BLENDING OF POLYETHYLENE MATERIALS

FOR PIPE APPLICATIONS

A thesis submitted for the degree of

Doctor of Philosophy

by

Wayne Clifton Augustus Wright

**Brunel, The University of West London,
Department of Materials Technology,
Uxbridge, Middlesex.**

January 1989.

To Joanne

He who finds a [true] wife finds a good thing, and obtains favour of the Lord.

Proverbs 18:22
(Amplified Bible)

Brunel, The University of West London,
Department of Materials Technology,
Uxbridge, Middlesex, UB8 3PH.

Wayne Clifton Augustus Wright

BLENDING OF POLYETHYLENE MATERIALS FOR PIPE APPLICATIONS.

Ph.D. Degree.

ABSTRACT

Melt blending of polyethylene, in particularly HDPE and LLDPE, have been shown to be a major success, especially in the film markets. In this thesis studies are reported on the stress rupture performance of pipes produced from selected polyethylene materials blended to a chosen MDPE pipe grade. The pipes were tested, notched or unnotched, at a single temperature of 80°C and at internal pressures designed to induce slit-mode failure. Results showed the simple concept of increasing the stress rupture performance of a pipe material by the addition of a higher molecular weight polymer was invalidated when applied to the blends system used in these studies. However molecular weight does have an influence to some degree as was illustrated by the addition of a very low molecular weight material, which produced the poorest stress rupture properties of the additives used.

Charaterization techniques, including Differential Scanning Calorimetry and Dynamic Mechanical Thermal Analysis, showed good compatibility of the blends at all addition levels studied, illustrating that there was no seperation of the polyethylene phases. Fracture analysis of pipe failures showed variations between the blends, except for a MDPE additive which had similar molecular characteristics to the base resin. Some of the blends fracture surfaces were found to vary in fibre height and distribution from the bore region to the outside of the pipe. On the morphological front spherulites from pipe samples were found to be a poor indication of stress rupture behaviour. Pipe blends were produced which had fine/featureless morphologies but whose 80°C stress rupture behaviour was found to be good *and* poor in comparison to the control MDPE pipe resin which had a spherulitic structure much larger than all the blends studied.

Models presented here infer that a number of mechanisms may be operating in producing these changes in stress rupture properties. One may be due to a dilution of a polyethylene system by materials of varying molecular weight and molecular weight distributions. This was evident in MDPE-A/MDPE-P blends (MDPE-P being a high molecular weight, low branch length additive), where the stress rupture performance initially decreased and then increased after addition levels of 10wt%. The main mechanisms for this system was postulated to be the initial dilution of octene branching levels within the MDPE-A blend causing a reduction in the ability of the branches to sterically hinder crack propagation under stress, to one of chain entanglement after sufficient levels of the additive was present in the blend to contribute to increasing the stress rupture behaviour. It was found that good blending can be produced using materials with similar branching types and distributions (especially in the high molecular weight tail), similar molecular weights and distributions and comparable crystallization temperatures.

ACKNOWLEDGEMENTS

I would like to thank the Science and Engineering Research Council for the award of a CASE studentship. DuPont UK Ltd provided additional funds, and I am grateful to Dr. David Hargett of DuPont for his guidance and help during the course of the project.

Thanks are also due to my Supervisor, Jeremy Bowman for his advice and support during the PhD, (your supervision is better than your football Jeremy), and to Bill Price for 3 years of fixing the tank heaters and putting up with me.

The manuscript was beautifully typed by Miss Patricia Healy and the final manuscript was produced in the Chemistry Department of Brunel University, of which I am extremely grateful for the use of their computer facilities.

But last and not least I am grateful to Jesus Christ for his love, strength and guidance during the PhD project. Without his support things may have been a little different. Thanks Lord.

Wayne Wright
January 1989

CONTENTS

CHAPTER 1

INTRODUCTION

Over 50 years have passed since the first patent for the production of polyethylene from ethylene was filed. It is sometimes difficult to realise that polyethylene, with one of the simplest molecular structures and having a wide range of properties, is still the largest tonnage plastic material, with total resin consumption of over 2.3 million tonnes in Western Europe during 1987 [1].

Due to increasing resin consumption, the demand for polyethylene resin continues to record good growth rates. However producers are now increasing prices to relatively high levels, making manufacturing profit margins very tight in major consumer areas. At present (Summer 1988) the UK price for film grade LDPE (Low Density Polyethylene) is £660-675/tonne and HDPE (High Density Polyethylene) blow moulding grade £660-700/tonne [2]. However for pipe grade resins the cost is approximately £900/tonne [3]. This premium for pipe grade material reflects the speciality of this engineering grade and the demands placed on it for overall short and long term strength.

In such a competitive market as the pipe industry the factors influencing the performance of the finished article need to be understood, to not only

influence the future choice of new raw materials but to maintain a company's edge over a rivals product.

In water and gas distribution, the pipe system is usually designed for a minimum lifetime of 50 years at 20°C, the design stresses for which are primarily derived from the results of long term hydrostatic tests [4]. The results of these hydrostatic tests are represented as double logarithmic plots of creep rupture time verses hoop stress in the pipe wall. An example of this is shown in Figure 1.1 [5]. Three regions can clearly be seen. The initial line (Stage 1) of small negative slope and ductile rupture behaviour is influenced by branching. Fractures which occur by brittle or slow crack growth fall on a steeper line (Stage 2) which intersects the ductile creep curve. The intersection point changes if the molecular weight or chain branching characteristics of the polymer are changed [5]. The infinite gradient region (Stage 3) results from chemical degradation of the material and is clearly evident when testing pipes at high temperatures [6]. Again brittle type failures are the resultant fracture feature of this region.

For design purposes the pipe system needs to perform above the service stress level after 50 years at 20°C. Because experimental data rarely has creep rupture times exceeding 10 years, it is necessary to predict the lifetime performance of the pipe by extrapolation techniques. There have been various methods used for predicting the lifetime of polyethylene pipes mainly based on empirical relationships between the hoop stress and the time to failure [7-13]. However the most common method is shown in Figure 1.1 where from observing the brittle fracture behaviour at 80°C, 60°C and 40°C it is possible to empirically extrapolate the data to 20°C by constructing an Arrhenius plot of the logarithm of the creep rupture life versus the reciprocal of the test temperature (in K). This is usually found

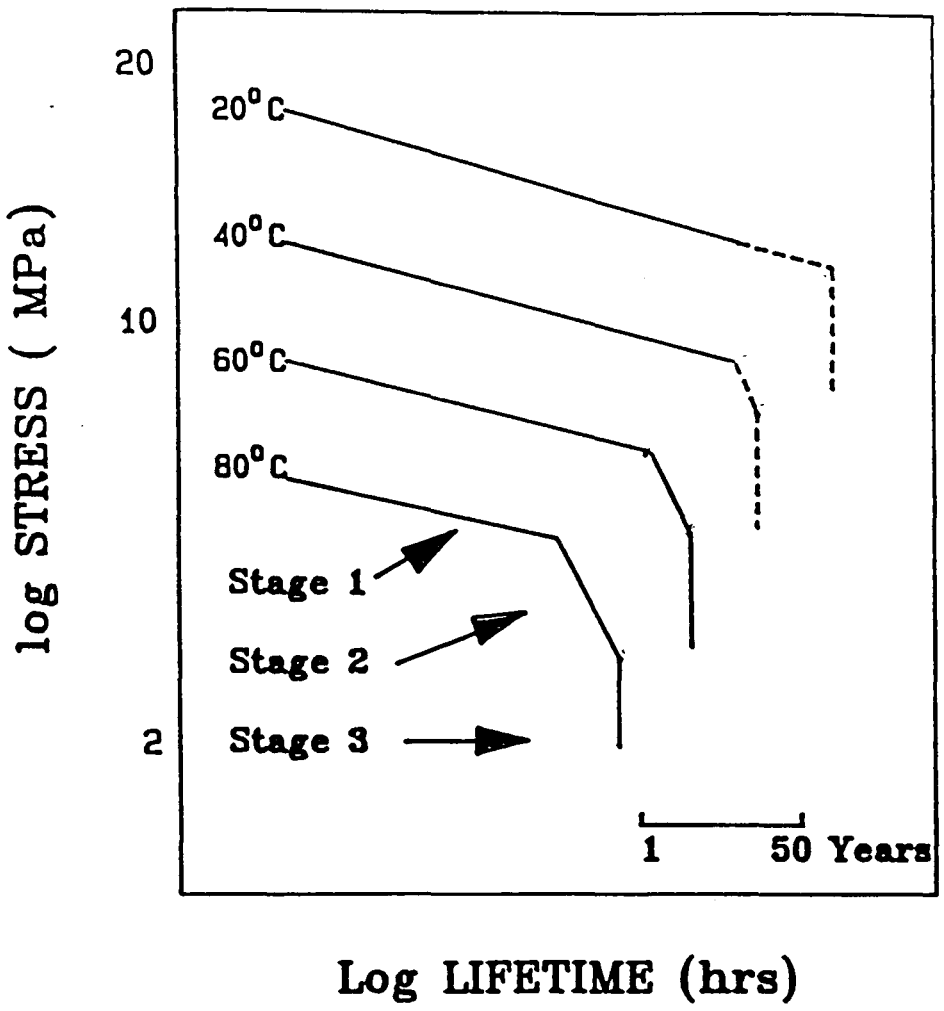

FIGURE 1.1: Typical stress rupture curves for polyethylene.

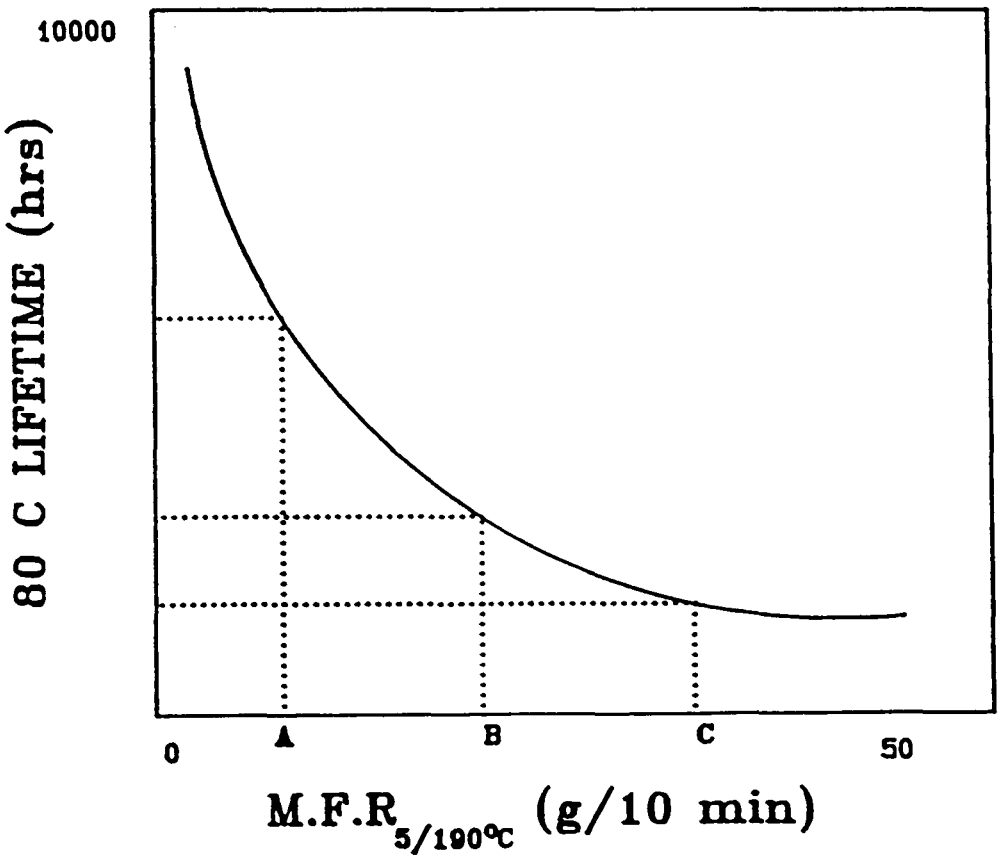

FIGURE 1.2: 80°C stress rupture variations with Melt Flow Rate [14]

to be a straight line graph which can be extrapolated to 1/293K . This procedure identifies the position of the brittle failure section of the stress rupture curve at 20°C and identifies if the design stress is based on ductile or brittle failures at 50 years.

It has been briefly mentioned that Stage 2 of the stress rupture curve is influenced by the molecular weight of polyethylene. Figure 1.2 illustrates the dependence of the long term testing times at 80°C and 5MPa for HDPE copolymers as a function of melt flow rate (MFR) [14]. The curve plainly illustrates how long term testing times can be affected by the melt flow rate. But let us examine the curve more closely. If we have a material of melt flow rate ***C*** which has poor 80°C stress rupture performance, by blending in a material of good stress rupture lifetime ***A***, we would expect a blend of ***B*** having a lifetime and melt flow rate in between ***A*** and ***C*** (assuming equal proportions and additivity of MFR properties). In this simple example we have altered the 80°C stress rupture performance of a poor pipe material. It is the use of these concepts that we aim to apply in this research programme. In other words can we by the addition of various polyethylene grade materials influence the stress rupture performance of pipe grade materials, and in doing so understand better the factors controlling pipe performance?

Blending of polyethylene materials is used extensively in the polymer industry and particularly in the polyethylene film business where recently there has been a spate of activity [2]. For pressure pipe applications it has been shown that high density polyethylene (HDPE), and the more recent medium density polyethylene (MDPE) grades, are the most suitable polyethylene materials. These resins are used unblended. It is with the MDPE pipe grade resins that we will concentrate on in this research

programme.

The objective of this research programme was to examine the influence of blending various HDPE and MDPE polyethylene grades into a known MDPE pipe resin. By producing blended pipe the project sought to identify the role of molecular weight and branching on the performance of the base resin. The work did not concentrate heavily on the influence of blending on the processing of pipe, but on the mechanical testing side, utilising notching of blended pipe to evaluate its surface damage resistance under stress rupture conditions. For long term data, creep rupture tests focused solely on the Stage 2 brittle region of the stress rupture curve, utilizing high testing temperatures in a water environment to induce short failure times. Because of this, thermal analytical tests were performed on the blended pipes to ensure that Stage 3 was not inadvertently reached from decreased antioxidant levels in the pipe [15].

CHAPTER 2

STRUCTURE AND PROPERTIES OF POLYETHYLENE AND POLYETHYLENE BLENDS

2.1 INTRODUCTION - MOLECULAR ARCHITECTURE

Polyethylene macromolecules form chains consisting of CH_2 links which may be branched in various ways to an extent depending on the catalyst system, comonomer (if present) and the polymerization conditions (Figure 2.1.). HDPE is frequently referred to as *linear polyethylene* because there are few branches in its molecular chains whereas LDPE is referred to as branched polyethylene.

Linear polyethylenes i.e. HDPE, MDPE and LLDPE (Linear low density polyethylene) are produced by the low pressure process. Short chain branches are admitted by copolymerizing the ethylene with α-olefins e.g. 1-butene, 1-hexene, 4-methyl pentene etc. Since MDPE and LLDPE contain higher mass fractions of comonomers than HDPE, they are more branched. If the proportion of comonomer further increases, the degree of branching may be so high that densities below 900kg/m^3 are attained. The product in this case is VLDPE (Very low density polyethylene). Polyethylenes of very high chain lengths are known commercially as ultra-high molecular weight polyethylenes (UHMWPE). These are speciality polymers with a molecular

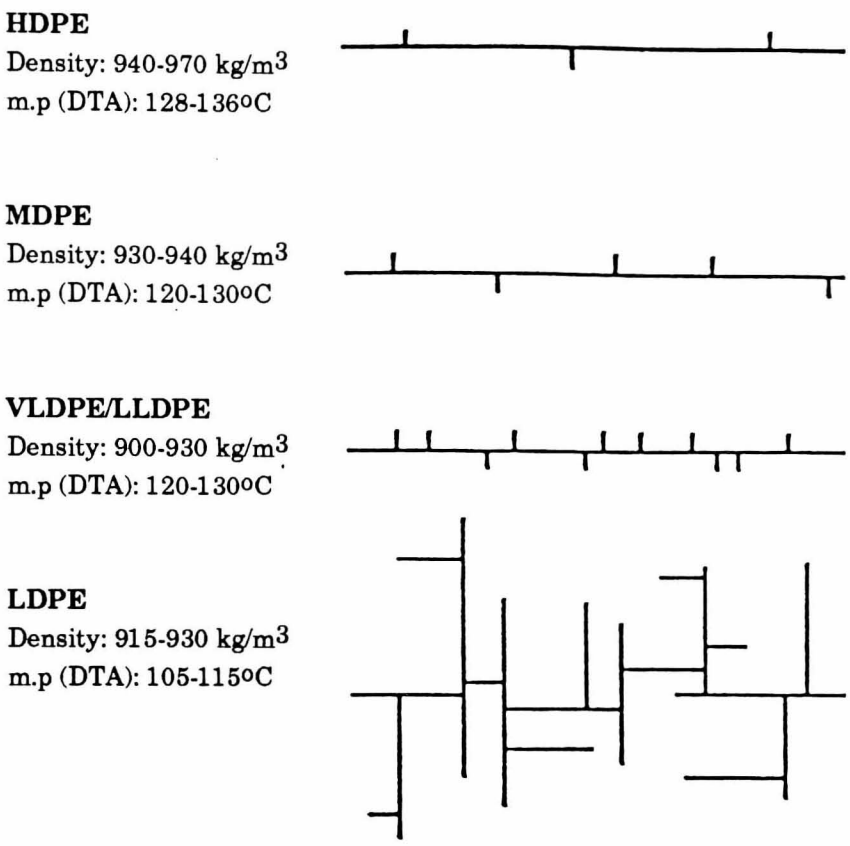

FIGURE 2.1: Basic representation of the different types of polyethylenes available

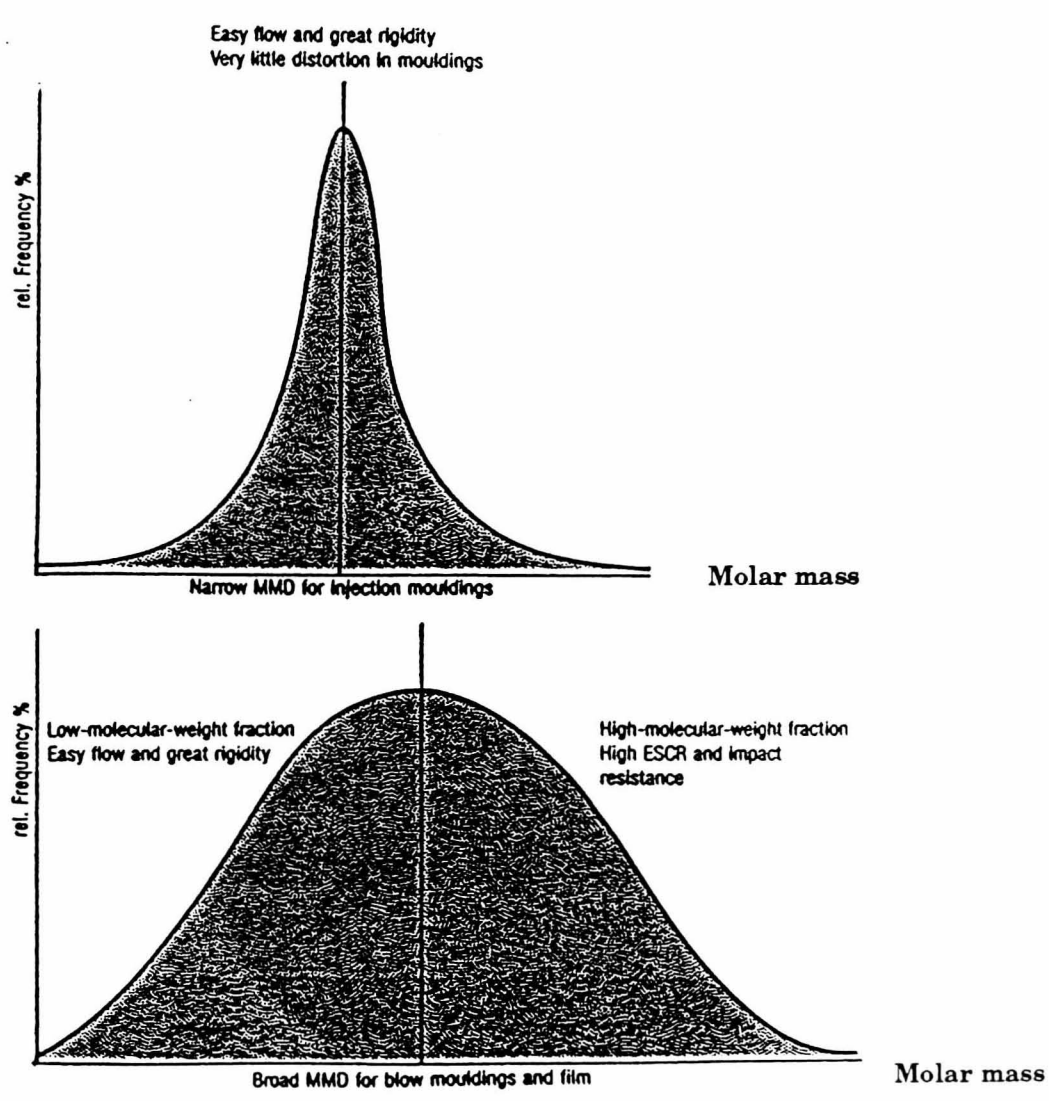

FIGURE 2.2: Properties variations with changes in molecular mass distribution

weight so high as to essentially inhibit flow of the polymer. They are essentially unbranched and require special synthesis and fabrication techniques.

Homopolymers and copolymers of ethylene (LDPE) obtained in the high pressure process contain branches of different length. The main chain, in contrast to that of linear polyethylene cannot be easily defined.

This chapter will highlight the principle factors influencing bulk properties of polyethylene and how they influence melting behaviour. On a microstructural basis we will discuss the morphology and the formation of spherulites of melt crystallized polyethylenes. Finally the use of polyethylene blending and mechanical properties of polyethylene/polyethylene blends is reviewed.

2.1.1 MOLAR MASS, MELT FLOW RATE, MELT VISCOSITY AND FLOW

Molecular mass is one of the most important parameters in distinguishing between grades of the same polymer. Differences in this property have a very important bearing on the polymers mechanical behaviour, morphology, kinetics of crystallization, thermodynamic properties and flow. Changes in molecular weight markedly influence the viscosity of the melt and therefore the ease with which products can be processed.

Commercial synthetic polymers have a range of molar masses and this distribution is most often illustrated as in Figure 2.2, but two of the most commonly used are the number average M_n and the weight average molecular weight M_w. They are defined as:

$$M_n = \Sigma (N_i M_i) / \Sigma N_i \qquad [2.1]$$

$$M_w = \Sigma (N_i M_i^2) / \Sigma (N_i M_i) \qquad [2.2]$$

where M_i is the molecular mass and N_i is the number of molecules of molecular mass M_i in the sample. A third measure describes the distribution of the high molecular mass portions of the sample and is known as M_z, it is defined as:

$$M_z = \Sigma N_i M_i^3 / \Sigma N_i M_i^2 \qquad [2.3]$$

As commercial polyethylenes consist of molecules of different chain lengths and molar masses, the frequency with which the molecules of different sizes are represented is described by the molar mass distribution. Characteristic ratios of the curve are:

$$Q = M_w / M_n \qquad [2.4]$$

$$Q' = M_z / M_w \qquad [2.5]$$

$Q = Q' = 1$ would correspond to a perfectly uniform or monodisperse polymer while a high Q ratio points to a low molecular weight tail whereas a high Q' ratio indicates the presence of a very high molecular weight tail.

2.1.2 DEGREE OF CRYSTALLINITY AND CHAIN BRANCHING

Figure 2.1 illustrates some of the various structures of polyethylene available. What can be seen is that a change in the length of the main

chain and branching substituents can influence the overall density of the polymer.

Density is an important parameter in the characterization of polyethylene and reflects the ability of the polymer to crystallize. The degree of crystallization is a term based upon the observation that there is a relatively large and measurable difference (up to 20%) between the densities of the crystalline and amorphous regions. From these differences in densities between the two phases it can be shown that a measure of crystallinity can be described by the following relationship:

$$X_c = \rho_c / \rho \, (\rho - \rho_a / \rho_c - \rho_a) \qquad [2.6]$$
$$= (V - V_a) / (V_c - V_a)$$

where ρ is the density (determined by floatation in a density gradient column). X_c is the degree of crystallinity and ρ_a and ρ_c are the densities of the 100% amorphous and 100% crystalline components. ρ_c is calculated from the knowledge of the crystal structure and ρ_a is measured directly if the polymer is obtained by rapid cooling (to suppress crystalline formation) or by extrapolation techniques [16]. V, V_c, and V_a are the specific volumes of the completely amorphous material and completely crystalline material respectively.

Next to molecular weight and molecular weight distribution, chain branching is the most important chain variable influencing the properties of polymers. Branching influences the proportion of crystalline matter and hence the density. In the Phillips process comonomers such as propylene, but-l-ene hex-l-ene etc., are used to produce a controlled degree of short chain branching in the polymer. The traditional method for their

measurement is by identification of the CH_3 distortion band at 1375cm-1 in the infra-red spectrum which measures the total content of branch ends [17]. However the ^{13}C chemical shifts from Nuclear Magnetic Resonance work on branched polyethylene has been found not only sensitive to stereochemical configuration but also to the type, length and distribution of branches [18,19].

2.1.3 PHASE TRANSITIONS AND RELAXATION PHENOMENA

We have seen how molecular weight and branching can effect the structural aspects of polyethylene. They also influence the melting and crystallization processes.

In linear polyethylene T_m is influenced by molecular weight. The decrease in molecular weight from for example $1x10^6$ to $4x10^4$ is accompanied by a decrease in T_m from 137 to 128°C. However the T_m of commercial HDPE depends mainly on branching as described by the following Flory equation [20]:

$$(1 / T_m) - (1 / T_m^0) = -(R / \Delta H_f) \ln p \qquad [2.7]$$

where T_m^0 is the melting point of a perfectly regular polyethylene,R the Gas constant, p a probability factor describing the structure of a copolymer and ΔH_f is the equilibrium heat of fusion. For copolymers with low α-olefin content, p is equal to the mole fraction of the comonomer in the copolymer. An example of the influence of branching on the T_m of HDPE is illustrated in Figure 2.3.

Relaxation spectrometry studies of semicrystalline HDPE using dynamic mechanical or elastic methods reveal four temperature ranges in which

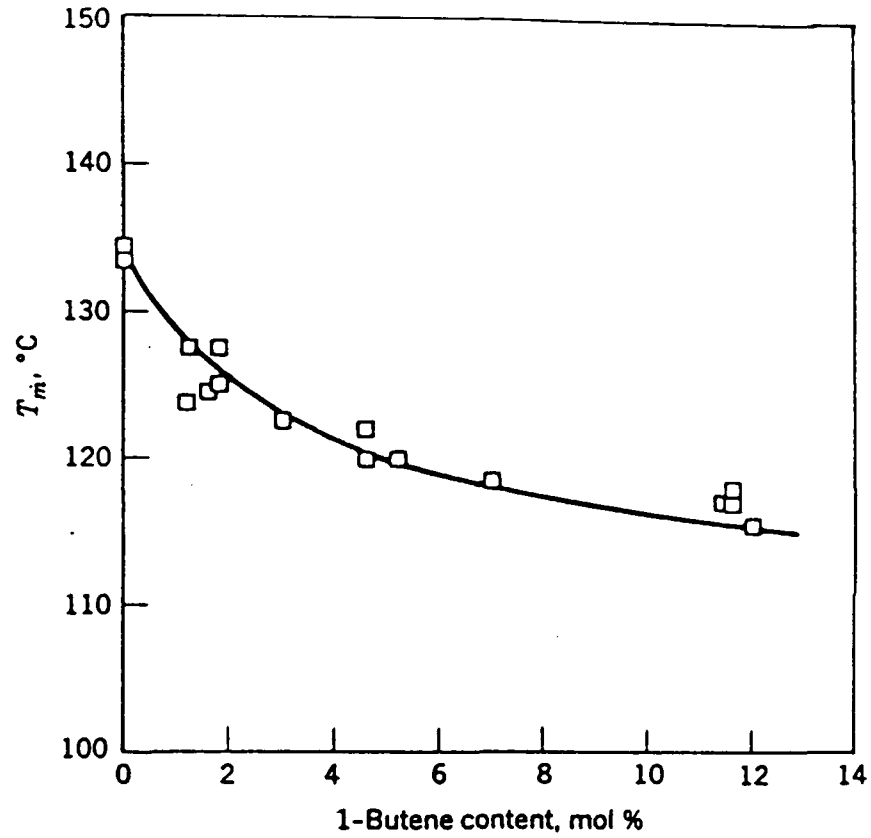

FIGURE 2.3: Influence of branching on the melting temperature of HDPE [20].

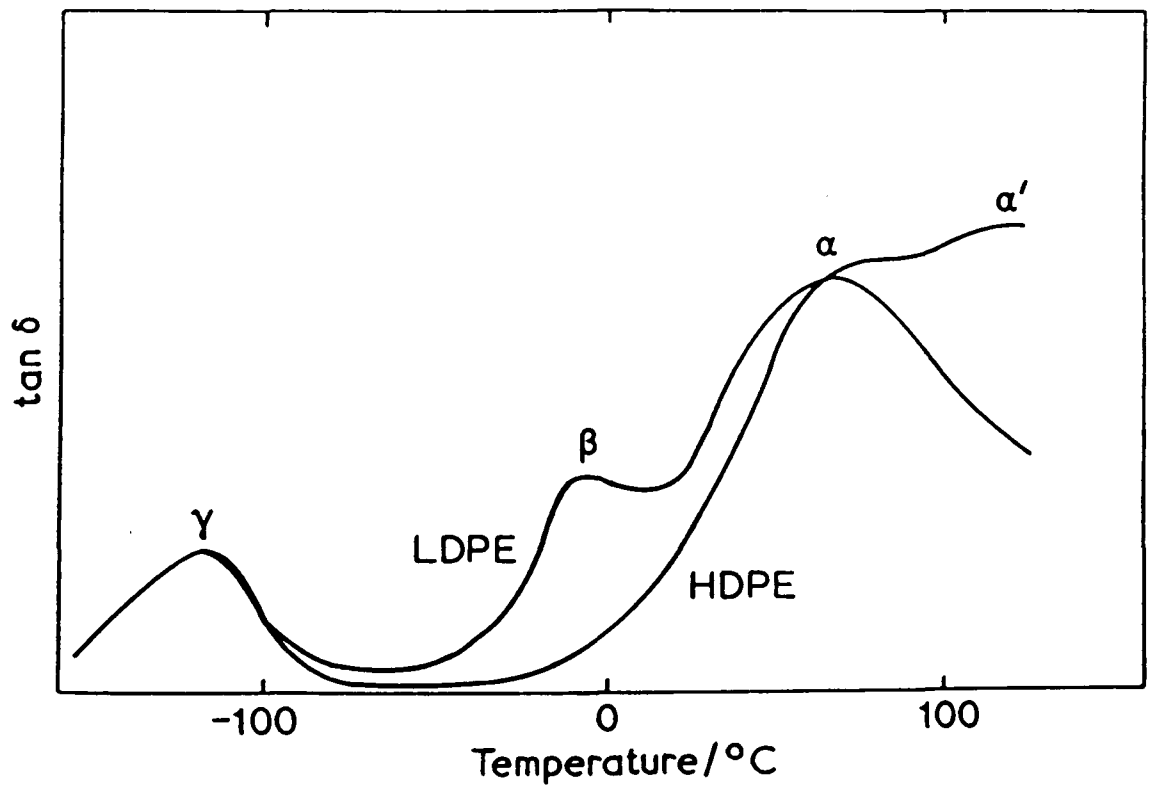

FIGURE 2.4: Relaxation transistions in LDPE and HDPE [20].

significant relaxation phenomena occur. Although it is not completely understood Figure 2.4 shows the variation of tanδ with temperature for HDPE and LDPE. The presence of branches in the polyethylene molecules reduces the degree of crystallinity, crystal size and its crystal perfection. This leads to complications in interpretation of the relaxation behaviour [21]. The intensities of the α' and α-relaxations decrease as the degree of crystallinity is reduced, implying that they are associated with motions within the crystalline regions. However the γ-relaxation *increases* with a reduction in crystallinity indicating that it is associated with the motions of small chain segments (3-4 CH_2 groups) in the amorphous phase, and has been tentatively assigned to a glass transition in the non-crystalline regions. The disappearance of the β-transition with the absence of branching has been taken as a strong indication that it is associated with relaxations at the large chain segments or branch points in the amorphous phase [21]. The transition as shown in Figure 2.4 is virtually absent in linear and highly crystalline HDPE, but in branched polyethylene the β peak is conspicuous and its maximum shifts to lower temperatures with increasing branching . In general the assignments of the peaks in crystalline polymers to particular types of molecular motion is rather difficult and often a matter for some debate .

2.2 MORPHOLOGY

2.2.1 SPHERULITES

The morphology of linear polyethylene as revealed by optical microscopy or small angle light scattering, depends on both molecular weight and crystallization temperature [21,22]. External factors such as pressure and shear or elongation forces acting during solidification also have a major

effect on the morphology. A number of possible morphologies may be obtained in equiaxed melt crystallized linear polyethylenes:

(a) Banded spherulite

(b) Non-banded spherulite

(c) Axialite

(d) Random lamellar structure

The banded spherulite is a common form seen in polyethylene morphologies and displays the familiar concentric rings first identified from the work of Keller [23] (Figure 2.5). The periodic changes in the birefringence along the radius of the spherulite were explained by Keller with reference to a regular smooth twisting of the lamellae along the radius of the spherulite (Figure 2.6). But more recent studies by Low et al [24] and Bassett et al [25] revealed results inconsistent with this regular twisting model. Instead Bassett presents microscopy data showing the presence of relatively untwisted S-shaped (as seen along the b-axis) lamellae in linear polyethylene with banded spherulites. He suggests that the variation in birefringence is caused by localized changes of the lamellar normal along the spherulite radius, possibly by screw dislocations.

2.2.2 CHAIN FOLDING

The origin of the twisting of the lamellae has been shown to be uncertain. However over the last decade controversy has raged over the detailed molecular level structure of lamellar melt crystallized polymers such as linear polyethylene. Although there is no doubt that their morphology is lamellar for the basic structural unit, no comprehensive agreement exists on the manner in which polymer molecules form these structural building

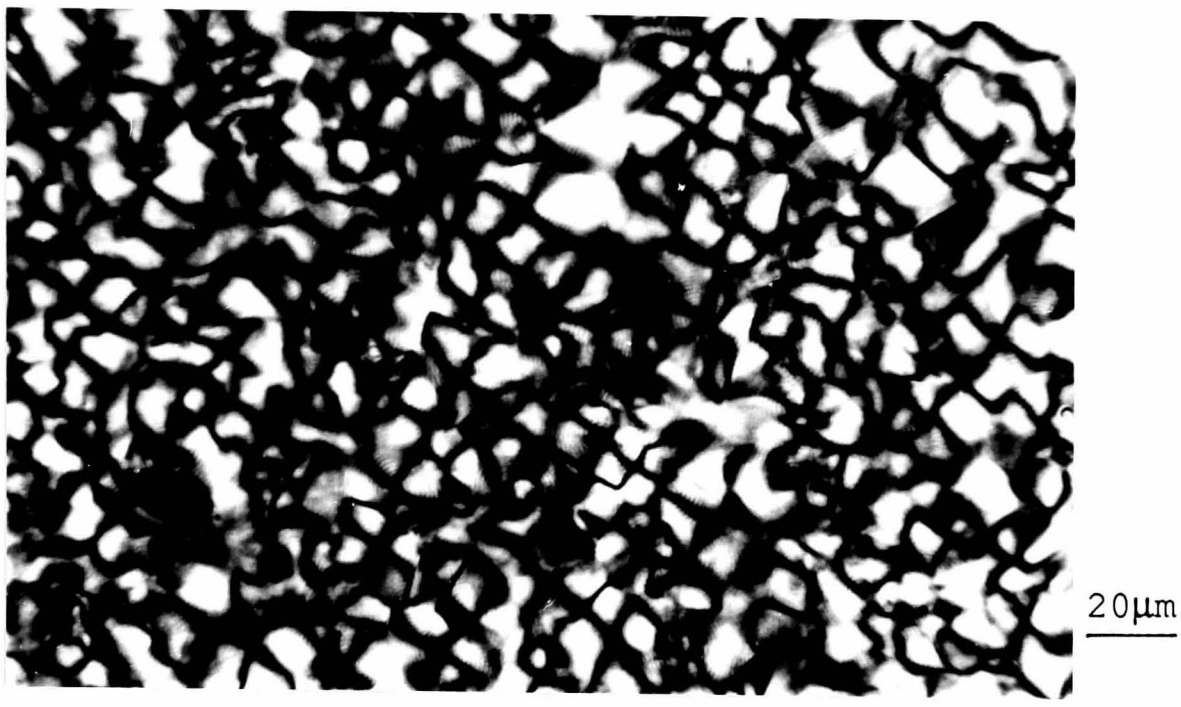

FIGURE 2.5: Banded spherulites in melt crystallized polyethylene.

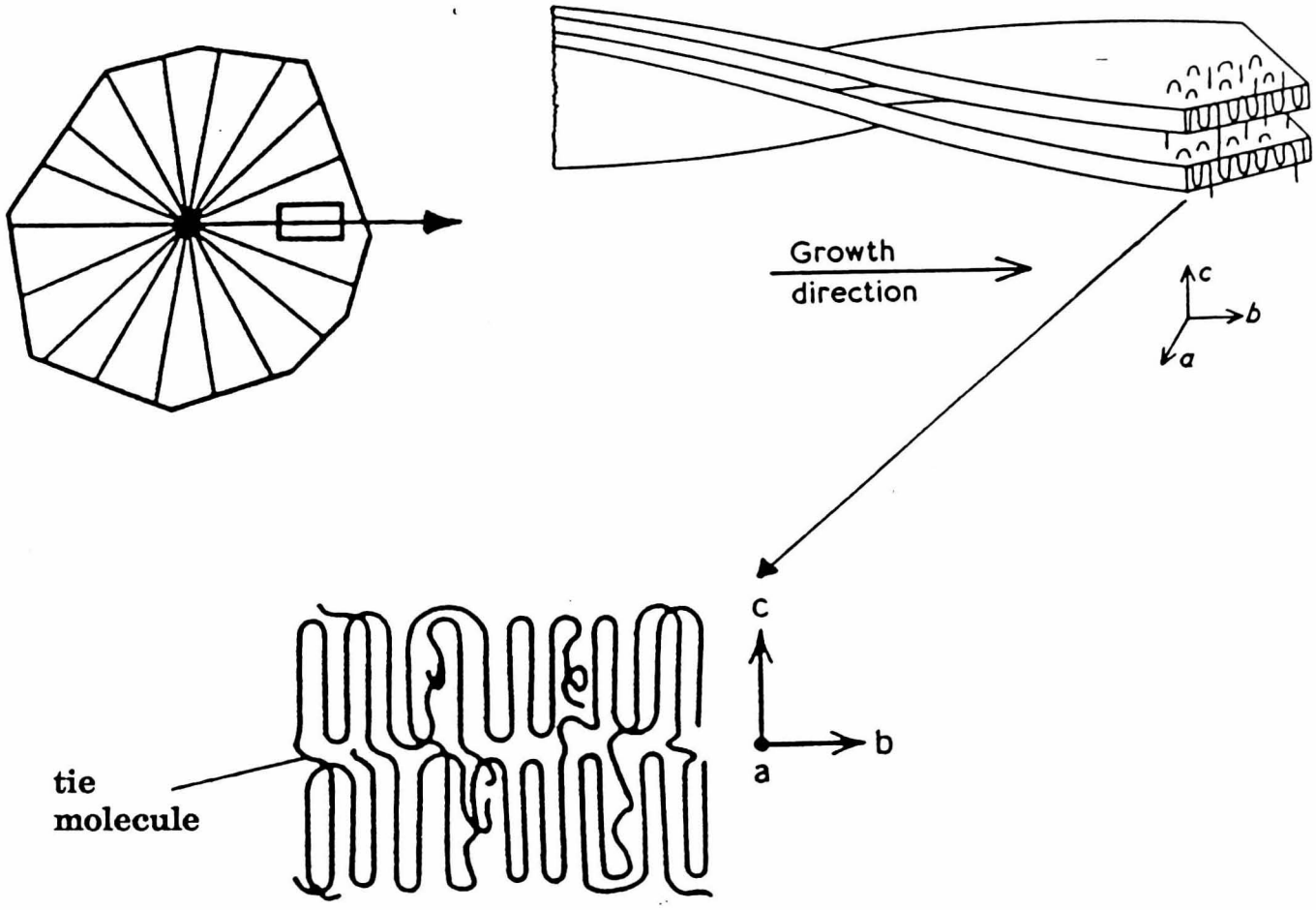

FIGURE 2.6: Model conformation of a spherulite and the chain organisation within a lamallae [21]

blocks. One school of thought favoured by Flory and many others [26,27] takes as its starting point the thesis that polymer melts are composed of randomly entangled molecules which on solidification form lamellae by a process which involves minimal movement of the chains during the crystallization process. The structure proposed is composed of chains translating through the lamellae in a random manner (Figure 2.7,I). Others feel that the structural unit is more typical of solution crystallized polymers i.e. the chain folded free lamellar is present in melt crystallized material and hence model II (Figure 2.7) is said to be closer to the structure of these materials. It is most likely that the true model is one composed of both points of view as experimental evidence neither fully supports or refutes one view from the other.

2.2.3 CHAIN BRANCHING AND INTERCRYSTALLINE LINKS

We have illustrated the influence that branching and molecular weight have on the structural properties of polyethylenes in previous sections; but on a molecular level the presence of branches is thought to retard lamellar growth and reduce the density. Many authors have thought that the branches as well as other defects are rejected to the amorphous regions [28,29]. However it is known that in LLDPE (where the length and distribution of branches is relatively uniform), the branches are accommodated into the crystalline lattice [30]. For polyethylene, Martuscelli [31], and Martinez de Salazar and Balta Calleja [32], have presented models showing their possible incorporation into the lamellae, (Figure 2.8.) In fact the change in lamellae thickness with branches is related to the melting temperature of the polymer in accordance with the Hoffman and Weeks relation [33].

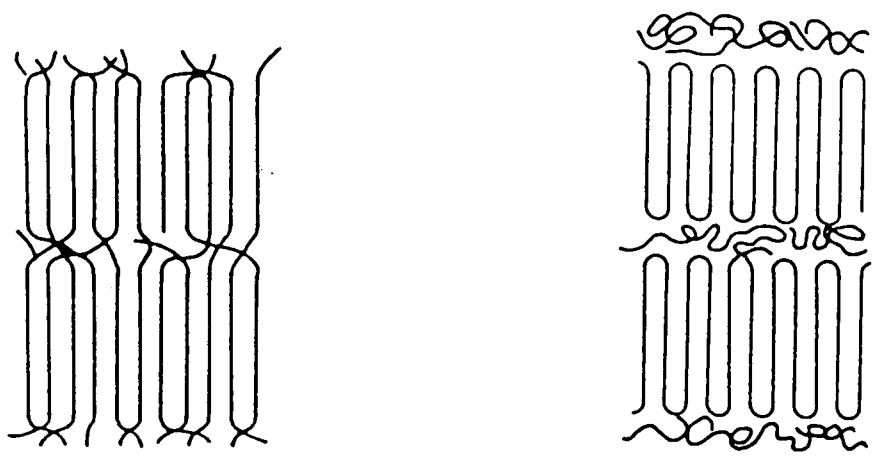

FIGURE 2.7: Crystallization lamellar model of Flory (I) and chain folded model (II).

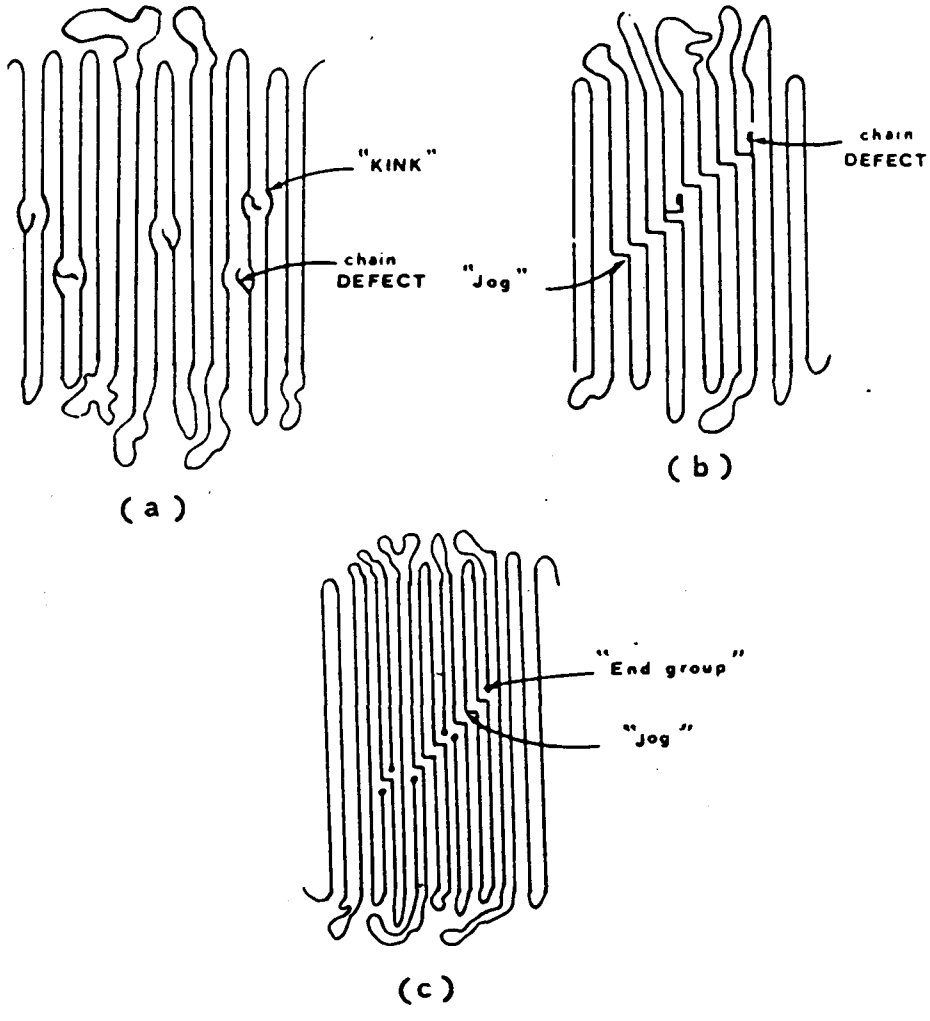

FIGURE 2.8: Incorporation of defects into crystalline lamellae [31].

$$T_m = T^o_m - (2 \sigma_e T^o_m / \Delta H_f L) \qquad [2.8]$$

Where ΔH_f is the enthalphy of fusion per unit volume of the crystals, L is the crystal thickness, σ_e the surface energy of the crystal, T^o_m is the melting temperature of an infinitely thick polymer crystal and T_m, the melting temperature of the polymer.

The picture we have built up is of a semicrystalline polymer made up of spherulites which are composed of lamellae containing some impurities in the form of branches. However this view is too simple as it does not account for the mechanical properties of such polymers; one might expect failure at interspherulitic boundaries and possibly within spherulites. It has accordingly been suggested that neighbouring lamellae are held together by intercrystalline links (tie molecules), as can be seen in Figure 2.6. Keith et al [34] provided evidence of intercrystalline links by crystallizing polyethylene in solution. The length and distribution of the branch in comonomers are thought to increase the number of tie molecules bridging crystallites [35,36] . However although their existence is widely accepted their determination and quantitative analysis in regard to physical properties has yet to be fully understood.

2.3 POLYETHYLENE BLENDING

2.3.1 INTRODUCTION - WHY BLEND !

There are five main reasons to employ polymer blends [37]

-higher performance at a reasonable price

-modification of performance as a market develops

-re-use of plastic scrap

-generation of a unique material as far as its processability and/or performance are concerned

-extending the performance of expensive resins

The main area of polyethylene blending is in the production of films where an extensive amount of literature and patent information is available [38], the pertinent blending systems being LLDPE/LDPE and HDPE/LDPE. However we will concentrate mainly on blend systems involving MDPE and HDPE mentioning other polymer blend systems wherever relevant to illustrate property trends.

2.4 MISCIBILITY AND METHODS OF DETERMINING MISCIBILTY

The blending of two polyethylenes immediately raises the question of their mutual compatibility. The term miscibility has been chosen to describe polyolefin blends with behaviour similar to that expected of a single phase system. Although miscibility does not imply ideal molecular mixing it suggests that the level of molecular mixing is adequate to yield macroscopic properties expected of a single phase material. So a miscible polyolefin blend is defined as a stable homogeneous mixture which exhibits macroscopic properties expected of a single phase polyolefin.

2.4.1 CALORIMETRIC METHODS

For polyethylene blends a reliable criterion of miscibility is the detection of the crystalline melting point of the blend and the comparison of the measured value to the individual components. This can be easily determined from calorimetric measurement [39]. A miscible polymer blend

exhibits a single crystalline melting temperature intermediate between those of the components, whereas two separate crystalline melting temperatures appear in the cases of immiscibility. A polymer blend with a single crystalline melting point is indicative of a homogeneous system. A blend with two separate crystalline melting points is indicative of a heterogeneous system. The melting behaviour for both miscible and immiscible systems are shown schematically in Figure 2.9 .

2.4.2 OPTICAL MICROSCOPY

Direct visual confirmation of the two phases has been used more often than any other method as a preliminary indication of the degree of miscibility of polyethylene blends. The formation of spherulites from the melt offers the ability of monitoring the morphology of blends of polymers with different spherulitic characteristics [40]. Although variations in blend morphology may not necessarily imply miscibility, the change in morphology with the second phase can clearly be seen in some polyethylene systems [41,42] .

2.5 MECHANICAL PROPERTIES OF POLYETHYLENE AND POLYETHYLENE BLENDS

Mechanical characteristics of polyethylene and polyethylene blends are related to numerous primary characteristics and in general the following parameters have the strongest influence on the mechanical properties.

(a) Molecular Weight and Molecular Weight Distribution

(b) Chain Branching

(c) Morphology

(d) Blend Ratios

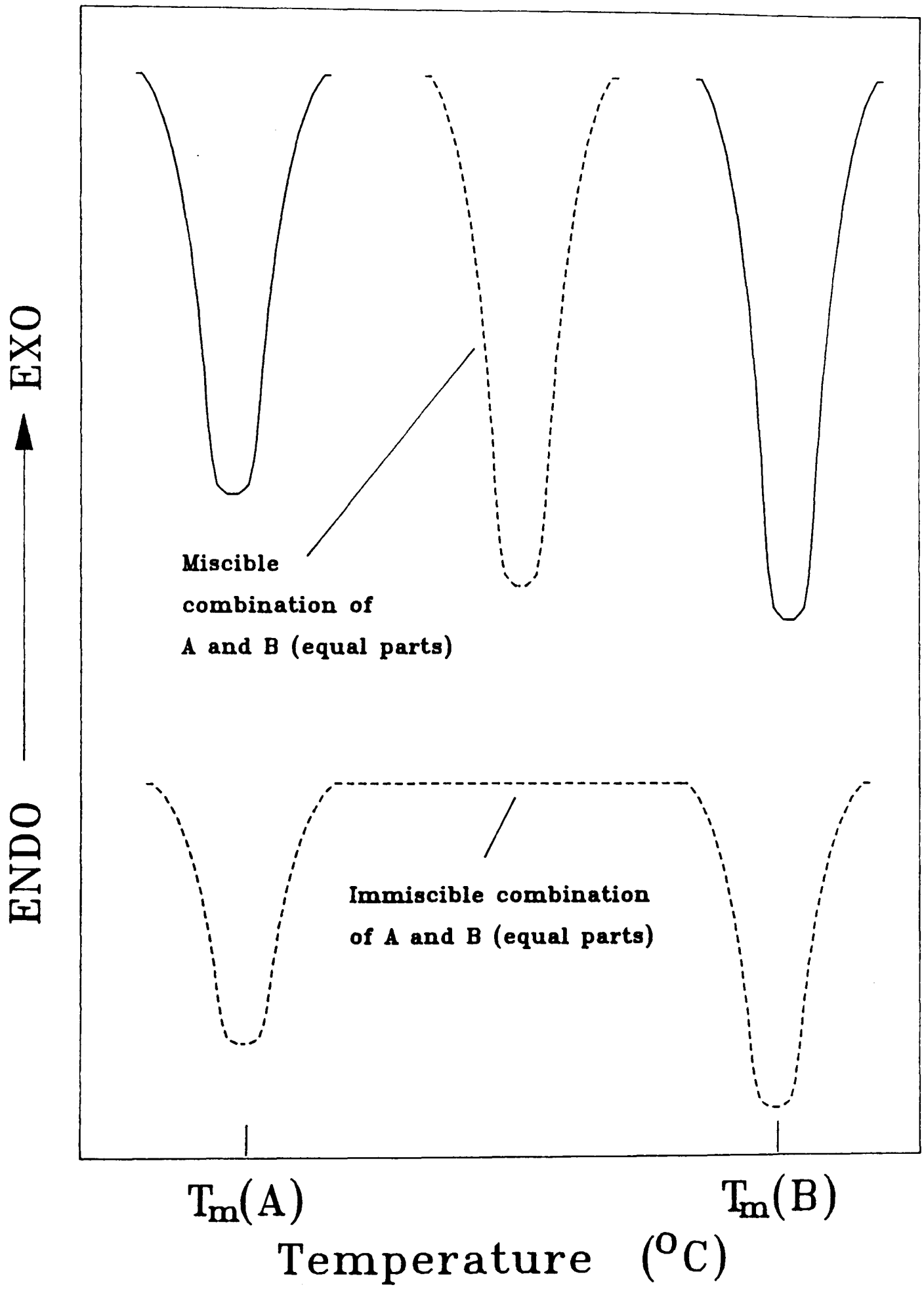

FIGURE 2.9: Melting behaviour for miscible and immiscible systems

Figs. 2.10 & 2.11 have been omitted.
Please refer to the references corresponding to each figure
(i.e. refs. 38, 40, 43, 44 for fig. 2.10; ref. 46 for fig. 2.11

With regard to properties, polyethylene blends may be expected to exhibit any of the three characteristics exhibited in Figure 2.10. Perhaps the most commonly anticipated property versus composition relationship is the concept of *additivity*. Such averaging of properties has many potential benefits for formulating new blends. Sometimes it is found that blend properties exhibit antagonistic behaviour. This situation could arise from a poor degree of interfacial adhesion between components [38,40]. A less observed feature from blending polyolefins is the property known as synergism. This is where the blended polymer produces better properties than either of the pure components. This kind of behaviour is known to be a rare occurrence and offers unique possibilities when it exists. An example is the commercial use of LLDPE/HDPE blends where there is a blend composition that has better mechanical properties than either of the pure components [43,44].

This section looks at the influences of the primary characteristics, molecular weight, branching and morphology on the mechanical properties of polyethylene and polyethylene blends. As was mentioned earlier we will be mainly concentrating on blends involving HDPE and MDPE using other polyolefin systems to highlight particular relationships.

2.5.1 INFLUENCE OF MOLECULAR WEIGHT

This parameter influences polyethylene properties mostly through its effect on crystallization kinectics, final crystallinity X_c and the morphological character of the sample. Margolies et al [45] found that the tensile strength of high density polyethylene increased with M_w to a M_w of 1.5×10^6. He postulated that increases in M_w led to an increase in the number of

intercrystalline tie chains that bridge crystallites. When the sample is stretched as in a tensile test, the tie chains are thought to restrain the crystallites from slipping with respect to each other and hence the observed increased tensile strength. Margolies et al [45] also showed that the Izod impact of HDPE increased with molecular weight up to a maximum of $1.75x10^6$. However Margolies et al [45] does not fully consider the molecular weight distribution of the polymer on its influence on the mechanical properties. Cohen [46] recognized this area and using the notched Izod test demonstrated that the M_W must be increased from $1.5x10^5$ to $2.75x10^5$ to achieve the same level of toughness when an end user shifts from a broad molecular weight distribution to a narrow molecular weight distribution grade during processing (Figure 2.11).

Due to the improvements of impact strength, tensile strength and environment stress cracking with increasing molecular weight, several workers have used these concepts of molecular weight blending for polyethylenes . Bhateja and Andrews [41] blended UHMWPE with linear polyethylene . They found that the properties of the blends were intermediate between the two polymers; yield stress and tensile modulus decreased with addition levels of UHMWPE whereas tensile strength increased with the high molecular weight additive. They explain these variations by stressing that the addition of UHMWPE decreases crystallinity and increases molecular entanglement formation. The crystallinity decrease was identified as influencing modulus and yield stress, whereas the entanglement network was said to have produced strain hardening and hence an increased tensile strength value. Dumoulin et al [42] added MDPE to UHMWPE and found similar relationships for yield stress and tensile strength.

2.5.2 INFLUENCE OF BRANCHING

An increase in branching reduces crystallinity and is accompanied by significant modification of mechanical characteristics.

The type of branch as well as the amount of branches and even the distribution of branches in the MWD of the polyethylene, has a profound affect on the physical properties of polyethylene. Bubeck et al [47] found that creep resistance, modulus and environmental stress cracking resistance all increased with branch length (methyl to hexyl) at a given density and molecular weight . Union carbide also found that the toughness of their polyethylene resins improved with increasing short chain branch length [48]. The change is shown not be that significant for LLDPE of low molecular weight compared to the high molecular weight material (Figure 2.12).

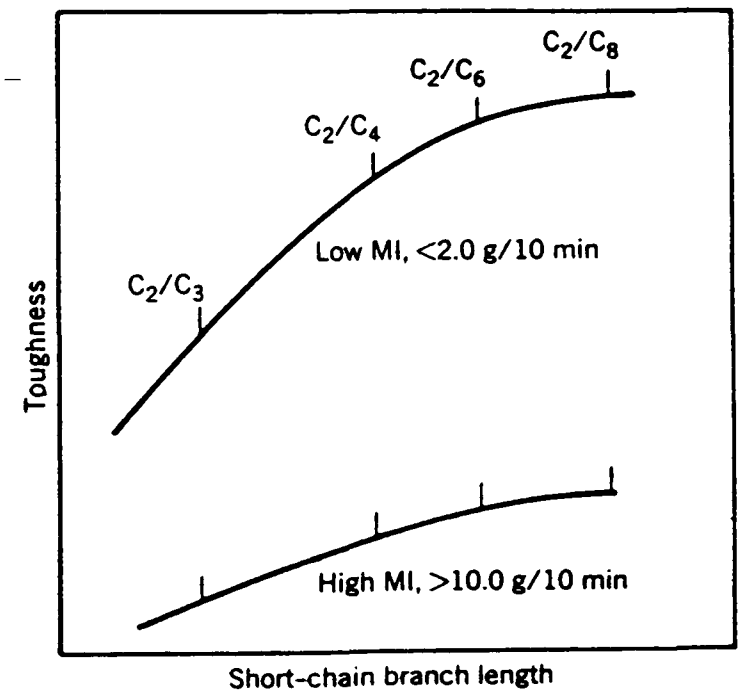

FIGURE 2.12: Molecular structure: Short chain branch length vs LLDPE toughness (MI = melt index) [20].

Seguela and Rietsch [49] found that branching increased the tensile strength of polyethylene . They suggest that during crystallization the branches are

rejected out of the crystallite into the amorphous regions enhancing strain hardening characteristics.

The branch distribution has now become the main concern of several investigations. Results from Cady's work [50] show that the distribution of branches plays a major role in the properties of LLDPE and that branches tailored on the high molecular weight component give better physical properties than branches that are evenly distributed along the chains . Ishikawa et al [51] have also found similar results from MDPE resins and found that the comonomer distribution as well as the comonomer type is also an important factor in the long term creep performance of polyethylene.

Again these concepts of chain branching have been applied to polyethylene blends. The most common (and commercial) group of blends in the literature concerns the LDPE/HDPE system which mainly has uses in the film blowing sector. Here the LDPE addition to HDPE produces tough films as a result of the inclusion of branches from LDPE [44] . Bailey and Whitte [52] in their patent of polyethylene blends found that when producing films of blends of high and low molecular weight polyethylenes that the high molecular weight portion which contained a hexene copolymer produced better tear strength and toughness than a high molecular weight linear grade.

2.5.3 INFLUENCE OF MORPHOLOGY

Since polyethylene crystallizes rapidly it is difficult to vary spherulite size, therefore the effect of morphological structure on the mechanical characteristics have not been studied in detail. However extensive work has been carried out on the variation of spherulitic morphology with

mechanical properties of polypropylene . Way et al [53] showed that there was a critical spherulite size for maximum yield stress. They used SEM and TEM to show that spherulite sizes greater than the critical spherulite size displayed poor mechanical properties due to the segregation of impurities at the boundaries.

With polyethylene Maxfield and Mandelkern [54] illustrated that increasing the short chain branching in LDPE changed the spherulitic structure from random spherulite sizes to poorly defined spherulites. However Bubeck and Baker [47] found that for a given density and molecular weight, short chain branching increases in the polymer, increased the spherulite size. To illustrate the complexities of allying mechanical characteristics with morphology, Mandelkern and Maxfield [55] noticed that different polymers having similar densities and molecular weights differed in morphological characteristics on quenching from the melt due to differences in polydispersities . Brown and Ward [56] correlated these morphological features to mechanical tests and found that the quenched material was less brittle and tougher than the slow cooled material. They proposed that differences in the samples were due to the number of tie molecules which held the crystals together, and that the number of tie molecules increased with the degree of supercooling and the length of the molecules (molecular weight).

In the literature little information is available on the influence of morphological variations of polyethylene blends on mechanical properties. Dumoulin et al [42] melt incorporated UHMWPE into MDPE and obtained antagonistic behaviour of modulus and tensile strength data with increase in UHMWPE levels. Optical microscopy of the samples showed particles of UHMWPE in a matrix of MDPE. They attributed the poor mechanical

properties to lack of molecular entanglements of the two phases. Similar mechanical relationships were determined for HDPE in UHMWPE by Bhateja and Andrews [41]. In their study no mechanical synergistic effects were observed from blends of the two polymers. However when they looked at the resultant morphology of the blends they observed that the addition of UHMWPE to HDPE increased the number of small spherulites (below 20μm) in the blend. This was found to be very much larger than either of the parent polymers morphology. Other authors have found similar morphological relationships with other polyethylene blend systems [57,58]. Unfortunately no correlations in these studies have been made with mechanical behaviour. What it appears from these authors is that the introduction of a second polyethylene phase disturbs the crystallization behaviour of the major phase and acts as a molecular nucleant for the production of smaller spherulites . The influence of this change in morphological feature on the mechanical behaviour of blends has yet to be fully understood; in particular to the mechanical synergism exhibited by blends of LLDPE/HDPE systems.

CHAPTER 3

PERFORMANCE OF POLYETHYLENE PIPES

3.1 INTRODUCTION

Creep rupture curves have been illustrated in Chapter 1 to represent the results of long term hydrostatic tests on pressure pipe. As Figure 1.1 illustrates, the testing times can be very high and hence extrapolation methods from high temperature tests are used to predict operating conditions at 20°C /50 years.

The purpose of this chapter is to describe the generation and utilization of pipe stress rupture curves. Predictive methods are highlighted which utilize short and long term data at elevated temperatures to predict pipe performance at 50 years at service temperatures. Fracture mechanics principles are also discussed, identifying their role in pipe performance predictions. A section on the factors controlling pipe performance will elaborate on the areas raised in Chapter 1. Also a section on principle fracture morphologies and failure mechanisms from pipe samples will be related to the stress rupture curve. Finally a discussion of the literature concerning blending of polyethylenes is reviewed in regard to their utilization for pressure pipe applications.

3.2 PREDICTING THE CREEP RUPTURE STRENGTH OF PIPE SYSTEMS

A number of methods have been developed for predicting the long term performance of pipe systems and these can be broken down into 3 major areas:

(a) Extrapolation Methods.

Larson - Miller Correlation.

European Graphical Method.

(b) Activated Rate Process.

(c) Fracture Mechanics (Discussed in section 3.3).

3.2.1 LARSON - MILLER CORRELATION

This method was primary developed for the production of creep rupture in metals [11]. It suggests that the applied stress and the time to failure are related by an expression of the form:

$$P = T (C + \log t_f) \qquad [3.1]$$

where P is the Larson - Miller extrapolation parameter. It depends only on stress. T is the temperature, C is the Larson - Miller constant and t_f is the time to failure. For polyethylene C was found to be approximately 21 [9].

Both Gloor [9] and Whyman and Szpak [60] have tried to adapt the method to predict the creep rupture strength of high density polyethylene. The reason for their limited success is that mechanical properties are very temperature dependant as shown by Barton and Cherry [61]. However Barton and Cherry

have shown that the Larson - Miller approach can be more accurately applied if the parameter C is assumed to change with temperature. As with the European Graphical method the Larson - Miller approach is only confined to the brittle region of the creep rupture curves.

3.2.2 EUROPEAN GRAPHICAL METHOD

The European Graphical Method, developed by Richard et al [7] has become the basis for creep rupture prediction in European standards based on ISO recommendations. This method assumes that the creep rupture data can be best represented by a linear relationship between the log (applied stress) and log (time to failure) as Figure 1.1 simply illustrates.

This approach stems from the relationship developed by Sherby [62] which is of the general form:

$$\log \sigma = M_1 + M_2 \log t_f \qquad [3.2]$$

where σ is the applied stress, M_1 and M_2 are temperature dependant constants and t_f is the time to failure. The spacing between the lines of the log (applied stress) log (time to failure) curves are supposed to be governed by the Arrhenius law, such that if $(t_f)_1$ and $(t_f)_2$ are the times to failure at temperatures T_1 and T_2 respectively then:

$$(t_f)_1 / (t_f)_2 = \exp(-\varepsilon_0/kT_1) / \exp(-\varepsilon_0/kT_2) \qquad [3.3]$$

where ε_0 is the activation energy term. The problem with this equation in trying to predict the shift in the $\log\sigma$ / $\log t_f$ curves is that it implies that the failure is a process which is controlled by the activation energy term.

However, the absence of a term dependant on stress in the above equation implies that this is not a stress activated process. This of course is not true and the equation needs to include a stress related variable to predict more accurately stress rupture behaviour.

3.2.3 ACTIVATED RATE PROCESS

The theory of activated rate process was initially applied to the prediction of creep rupture strength by Zhurkov and his colleagues [10] , although the theoretical foundation was developed by Eyring et al [12]. Coleman assumed the activated complexes pass over an energy barrier [13]. This approach led to:

$$d_n/d_t = (kT/h) \exp (-E_0/kT) \exp (\beta\sigma/2kT) \qquad [3.4]$$

where d_n/d_t is the number of activated complexes passing over an energy barrier in unit time, E_0 and β are the activation energy and the activation volume of the process which leads to failure, h and k are Plank's and Boltzmann's constants respectively, σ is the local stress and T is the absolute temperature. From this Coleman [13] showed that by assuming a local critical strain he could derive an expression for the time to failure (t_f) under creep rupture conditions of the form:

$$t_f = (Nh/kT) \exp (E_0/kT) \exp (-\beta\sigma/2kT) \qquad [3.5]$$

where N is a constant. Taking logs of both sides and transposing gives the form:

$$\sigma = 2kT/\beta (\ln N - \ln kT/h + E_0/kT) - (2kT/\beta) \ln t_f \qquad [3.6]$$

The equation implies a linear stress-log (time to failure) relationship with a slope of $2kT/\beta$. Equation [3.6] can be written in the general form:

$$\sigma_1 = A - B\,T \ln t_f \qquad [3.7]$$

where σ_1 = wall stress, and A and B are constants. Zhurkov [10] and Bartenev and Zuyev [63] have applied this equation to 50 organic and inorganic materials and found B to be independent of temperature and β to be constant. However Cherry and Holmes [64], McGinley [65] and Kubat et al [66] have shown that β not only varies with temperature but even stress.

Bragaw [67] has utilized the modified Coleman equation to form the Rate Process Method. This method is currently being added to the current rating method ASTM D 2837. The general form of the equations relating to ductile and brittle failure deviate from the linear stress/log failure time relationships and take on the modified form of:

$$\log \sigma = A_1 - B_1\,T - C_1\,T \log t_f \qquad [3.8]$$

where A_1, B_1, C_1, are constants. The equations have been found to be suitable for a wide range of polyethylene resins. However the tougher grades currently on the market show anomalies to the method. Ayres [68] points this out when applying the method to some Phillips resins. Four areas were identified for future modification of the method:

(a) Equation to take into account expansion of the pipe during creep testing.

(b) The change in the material being tested due to antioxidant levels

being exhausted.

(c) Modification for chemical environments in the equation for buried ground environments.

(d) The need for more stress points from the method which would better define the slopes or change of slope.

The work by Ayres [68] does not invalidate the Rate Process Method; on the contrary the basic tests that were carried out validate the method. However the suggestions will have to be applied for the future predictions of polyethylenes resins far superior than some of the grades currently on the market.

3.3 DESCRIBING PIPE PERFORMANCE USING FRACTURE MECHANICS

Materials contain flaws such as inhomogeneities or voids from which cracks may initiate and propagate and thus lead to failure of the finished component. Under a given stress the risk of failure depends not only on crack size and notch tip radius but also decisively depends on the resistance shown by the material to crack propagation i.e. the energy required per unit of crack surface in material separation. If the material toughness is low and the stress and temperature high, the crack can propagate slowly through the wall of a pipe, with the risk of considerable damage. The raw material producers make considerable efforts to increase the safety allowances of their materials and have to use creep rupture tests under internal pressure to specify the quality of their materials. The test procedures are extensive and time consuming to characterize new materials. Therefore attempts have been made during the last few years to supplement, or to replace the creep rupture test on pipe by test methods

deriving from the fracture mechanics approach to characterize material strength [69,70].

Fracture mechanics seeks to establish a suitable parameter to characterize the fracture of a cracked body under load. In linear elastic fracture mechanics (LEFM) a single parameter K, the stress intensity factor, characterizes a material's resistance to crack growth. Increasing K gives a critical condition at which the crack will begin to grow. This case is referred to as the critical stress field intensity factor K_C, provided the plastic zone size adjacent to the crack tip is small compared to the relevant specimen dimensions of crack length and width [71]. K_C is defined as:

$$K_C^2 = Y^2 \sigma^2 \pi a \qquad [3.9]$$

where σ is the gross applied stress, a, the crack size and Y the finite width correction factor. The Y factor is a dimensionless number and is dependant on the geometry and mode of loading. The Y factors have been measured or calculated for many test geometries and are available in the literature [72].

3.3.1 SLOW STABLE CRACK GROWTH IN POLYETHYLENE MATERIALS

Slow crack propagation in polymers is of considerable practical importance since it occurs at low stresses and is seen to be the major cause of long term failures in polyethylene pipes. The presence of active environments can promote this process with crack growth occurring at even lower stresses. In many cases of long-term failures, crack growth initiates from an inherent flaw in the material and extends as a single macroscopic crack until final failure. For a test specimen subject to constant load, the whole process from

the application of the load to ultimate failure can be broadly divided into four different stages [71] illustrated in Figure 3.1 .

(a) An incubation period from the application of the load to the initiation of crack growth.
(b) A period of unsteady crack growth following crack initiation (this is manifested by non-unique critical stress intensity/crack length (K_C-a) curves at different starting values of critical K).
(c) Crack growth which is characterized by a unique K_C-a curve (known as steady crack growth).
(d) Final instability.

The four stages are not separated and each stage contributes its proportion to the final failure time. However by using the concepts of fracture mechanics we will concentrate on the steady growth behaviour (Stage (c) of (Figure 3.1)).

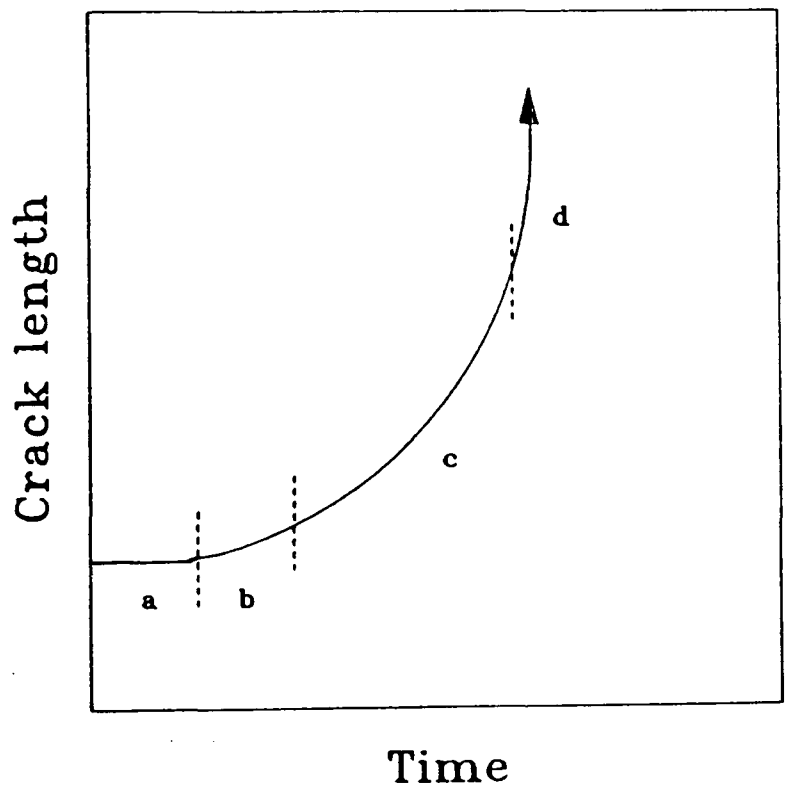

FIGURE 3.1: Crack length / time variation in a specimen under constant load.

3.3.2 PIPE PERFORMANCE PREDICTIONS USING FRACTURE MECHANICS

Fracture mechanics describes the propagation of cracks from pre-existent flaws and these concepts can be applied to polyethylene pipes for brittle failure.

Gray et al [73] applied fracture mechanics concepts to the case of slow stable crack growth in polyethylene pipe materials and found that the rate of crack growth d_a/d_t could be given by the power law relation:

$$d_a / d_t = D\, K_c^m \qquad [3.10]$$

where D and m are material constants and K_c is the critical stress intensity factor at the tip of the growing track and is given by:

$$K_c = Y \sigma (\pi a)^{1/2} \qquad [3.11]$$

where Y is a geometrical correction factor, a is the crack length and σ is the applied stress. The propagation time required for a flaw to grow through the pipe wall can be derived by integrating between the initial and final values of K_c, and substituting for K_c to yield:

$$t = (2/Y^2\pi\sigma^2)\, [D(2-m)]^{-1}\, [K_c^{(2-m)}_{final} - K_c^{(2-m)}_{initial}] \qquad [3.12]$$

The above equation can be modelled to include the influence of flaw size by integrating between the initial flaw size a_0 and the pipe wall thickness w to obtain:

$$t = 2/2\text{-}m\ [\ w^{1-(m/2)} - a_0^{1-(m/2)}\ ]\ [D(Y.\sigma^{1/2})\text{-}m] \qquad [3.14]$$

Assuming that equation [3.14] is obeyed by the material, then the lifetime of the pipe is dependant upon the initial defect size. It also implies that the initial crack growth dominates the lifetime of the pipe.

Gray et al [73] applied this work to BP Chemicals Ltd Rigidex HDPE 006-60 processed into pipes and found the equation evaluated a lower and upper bound region of flaw sizes between 10 and 100 μm . This region hence described the distribution of pipe failures within that range (Figure 3.2).

Although this model behaved reasonably for a low toughness HDPE a much tougher material such as BP Chemicals Rigidex MDPE 002-40, could not be described by the simple power law relation (Figure 3.3). However, the authors stress that a modification of the treatment to include plastic flow at the crack tip would rectify any difficulties [73].

Nevertheless the model proposed by Gray et al [73] does not include an incubation period, a period spent initiating the growth of cracks. Bragaw [67] illustrates this incubation period with MDPE pipe systems. From his analysis on the systems he casts doubt on the fracture mechanics approach without considering the incubation period. Gray et al [73] however illustrate that their model fits experimental work on standard pipe manufactured from the non-pipe grade resin Rigidex 006-60, which they say has an insignificant incubation period. Birch et al [74] stress that this could be the case if tests were conducted on thin samples. Their work and several other workers [71,75] show that sample thickness has an effect on the stress intensity factor K_C. It is also noted that Gray et al [73] determined the

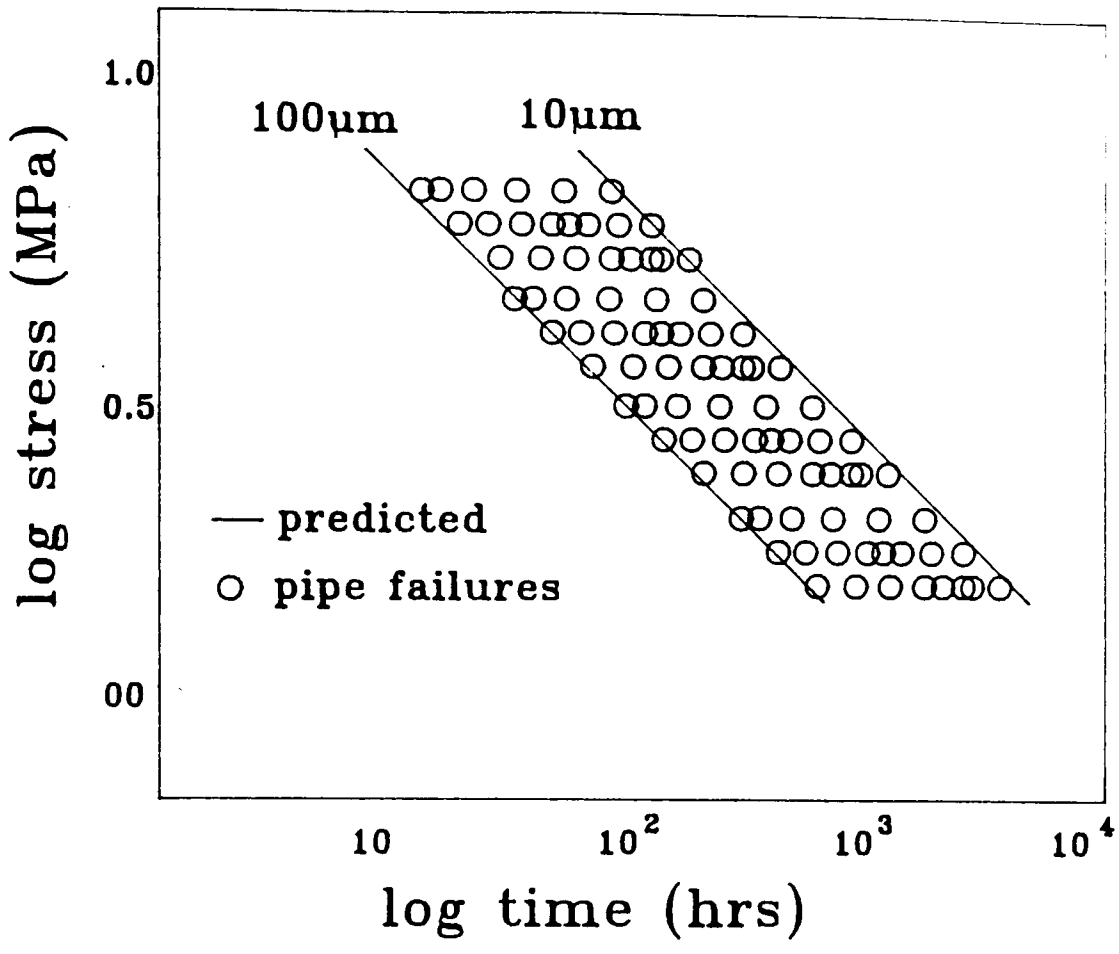

FIGURE 3.2: Fracture mechanics prediction of the lifetime of pipes made from Rigidex 006-60 showing upper and lower bound defect size predictions [73].

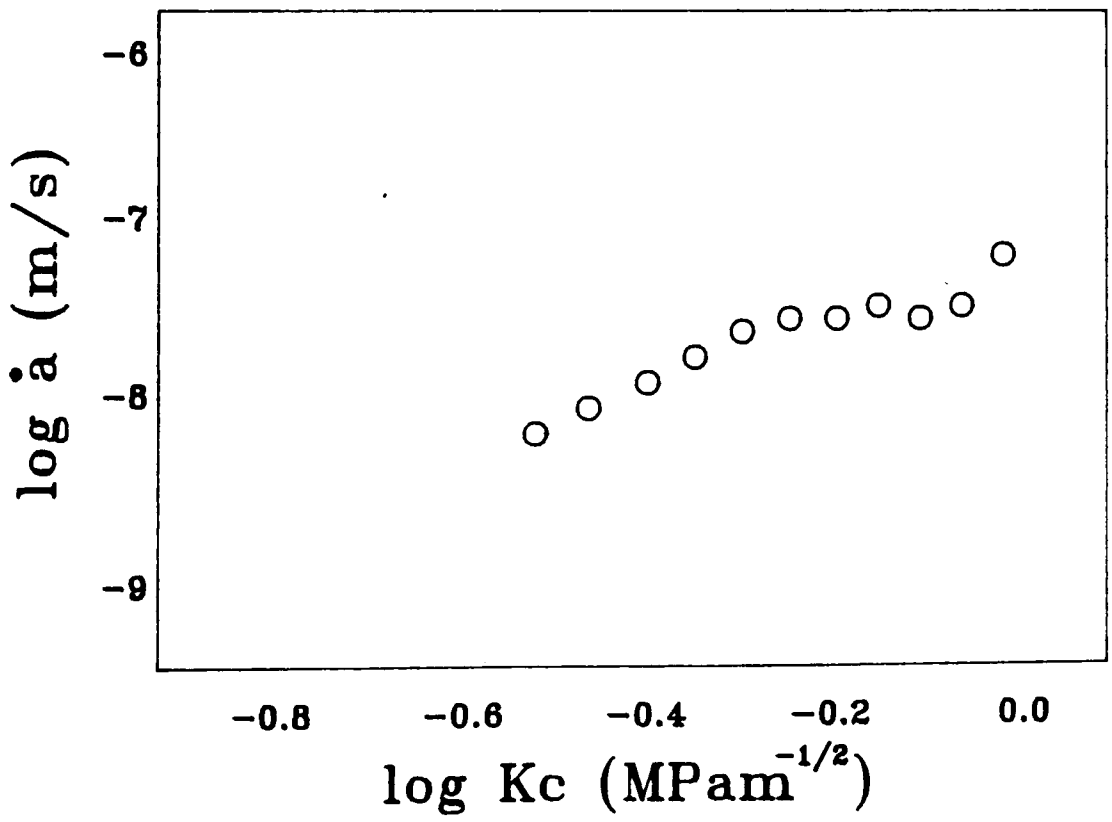

FIGURE 3.3: Crack growth / K_c curve for Rigidex MDPE 002-40 [75]

kinetics of slow crack growth using a single edge notch (SEN) specimens in uniaxial tension, a method that for polyethylene has been shown to unreliable by Chan and Williams [71,75] due to localized stresses from the test. Chan and Williams and Birch et al [74,75] have shown that SEN three point bend specimens can give stable crack growth at room temperature for HDPE but not for the tougher pipe grades (e.g 002-40).

For fracture mechanics to be used as a predictive technique a more rigorous analysis involving theoretical and/or practical measurements of the full initiation growth and crack growth phase is necessary. However it is relevant to indicate that the work referred to is of great use and points the way to further study.

3.4 FACTORS CONTROLLING PIPE PERFORMANCE

We have identified several ways in which polyethylene pipe materials can be evaluated in regards to their long term performance. However laboratory predictions and stress rupture curves on pipes are not always equivalent to production made pipes. The implications for adequate design are that additional factors have to be considered for the installations to be viable. This section will highlight principal factors which affect polyethylene pipe performance.

3.4.1 MOLECULAR WEIGHT

It has been found from early work by Niklas [76] and Gaube [77] that the average molecular weight or molar mass of a given density or structure of the polyethylene has a decisive influence on the brittle-mode rupture strength, with increases in molecular weight shifting the brittle region to

longer times as illustrated in Figure 3.4. An interesting note from Figure 3.4 is that crosslinking the polymer practically eliminates the slow crack growth failure regime. Work at Studsvik [78] found this behaviour with their crosslinked polyethylene pipes, finding that their stress rupture results indicated an intersection of the third (Stage 3) region from the extension of the ductile region.

In explaining lifetime variations with molecular weight, Muller and Gaube [5] suggest that the longer chains in a high molecular weight material engenders more connecting points (interlooping with neighbouring molecules) per macromolecule than a low molecular weight product. They cite that the good stress rupture performance of the crosslinked polyethylene is due to increasing the connecting points (tie molecule concentration) in the amorphous region between lamellae.

3.4.2 DENSITY

Figure 3.5 illustrates how the position of *the low slope start* to the creep rupture curve of polyethylene pipes depends on density [5]. The inclines of the graphs are due to structural differences of the macromolecules in the shape of branchings. In fact Fleißner [79] has shown that the stress rupture behaviour is influenced more strongly by density (by adding short chain branches) than by molecular weight . He found that the additions of comonomers (butene or hexene) move the brittle region of the stress rupture curve to higher failure times. Hexene comonomers were found to produce better stress rupture behaviour than butene comonomers in the Stage 2 brittle region.

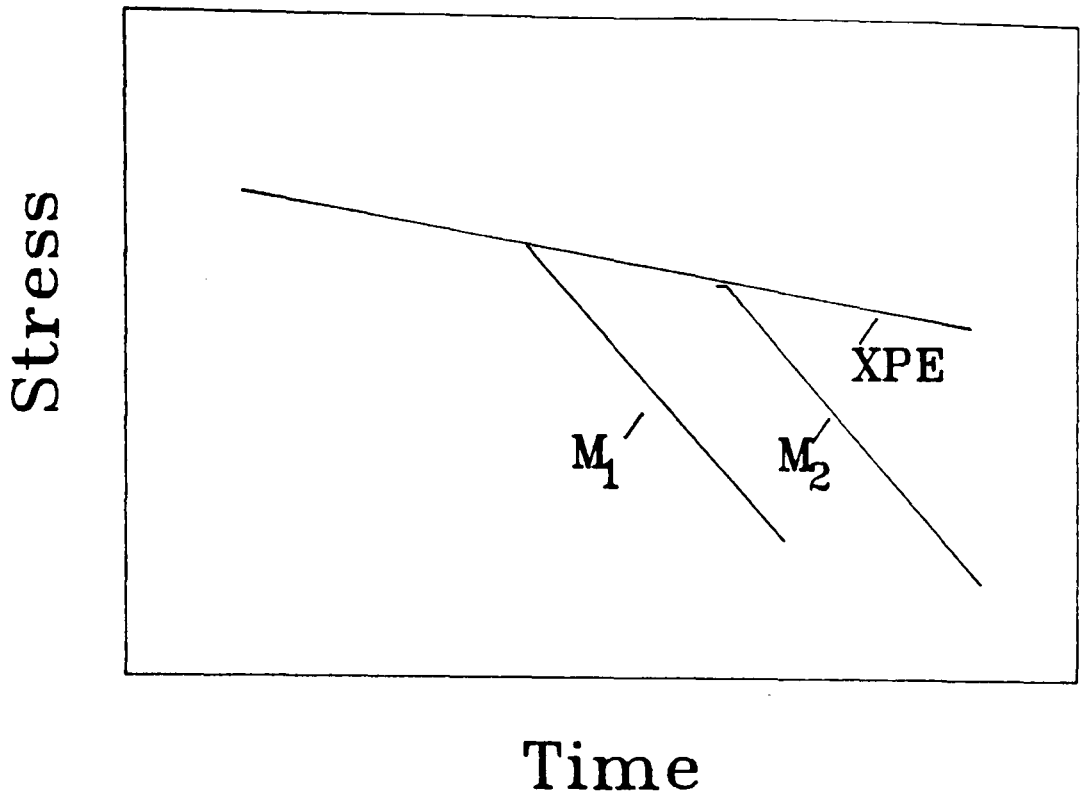

FIGURE 3.4: Molecular weight variations on the brittle region of the stress rupture curve [5].

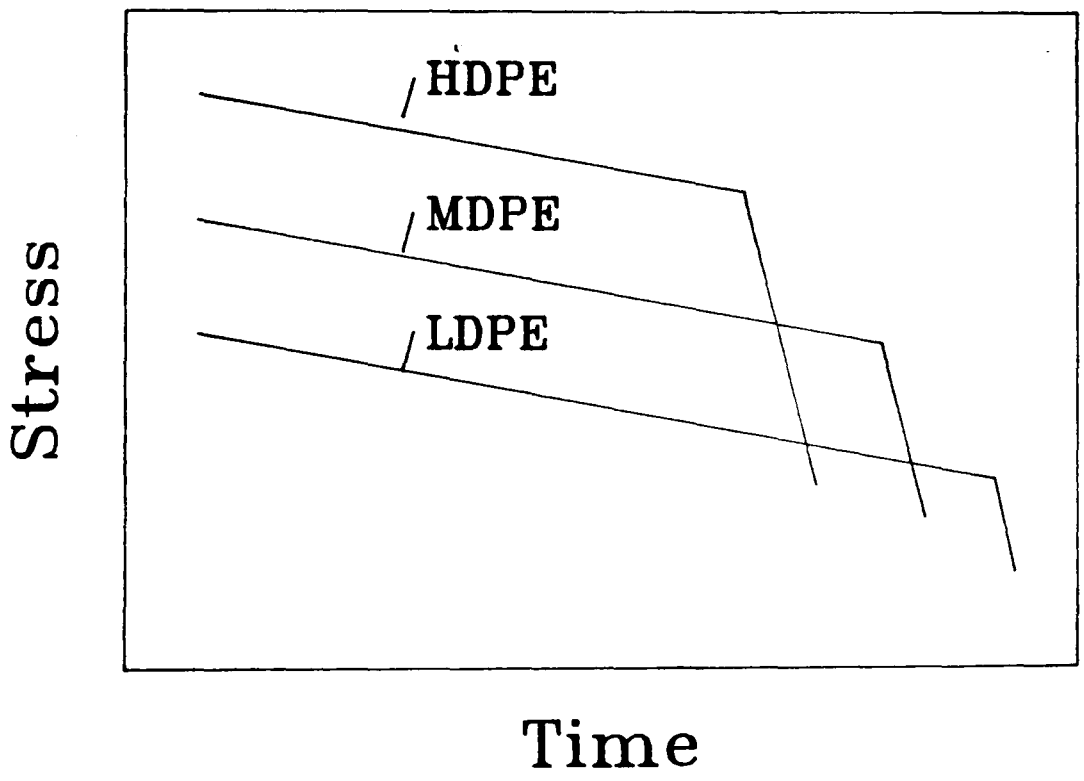

FIGURE 3.5: Density influences on the stress rupture curves (all curves at a single temperature) [5].

The influence of the type of branching and also its distribution along polymer chains on stress crack resistance have been investigated by Ishikawa et al [51] for polyethylene pipe materials. They identified that good stress rupture performance was obtained for materials which had a high degree of chain branching in the high molecular weight chains. This work illustrates that it is not only the length of the branching that may influence stress rupture behaviour but its distribution within the polymer that influences long term properties.

3.4.3 PROCESSING

It has been known for many years that processing can significantly influence the mechanical properties of a large number of polymers. However, in the case of polyethylene it is generally agreed by manufacturers that the polymer is less sensitive to processing than other polymers processed into pipe such as polyvinyl chloride. Marshall et al [80] have come to a similar conclusion on their work with MDPE pressure pipes. They attempted using high temperature stress rupture testing (80^{o}C) and fracture tests to identify if processing variations influenced pipe performance and found minimal variations.

Other authors such as Gebler et al [14] found that extrusion speed influenced pipe performance, too high a speed and the quality of pipe declined as well as a decrease in lifetime ; too slow a speed and thermo-mechanical damage was evident when the pipe was inspected. Edwards et al [81] have found that if the line speed is reduced then cooling of the pipe is more effective, minimizing residual stresses in the component.

IngenHousz [82] has shown that internally cooling the inside of the pipe from the extrusion process changes the stress in the pipe giving a compressive stress in the inside as well as the outside of the pipe. The tensile stresses are moved to the middle of the pipe and oxidative and thermal degradation of the material on the inside pipe reduced. Highly crystalline materials have been shown to have very coarse spherulitic structures at the inner surface of large diameter production pipes, which is said to be due to oxidation of the bore [14,83,84]. This region has been identified as a low molecular weight material and is thought to influence the crack propagation characteristics of the pipe [85].

3.4.4 ENVIRONMENTAL STRESS CRACKING

Polyethylenes on the whole possess good resistance to chemicals. However under the simultaneous conditions of stress and certain chemical media failure can occur in a relatively short time. This phenomenon is referred to as environmental stress cracking (ESC).

The mechanism of ESC in polymers has been a point of contention for many years where two questions surface. How much ESC is due to plasticization of the material and how much is caused by a reduction in surface energy.

Hannon [85] suggests that brittle failure in polyethylene was due to nucleation and growth of voids followed by craze formation and breakdown. Brown [86] however points out that ESC is due to stress induced swelling and plasticization of the amorphous regions in the stressed polymer.

Diedrich et al [87] found that natural gas as well as the presence of alkanes in the vapour phase (methane and ethane) do not adversely affect

polyethylene pipe stress rupture performance but the higher hydrocarbons (propane, butane, heptane etc) have a greater influence on lifetime . They developed a resistance factor in their safety design calculation for polyethylene pipe. Wolters [88] has pointed out that liquid gas condensate does have a significant effect on the properties of the pipe resulting in a softening and weakening of the material and reduction in service life.

3.5 FAILURE MECHANISMS AND FRACTOGRAPHY

Figure 3.6 illustrates the general stress rupture curve exhibited by polyethylene pipe materials. From the Stage 1 region ductile fracture is observed and its principal features are the typical parrot beak failure where extensive yielding is clearly visible (Figure 3.6 (a)). At low stresses (Stage 2) brittle fracture occurs by the process of slow crack growth which involves the formation of a craze, craze breakdown and slow crack propagation . Macroscopically the fracture surface of this region shows that the extent of deformation is negligible with the region being macroscopically flat. However at high magnification this region is not flat but consists of locally drawn material that has undergone extensive microductility (Figure 3.7). This rough region shows river markings which are lines of roughness elongated in the direction of crack propagation. The increase in roughness can be attributed with an increase in crack velocity [89,90] .

During manufacture, transportation and installation, it is possible that defects may be introduced into the pipe. Various authors have identified brittle failure from field pipes as being initiated from defects [91,92]. Erickson and Ifwarsson [91] have identified three main areas where fracture initiation takes place.

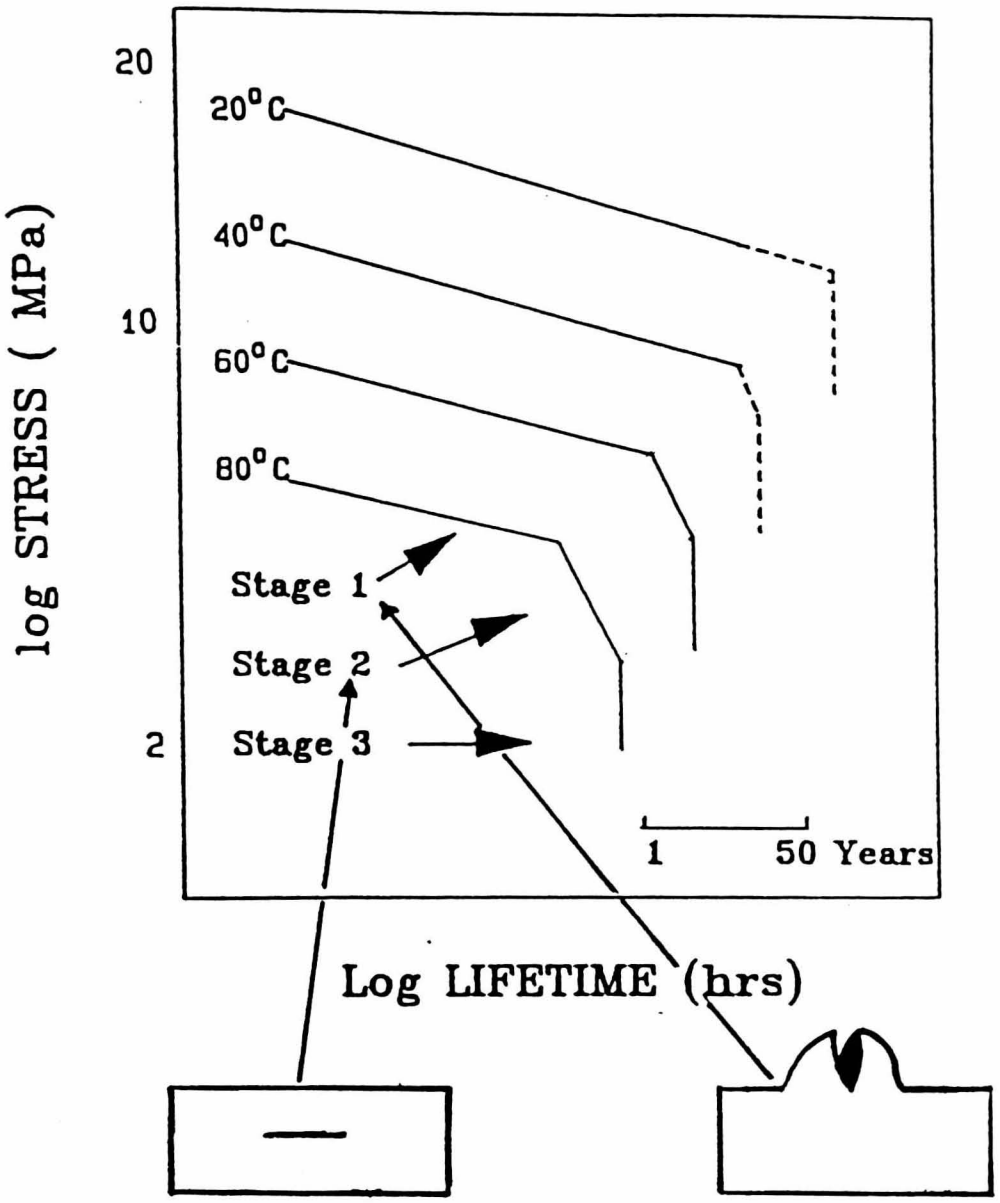

FIGURE 3.6: Typical fracture features from the stress rupture testing of polyethylene pipes.

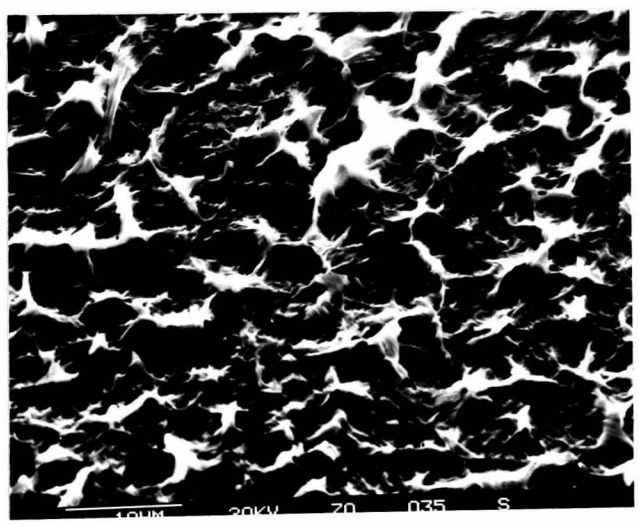

FIGURE 3.7: Typical britle fracture surface of a polyethylene pipe sample showing slow crack growth characteristics.

i) Initiation at particles or pores.

ii) Initiation on the inside in areas without a fibril.

iii) Initiation in degraded areas known as spiders .

They found i) to be in the transition area of Stage 1 and 2, ii) to be predominantly in Stage 2 and iii) in Stage 3 where chemical degradation of the material produces these voided spider regions.

The fibrous nature of the surface of brittle fracture has been an indication of the materials behaviour under slow crack growth. Lee and Epstein [93] observed that tougher polyethylene materials had fibre heights on the brittle fracture surface greater than other polyethylene grades. They assumed that crack growth resistance is related to the work in forming the fibrous texture and hence its height. Lustiger and Markham [94] have investigated this fracture behaviour and postulated that resistance to slow crack growth was due to the number of entangled tie molecules in the amorphous regions of the polymer. They suggested that materials with a significant low molecular weight fraction or short chain branch length (1-butene compared to 1-hexene) would exhibit lower slow crack resistance than high molecular weight, high branch length polymers.

3.6 BLENDING TO IMPROVE THE PERFORMANCE OF PE PIPE

The use of blending materials in pipe production is already a common art. Masterbatches are added to the virgin polymer to produce the desired coloured and stabilized pipe product. Some masterbatches have a low molecular weight carrier to help the additives distribute themselves into the polymer. Standards exist to ensure that good blending takes place from the mixing of the masterbatch into the virgin polymer [4].

Chapter 2 has shown how the blending of two PE grades could impart favourable mechanical properties to blown films. With the advent of increasing prices it should be thought that a similar approach would be made in the pipe production area.

In the literature only Dumoulin et al [42] have attempted to assess the viability of blending for pipe production. They attempted to incorporate ultra high molecular weight polyethylene into a MDPE pipe grade to try and impart the good toughness properties of UHMWPE to MDPE, whilst utilizing the easy processing properties of MDPE. They found difficulties in getting any level of blending due to poor mixing of the components . This was reflected in antagonistic mechanical behaviour. No stress rupture tests were carried out on the material.

The patent area appears to be the main source of information for the blending of polyethylene materials into pipe with the Japanese leading the way.

Showa Denko company [95] used a blend of high pressure polyethylene (910-935 kg/m^3 , MFR up to 1.0 g/ 10 min and 97- 70 wt%). Other Japanese patents [96,97], utilize similar blending methods, finding that the combination of alpha-olefins and high molecular weight resin can influence mechanical properties and stress cracking of the material. Bailey and Whittle [52] also found that by mixing a high molecular weight ethylene copolymer (ρ, 930-940 kg/m^3) and a low molecular weight homopolymer (essentially linear, ρ > 950 kg/m^3), good environmental stress cracking was obtained compared to conventional resins.

All the above patents however negate work related to stress rupture testing, citing good ESCR results for the applicability to pipe materials. Peter Lucchesi of Union Carbide [48] produced medium density blends from HDPE and LDPE materials. He found that the best compositions composed of a 70 wt% high molecular weight HDPE and a 30 wt% low molecular weight LDPE copolymer (1-butene). With this blend good burst stress rupture results were obtained. But it must be said that brittle stress rupture results were not obtained. We have already shown in this chapter that the full stress rupture curve, especially the brittle region, which is indicative of field failures, needs to be fully evaluated before a new material can be utilized.

However a spin off from the work on the stress rupture behaviour of recycling polyethylene pipe by Sandilands and Bowman [98] identified that the addition of a manufacturers MDPE pipe grade to another manufacturers pipe material produced an increase in stress rupture performance in the brittle region. It is this area that we are looking to explore in this thesis and hence try to understand the factors governing pipe performance in the brittle region.

CHAPTER 4

EXPERIMENTAL

4.1 SELECTION OF MATERIALS

4.1.1 CONTROL MATERIAL

The polyethylene material used as a control for blending was a MDPE pipe grade containing octene as the comonomer. This pipe grade was pigmented yellow and contained stabilizers, antioxidants and other additives needed in the manufacturer and long term performance of the extruded article. Some of the physical properties of this material are displayed in Tables 4.1 and 4.2 .

4.1.2 ADDITIVE MATERIALS

To the control resin a number of polyethylene materials were added. Three HDPE materials were chosen, primarily to identify the influence of the molecular weight of the second material on the performance of blends produced with the control material. These HDPE grades contained no pigments but a small amount of stabilizer sufficient for primary processing. Of these materials HDPE-B is the code for for an injection moulding grade with a low molecular weight. HDPE-F is an extrusion grade with a similar molecular weight value to the control material, and HDPE-M is a blow

	DENSITY (kg/m3)	MFR (g/10min)	MMI (%)	M_w x10⁴	M_n x10⁴	M_z x10⁴	M_w/M_n
MDPE-A	937.8	2.75	28.3	11.8	1.48	53.4	7.97
HDPE-B	949.2	26.2	14.5	5.94	1.12	19.3	14.5
HDPE-F	953.8	1.45	31.7	12.1	1.75	43.5	6.91
HDPE-M	944.8	0.14	17.9	23.5	1.32	109.0	17.8
MDPE-P	937.8	0.67	41.2	17.0	0.97	89.5	17.5
MDPE-D	936.2	2.98	25.1	10.4	1.32	42.3	7.87

i) Density determined in a gradient column on compression moulded sheets.
ii) Melt Flow Rate (MFR) and Melt Memory Index (MMI) values at 190°C and 5kg load.
ii) Molecular weight and values from RAPRA Technology Ltd. (Section 4.2.5).

TABLE 4.1: Selected structural properties of Polyethylenes used in the blending trials.

	VISCOSITY (MPas)	O.I.T (oC)	T_c (oC)	T_m (oC)	Ten' Stress (MPa)	Ten' Modulus (MPa)
MDPE-A	1574.3	28.2	114.35	119.03	13.85	553.5
HDPE-B	452.2	7.0	116.87	121.75	21.73	1054.5
HDPE-F	1841.5	5.2	119.20	124.8	24.58	1388.5
HDPE-M	1948.8	0.5	118.64	120.47	20.22	877.9
MDPE-P	1474.3	>30.0	115.95	116.41	-	-
MDPE-D	1799.4	>30.0	114.95	120.17	-	-

i) Viscosity at a temperature of 190oC and a shear rate of $100s^{-1}$.
ii) Oxidation Induction Time (O.I.T) and melting and crystallization values from the Differential Scanning Calorimeter. (Section 4.2.7).
ii) Tensile stress and modulus values from compression moulded sheets at a strain rate of 100mm/min.

TABLE 4.2: Selected structural properties of Polyethylenes used in the blending trials.

moulding grade which has a molecular weight value greater than the base resin and has a density lower than the other HDPE materials. All three polyethylene materials had hexene as a comonomer in their synthesis to produce short chain branching.

Two further polyethylene grades were blended with the control material during this programme of work. Both were MDPE pipe grade resins. They were chosen to establish whether there were any differences from adding pipe grade and non-pipe grade resins to the control material, in terms of the performance of pipe produced from the blends.

Both medium density grades were non-pigmented, with one supplied already stabilized, the second requiring a stabilizer package. Properties of all the additives discussed are compared with the base resin in Tables 4.1 and 4.2. It can be seen that of the two pipe grades, MDPE-D has very similar properties to the control material, including comonomer type, density and melt flow rate. The MDPE-P resin has a high molecular weight (M_W and M_Z) compared to the control material, and also differs in the comonomer type.

4.2 MATERIALS CHARACTERIZATION

This section describes the characterization techniques used in producing the data of Tables 4.1 and 4.2, and on the samples produced from blending these materials into pipe.

4.2.1 SAMPLE PREPERATION - COMPRESSION MOULDING

The use of compression moulded sheets provided samples for density,

Dynamic Mechanical Analysis (DMTA) and Differential Scanning Calorimetry (DSC) work.

The pellets of material were placed into a mould to produce a 300x300x3mm plaque. The mould was placed into a Moore compression moulder, with compression faces set at 180°C, and left for 4 minutes without applied pressure. 40kN clamping force was then applied to the plaque causing the pellets to conform to the shape of the mould. This clamping force was maintained for a further 3 minutes after which the mould was removed and transferred to a second compression moulder whose mould faces were water cooled to room temperature (20°C). A 40kN clamping force was applied during cooling before the sample was removed.

4.2.2 DENSITY

The density gradient column technique is frequently employed as a rapid means of accurately determining the densities of plastics. The apparatus consists of a column which contains a liquid whose density increases uniformly from the top to the bottom of the tube. The entire tube is surrounded by a constant temperature water jacket which is kept at 20°C. Samples approximately 7x7x3mm were cut from compression moulded sheets and placed into the column to determine their densities.

The density gradient column was prepared in accordance to ASTM D505 method B using a propan-2-ol water mixture having a density range of 930.0 to 970.0 kg/m^3 at 20°C.

4.2.3 BRANCHING AND BRANCH DISTRIBUTION DETERMINATION

The physical and mechanical properties of polyethylene are dependant not only on the type of branches but also on comonomer distribution within the molecular weight spectrum. This area of work was undertaken by technicians at the Conaco Research and Development Laboratories, Ponca City, Oklahoma, USA and is an adaption of the work undertaken by Ishikawa et al [51].

The work by Ishikawa et al [51] involved the fractionation of the polymer into several molecular weight fractions using mixtures of good and poor solvents. These fractions were passed through a GPC instrument for molecular weight determination. Each fraction was then characterized for comonomer type and degree of branching using ^{13}C NMR. A schematic diagram in Figure 4.1 summarizes these steps.

4.2.4 MELT FLOW RATE (MFR) AND MELT MEMORY INDEX (MMI) DETERMINATION

The MFR of a thermoplastic (units of g/10min) is usually the measured gravimetric flow rate of the sample melt expressed through a die using a defined weight acting on the melt which is maintained at a set temperature. MFR is generally regarded as an indicator of molar mass with the low rate indicative of a high molar mass.

This method was carried out to ASTM D1238-79 (condition E) at 190°C with a 5kg load using a Davenport Melt Indexer 3/80. Pellets from the materials were used for the te extruded through a die with a diameter of

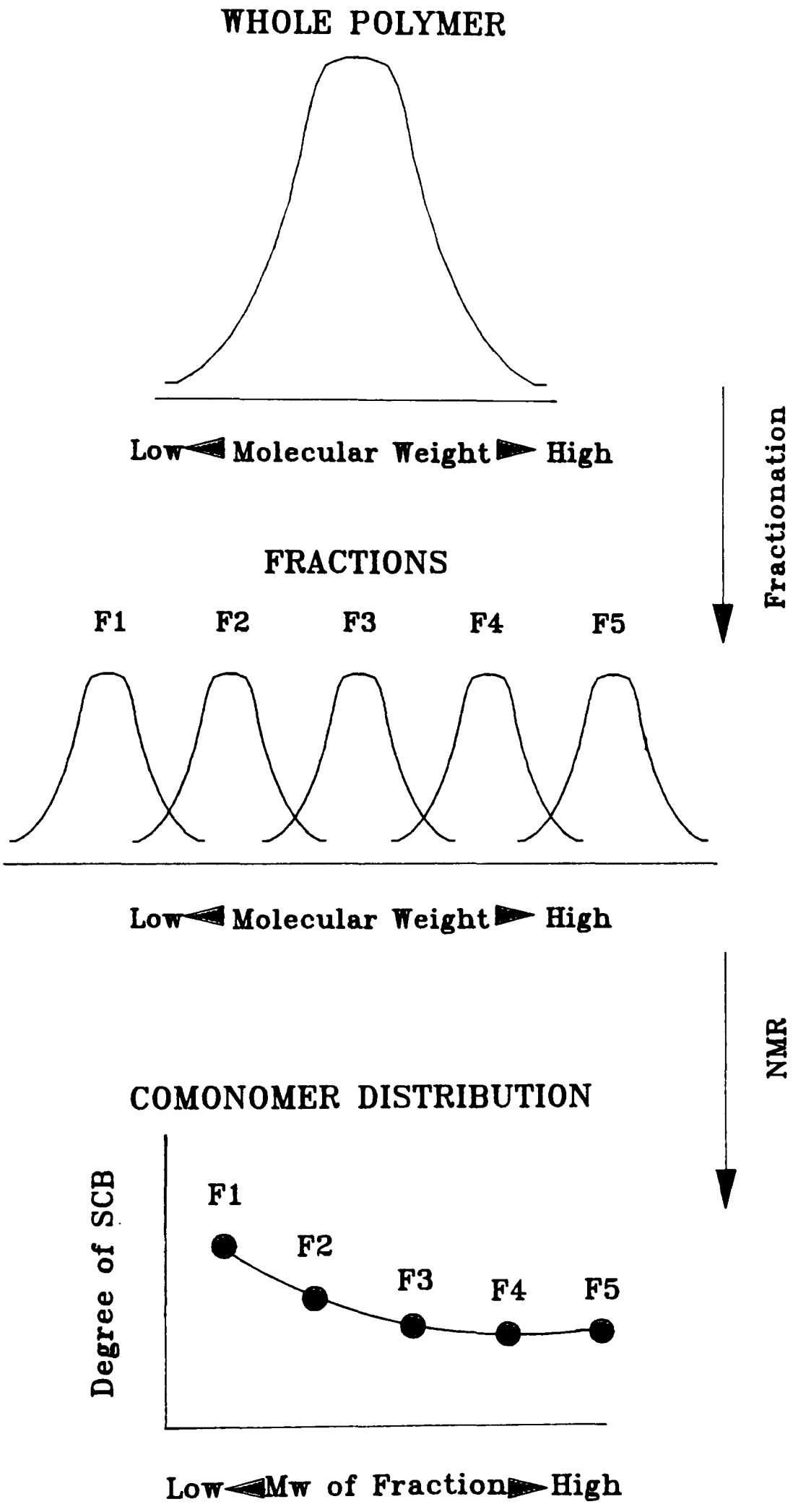

FIGURE 4.1: Summarization of the steps involved in the branching distribution method.

2.095mm.

Melt memory index (MMI) or, more precisely, the extrudate swell of the melt flowing out of the die of the melt indexer is widely used in the plastics industry as a quick indication of melt elasticity. This parameter is measured with the extrudate from the MFR in the Davenport melt indexer under the same experimental conditions. Melt memory index is calculated from the following equation and is expressed in percent .

$$\text{Melt Memory Index (MMI)} = [(\, d_e - d_d \,) / d_d \,] \times 100\% \qquad [4.1]$$

where: d_e= Diameter of the extrudate (mm).

d_d= Diameter of the die = 2.09mm

All extrudate specimens were cooled in air and the average diameter for all the specimens recorded.

4.2.5 MOLECULAR WEIGHT DETERMINATION

Gel permeation chromatography (GPC) is a rapid efficient and reliable method of assessing molecular mass distribution. The principle of the technique involves a solution of the polymer being injected into a column of porous gel beads. During the flow of the solution down the column, larger molecules spend less time within the porous gel and are elluted first whereas small molecules are retarded and are elluted last. Analysis of the solution using refractive index or low angle light scattering reveals a distribution of the molar mass.

This procedure was carried out by the Rubber and Plastic Research

Association (RAPRA) using Waters Associates ALC/GPC-501/502 equipment. Pellets of the materials or pipe samples were sent for analysis using this technique.

4.2.6 RHEOLOGICAL BEHAVIOUR

A Davenport capillary rheometer was used to provide information about the shear flow behaviour of the polyethylene materials. The polymer sample (pellets) was placed in a heated barrel and extruded through a precisely dimensioned extrusion die. When the sample reached the desired test temperature, it was extruded through the die at a predetermined shear rate, by a power driven piston, the control forward speed of which could be accurately controlled. Material was forced through the die and the pressure drop in the capillary die was measured by a calibrated Dynisco pressure transducer whose sensing head was fitted at the end of the barrel and before the entry to the capillary. The pressure drop was recorded on a chart recorder. From the piston speed and the pressure drop corresponding thereto, shear rate, shear stress and viscosity could be calculated.

Four test temperatures were used, 170, 190, 210, 230°C. At each temperature for each material two dies were used to obtain the end correction factor for the calculations of shear stress. These dies had a length/diameter ratio (L/D) of 25:2 and 40:2. The entry of the die was at an angle of 180^{o}. The barrel diameter was 19mm.

The derivation of the Poiseuille law for capillary flow is available in standard text books [106] and yields:

$$Q = (\pi R^4 \Delta P) / (8 \mu L) \qquad [4.2]$$

where: Q = The volumetric flow rate (m^3/s)

ΔP = Pressure drop (Pa)

R = Capillary radius (m)

L = Capillary length (m)

μ = Viscosity (Pas)

For Newtonian behaviour the wall shear stress and wall shear rate are given by the following equations:

$$\tau_w = (\Delta P \, R) / (2 \, L) \qquad [4.3]$$

$$\gamma = (4 \, Q) / (\pi \, R^3) \qquad [4.4]$$

where: τ_w = Wall shear stress

γ = Wall shear rate

ΔP, R, L, Q = as defined above

Rearranging equation 4.2 gives:

$$(\Delta P \, R) / (2 \, L \, \mu) = (4 \, Q) / (\pi \, R^3)$$

Therefore : $\tau_w / \mu = \gamma$ [4.5]

$$\mu = \tau_w / \gamma \qquad [4.6]$$

This equation only applies for Newtonian behaviour. However for non-newtonian behaviour (in the case of polymer melts) correction factors have

to be applied to account for non-uniform flow of the material within the capillary and die regions. Two corrections were applied, one for the shear stress, the other for the shear rate. For the shear stress Brydson [100] has adapted the Bagley correction to account for only two dies. The dies have different L/R ratios designated below as a_1 and a_2 . For each die the true shear stress at the wall is given by:

$$\tau_W = P_1 / [\, 2\,(a_1 + n\,)] \qquad [4.7]$$

$$\tau_W = P_2 / [\, 2\,(a_2 + n\,)] \qquad [4.8]$$

If the pressure values, P_1 and P_2 are at a common value of wall shear rate (or apparent wall shear rate $4Q/\pi R^3$), the two equations will be equal and hence the Bagley correction factor n for viscous drag at the entry of the die can be found from the equation:

$$n = (\, P_2\, a_1 - P_1\, a_2\,) / (\, P_1 - P_2\,) \qquad [4.9]$$

Modification of the shear rate as applied to polymer melts was carried out by using the Rabinowitsch-Mooney equation [100] :

$$\gamma_W = \gamma_{app}/4\, [\, 3 + (\, d\ln \gamma_{app} / d\ln \tau_W\,)\,] \qquad [4.10]$$

where: γ_W = True shear rate

γ_{app}= Apparent or Newtonian Shear rate

τ_W = True shear stress

By applying a graph of τ_W against γ_{app} the slope $d\ln \gamma_{app} / d\ln \tau_W$ could be calculated.

Appendices 9.1 to 9.6 display the values obtained from this test for all the materials used in this research programme. For an extruder a typical shear rate for the melt is approximately 100s-1 101 using equation [4.5]:

$$\tau_w / \gamma = \mu$$

$$\mu = \tau_w / 100 \qquad [4.11]$$

Therefore as the shear stress is known one can calculate the viscosity at that temperature. The viscosity values of these materials are displayed in Table 4.2 .

4.2.7 THERMAL ANALYSIS OF MATERIALS

Differential Scanning Calorimetry (DSC) is a technique which involves measuring the energy change due to a phase transformation or transition in polymers and other materials. Figure 4.2 is a schematic representation of the apparatus . Reference and sample pans are maintained at the same temperature, predetermined by the programme even during a thermal event. The amount of energy which has to be supplied to or withdrawn from the sample to maintain zero temperature differential between the sample and the reference is the experimental parameter displayed as the ordinate of the thermal analysis curve. This heat or energy flow is displayed in units of milli watts.

i) Crystallization Temperature.

The application of DSC to the polyethylene materials and various blends

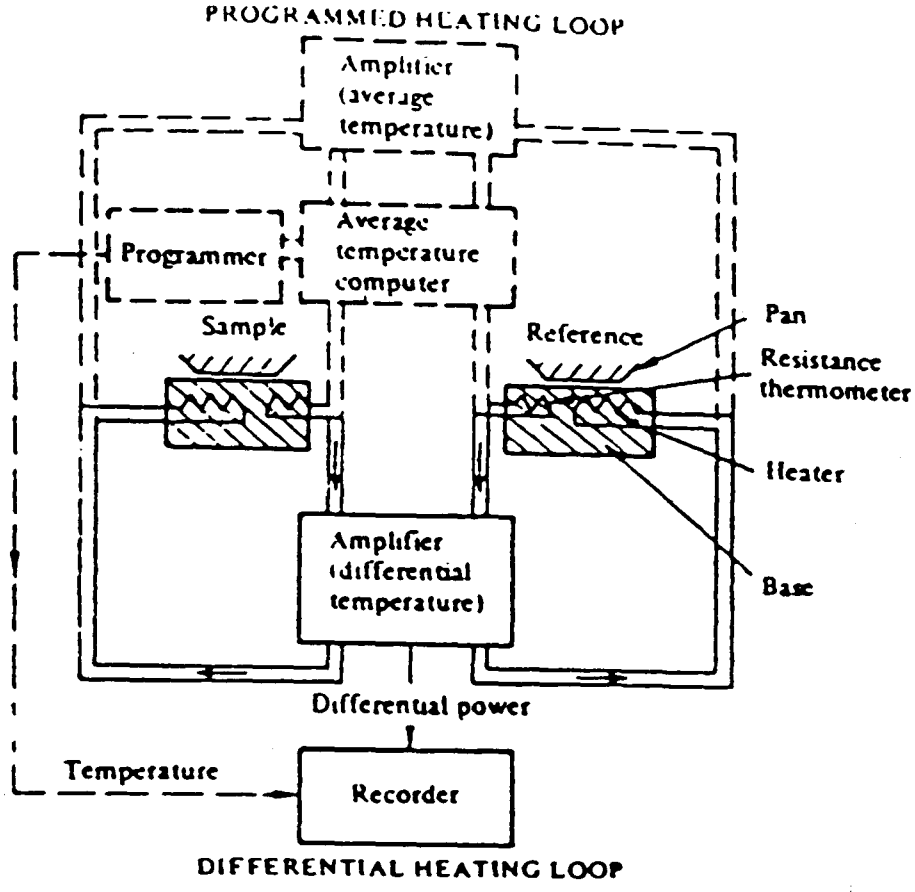

FIGURE 4.2: Schematic representation of the DSC apparatus.

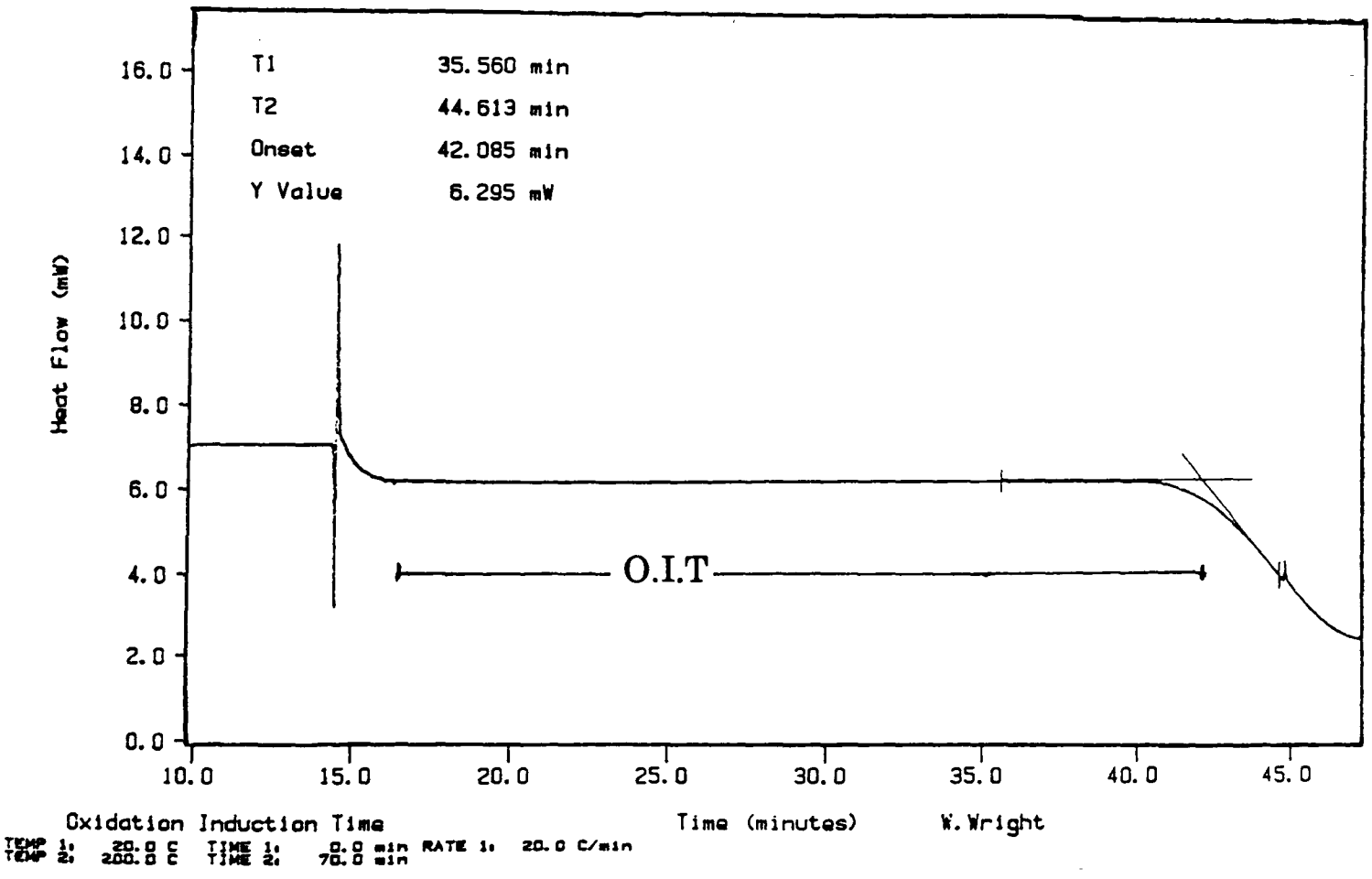

FIGURE 4.3: Typical oxidation induction time curve from the DSC.

identified the melting and crystallization of the materials. A sample (approximately 5-10mg) from a pellet was encapsulated in an aluminium pan and placed into a Perkin Elmer DSC 7 sample holder under a nitrogen atmosphere (flow rate 20ml/min). The sample was then heated from 20 to 170°C at a heating rate of 10°C/min and held there for 5 minutes to obtain thermal equilibrium. After this time it was then cooled at the same rate of 10°C/min to obtain the cooling exotherm. By now the sample would have lost the majority of its previous thermal history. It was then rerun to obtain the second heating endotherm; this endotherm was used for the onset of melting and heat of fusion values, whereas the exotherm was used for the onset of crystallization of the material.

ii) Oxidation Induction Time.

The oxidation induction time test is an indication of the thermal stability of the polymer compound due to the presence of an antioxidant package. The procedure described below is an adaption from the British Gas Standard PS/PL2: Part 1 Appendix D where a DSC was used instead of a Differential Thermal Analyzer (DTA) and the sample weights were between 5-10mg rather than the 15mg stipulated in the standard.

Samples 5-10mg in weight were taken from a compression moulded sheet or the internal bore of a pipe sample and placed in an open aluminium pan in the DSC. The sample was heated up at a rate of 20°C/min. After steady state conditions in nitrogen for 5 minutes at 200°C, a switch to a pure oxygen atmosphere was made. The thermal stability of the specimen as shown in Figure 4.3 is the time taken in minutes from the introduction of oxygen to the onset of the exotherm curve. The change in oxygen and nitrogen baselines (as shown in Figure 4.3) reflects the differences in the

thermal conductivity of the two gases.

iii) Dynamic Mechanical Thermal Analysis

Relaxation spectrometry of polyethylene blends is also a routine technique for localizing the molecular and supermolecular motions on the energetic (temperature and/or frequency) scale. Using Dynamic Mechanical Thermal Analysis (DMTA), relaxation spectrometry of polyethylene blends have been employed in studying compatibility, blend structure and blend ratios [40].

A Polymer Laboratories DMTA was used to evaluate the loss modulus and the tanδ of the sample. Samples from a compression plaque, (of dimensions 25x7x2mm) were placed into a 3 point bend jig and enclosed in a chamber which was set to decrease to -150°C. The frequency of the oscillation was 3Hz and the strain of the sample set to x4. By increasing the temperature at 10°C/min intervals using the conditions identified above the log modulus and tanδ values were displayed against temperature on a computer screen and the data stored on computer disk.

4.2.8 MECHANICAL PROPERTIES OF MATERIALS

i) Tensile Tests

Tensile properties (yield strength and tensile modulus) were determined according to BS 2782: Part 3: Method 320C using an Instron model 1195 tester. Tensile specimens from compression moulded sheets were machined from a rectangular blank which was traversed by a high speed router-cutter guided by a shaped template. Tensile tests were carried out at a crosshead speed of 500mm/min at 21°C. A minimum of 3 specimens were tested and

the average of the tensile strength and modulus displayed. For the materials used in this research programme, yield stress and modulus values are illustrated in Table 4.2 .

ii) Impact Tests

The samples were prepared from compression moulded plaques of 6.9mm thickness. Specimens were cut parallel and perpendicular from it. Notched samples with dimensions of 80x10x6.9mm were placed into a Ceast charpy impact tester with a 2J energy pendulum. The notch was formed using a Blacks equipment notcher which produced a notch of root radius 0.25mm with an included angle of 45º and a depth 20% of the width.

The test was carried out to BS2782: Part 3:Method 359 at room temperature. The energy per unit area of an impact sample is known as its Impact Energy, its units are J/m^2:

$$E_i = E / (l \times l_n) \qquad [4.12]$$

where E_i = Impact energy (J/m^2)

E = Energy value indicated by Pendulum (J)

l = Thickness of sample (m)

l_n = Width at notch (m)

= width - notch depth

4.3 PRODUCTION OF BLENDED PIPE

The production of blended pipe involved several areas of research. Initially the work involved the investigation of precompounding the blends using a

co-rotating twin screw extruder before extrusion into pipe, as compared with simply hand mixing the blends prior to extrusion. For this line of work the HDPE-F material was used with the control material to produce blended pipe. The second area involved looking at the influence of molecular weight on pipe performance. Selected addition levels of HDPE-B and HDPE-M materials were added to the control material to give blended pipe which could be compared with the blends using HDPE-F as the additive material. These two areas of research were for 32mm pipe, produced using a Rheiffenhauser S45 40mm single screw extruder.

The final area of research involved the use of pipe grade resins as blending additives and their influence on pipe performance; MDPE-D and MDPE-P material were utilized in producing blended pipe. Further batches of HDPE-B and HDPE-M at an expanded range of weight additions were also produced, supplementing the 32mm pipe work. 55mm diameter pipe produced from this line of research involved the use of a Betol Model 5025, 50mm single screw extruder.

In all the trials to produce pipe, efforts were maintained in producing pipe conforming to the British Gas standard PS/PL2: Part 1. The materials used and their additive levels to the control pipe grade resin in the production of 32mm and 55mm pipe are shown in Tables 4.3 and 4.4 .

4.3.1 PRECOMPOUNDING OF BLENDS

Twin screw compounding has been found to give better dispersion and temperature control over single screw extrusion and over melt mixing techniques **102**. For this work twin screw extrusion equipment of the intermeshing co-rotating type was used; the designated model TS40-DV-L

SAMPLE CODES FOR 32mm BLENDED PIPE WITH MDPE-A

	ADDITION LEVEL (wt%)			
BLEND RESIN	**0**	**2**	**10**	**20**
Uncompounded HDPE-F BLENDS	MDPE-A/32	HDPE-F/2	HDPE-F/10	HDPE-F/20
Compounded HDPE-F Blends	-	CHDPE-F/2	CHDPE-F/10	CHDPE-F/20
HDPE-B	MDPE-A/32	-	HDPE-B/10/32	-
HDPE-M	MDPE-A/32	-	HDPE-M/10/32	-

TABLE 4.3: Sample codes for 32mm pipe blends.

SAMPLE CODES FOR 55mm BLENDED PIPE WITH MDPE-A (wt%)

	ADDITION LEVEL (wt%)				
BLEND RESIN	**0**	**2**	**5**	**10**	**20**
HDPE-B	MDPE-A/55	HDPE-B/2	HDPE-B/5	HDPE-B/10	HDPE-B/20
HDPE-M	MDPE-A/55	HDPE-M/2	HDPE-M/5	HDPE-M/10	HDPE-M/20
MDPE-P	MDPE-A/55	MDPE-P/2	MDPE-P/5	MDPE-P/10	MDPE-P/20
MDPE-D	MDPE-A/55	MDPE-D/2	MDPE-D/5	MDPE-D/10	MDPE-P/20

TABLE 4.4: Sample codes for 55mm pipe blends.

manufactured by Betol Machinery of Luton, England. Screw and barrel assemblies were in the 17:1 L/D ratio. Temperature was monitored by thermocouples on each of the five barrel sections. A pellet strand head was used to produced strands which were taken through a water bath by a haul-off and pelletized in a strand pelletizer.

Samples were first hand blended according to weight percent and were approximately 7kg each in weight. Table 4.3 shows the addition levels of the HDPE-F material to the control pipe grade in this study. A low density blue masterbatch was added at the hopper to distinguish between batches. Conditions for producing the precompounded blends are shown in Appendix 9.7.

4.3.2 PRODUCTION OF 32mm PIPE

A Rheiffenhauser S45 single screw extruder was used to make nominal 32mm SDR11 pipe. The screw contained no mixing sections and had a L/D ratio of 24 : 1. A sizing die on the vacuum bath ensured uniform wall thickness. A screen pack of 254μm mesh was inserted at the interface between the extrusion die and the extruder, to filter extrenuous material that would act as initiation sites in the pipe under stress rupture testing conditions [73]. The pipe was extruded into a vacuum bath between a vacuum gauge value of 11.9 to 13.3x10^{-2}MPa and hauled off onto an automatic cutter, cutting the pipes into lengths of approximately 850mm. The lengths of pipe were then numbered so that the *beginning* and the *end* of a batch could be easily identified.

In the production of 32mm pipe blends, the control material was extruded first and the blends added in increasing weight addition. This enabled

extrusion conditions to be carefully monitored and corrected if any variation in pipe specification took place. The wall thickness was controlled to give nominal SDR11 pipe.

A schematic of the extrusion line for 32mm pipe production is illustrated in Appendix 9.8a) and the extrusion conditions displayed in Appendix 9.9 and 9.10 for the hand mixed blends.

4.3.3 PRODUCTION OF 55mm PIPE

The arrival of the new Betol 5025, 50mm single screw extruder enabled 55mm SDR 11 pipe to be produced. The screw was of a general purpose type with no mixing sections and a 25:1, L/D ratio. A screen pack of 170-430μm mesh was inserted at the breaker plater. The new extruder enabled conditions to be monitored more accurately than the Rheiffenhauser and pressure transducers were inserted at the die, breaker plate and the barrel zone to monitor melt pressure for the various blend additions. A melt temperature transducer was also inserted at the die to enable the temperature of the melt, before it leaves the die, to be accurately measured.

All the blends were hand mixed into 15kg batches and added to the hopper. It was easy to identify changes from one batch (blend) to another due to the pressure drop registered by the pressure transducers from a batch changeover. Each pipe was numbered sequentially so that variations within a batch/blend could be identified.

Due to the slow output rates of the extruder (1 metre of pipe every minute) it was difficult to have control over the wall thickness of the pipe by using the normal methods of increasing/decreasing the haul-off or screw speed.

Increasing the screw speed increased the shear on the material and increased the screw melt zone temperatures, while increasing the haul-off produced problems at the vacuum bath end in maintaining a steady vacuum. To overcome these wall thickness difficulties an oil/water solution was mixed and allowed to continuously flow over the molten polyethylene pipe before it entered the sizing die on the vacuum bath. This enabled the friction between the melt and the vacuum sizing die to be greatly reduced and produced a greater leeway for extrusion conditions to be altered. The oil was water soluble and mixed into a solution with water.

Pipe samples had their wall thicknesses and outside diameters regularly monitored during extrusion to give 55mm SDR11 pipe. Sample lengths were of the order of 1m. Extrusion conditions for all the blended pipe produced are summarized in Appendices 9.11 and 9.12. A schematic diagram of the extrusion layout is illustrated in Appendix 9.8b).

4.4 STRESS RUPTURE TESTING

All the pipe samples were stress rupture tested using an arrangement shown in Figure 4.4 . The test was carried out in accordance with ASTM D1598. Samples were water filled and top loaded with compressed air. The pipe systems were placed into a tank filled with tap water and controlled at the desired temperature. A normally open three-way solenoid valve, positioned between the pressure source and the test samples was activated when a failure was detected. On activation the valve closed, depressurized the sample, cutting it off from the supply of compressed air. At the same time the timer on the Failure Detection Unit would stop to record failure times, and allow a calculation of the sample's stress rupture lifetime. All the stress rupture tests were conducted at a bath temperature

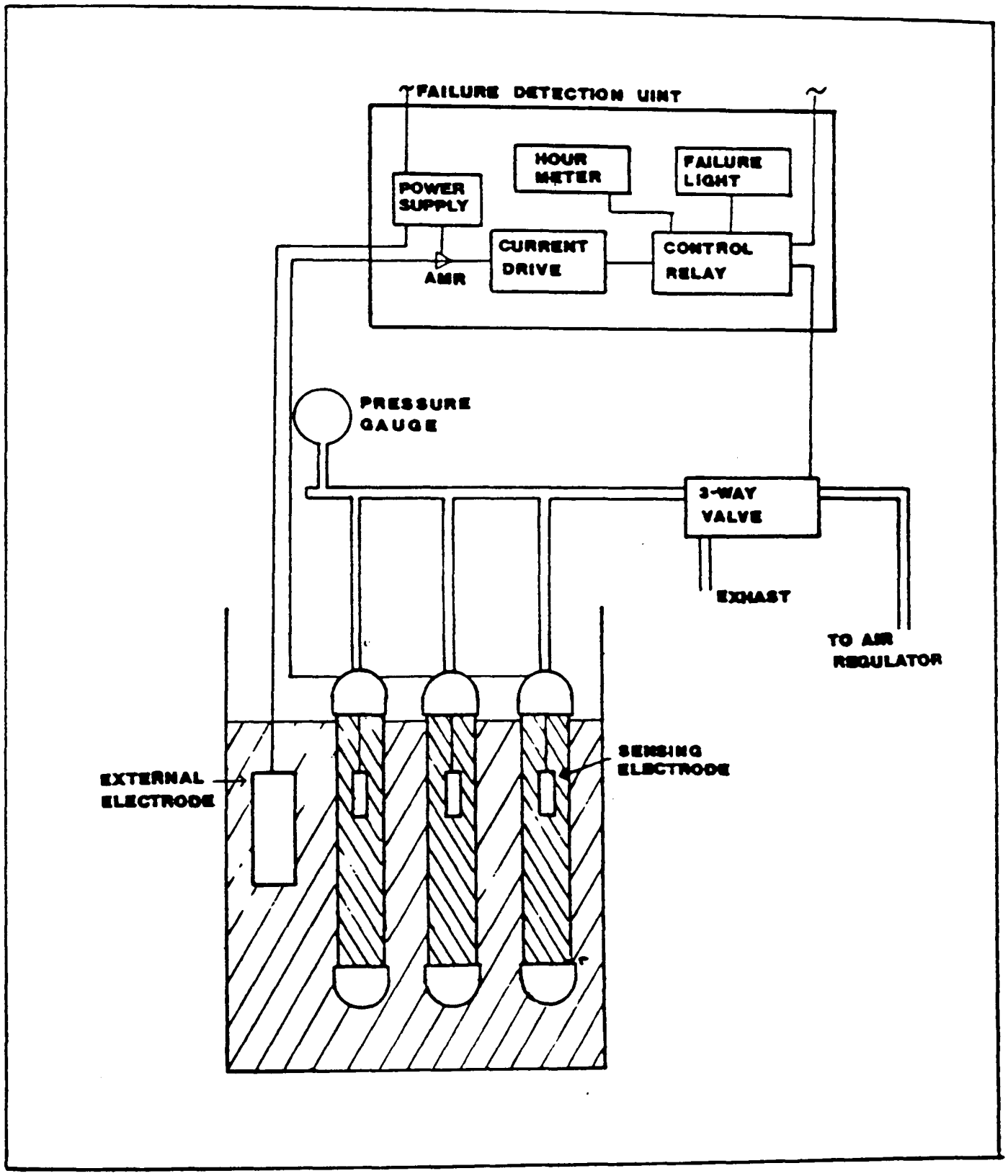

FIGURE 4.4: Schematic presentation of stress rupture testing facilities.

of 80 ±1°C . For all the 32mm pipes, the gauge pressure applied to the samples was 0.95 MPa. For 55mm pipes the three gauge pressure levels administered were 0.9, 0.8 and 0.7 MPa.

4.4.1 STRESS RUPTURE TESTING EQUIPMENT

The samples were placed in a glass reinforced polyester water bath. The temperature in the bath was maintained by UTAC heaters which pumped water from an inlet connection on the side of the bath. Temperature was monitored by a calibrated digital thermometer. The circulating action of the water prevented thermal layering occurring within the bath.

A schematic representation of the failure detection device is shown in Figure 4.4 . The technique for detection relies on the fact that water is within and around the pipe; the pipe walls being the insulating barrier between the liquids. Electrodes were inserted internally and externally to the pipe system. The external electrode was connected to the positive bias voltage derived from the amplifier power supply, thus sustaining a potential between both electrodes. When a crack propagates through the wall of the pipe, water connects the inside of the pipe with the outside of the pipe, opening the circuit between the internal and external electrodes. This signal current (microamps) turns on the amplifier which is biased off with a small negative charge, and operates a relay, stopping the timer and closing the 3-way solenoid valve. The system is automatically isolated at the 3-way solenoid valve which shuts off the applied pressure to the system and vents any excess pressure remaining. A red light on the control panel indicated that a sample had failed.

4.4.2 32mm AND 55mm PIPE TEST SAMPLES

For pressure tests the specimens conformed to the British Gas Standard PS/PL2, Appendix I, and were 400mm in free length between end fittings for 32mm pipe specimens and 500mm for 55mm pipe specimens. Figure 4.5 illustrates the top end cap which involved boring a 15.8mm diameter hole through the end cap and tightening a 15.8mm bulk head fitting through it before welding to the pipe. The samples ends were not constrained. This system was employed for both 32 and 55mm end caps. The polyethylene end caps were welded to the pipe ends using a socket fusion tool at 210°C (Figure 4.6) .

Test samples were filled with water and conditioned in the bath for 24 hours at 80°C before stress rupture testing commenced. A minimum of 3 samples for each blend addition level were tested so that an average lifetime could be recorded.

4.4.3 NOTCHING OF TEST SAMPLES

External notching has been shown by Dickinson to reduce the lifetime of polyethylene pipe [103]. The need for reducing the lifetime of pipe was needed as failure times could be excessively large (greater than 1 year). The notching of 32mm pipe supplemented the stress rupture testing of 32mm straight pipe, whereas all the 55mm pipe blends were notched prior to testing.

The notching procedure used was a modified version of the British Gas standard BGC/PS/PLC, Part 1, Appendix O. The only major change was the table feed rate of 5.2 in/min (132.08 mm/min) and the cutter rotating at 600

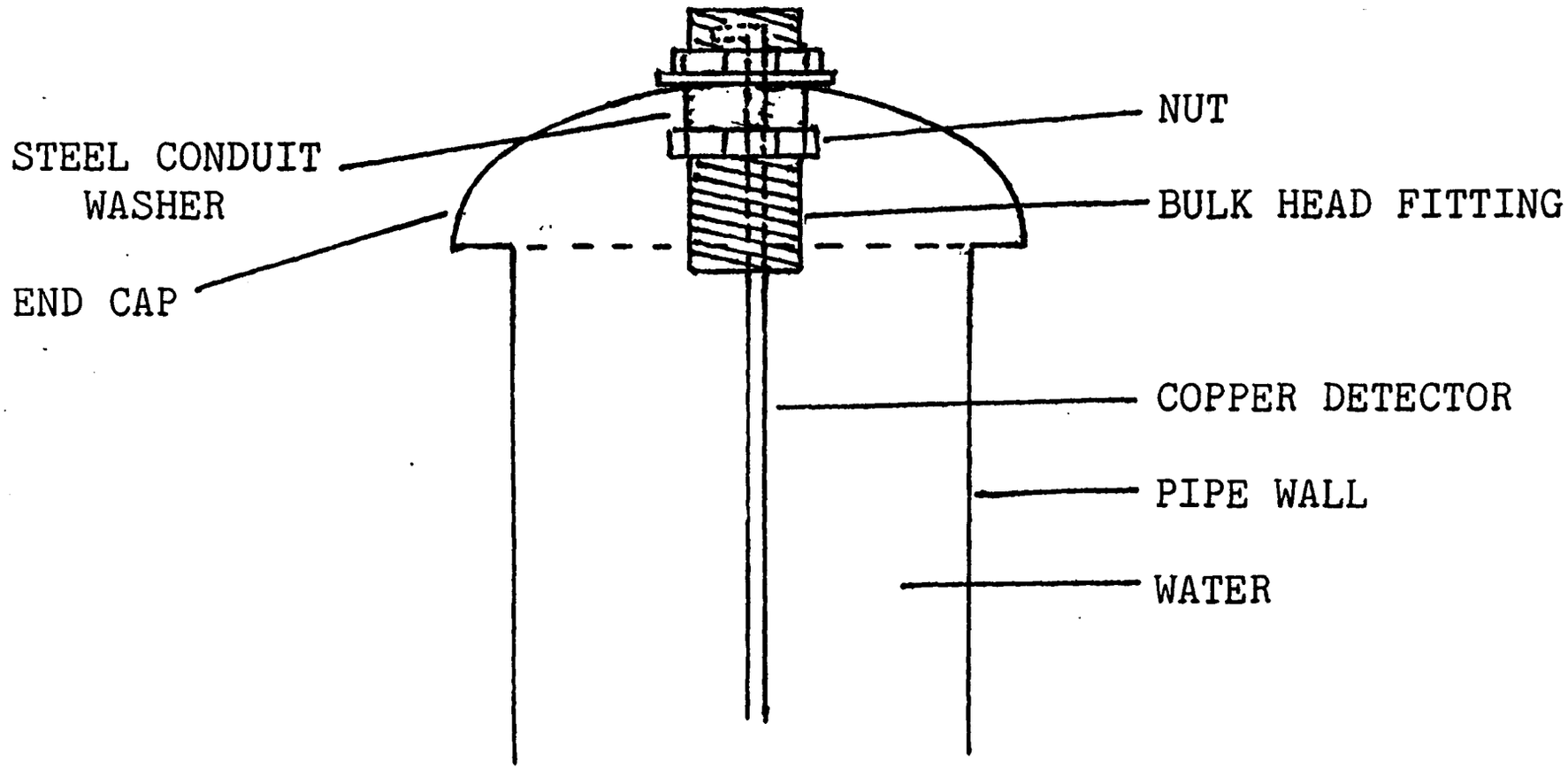

FIGURE 4.5: Schematic representation of the pipe end cap with detector electrode.

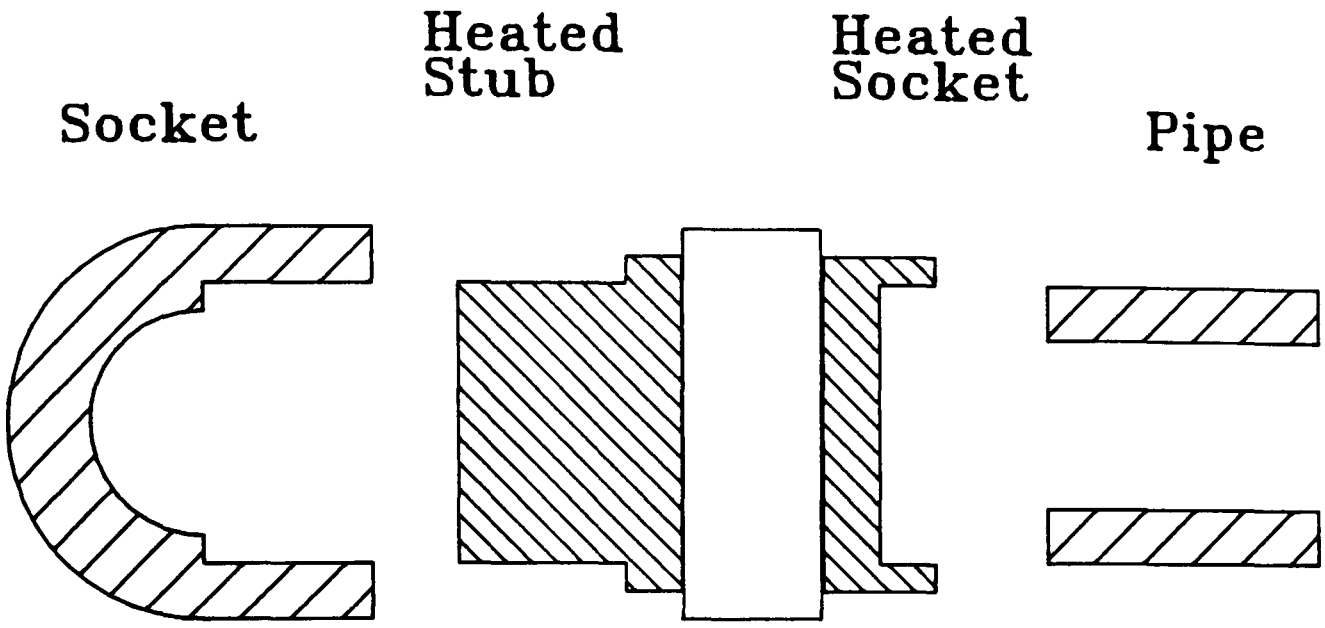

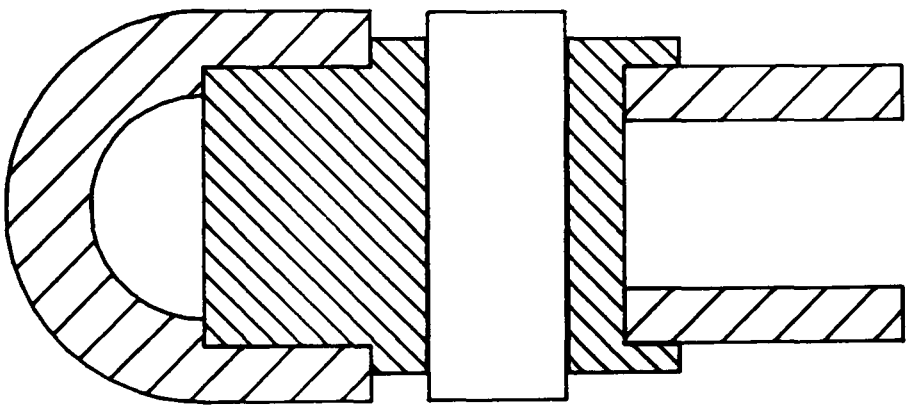

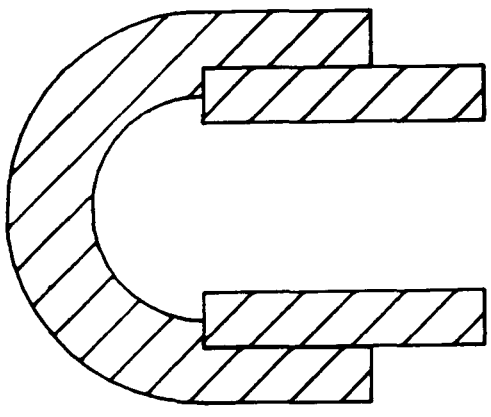

FIGURE 4.6: Fusion of end caps onto pipe sample.

rpm. The samples were prepared by marking circumferential lines 125mm apart along the pipe axis. The wall thicknesses were accurately measured prior to notching using a ball micrometer and a calculation made of the notch depths (20% of the wall thickness) for each of the 4, 125mm lines. Marking the pipe before notching provided an easy means of seeing the cutter touch the pipe. The notches were numbered on the pipe so that a record was made of which notch failed after stress rupture testing. The length of the notch for the 55 and 32mm pipes was 125mm and four notches were placed 90° apart.

4.4.4 STRESSES IN PIPES UNDER INTERNAL PRESSURE

If a thin-walled cylinder or pipe is allowed to expand and extend freely and is subjected to an internal pressure, three mutually perpendicular stresses will be produced as shown in Figure 4.7 . Such stresses are generally termed hoop or circumferential, axial or longitudinal and radial stresses . Hearn [104] assumes that if the ratio of the wall thickness to the inside diameter of the pipe is less than 1/20; then the hoop and axial stresses remain constant though the wall thickness and the radial stress is small enough to be neglected. Therefore the hoop stress is given by:

$$\sigma_h = (P\, d) / (2\, t) \qquad [4.13]$$

where σ_h = The hoop stress

d = The internal diameter

t = The wall thickness

P = The applied internal pressure

The longitudinal stresses are half the hoop stresses for axially

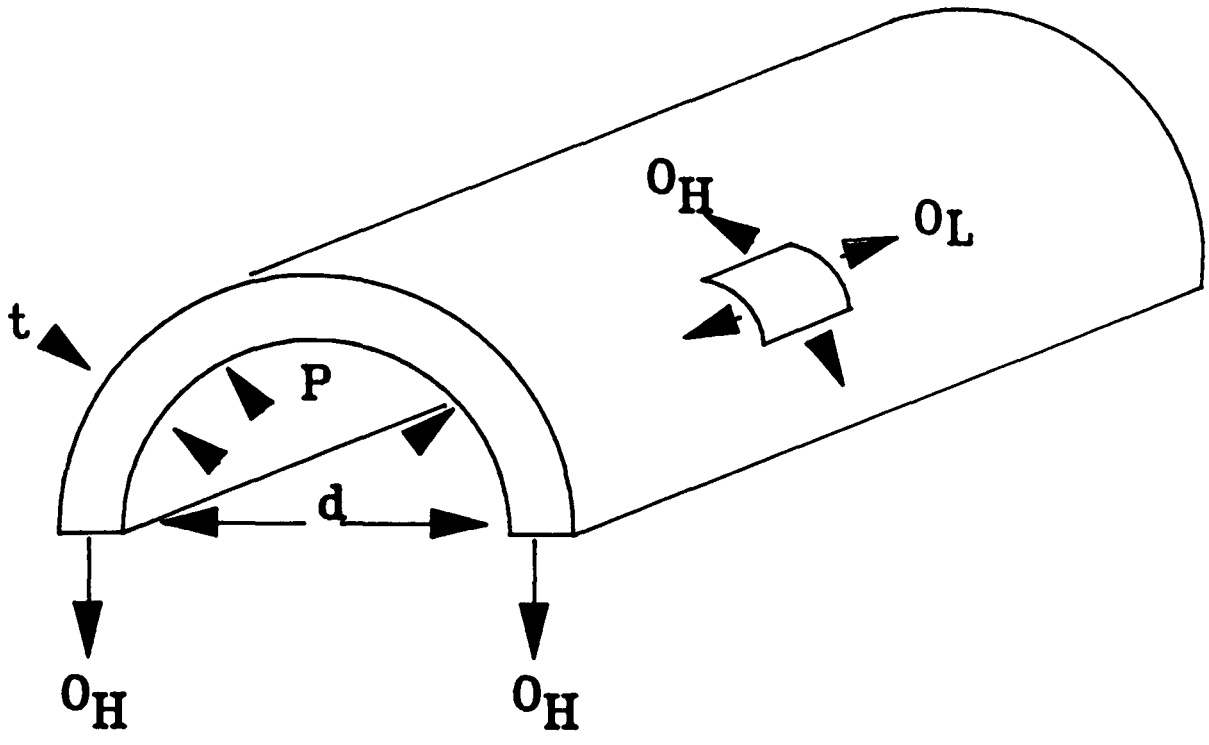

FIGURE 4.7: Stresses in thin walls.

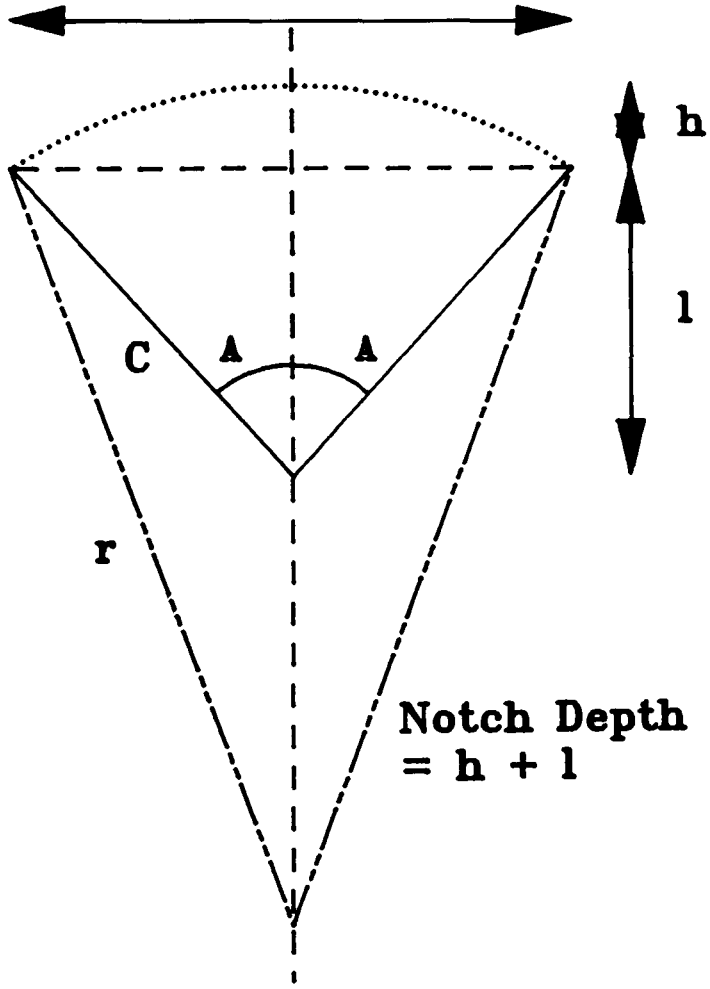

FIGURE 4.8: Notch segment of pipe showing parameters for notch depth calculation.

unconstrained pipes. However the assumptions above are invalid for thick-walled pipes or cylinders and in reality the hoop stress will vary in all SDR11 pipes. (SDR is the standard dimension ratio and is equal to the minimum outside diameter over the minimum wall thickness). The hoop stress on the inside surface of the pipe can be greater by about 25% than the hoop stress experienced on the external surface. The expression describing this variation is developed from the Lame equation 104.

$$(\sigma h)_r = P\,[\,(r_1^2)\,/\,(r_0^2 - r_1^2)]\,[\,1 + (r_0^2/r^2)] \qquad [4.14]$$

where: $(\sigma h)_r$ = Hoop stress at radius r

r_1 = Inside radius of the pipe

r_0 = Outside radius of the pipe

r = Radial position at which the hoop stress is being calculated.

The Nadai formula is a simplification of the Lame equation and is given by:

$$\sigma h = P\,(\,d - t\,)\,/\,2t \qquad [4.15]$$

The hoop stress calculated by equation [4.15] is within 5% of the hoop stress on the bore of a thick walled SDR11. This equation is the one applied to all hoop stress calculations in the later chapters. For example using the values of 32mm pipe at an applied pressure of 9 bar and a wall thickness of 3mm, equation 4.15 becomes:

$$\sigma h = [\,9\times10^5 Pa \times (3.2\times10^{-2} m - 0.3\times10^{-2} m)]\,/\,[\,2 \times 0.3\times10^{-2} m]$$

$$= [\,9\times10^5 \times 0.029\,]\,/\,[\,0.006\,]$$

$$= 4.35\ MPa$$

4.4.5 NOTCH DEPTH DETERMINATION AND CALCULATION OF K

On failure of a notched pipe, the fracture surfaces were fully exposed by breaking the pipe open using a hammer or immersing the sample in liquid nitrogen and cracking open the notch. Once the fracture surface was exposed a travelling microscope was used to measure the face that was notched, (c) . This is illustrated in Figure 4.8 . As can be seen from the diagram this depth is different from the true notch depth (l+h). Using simple geometrical equations the true notch depth can be evaluated. Using Figure 4.8 as a basis, an example calculation is performed below for a 55mm diameter pipe which has c measured by a travelling microscope of 1.12mm. The width of the notch k is given by:

$$k = 2 \sin A \, C \qquad [4.16]$$

where: A = half the angle of notch cut = 30^o

$$k = 2 \sin 30 \times 1.12$$

$$= 1.12\text{mm}$$

h is a part of the segment of pipe removed; it is represented by:

$$h = r - 1/2 \, (4 r^2 - k^2)^{1/2} \qquad [4.17]$$

where: r = pipe radius = 27.5mm

$$\therefore \quad h = 27.5 - 1/2 \, [4x(27.5)^2 - (1.12)^2]^{1/2}$$

$$= 27.5 - 1/2 \, [3023.7]^{1/2}$$

$$= 27.5 - 1/2 \, [54.9]$$

$$= 5.7 \times 10^{-3} \text{ mm}$$

l represents the height of the rest of the segment removed and is described by the following equation:

$$l = \cos A \; C \qquad [4.18]$$

$$\therefore \quad l = \cos 30 \times 1.12$$

$$= 0.97 \text{ mm}$$

Therefore the notch depth cut is described by:

$$\text{Notch Depth} = h + l = a \qquad [4.19]$$

$$\therefore \quad = 5.7 \times 10^{-3} + 0.97$$

$$= 0.9757 \text{ mm}$$

Which is ~ 19% of a wall thickness of 5mm.

The value of *a* for the notch depth can be used in equation [3.11] discussed in section 3.3.1 for calculating K_c. Although K_c was previously defined as the limit which a flawed system would attain before a fast unstable crack propagates, the value of K will be used to define the intensity of the stress system at the tip of the crack before propagation, $K_{initial}$ or K_{int}. For example using equation [3.10] for a pipe with a hoop stress of 4.6 MPa and containing a 1mm deep outside notch, and a geometry factor of 1.31 for 55mm pipe from Rooke and Cartwrights Compendium of Stress Intensity Factors [72], K_{int} can be expressed as:

$$K_{int} = \sigma Y (\pi a)^{1/2} \qquad [4.20]$$

where : σ = Applied hoop stress at start of crack growth.

Y = Geometry parameter.

a = Crack length.

K_{int} = Stress intensity factor at start of crack growth.

$$\therefore \quad K_{int} = 4.6 \times 1.31 \, (\pi \times 0.001)^{1/2}$$

$$= 0.34 \text{ MPa.m}^{1/2}$$

For further information Figure 156 from Rooke and Cartwrights manual [72] is represented here as Figure 4.9 showing the condition for an edge crack in a tube subjected to a uniform internal pressure. K_i is equivalent to equation [3.11] and K_o is the stress intensity factor for a crack in a sheet subjected to a uniaxial tensile stress remote from the crack.

4.5 MICROSCOPY AND FRACTOGRAPHY

4.5.1 MICROTOMY AND LIGHT MICROSCOPY

For birefringent polymers such as polyethylene a useful microstructural analytical technique is the use of microtomy coupled with microscopy . In the experimental method a sledge microtome with a Mettler cold stage was used for preparing sample sections of 6μm thickness. For the control material this was found to be of sufficient thickness to let light through the sample for the microstructure to be viewed. All sections were transferred to clean microscopy slides, immersed in a setting oil and protected with glass cover-slips. These microscopy slides were subsequently viewed by means of a Reichert Zetopan microscope, with camera attachment, set up for

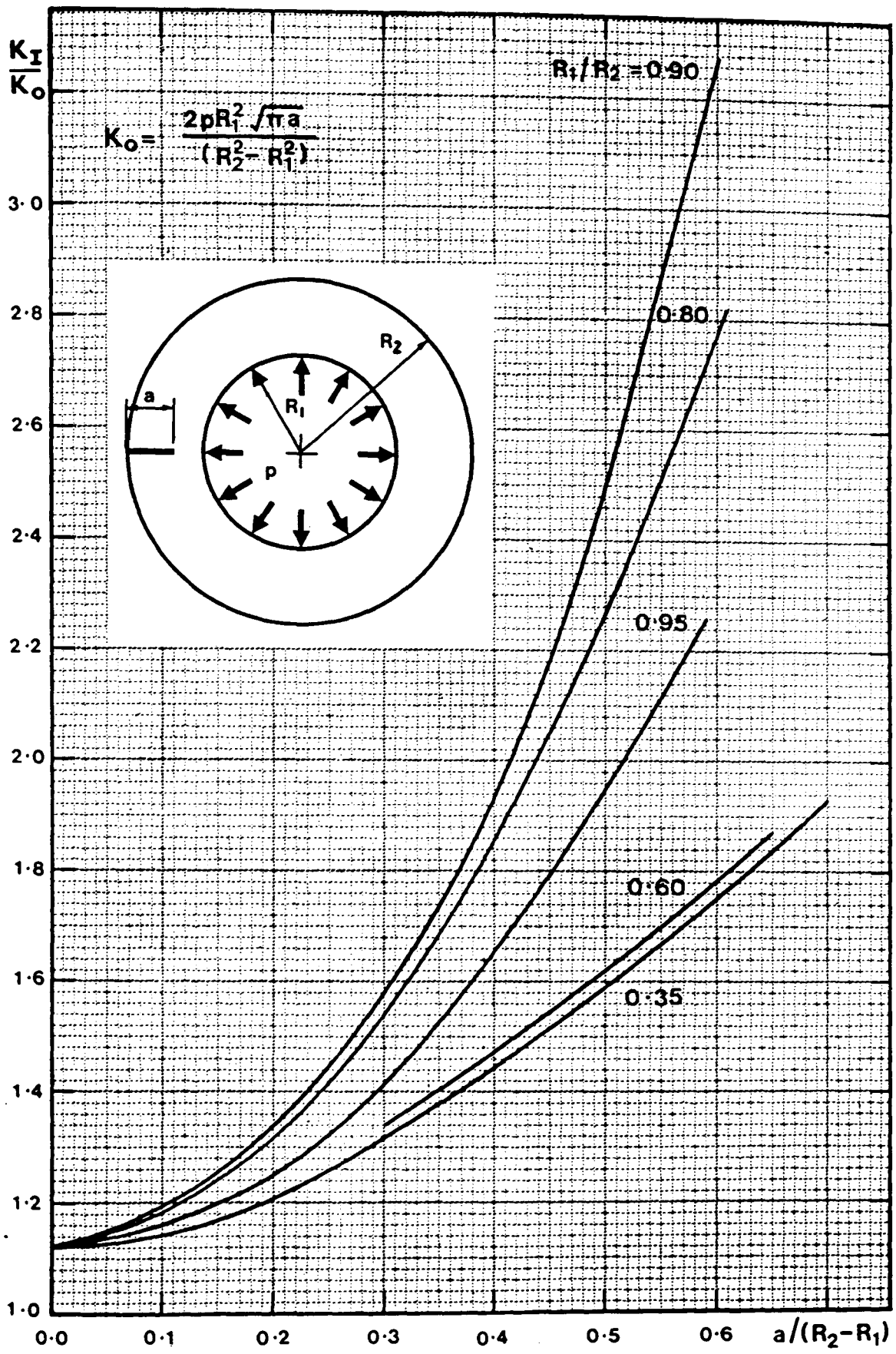

FIGURE 4.9: K_I for an external radial edge crack in a tube subjected to a uniform pressure. [72]

transmission polarized light microscopy with the polarizer and analyzer crossed.

This microscopy set-up was used to evaluate the microstructure of blended pipe samples . Figure 4.10 shows the location at which samples were removed from the wall of the pipe. Materials that were not extruded separately into pipe (for example) HDPE-F, HDPE-M, HDPE-B and MDPE-P, had their samples taken from compression moulded sheets. The variation in processing conditions between compression moulding of sheet and extrusion of pipe was found not to have an influence on spherulite size.

4.5.2 HOT-STAGE MICROSCOPY

A simple technique was developed to identify the changes in spherulitic formation of two polyethylene materials of differing crystallization temperatures. In this study a section of MDPE-A was microtomed from pipe and a separate section of HDPE-F was microtomed from a compression moulded sheet. Both samples were cut to 10μm thickness. They were placed side by side on a microscopy slide with a section from each microtome overlapping the other. A separate slide was then placed onto the samples sandwiching the samples between the slides. The sample with the slides were then placed onto a Reichert hot-stage which was heated to 170°C and left for 10 to 15 minutes. Once the spherulitic structure of the samples had disappeared, the stage was allowed to cool to room temperature. The sample was examined microscopically using transmitted light to view the spherulitic structure reappearing once the crystalline melting point was reached. A Reichert Zetopan microscope was used to view the spherulitic formations of the samples at room temperature.

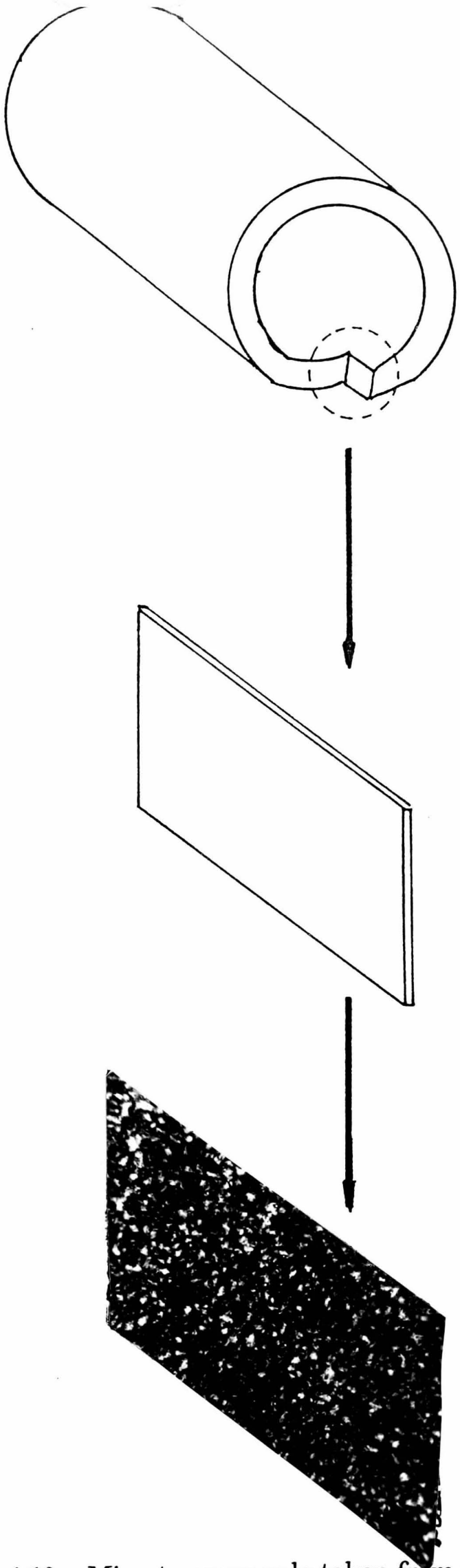

FIGURE 4.10: Microtomy sample taken from pipe in the extrusion direction.

4.5.3 FRACTURE SURFACE ANALYSIS

All pipe samples which failed in a brittle manner were opened up using a hammer or by immersing the sample in liquid nitrogen and revealing the fracture surface by hand.

The macro features of the fracture surfaces were examined with the aid of a Wild Heerbrugg microscope, under low angle illumination and employing a intralux fibre optics light source.

The micro-features were examined by a Cambridge 5250 and a Jeol SM480A scanning electron microscope (SEM) with the accelerating voltage for the beam set at 10KV. The samples were firstly placed into a Polaron E5000 sputter coater which gave a coating of gold of approximately 70nm. The coated sample was then clothed around the edges with silver dag to prevent excessive charging when the sample was observed in the SEM.

Once the sample was in the SEM, energy dispersive X-ray analysis (EDAX) could be performed on the fracture surface to determine the elemental composition of inclusions or other substances present. A Links system 860 analyzer was used to generate and collate data. The technique is limited to detecting the presence of those elements whose atomic number are above that of oxygen.

CHAPTER 5

CHARACTERIZATION AND MECHANICAL TESTING OF BLENDED POLYETHYLENE PIPES

5.1 INTRODUCTION OF RESULTS

The results generated from this research programme are presented in three chapters. This chapter, covering the characterization and mechanical testing of the polyethylene blends, is broken down into three main sections. The first section presents a brief summary of the production of these blended materials into pipes. The second section focuses on the short term mechanical properties of the materials and outlines testing on HDPE-F blends. The final section reviews the 80°C stress rupture performance of the blends for unnotched and notched pipe.

Chapter 6 continues the characterization work on polyethylene pipe blends, focussing on results obtained from compatibility or miscibility studies and qualifying blend quality in relation to stress rupture performance.

Finally Chapter 7 reviews results of the fracture surfaces of failed pipe samples and attempts to correlate the features with stress rupture performance. The chapter concludes with simple morphological models to explain the brittle fracture behaviour of polyethylene pipe blends under

80°C stress rupture conditions.

5.2 PRODUCTION OF PIPE BLENDS

5.2.1 EXTRUSION AND QUALITY CONTROL

The extrusion of the MDPE-A material into pipe produced a product with a smooth gloss finish on the internal and external areas of the pipe. The appearance of the pipe was of great benefit in assessing the behaviour of polyethylene blends for producing quality pipes.

i) 32mm Pipe Production

The surface finish exhibited by the MDPE-A material was apparent in the manufacture of HDPE-F blends into 32mm pipe. Both compounded and uncompounded batches of materials produced pipe that had a good surface finish on the inside and the outside of the pipe, illustrating the similarity in the materials viscosity values and general molecular characteristics (Table 4.1). The similarity in the materials flow behaviour ensured that there was no need for changes in extrusion conditions for all HDPE-F blends.

ii) 55mm Pipe Production

The extrusion of 55mm pipe provided a better opportunity to evaluate the additives influence on blending with the MDPE-A base resin. The recorded melt pressures at each zone along the extruder regions and at the die are reproduced in Figures 5.1 - 5.4. It can be readily seen that the increase in viscosity at 190°C for the HDPE-M and MDPE-P materials have increased the pressure profiles of the blends as expected. This resulted in a need to

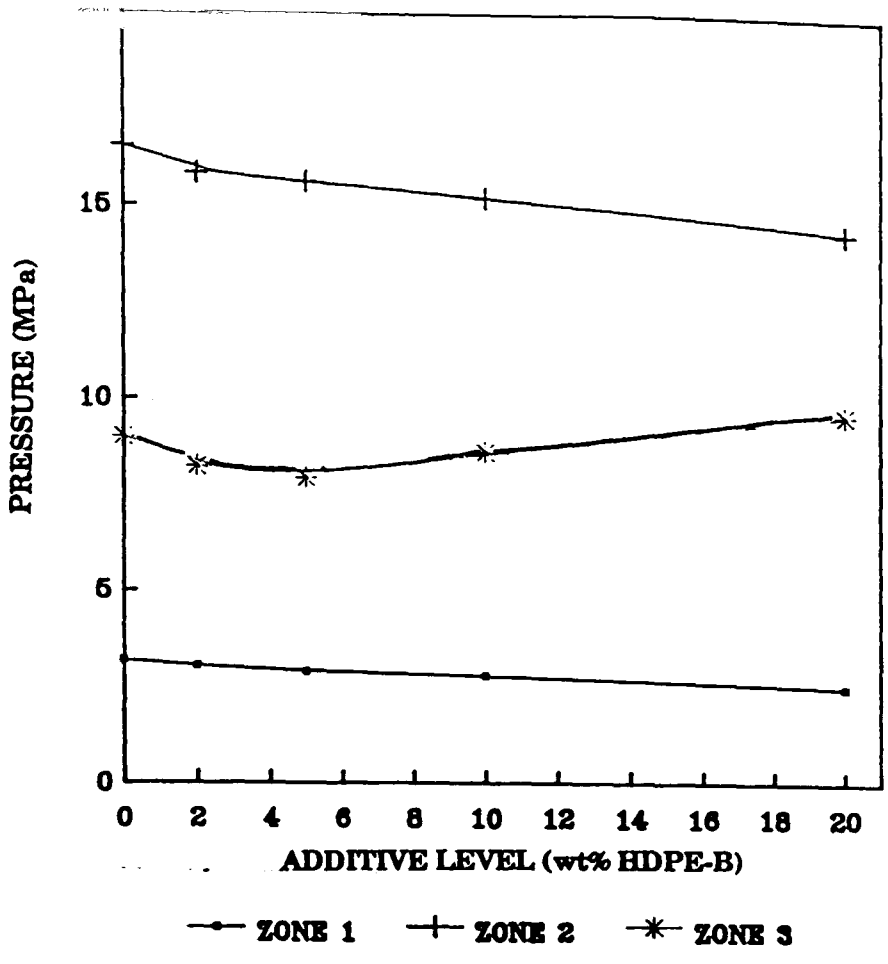

FIGURE 5.1: Melt pressure extrusion profiles for HDPE-B blends.

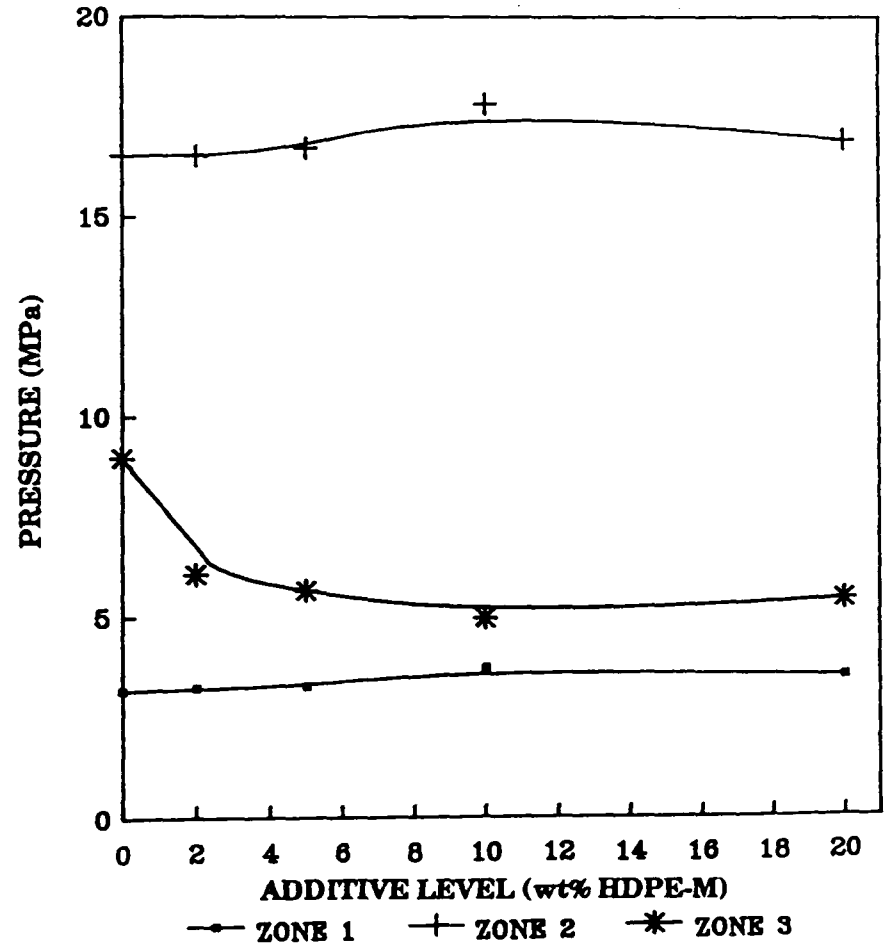

FIGURE 5.2: Melt pressure extrusion profiles for HDPE-M blends.

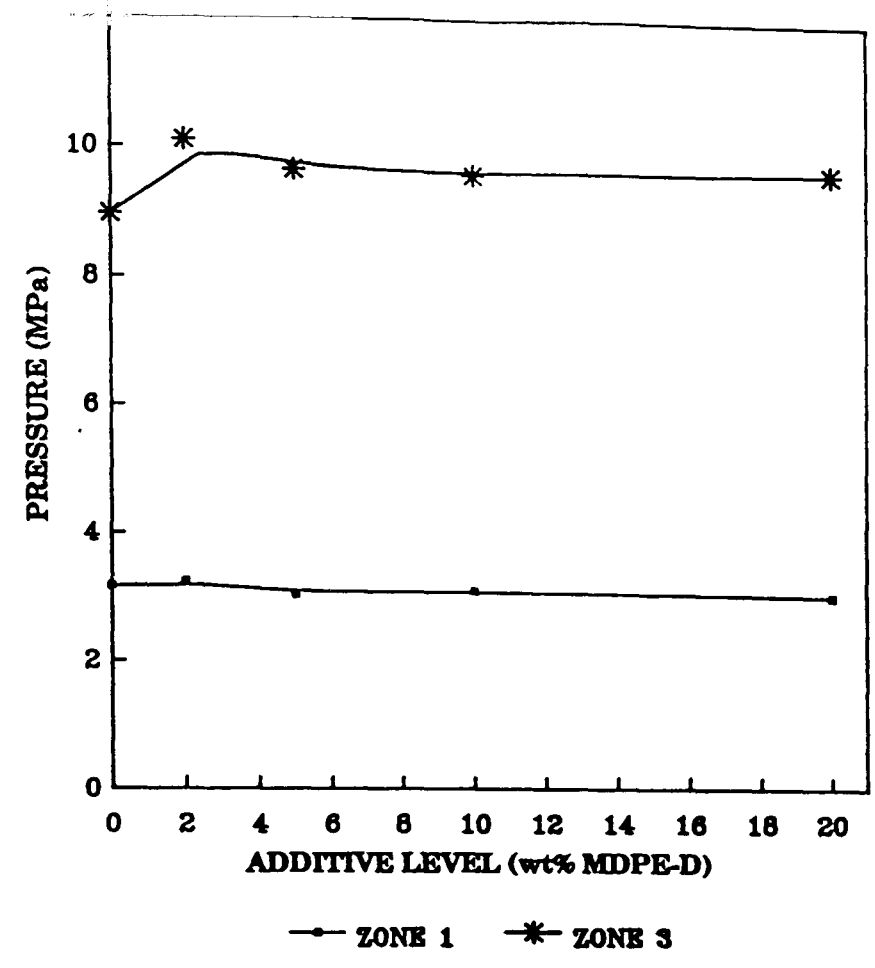

FIGURE 5.3: Melt pressure extrusion profiles for MDPE-D blends.

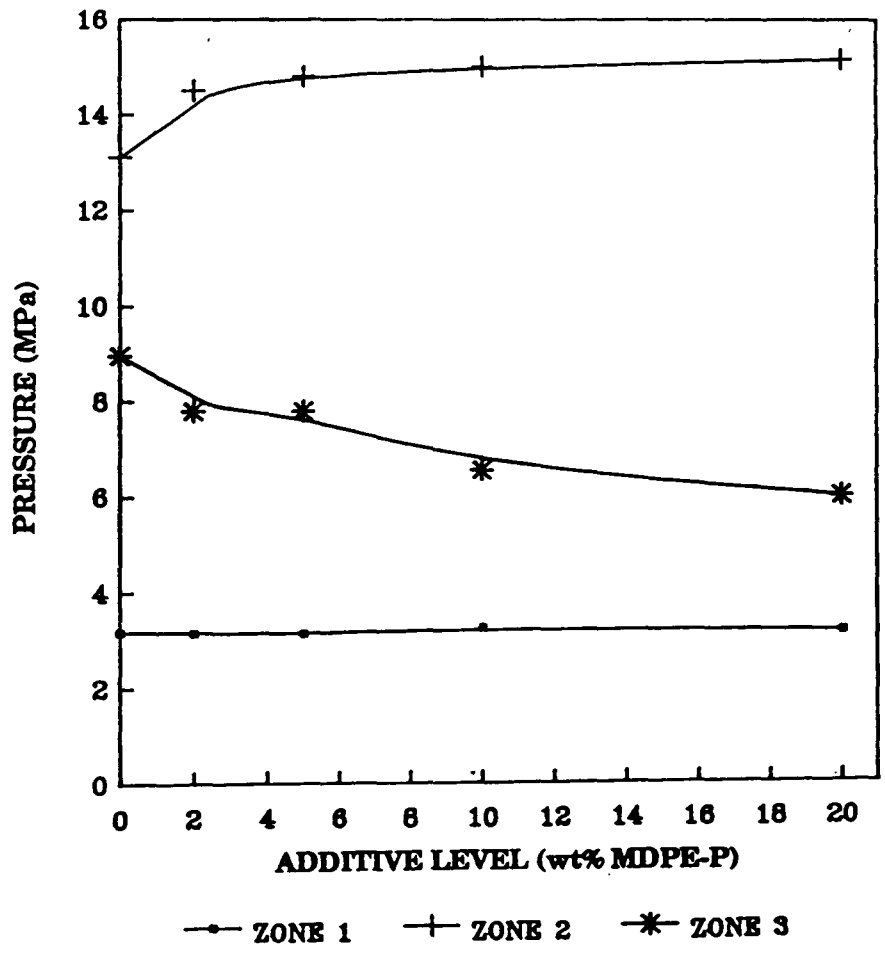

FIGURE 5.4: Melt pressure extrusion profiles for MDPE-P blends.

increase screw speeds during the trials to ensure that wall thicknesses were maintained to specification.

The pressure profile however decreased for the HDPE-B blends, which was expected due to the HDPE-B material having a lower viscosity at 190°C when compared to the MDPE-A resin (Table 4.1). This was reflected during the trial by decreasing the extrusion speed so that wall thicknesses could be reduced.

The MDPE-D material proved to be the easiest material to extrude in that no major changes were needed in changing from one blend to another. This can be seen as a constant melt pressure profile for all blends in Figure 5.3. This was reflected in the quality of the pipe blends, which all had the excellent surface finish of the MDPE-A resin. The HDPE-M blends produced the poorest visual quality pipe with an uneven surface finish on the bore of the pipe. This feature was less characteristic for MDPE-P blends, whereas the HDPE-B blends had the least surface irregularities on the bore.

5.2.2 IDENTIFICATION OF PIPE BLENDS AFTER PRODUCTION

Due to the monitoring of the melt pressure readouts by a chart recorder, it was possible to note the changeover from one blend to another. However a further technique enabled batches to be accurately determined during a changeover of blends. Table 5.1 illustrates this simple technique using 32mm HDPE-F pipe blends. These data shows that by using either MFR or density the variation in property between the first sample of pipe removed and the last sample of the extrusion process can be monitored. This

	COMPOUDED BLENDS (wt% HDPE-F)			UNCOMPOUNDED BLENDS (wt% HDPE-F)		
	2/98	**10/90**	**20/80**	**2/98**	**10/90**	**20/80**
M.F.I (g/10min)	2.90/ 3.12	2.72/ 2.74	2.58/ 2.59	3.17/ 3.21	3.05/ 3.01	2.80/ 2.81
DENSITY (kg/m^3)	940.5/ 940.0	940.7/ 940.6	941.1/ 941.0	939.0/ 940.0	938.0/ 940.9	941.6/ 941.9

TABLE 5.1: Comparison of Uncompounded and Compounded pipe blends.

technique was used to distinguish the beginning and the end of a batch and hence consistent blend samples were selected for experimental testing

5.3 CHARACTERIZATION AND SHORT TERM MECHANICAL PROPERTIES OF PIPE BLENDS

5.3.1 DENSITY AND BRANCH DISTRIBUTION

For HDPE-F blends the density results are shown in Table 5.2 for both uncompounded and compounded pipe blends, illustrating the similarities between the materials. As expected density increases as the HDPE-F additive level increases (Figure 5.5).

Density variations are more pronounced for 55mm pipe blends. Figures 5.6 and 5.7 reflect this change in behaviour from values expressed in Tables 5.2 . However the density trends are what would be expected from the knowledge of the additives density (Table 4.1).

Branching has been shown in the earlier chapters to influence the density of the material. The results from fractionating MDPE-A,D and P materials are displayed in Table 5.6. The data reported shows the similarity of the MDPE-A and D resins in regards to molecular weight and branching levels. The MDPE-P resin although having butyl side chains in comparison with hexyl for the other materials, has a *significant* high molecular weight tail. Similarly a significant low molecular weight tail is present compared to the MDPE-A and D materials.

ADDITIVE LEVEL (wt% in MDPE-A)	DENSITY (kgm^{-3})			
	HDPE-B	HDPE-M	MDPE-P	MDPE-D
0	945.10 944.85 943.40	945.10 944.85 943.40	945.10 944.85 943.40	945.10 944.85 943.40
Average	944.45	944.45	944.45	944.45
2	946.24 945.53	944.93 944.67	944.80 945.56	945.00 945.00
Average	945.88	944.80	945.18	945.00
5	945.72 945.98	945.60 944.89	945.40 944.80	945.10 945.10
Average	945.85	945.24	945.10	945.10
10	946.66 946.77	945.16 944.08	945.10 944.90	944.60 945.10
Average	946.71	944.62	945.00	944.85
20	947.47 947.53	945.17 944.96	944.70 944.60	944.20 944.30
Average	947.50	945.06	944.65	944.25
100	949.20	944.80	937.80	936.20

TABLE 5.2: Density values from 55mm pipe blends.

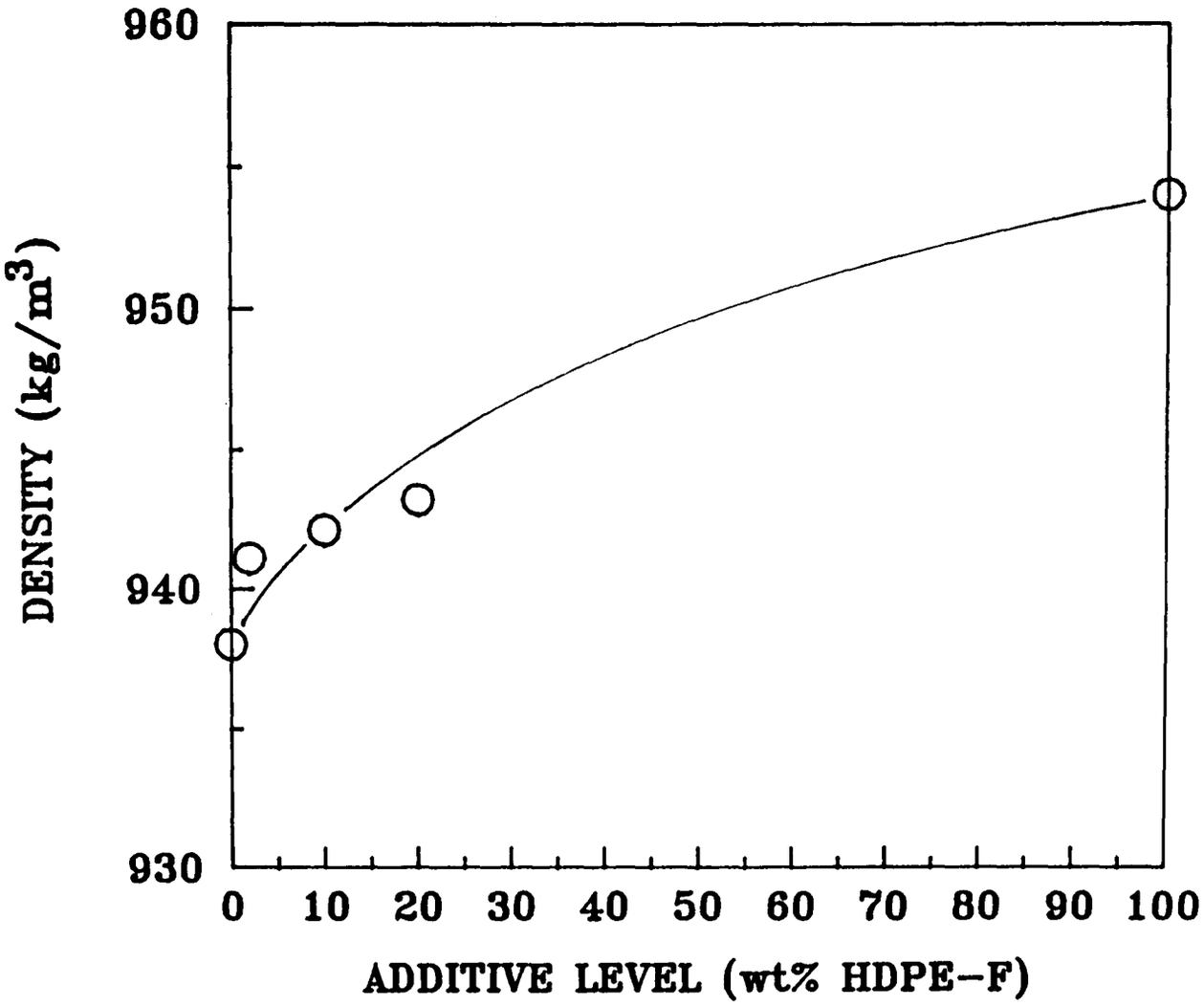

FIGURE 5.5: Density variations in compounded HDPE-F blends. (from compression moulded sheet).

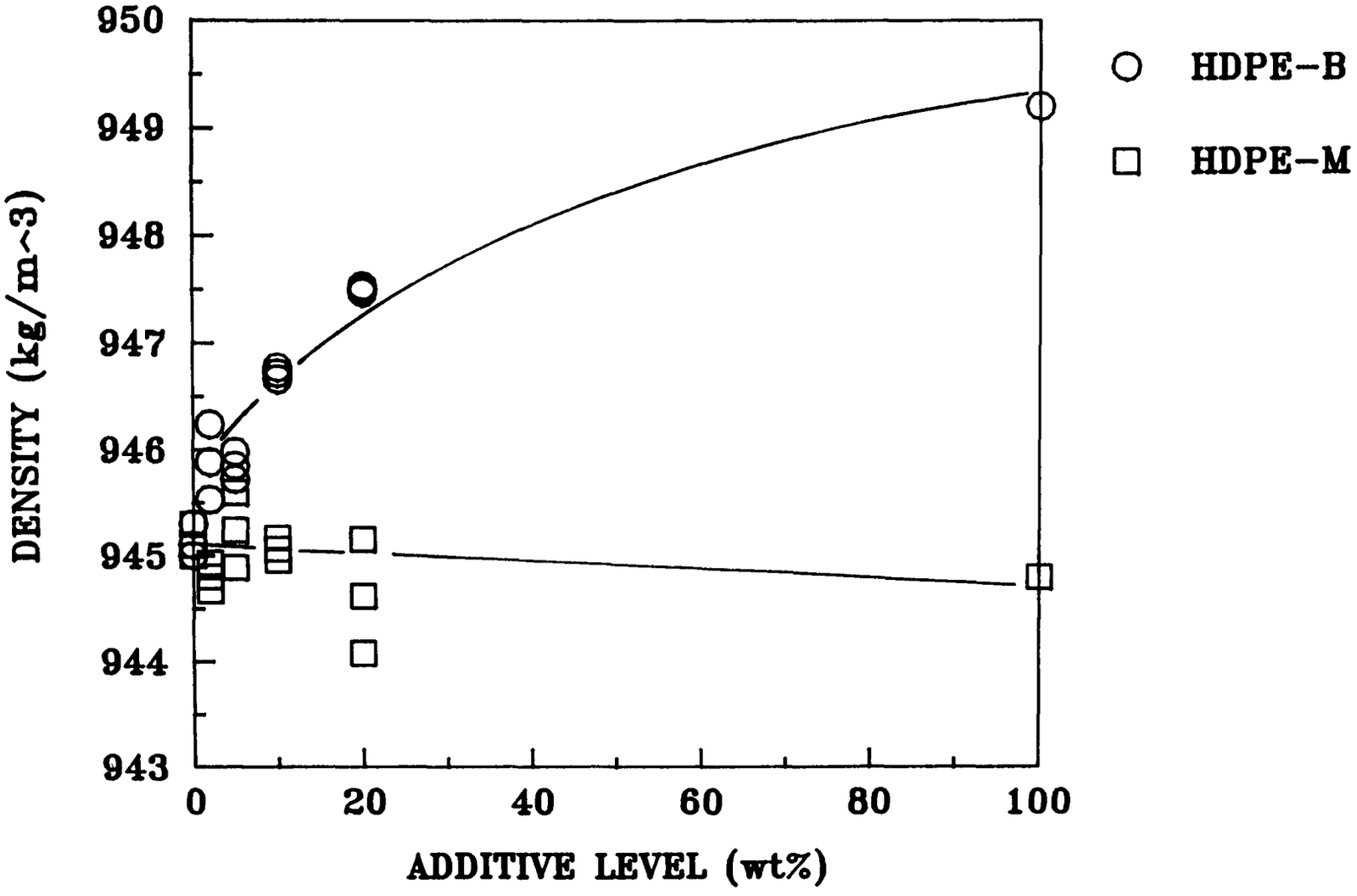

FIGURE 5.6: Density variations in HDPE-B and HDPE-M pipe blends.

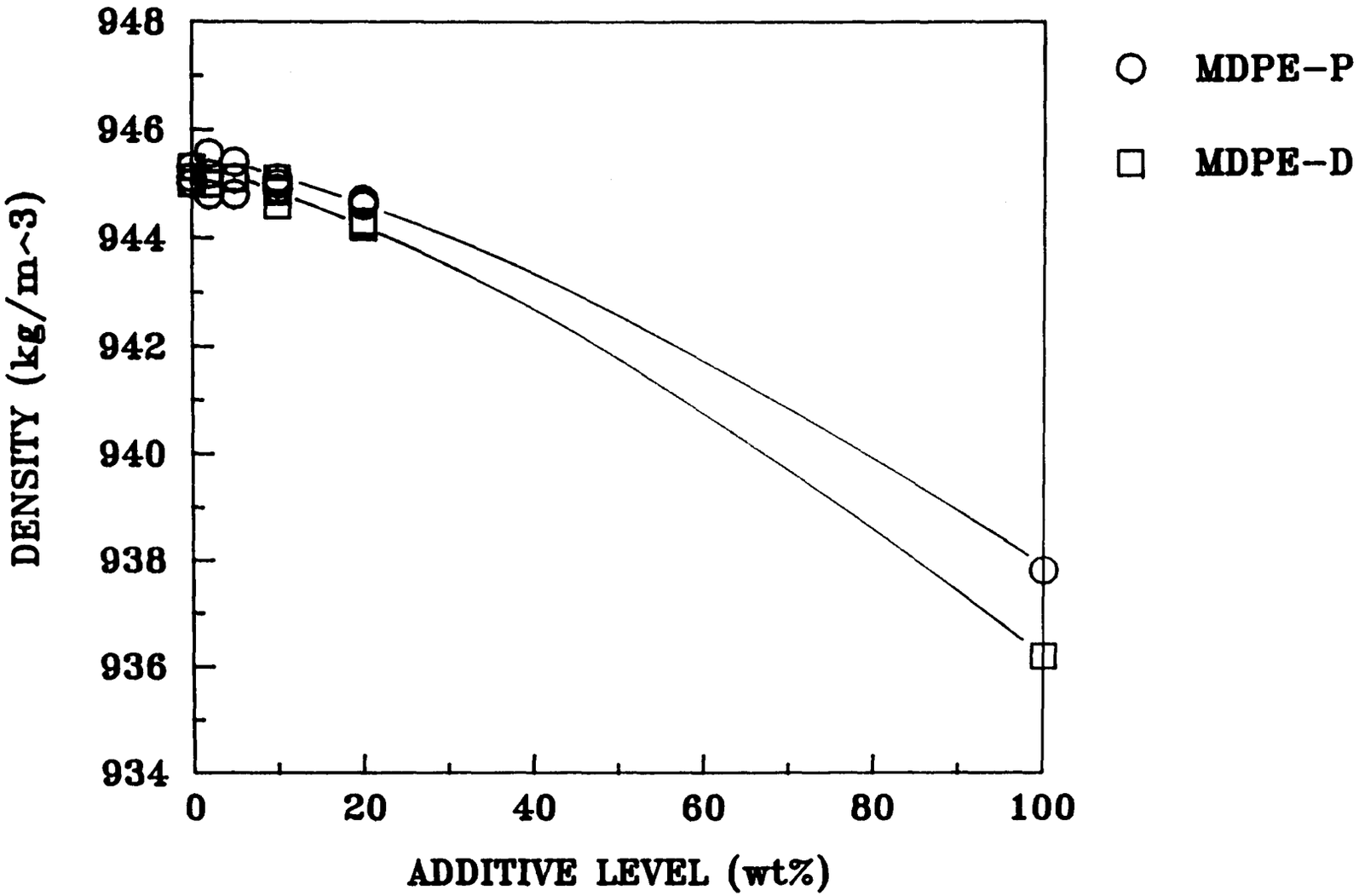

FIGURE 5.7: Density variations in MDPE-P and MDPE-D pipe blends.

	COMONOMER TYPE	FRACTION 1 (/1000CH_2)	FRACTION 2 (/1000 CH_2)	FRACTION 3 (1000 CH_2)	OVERALL BRANCHING (/1000 CH_2)
MDPE-A	Octene	4.4	3.3	2.2	4.5
MDPE-P	Hexene	9.2	9.2	4.3	7.4
MDPE-D	Octene	5.5	5.5	4.2	4.8

i) Fraction 1 refers to the low molecular weight portion of the distribution curve.
ii) Fraction 2 refers to the middle molecular weight portion of the distribution curve.
iii) Fraction 3 refers to the high molecular weight portion of the distribution curve.

TABLE 5.3: Chain branching distribution in selected pipe resins.

5.3.2 MELT FLOW RATE AND MOLECULAR WEIGHT

The MFR values from pipe samples are tabulated in Table 5.1 for HDPE-F uncompounded and compounded blends, showing the expected decrease in MFR value with increasing additive addition. However molecular weight values, (as shown in Table 5.4 for compression moulded samples) are inconsistent and show the variations associated with the GPC techniques from materials with similar molecular weight values.

For 55mm pipe blends variations in molecular weight are not clearly visible with HDPE-B, M and MDPE-P materials. (Tables 5.5 - 5.7). With the MDPE-D blends the similar molecular weight mean values (to MDPE-A) trends are not clearly seen (Table 5.8). As expected from these results all the blends produced MFR values between the parent materials (Figure 5.8).

5.3.3 TENSILE AND IMPACT TESTING

Table 5.12 displays the results of the tensile behaviour of HDPE-F compounded blends. These are graphically expressed in Figure 5.9 showing the good short term properties of yield stress and modulus from the increases in additive addition.

Impact strength data are reported for the HDPE-F compounded and uncompounded blends in Table 5.10. The values expressed show that this particular test procedure was unable to discern major variations within the blends. This was thought to be due to the pendulum weight which needed to be of a greater energy value. Observation of the fracture surfaces highlighted this point clearly by displaying an *hinge* type failure, in comparison to a 10% HDPE-B blend which fractured completely producing a

	ADDITIVE LEVEL IN MDPE-A (wt%)				
	MDPE-A	**2**	**10**	**20**	**HDPE-F**
M_n (x10^4)	1.48	2.35	1.38	1.45	1.73
M_w (x10^4)	11.8	9.6	10.5	10.4	12.1
M_z (x10^4)	53.4	28.8	41.2	40.5	43.5
M_w/M_n	7.97	4.08	7.61	7.17	6.99

i) Data taken from compression moulded sheet.
ii) Blend data from compounded compression moulded sheet.

TABLE 5.4: Molecular weight data for HDPE-F blends.

	ADDITION LEVELS IN MDPE-A (wt%)					
	MDPE-A	**2**	**5**	**10**	**20**	**HDPE-B**
MFR (g/10min)	2.84	2.90	3.03	3.40	3.1	26.2
MMI (%)	24.1	24.3	25.6	25.2	25.0	14.5
M_n (x10^4)	1.48	1.44	1.45	1.73	1.40	1.12
M_w (x10^4)	11.8	11.0	11.0	9.80	9.70	5.94
M_z (x10^4)	53.4	45.9	44.1	32.2	35.6	19.3
M_w / M_n	7.97	7.64	7.58	5.66	6.93	14.5

i) MFR and Molecular weight values of blends, from pipe except HDPE-B (pellets).

TABLE 5.5: M.F.R and Molecular weight variations in HDPE-B pipe blends.

	ADDITION LEVELS IN MDPE-A (wt%)					
	MDPE-A	**2**	**5**	**10**	**20**	**HDPE-M**
MFR (g/10min)	2.84	2.68	2.40	2.20	1.70	0.14
MMI (%)	24.1	28.5	33.4	36.9	41.6	17.9
M_n (x10⁴)	1.42	1.59	1.42	1.34	1.41	1.32
M_w (x10⁴)	8.4	12.5	11.6	12.6	12.0	23.5
M_z (x10⁴)	24.1	54.3	49.6	59.6	52.5	109.0
M_w / M_n	5.91	7.86	8.17	9.40	8.50	17.8

i) MFR and Molecular weight values of blends, from pipe except HDPE-M (pellets).

TABLE 5.6: M.F.R and Molecular weight variations in HDPE-M pipe blends.

	ADDITION LEVELS IN MDPE-A (wt%)					
	MDPE-A	**2**	**5**	**10**	**20**	**MDPE-P**
MFR (g/10min)	2.84	2.77	2.68	2.67	2.37	0.67
MMI (%)	24.1	24.7	29.7	30.7	37.1	41.2
M_n (x10^4)	1.42	1.55	1.45	1.43	1.25	0.97
M_w (x10^4)	8.4	10.6	11.5	10.7	9.7	17.0
M_z (x10^4)	24.1	41.4	44.5	43.4	44.5	89.5
M_w / M_n	5.91	6.84	7.93	7.48	7.76	7.87

i) MFR and Molecular weight values of blends, from pipe except MDPE-P (pellets).

TABLE 5.7: M.F.R and Molecular weight variations in MDPE-P pipe blends.

	ADDITION LEVELS IN MDPE-A (wt%)					
	MDPE-A	**2**	**5**	**10**	**20**	**MDPE-D**
MFR (g/10min)	2.84	2.84	2.83	2.85	2.85	2.98
MMI (%)	24.1	22.9	24.6	24.3	22.2	25.1
M_n (x10⁴)	1.42	1.28	1.45	1.50	1.50	1.32
M_w (x10⁴)	8.4	9.8	10.7	10.4	10.4	10.4
M_z (x10⁴)	24.1	43.8	43.3	39.2	37.2	42.3
M_w / M_n	5.91	7.65	7.38	6.93	6.93	7.87

i) MFR and Molecular weight values of blends, from pipe except MDPE-D (pellets).

TABLE 5.8: M.F.R and Molecular weight variations in MDPE-D pipe blends.

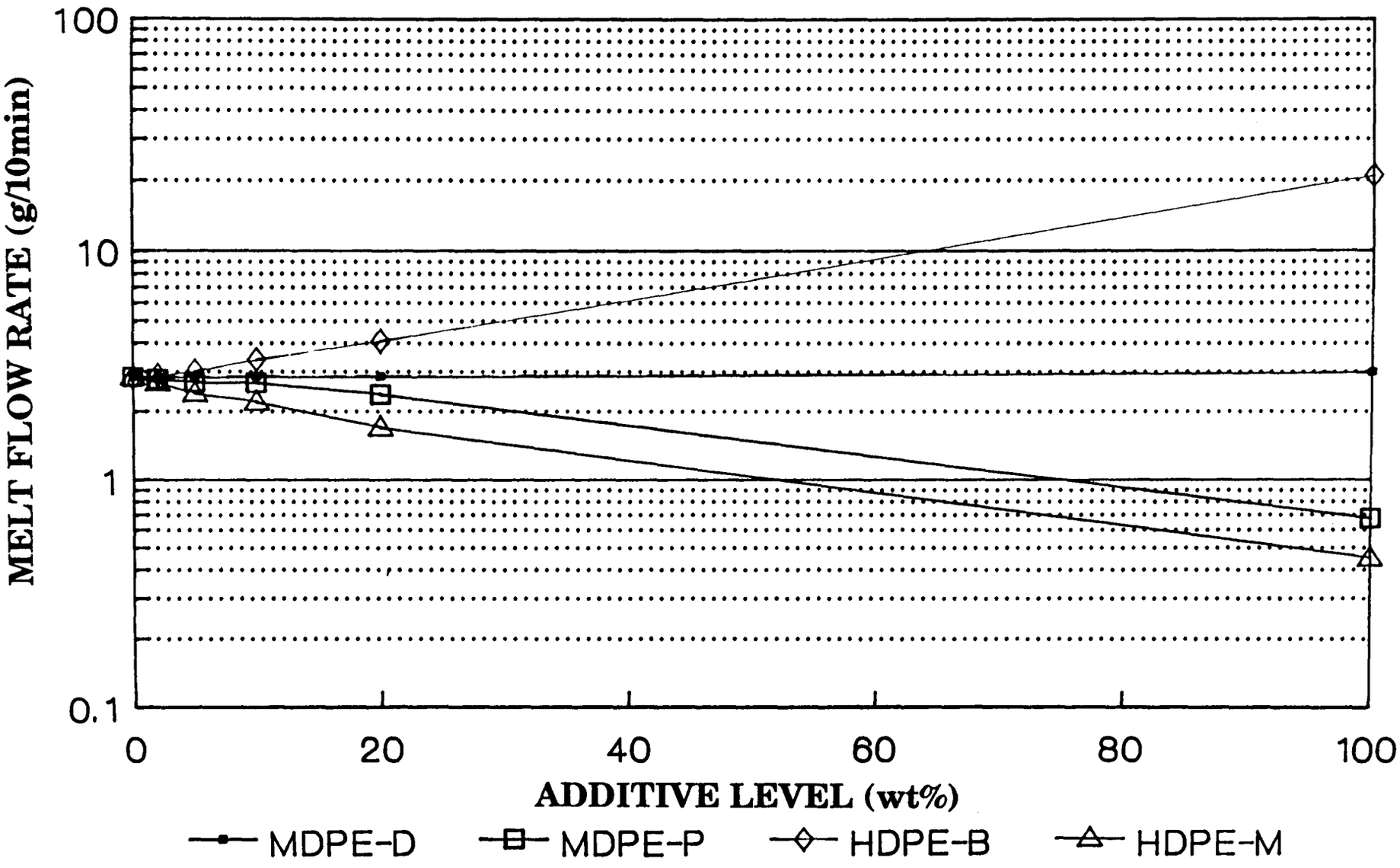

FIGURE 5.8: Melt flow rate variations in 55mm pipe blends.

	ADDITIVE LEVEL IN MDPE-A (wt%)				
	MDPE-A	**2**	**10**	**20**	**HDPE-F**
TENSILE MODULUS (MPa)	496	443	475	536	1044
YIELD STRESS (MPa)	16.55	16.17	16.88	18.66	27.43

i) Data taken from compression moulded sheet.
ii) Blend data from compounded compression moulded sheet.

TABLE 5.9: Short term mechanical data for HDPE-F blends.

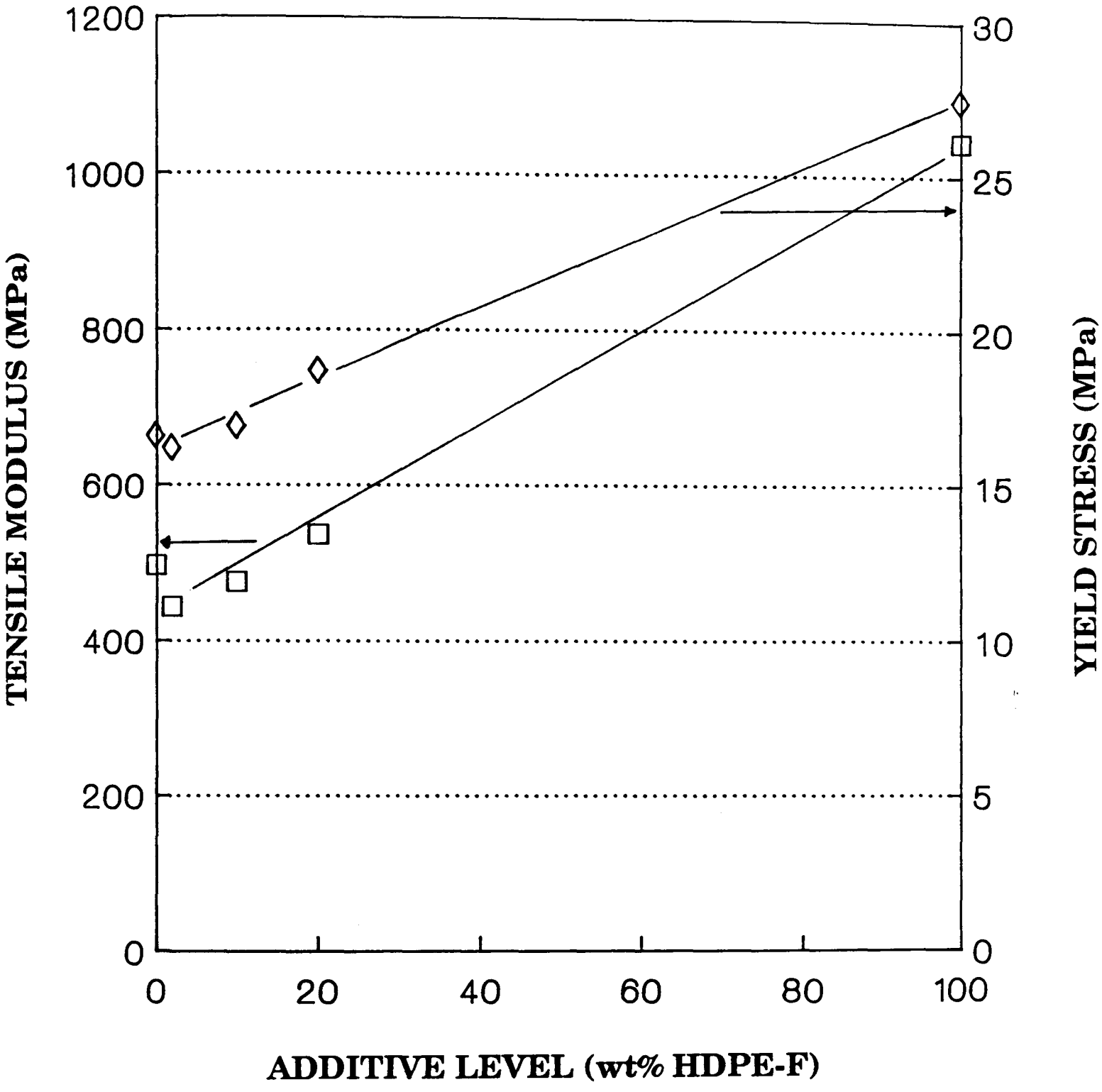

FIGURE 5.9: Tensile modulus and yield stress curves for HDPE-F compounded blends (from compression moulded samples).

		COMPOUNDED PIPE			UNCOMPOUNDED PIPE			
	MDPE-A	**2**	**10**	**20**	**2**	**10**	**20**	**HDPE-F**
IMPACT ENERGY (kJ/m^3)	24.99	23.25	25.66	25.72	26.05	25.69	26.60	26.49
STANDARD DEVIATION (kJ/m^3)	0.46	2.55	0.87	1.24	1.44	0.88	1.76	1.35

i) Impact energy values from pipe pressed into compression moulded sheets. Except HPDE-F (pellets).
ii) Impact energy values are the average of 6 samples.

TABLE 5.10: Impact data for compounded and uncompounded blends.

brittle fracture surface texture.

5.4 STRESS RUPTURE PERFORMANCE OF BLENDED PIPES

5.4.1 UNCOMPOUNDED AND COMPOUNDED BLENDS OF HDPE-F AND MDPE-A MATERIALS

The first line of work involved the investigation into the influence of precompounding the blends on the stress rupture performance of 32mm pipe. These results are displayed in Table 5.11 and plotted in Figure 5.10. All the data are from brittle failures. What can be seen is a dramatic fall off in stress rupture performance at 80°C. Using the average times shown in Table 5.11 there is a 14% reduction in performance with uncompounded blends at 2wt% with an incredible 90% fall off in performance for compounded blends at the same weight percent. However at 20wt% both uncompounded and compounded blends illustrate similar failure lifetime with a 99% decrease in performance. The great change in the stress rupture performance of the HDPE-F blends is in stark contrast to the good short term mechanical properties of the blends shown in Figure 5.9.

5.4.2 STRESS RUPTURE PERFORMANCE OF 32mm HDPE-B AND HDPE-M BLENDS

The dramatic performance changes associated with the addition of the HDPE-F material to the MDPE-A resin was compared to blends of MDPE-A with 10wt% of HDPE-M and HDPE-B materials. Table 5.11 (for 32mm pipes produced from uncompounded blends) shows the stress rupture performance with the addition of these HDPE resins. Figure 5.11 graphically illustrates these materials in comparison with the 10wt%

SAMPLE	FAILURE TIME (hrs)		MEAN FAILURE TIME (hrs)
MDPE-A/32	>15,000		>15,000
HDPE-F/2	15,000 13,739 13,035	14,197 12,060 9,577	12,935
HDPE-F/10	14,095 3,108 1,645	5,576 2,942 366	4,622
HDPE-F/20	226 236 187	237 160 246	215
CHDPE-F/2	1,998 2,663 866	1,655 1,454 871	1,584
CHDPE-F/10	365 258 311	202 193 360	281
CHDPE-F/20	208 155 130	161 157 121	155
HDPE-B/10/32	469 536 835	685 1,596 469	765
HDPE-M/10/32	1,132 1,426 5,199	2,132 4,388 >6,000	>3379

TABLE 5.11: Unnotched HDPE-F, HDPE-B and HDPE-M 32mm pipe stress rupture results at 80°C and 0.955MPa pressure.

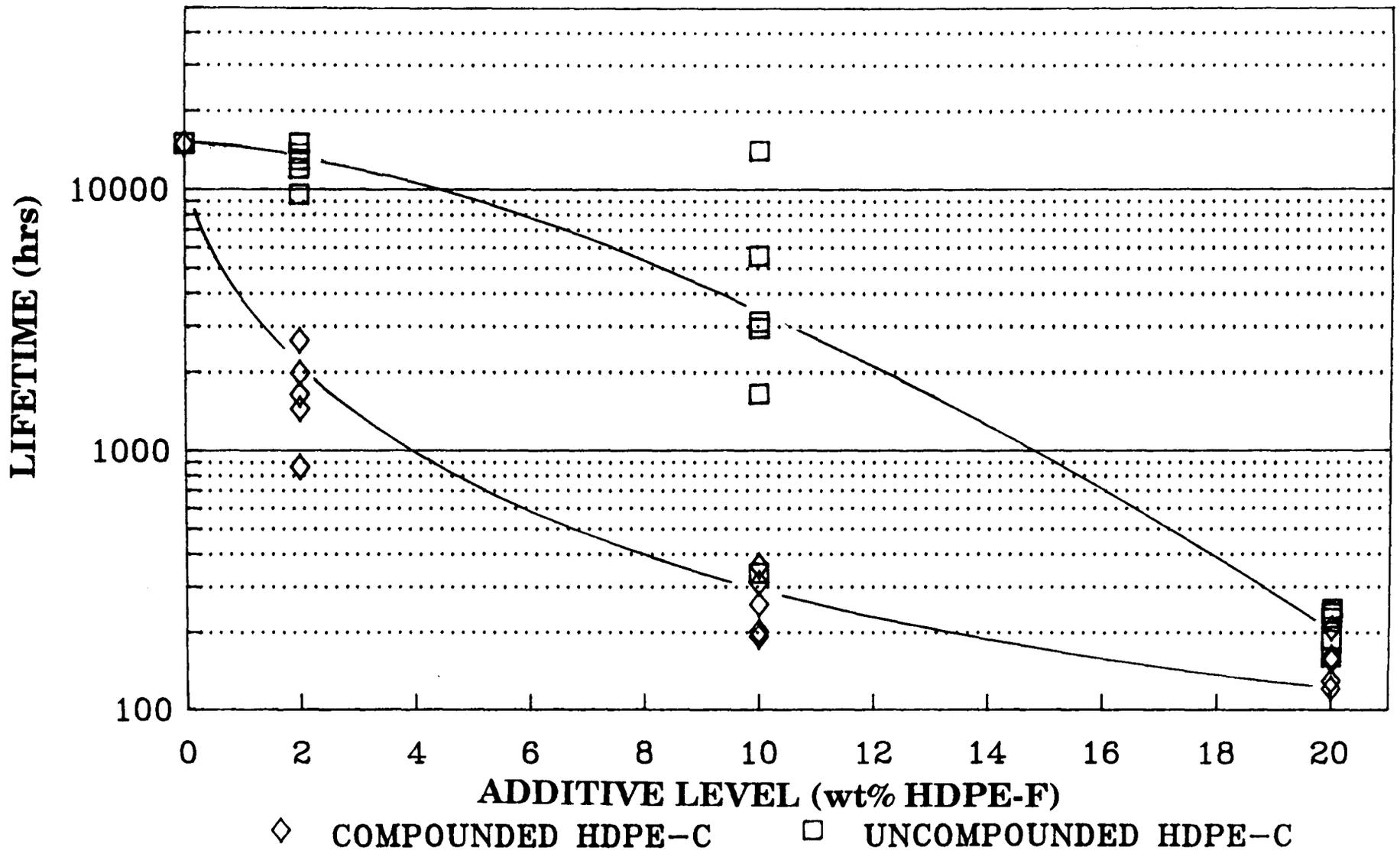

FIGURE 5.10: 80°C stress rupture curves for 32mm HDPE-F compounded and uncompounded pipe blends.

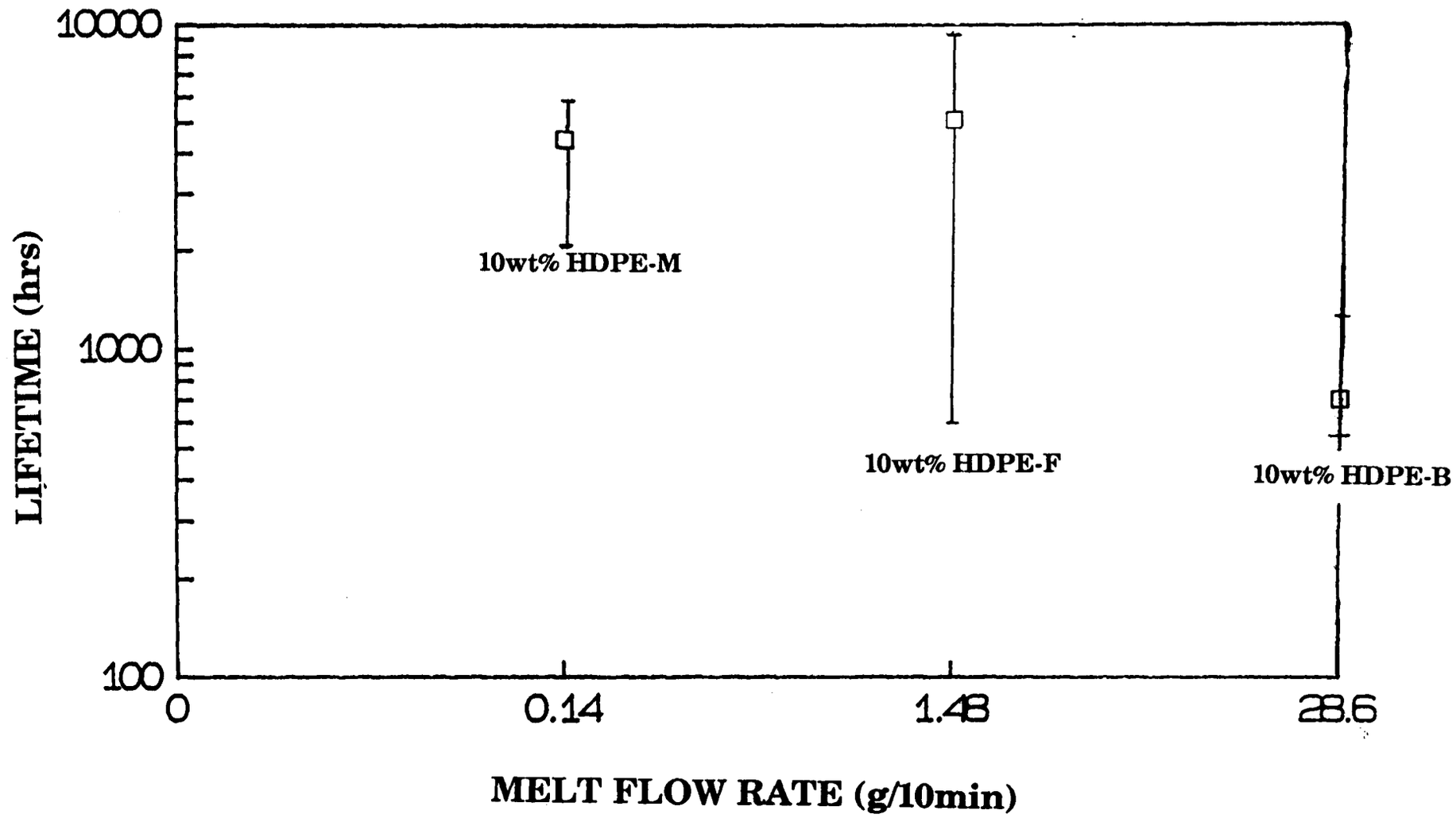

FIGURE 5.11: Stress rupture lifetime variations in 32mm pipe blends as a function of melt flow rate.

HDPE-F blend lifetimes as a function of melt flow rate of the base resin with the added polymer. The graph shows how molecular weight, to a degree, influences the fall off in stress rupture performance. However these results show that regardless of a large change in molecular weight of the additive, there still remains a disturbing decrease in 80°C stress rupture lifetime of the MDPE-A resin with the addition of a second phase.

5.4.3 STRESS RUPTURE PERFORMANCE OF 32mm NOTCHED PIPE BLENDS

Notching has been used as a means of pipe quality control [4] and has been shown to lower the overall failure time of the pipe product under stress rupture conditions [107]. This was seen as a valid route by which to evaluate the stress rupture performance of the 32 and 55mm pipe blends in reasonable test times.

Initially comparisons between unnotched and notched 32mm pipe lifetimes were made using HDPE-F uncompounded blends. Table 5.12 shows the stress rupture lifetimes of notched and unnotched pipe while Figure 5.12 illustrates their relationship with one another in graphical form. Unfortunately no notch data was available for the MDPE-A material due to limited samples. Figure 5.12 illustrates the fact that notching produces a decrease in performance of the blends but its influence on the pipe decreases as the additive addition is increased. The data from Table 5.12 shows that at greater additive addition levels the blend material became less notch sensitive and the failure times were comparable with the unnotched data (Figure 5.12). This was evident in several samples where some of the data originated from pipe failures remote from the notch, especially at high blend

SAMPLE	NOTCH FAILURE TIME (hrs)		MEAN FAILURE TIME (hrs)
MDPE-A/32	-		-
HDPE-F/2	4,376 4,709 4,851	6,435 6,916	5,269
HDPE-F/10	1,654 977	1,598* 948	1,294
HDPE-F/20	125 322 243	216 269 213	231
CHDPE-F/2	-		-
CHDPE-F/10	408* 177* 127	318 359* 168*	259
CHDPE-F/20	141 88 121	118 68 50	97

* Pipe Failure.

TABLE 5.12: Notched HDPE-F 32mm pipe stress rupture results at 80°C and 0.955MPa internal gauge pressure.

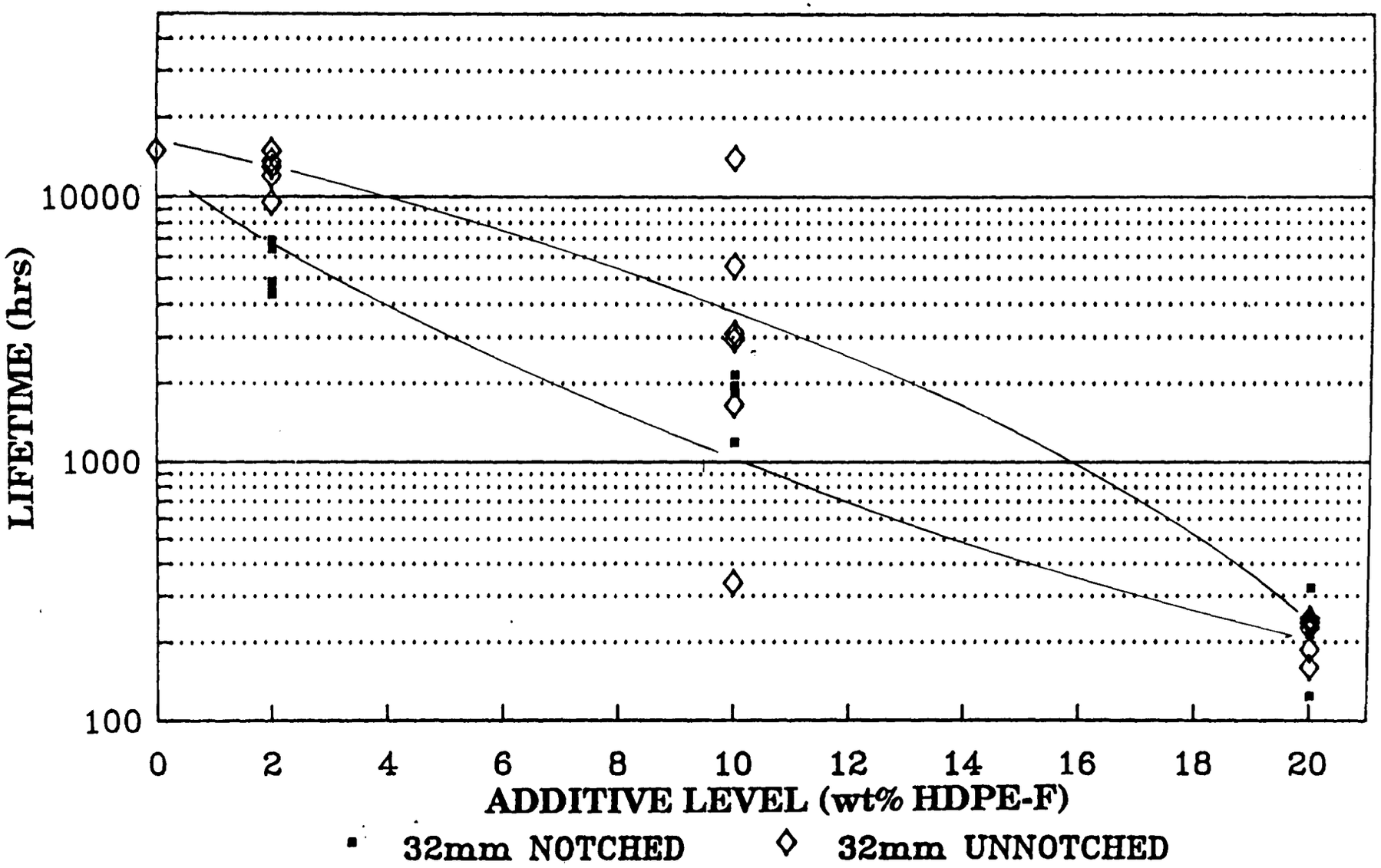

FIGURE 5.12: 80°C stress rupture lifetime of HDPE-F 32mm notched and unnotched uncompounded pipe blends.

additions (Table 5.12).

Therefore from the results discussed above, the use of notching provided a means of assessing trends in blend quality at reasonable failure times. However the results show that care must be taken in interpreting notch pipe lifetime data.

5.4.4 STRESS RUPTURE PERFORMANCE OF 55mm PIPE BLENDS

Figure 5.13 is a graphical presentation of the mean lifetime data recorded in Tables 5.13 - 5.16 which is for blended pipe tested at 0.9 MPa pressure at 80°C. This graph is characteristic of the trends displayed by the blends at all pressure levels (Figures 5.14 - 5.17). The distinguishing feature of Figure 5.14 is that the additives that use hexene as a comonomer (MDPE-P, HDPE-M and HDPE-B) all caused a deleterious effect on the base material, whereas the additive with octene as its comonomer had very little influence on pipe lifetime over the whole additive range investigated.

One unusual variation in the data appears to be the curve exhibited by the MDPE-P blends. Figure 5.16 shows a minima in lifetime occurring about 5wt% and then increasing to MDPE-A performance levels at 20wt% at all pressure levels.

Figures 5.14 and 5.15 show the expected variation of the HDPE pipe blends tested at pressures of 0.7, 0.8 and 0.9 MPa. However this is not repeated in Figures 5.16 and 5.17 for the MDPE pipe blends where the 0.8 MPa data overlaps the 0.7 MPa data. The 0.8 MPa samples were the last to be notched prior to testing. What could be seen in Figures 5.16 and 5.17 is the

ADDITIVE LEVEL (wt% in MDPE-A)	0.7MPa			0.8MPa			0.9MPa		
	NOTCH FAILURE TIME (hrs)		MEAN TIME (hrs)	NOTCH FAILURE TIME (hrs)		MEAN TIME (hrs)	NOTCH FAILURE TIME (hrs)		MEAN TIME (hrs)
0	777 1,201	1,496 1,695	1,292	658 1,933	1,530 2,189*	1,577	385 351	345 511	398
2	-	-	-	-	-	-	340 257	263	286
5	663 534	698 212	527	506 339	575 164	396	92 163	131 153	135
10	-	-	-	-	-	-	104 176	167	149
20	62 145	171	126	97 116	132 156	125	34 61	61 59	54

* Pipe failure

TABLE 5.13: 80°C Stress rupture data for HDPE-B blends at 0.7, 0.8 and 0.9MPa pressure.

ADDITIVE LEVEL (wt% in MDPE-A)	0.7MPa			0.8MPa			0.9MPa		
	NOTCH FAILURE TIME (hrs)		MEAN TIME (hrs)	NOTCH FAILURE TIME (hrs)		MEAN TIME (hrs)	NOTCH FAILURE TIME (hrs)		MEAN TIME (hrs)
0	777 1,201	1,496 1,695	1,292	658 1,933	1,530 2,189*	1,577	385 351	345 511	398
2	-	-	-	-	-	-	427 241	332 289	322
5	652 1,113	803 1,246	953	664 688	1,156 914*	855	163 297	175 226	215
10	-	-	-	-	-	-	160 157	176 197	172
20	979 1,174	606	919	170 180	300 230	220	140 110	107 132	122

* Pipe failure

TABLE 5.14: 80oC Stress rupture data for HDPE-M blends at 0.7, 0.8 and 0.9MPa pressure.

ADDITIVE LEVEL (wt% in MDPE-A)	0.7MPa NOTCH FAILURE TIME (hrs)		MEAN TIME (hrs)	0.8MPa NOTCH FAILURE TIME (hrs)		MEAN TIME (hrs)	0.9MPa NOTCH FAILURE TIME (hrs)		MEAN TIME (hrs)
0	777 1,201	1,496 1,695	1,292	658 1,933	1,530 2,189*	1,577	385 351	345 511	398
2	-	-	-	-	-	-	293 209	313 421	309
5	710 975	570 486	685	1,101 1,074	624 1,674	1,118	255 313	216	261
10	-	-	-	-	-	-	626 595		610
20	1,179 948	682 977	946	>1,900 >1,900	1,544 1,376	>1,680	318 385	304	335

* Pipe failure

TABLE 5.15: 80oC Stress rupture data for MDPE-P blends at 0.7, 0.8 and 0.9MPa pressure.

ADDITIVE LEVEL (wt% in MDPE-A)	0.7MPa NOTCH FAILURE TIME (hrs)		MEAN TIME (hrs)	0.8MPa NOTCH FAILURE TIME (hrs)		MEAN TIME (hrs)	0.9MPa NOTCH FAILURE TIME (hrs)		MEAN TIME (hrs)
0	777 1,201	1,496 1,695	1,292	658 1,933	1,530 2,189*	1,577	385 351	345 511	398
2	-	-	-	-	-	-	481 450	667 693	573
5	1,461 1,297	1,629 1,007	1,348	>2,200		>2,200	342 353	306 384	346
10	-	-	-	-	-	-	562 440	603 450	513
20	1,423 1,438	1,852 1,231	1,486	2,182 1,843	1,197 1,600	1,705	338 338	342 410	345

* Pipe failure

TABLE 5.16: 80oC Stress rupture data for MDPE-D blends at 0.7, 0.8 and 0.9MPa.

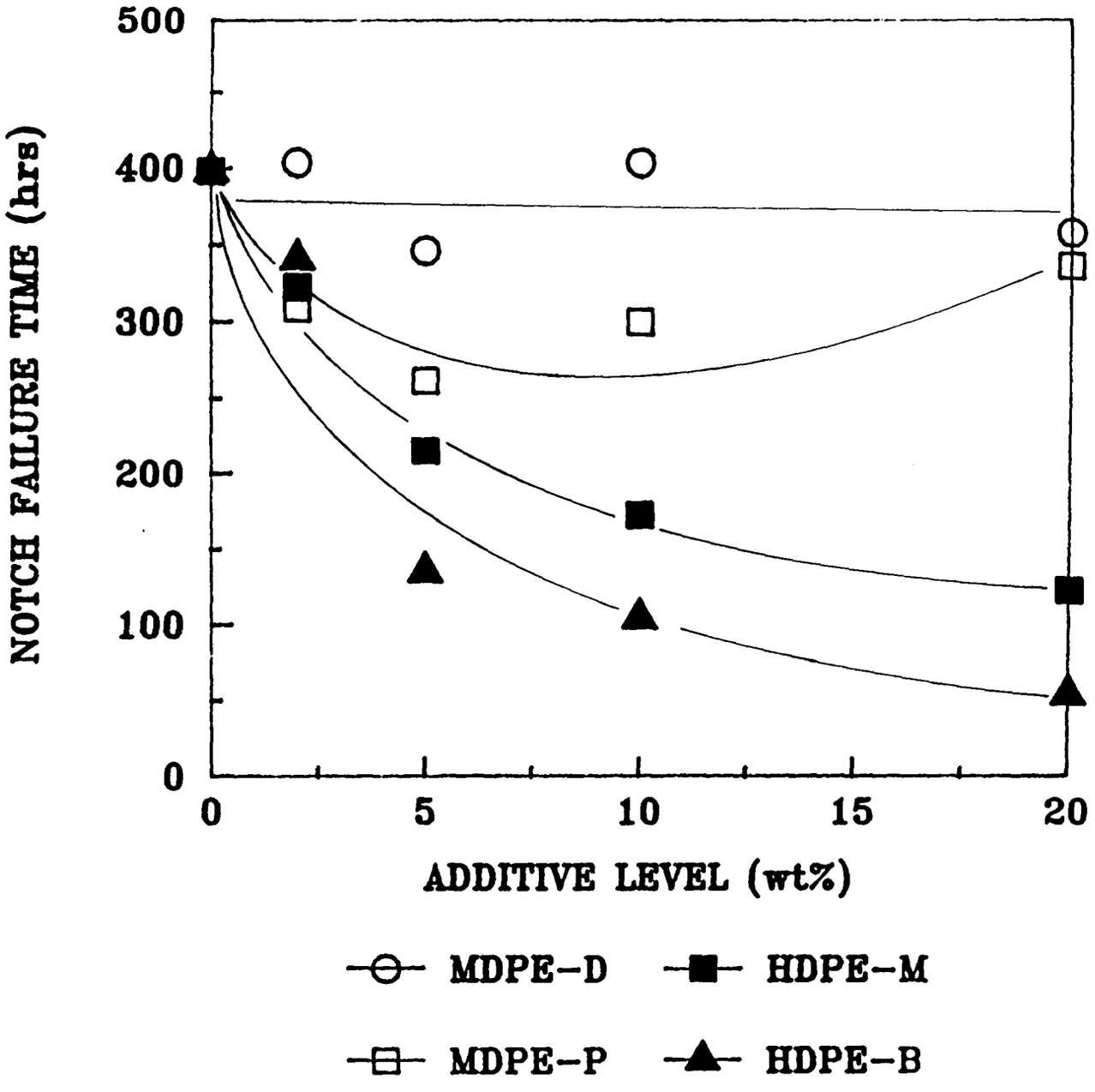

FIGURE 5.13: 80°C stress rupture lifetime of 55mm pipe blends at 0.9MPa pressure.

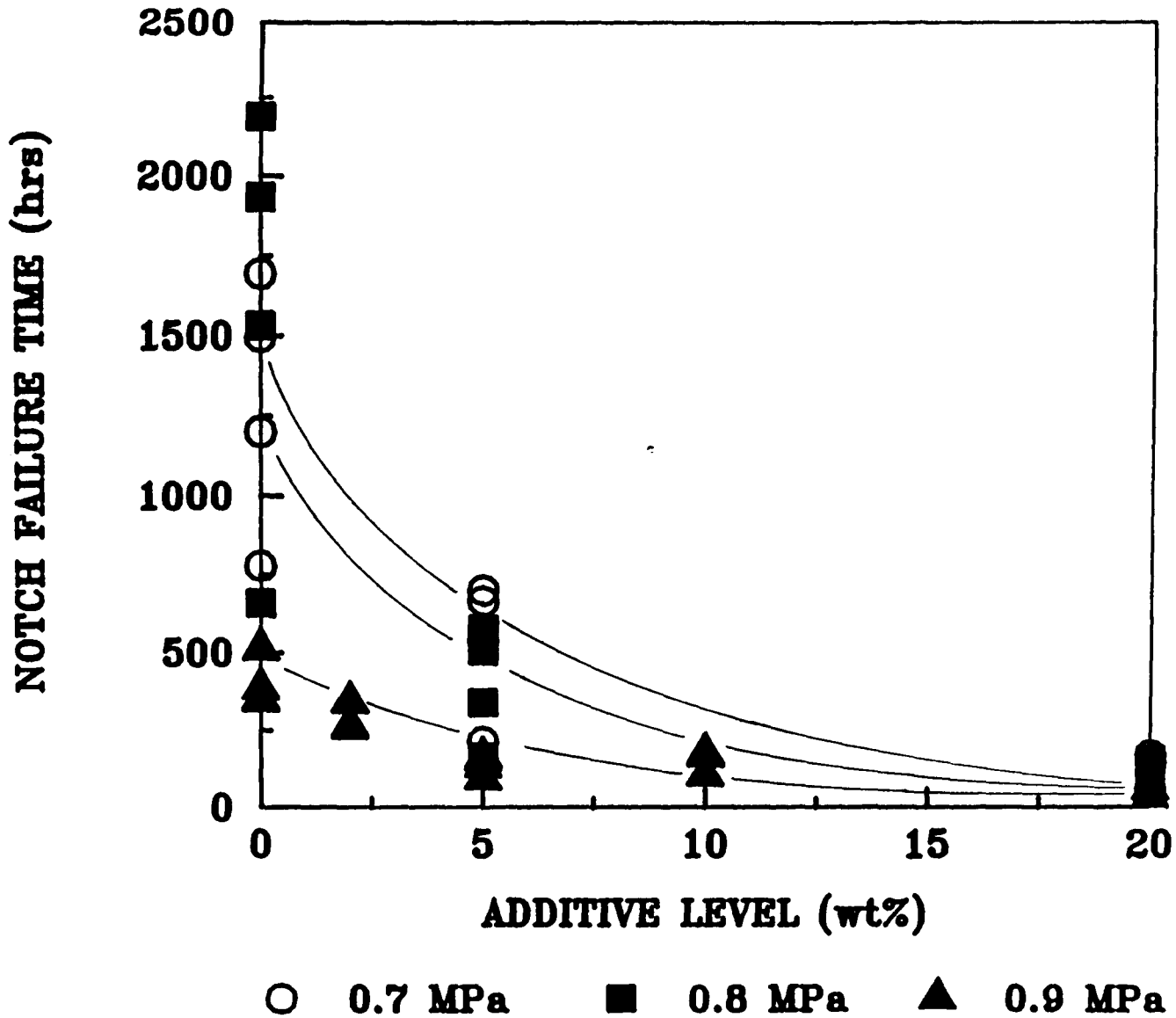

FIGURE 5.14: 80°C stress rupture lifetimes of HDPE-B 55mm pipe blends.

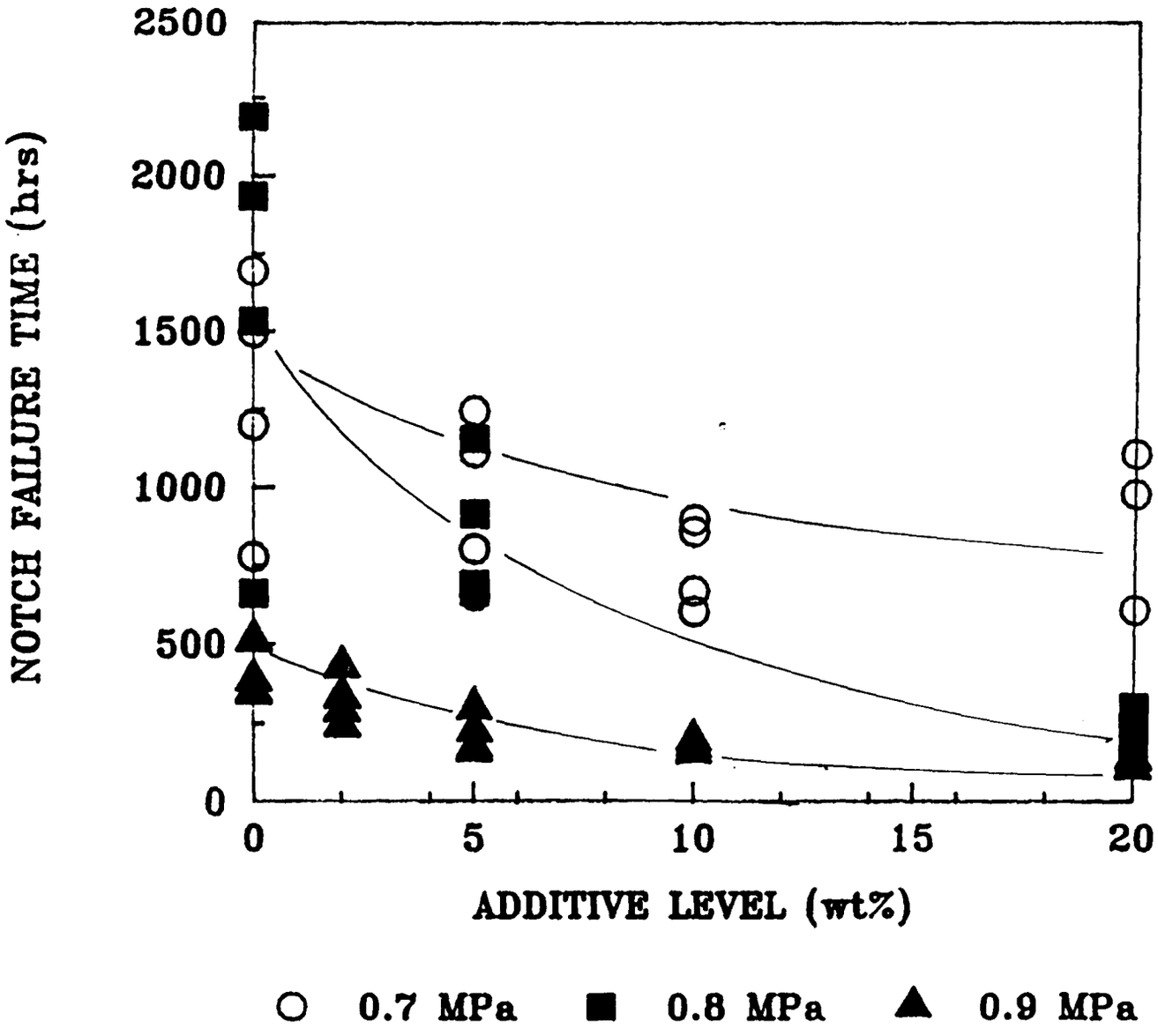

FIGURE 5.15: 80°C stress rupture lifetimes of HDPE-M 55mm pipe blends.

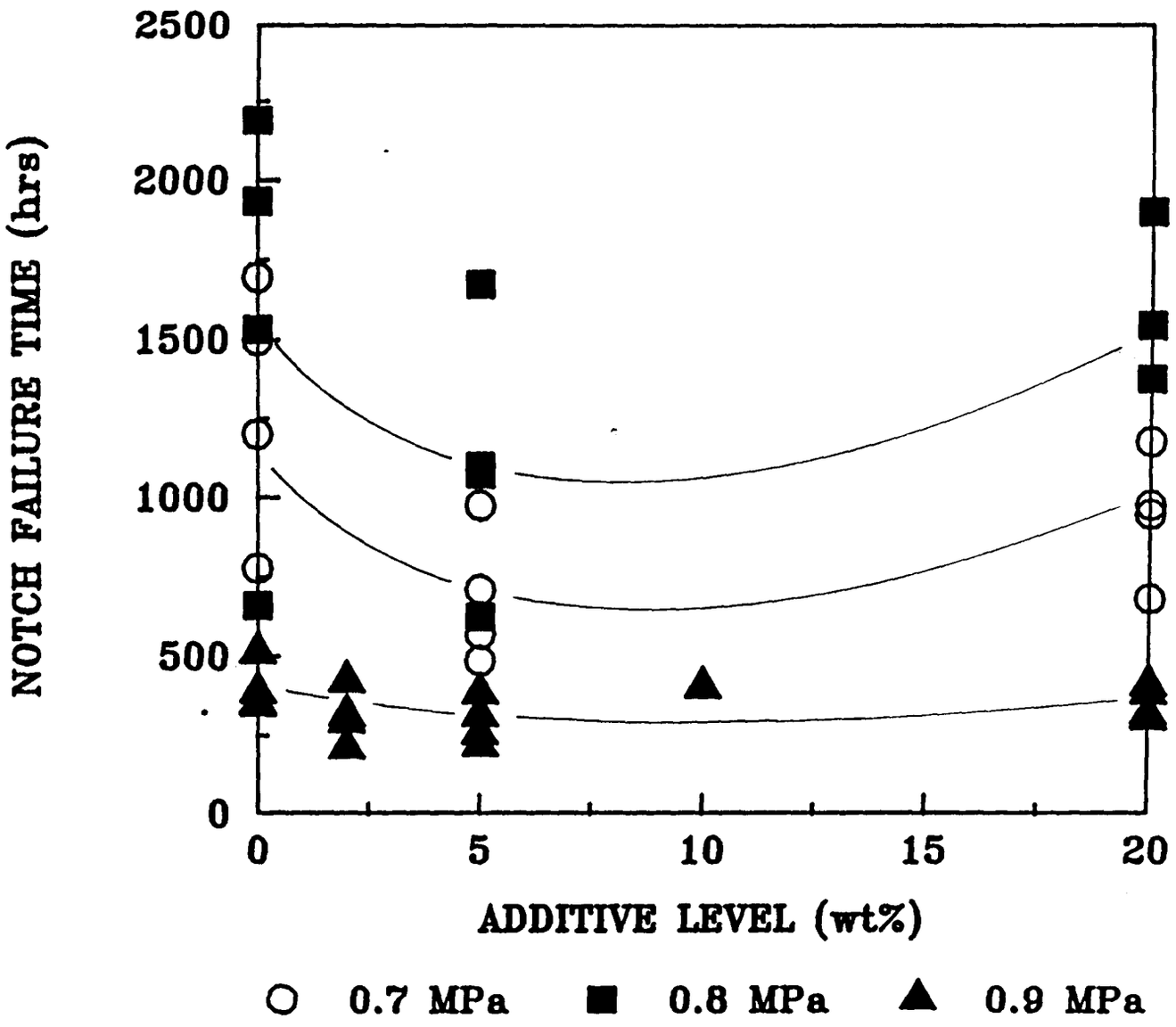

FIGURE 5.16: 80°C stress rupture lifetimes of MDPE-P 55mm pipe blends.

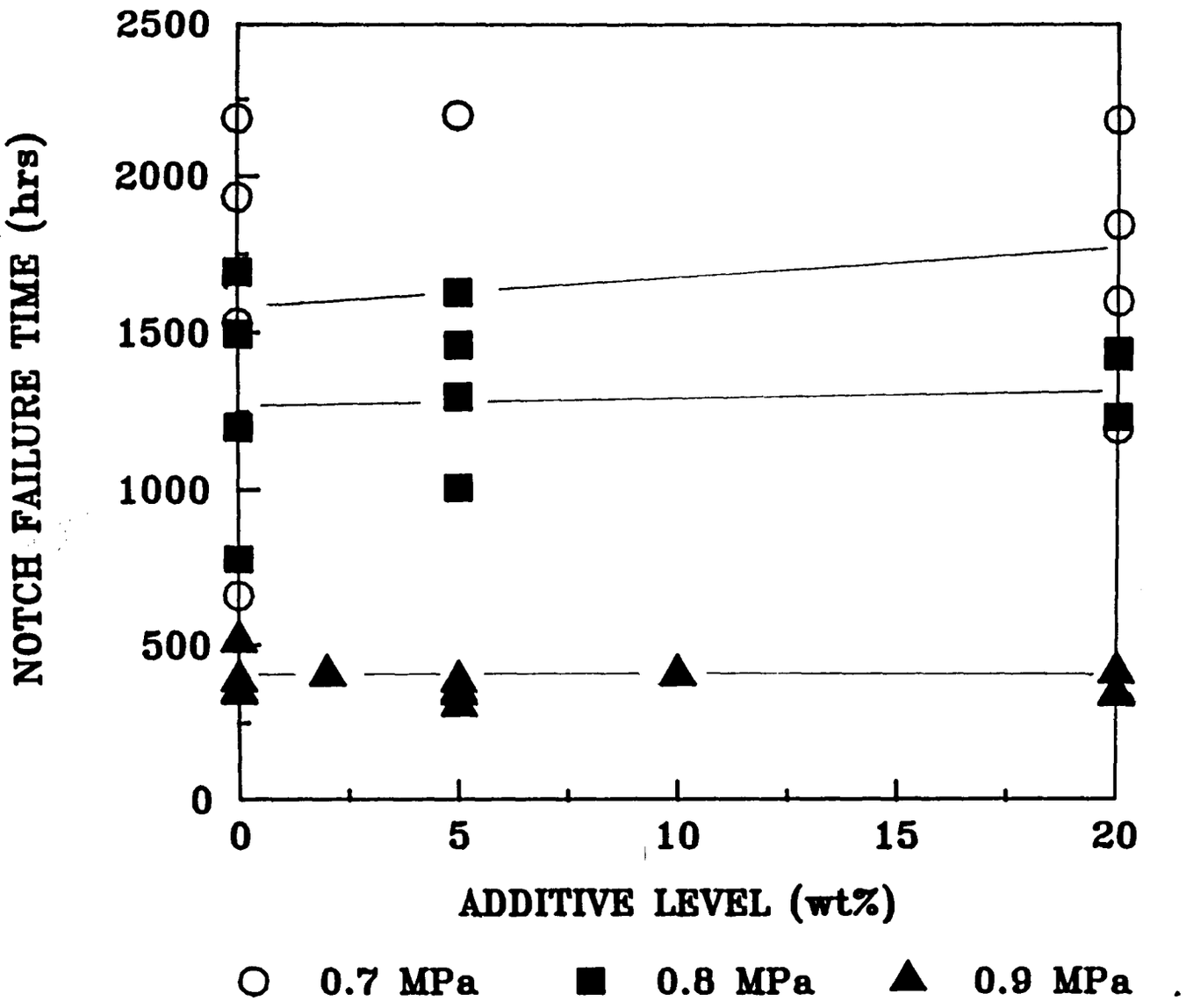

FIGURE 5.17: 80°C stress rupture lifetimes of MDPE-D 55mm pipe blends.

influence of notch blunting on the specimens from a cutter that was used for all the notched samples in this study. This area will be further discussed in Chapter 7.

5.5 DISCUSSION

5.5.1 SHORT AND LONG TERM PERFORMANCE OF HDPE-F BLENDS

The good short term mechanical properties of HDPE-F blends were in stark contrast to the poor long term stress rupture performance of the blends outlined in section 5.4. The results emphasize the need to test the pipe product correctly in order to distinguish its long term behaviour in the ground.

The differences in performances between uncompounded and compounded blends shows that precompounding of the materials does not offer any advantage over mixing in the hopper. The extra distribution of the two components by twin screw compounding affects the stress rupture behaviour to the degree that the blends at 2wt% reduced the performance by 90% compared to 14% for the uncompounded blends. These changes in failure times were reflected in the fracture surface features and the morphology. These areas are more fully discussed in Chapters 6 and 7.

The stress rupture testing of HDPE-M and HDPE-B blends at 10wt% confirmed the trends exhibited by HDPE-F blends. The addition of HDPE-M and HDPE-F materials to the MDPE-A resin decreased the MFR (which is a guide to molecular weight) as the additive levels were increased (Table 5.6). From the hypothesis outlined in Chapter 1 using the work of Gebler

[14] , it was postulated that 80oC lifetime would increase in a blend in which a higher molecular weight material was added to one of a lower molecular weight. The results do not confirm this hypothesis and shows that the addition of a second polymer with a large high molecular weight tail (HDPE-M, Table 4.1, M_z value) progressively reduced stress rupture performance with increasing additions . This can be illustrated by looking at the molecular weight distribution curves of HDPE-M compared with HDPE- F, showing not only the increased high molecular weight portion of the HDPE-M material but the more significant low molecular weight species (Figure 5.18). What may be happening is that the presence of a low molecular weight species may outweigh the advantage of having a high molecular weight tail. The results here show that molecular weight is only one of may factors contributing to the stress rupture performance of pipe materials [109].

5.5.2 LONG TERM BEHAVIOUR OF 55mm PIPE BLENDS

The results for 55mm pipes continue to show the deleterious influences of blending certain polyethylene materials into pipe grade polyethylene resins. However the MDPE pipe blends proved to be the most interesting showing that the MDPE-D material with octene as its comonomer produced blends that practically maintained the performance levels at increasing additive additions (Figure 5.17). This is in contrast with the MDPE-P material which had hexene as its comonomer. These blends were shown to reduce the stress rupture performance of the MDPE-A base resin up to about 5wt% and then increasing lifetimes up to 20wt% at all test pressure levels. What is enlightening is that the MDPE-D material has a lower high molecular weight tail than the MDPE-P material (Table 4.1). This was also illustrated in Table 5.3 which showed the fractionation results of branching

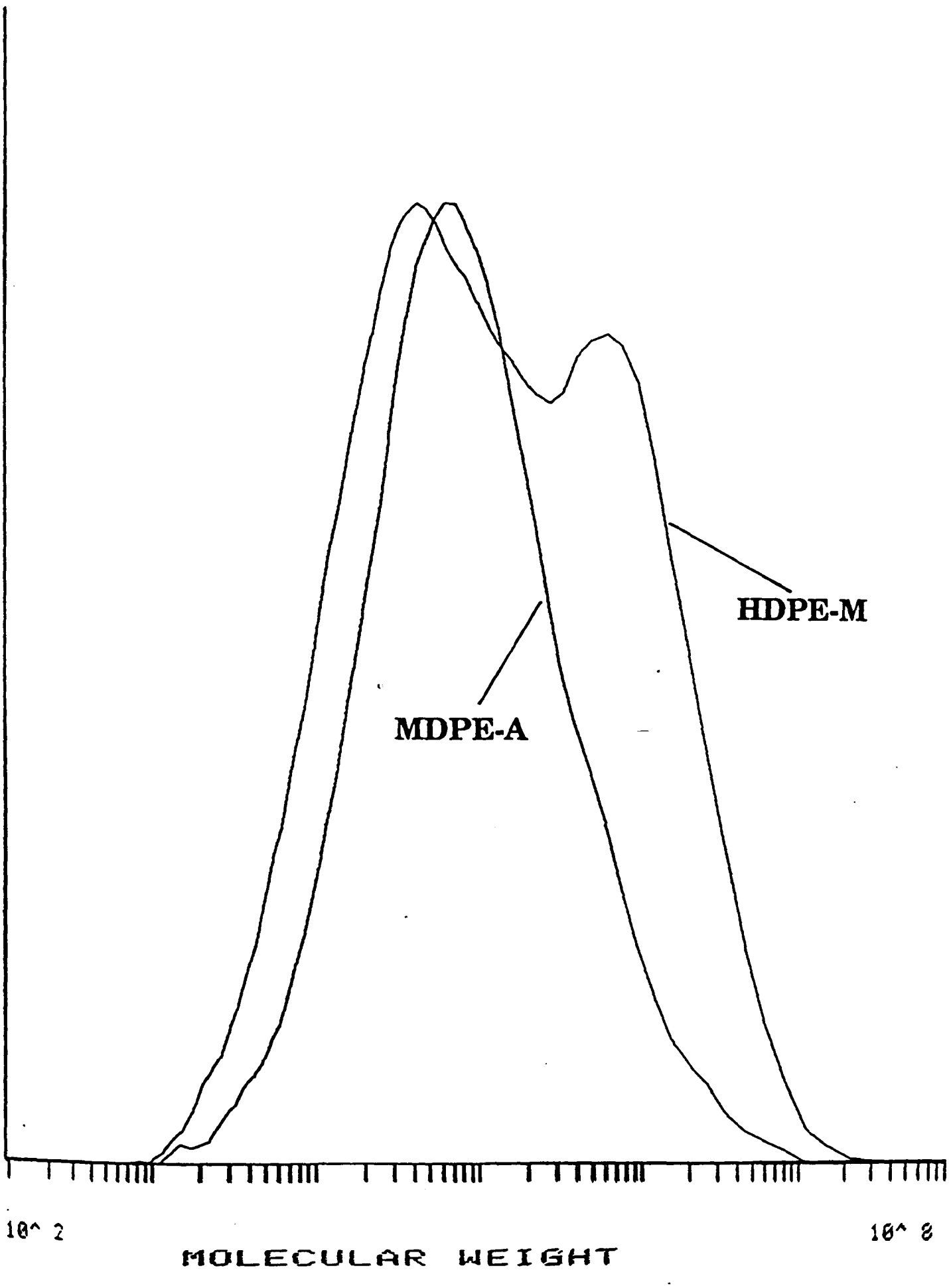

FIGURE 5.18: Molecular weight distributions of MDPE-A and HDPE-M materials.

levels in the MDPE pipe materials. Although the branching levels in the MDPE-P material are higher than the MDPE-D resins, (7.4 branches to 4.8 branches /1000 CH_2), the performance of the MDPE-D blends are overall slightly better than the MDPE-P blends. What we may be observing is the greater influence of longer *short* chain branching than molecular weight on the 80°C brittle lifetimes of these blends; which has been shown by many authors to significantly influence the brittle region of the stress rupture curve [51,79].

5.5.3 CHARACTERIZATION OF PIPE

Although the majority of the HDPE blends severely reduced 80°C performance, a logical reason for this could be based from O.I.T values in Table 4.2. Due to the additives having little stabilization, degradation could have resulted in the blends. The hypothesis would particularly address the HDPE-F compounded blends where the added thermal history (from twin-screw compounding) would have reduced stabilization levels to very low proportions.

Table 5.17 displays the O.I.T values of HDPE-F uncompounded and compounded blends before stress rupture testing, showing the good O.I.T. for all the blends; even in the bore region which for large diameter pipes has been shown to be easily depleted of stabilizer [82]. Table 5.18 shows the values after stress rupture testing for the 55mm pipe blends at 20wt% additive levels showing that even the largest additive additions the O.I.T. values are very good. Thus, the evidence in Tables 5.17 and 5.18 shows that both the 32 and 55mm blended pipes contained sufficient stabilizer to avoid failure due to a depolymerization process [91].

SAMPLE	POSITION	O.I.T (min)
MDPE-A/32	Bore Outside	25.6 27.1
HDPE-F/2	Bore Outside	24.6 25.7
HDPE-F/10	Bore Outside	25.2 27.0
HDPE-F/20	Bore Outside	29.8 29.8
CHDPE-F/2	Bore Outside	19.2 24.5
CHDPE-F/10	Bore Outside	26.7 24.6
CHDPE-F/20	Bore Outside	28.1 26.1

TABLE 5.17: Oxidation induction time of 32mm HDPE-F pipe blends.

SAMPLE	O.I.T (min) 0.7MPa	0.8MPa	0.9MPa
MDPE-A/55	>30	>30	>30
HDPE-B/20	>30	21	>30
HDPE-M/20	>30	20	23
MDPE-P/20	>30	>30	16
MDPE-D/20	>30	>30	>30

i) All samples taken from the bore region of the pipe.

TABLE 5.18: Oxidation induction time values of 55mm pipe blends.

The results of the lifetimes of blended pipes have not supported the simple concept of increasing molecular weight to improve pipe lifetime. We have shown that the presence of a low molecular weight species and different branch sizes and content in an high molecular weight polymer can easily reduce the overall 80°C performance of the base resin. Also the good short term properties obtained from blending polyethylenes are in stark contrast to the stress rupture performance of those blends. However the good short term properties may be a guide to the poor behaviour of these materials under stress rupture conditions. Table 5.2 shows the increasing density of the blends with increases in additive content. It is known that as the density increases the yield stress and modulus increase due to the load bearing capacity of the extra crystalline regions [21]. However, for a fixed molecular weight this usually reduces the tie molecule concentration within the sample which is thought to confer the good toughness characteristics of the sample [110]. From these observations we will proceed in identifying their role in the changes associated with the blending of polyethylenes under 80°C stress rupture conditions.

CHAPTER 6

MISCIBILITY STUDIES

6.1 INTRODUCTION

The previous chapter has shown that by adding HDPE materials to the MDPE-A resin we are in the majority of cases reducing the overall stress rupture performance of the base resin. This chapter presents techniques which were used to evaluate the blending quality of the two polyethylene phases, and whether there was segregation of the components in the blends that led to the drastic changes in 80°C lifetimes of blends when compared to the base MDPE-A resin.

6.2 EVALUATION OF BLEND QUALITY

6.2.1 DYNAMIC MECHANICAL THERMAL ANALYSIS

Section 2.4.3 has outlined the advantages of DMTA as a powerful tool for blend characterization and miscibility determination. Table 6.1 illustrates the results of the measurement of the α and γ peak heights from compression moulded plaques of HDPE-F compounded blends; peaks were evident in the samples for 10 and 20wt% blends. What can be seen is that there is only one peak for the α and γ peaks which changes with increasing additive levels (Figure 6.1). The loss modulus values are also in line with

	ADDITIVE LEVEL IN MDPE-A (wt%)				
	MDPE-A	**2**	**10**	**20**	**HDPE-F**
TEMPERATURE (°C)	-101	-102	-102	-102	-106
TAN δ	0.057	0.049	0.057	0.048	0.082
LOG E (Pa)	9.66	9.63	9.49	9.08	9.04

i) Data taken from compression moulded sheet.
ii) Blend data from compounded compression moulded sheet.

TABLE 6.1: γ peak variation with temperature, tanδ and LogE for HDPE-F blends.

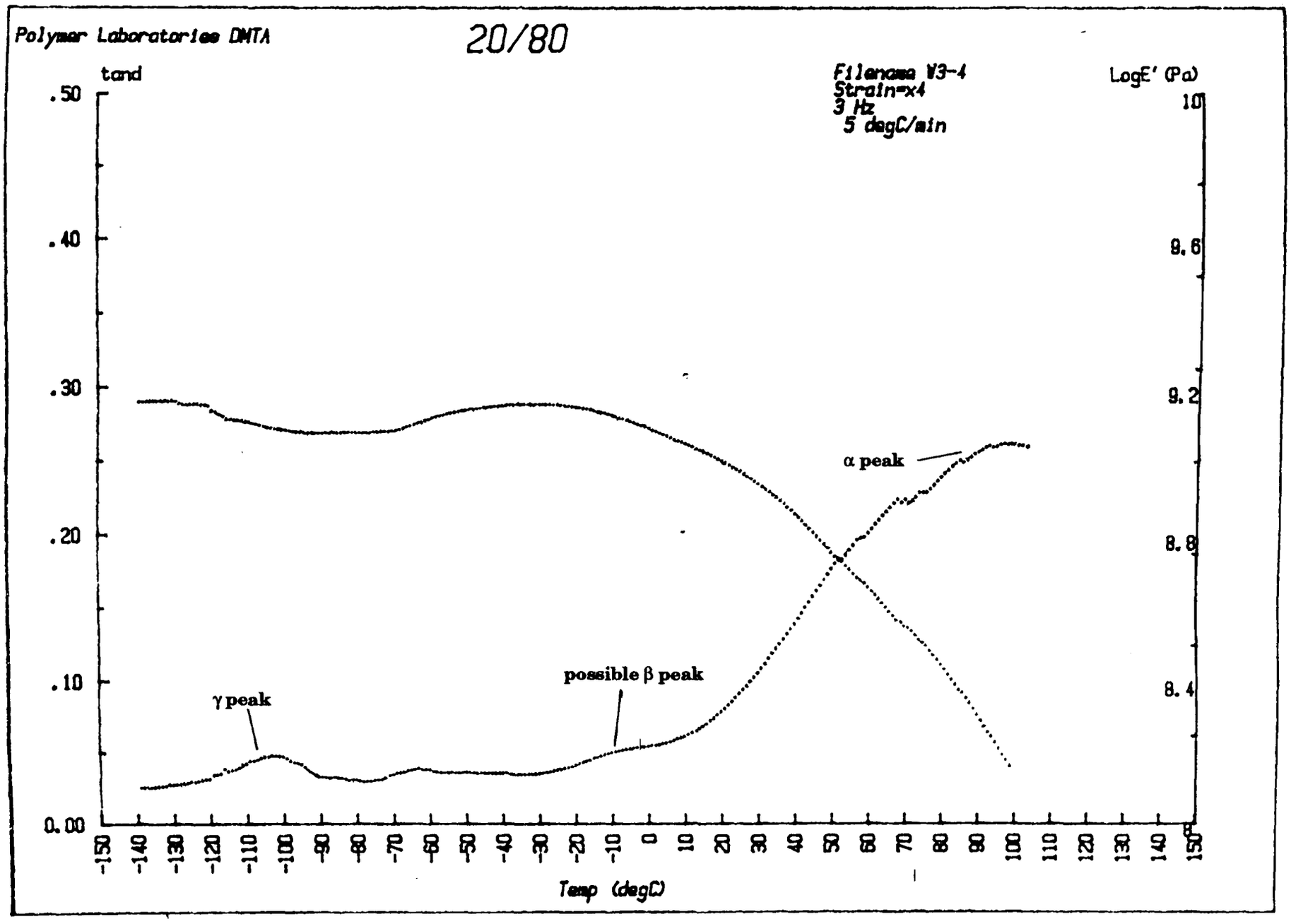

FIGURE 6.1: Typical DMTA curve for a 20wt% compounded HDPE-F blend.

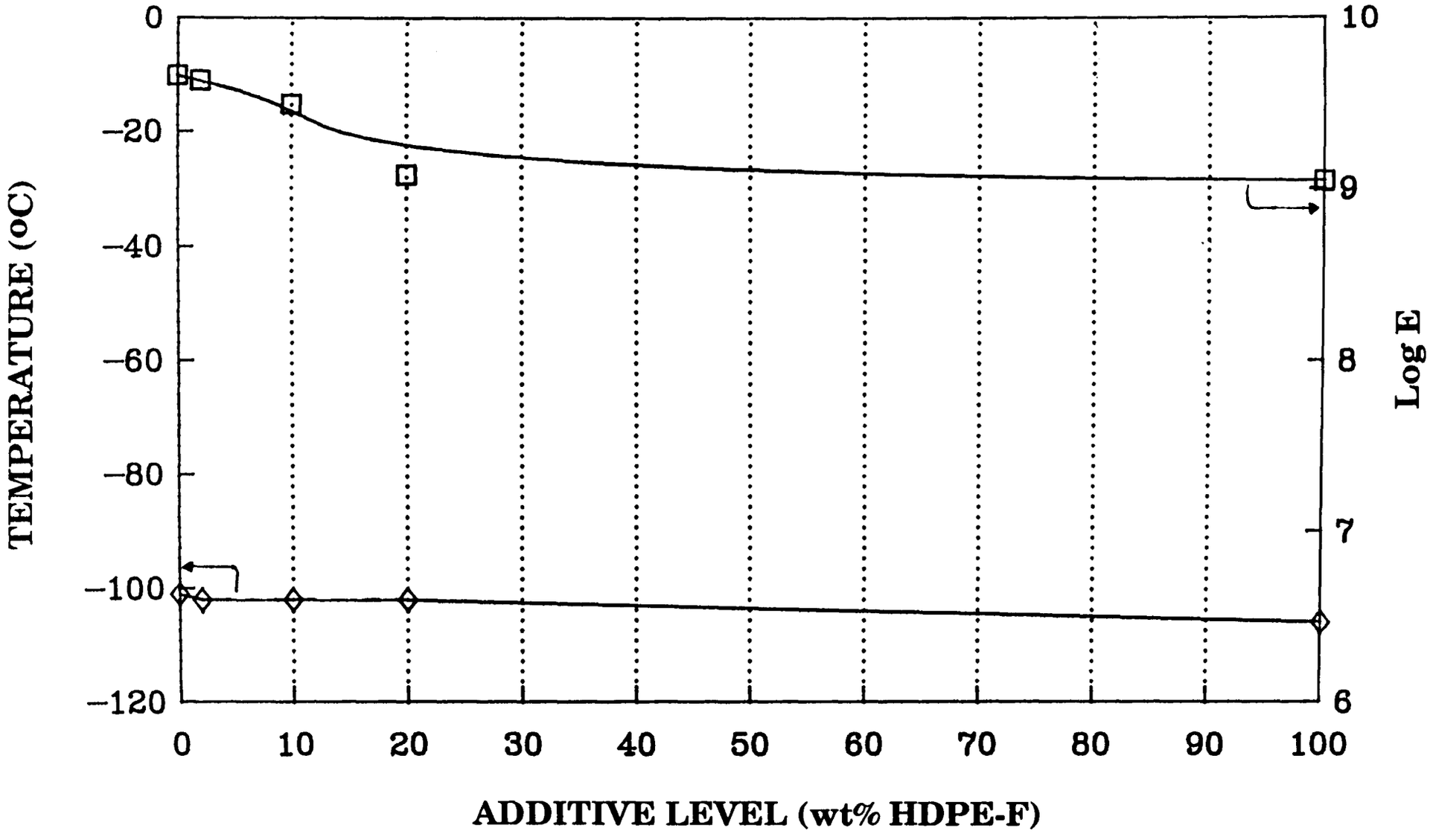

FIGURE 6.2: Temperature and logE variations in HDPE-F compounded blends.

the tensile strength data and reflect the materials overall mechanical properties (Figure 6.2). Therefore this technique has shown that there is no variation in compatibility of the two polyethylene phases and that the materials mixed adequately.

6.2.2 DIFFERENTIAL SCANNING CALORIMETRY

Differential Scanning Calorimetry (DSC) on compression moulded blends supported the work of DMTA, showing single melting and crystallization peaks at all blend addition levels. These are tabulated for HDPE-F blends in Table 6.2. Figure 6.3 and 6.4 illustrates the uniform change in crystallization and melting behaviour of the blends. The influence of the additive is to move the base resins crystallization temperature to higher temperatures. A fast cooling rate was chosen to simulate the cooling conditions experienced by the pipe when it enters the water bath from the molten state. Figure 6.5 illustrates a typical DSC curve still maintaining the characteristic single peak of compatible polymeric blends [44].

The crystallization and melting temperature behaviour of HDPE-M, HDPE-B, MDPE-P AND MDPE-D blends are tabulated in Table 6.3 and graphically presented in Figures 6.6 and 6.7. All the values are from pipe samples prior to testing. Again the interesting observation of these blends is that every one of them exhibited a single peak under heating and cooling regimes showing no major segregation of the two polyethylenes. The values identify the blends in all cases to shift the T_c of the base resin to higher temperatures (Figure 6.7).

	MELTING VALUES			CRYSTALLIZATION VALUES		
	ΔH_h (J/g)	$PEAK_h$ (°C)	$ONSET_h$ (°C)	ΔH_c (J/g)	$PEAK_c$ (°C)	$ONSET_c$ (°C)
MDPE-A	112.4	123.8	117.5	-115.9	109.4	112.3
HDPE-F/2	118.7	124.5	118.7	-111.9	110.8	113.0
HDPE-F/10	128.3	125.2	119.4	-117.3	111.4	113.6
HDPE-F/20	130.9	127.3	118.9	-119.8	111.7	114.5
HDPE-F	185.0	133.3	124.8	-174.8	116.4	119.2

i) Data from compression moulded sheet except HDPE-F (pellets).
ii) Subscript h refers to the heating cycle, c to the cooling cycle.

TABLE 6.2: Heating and crystallization data from HDPE-F compounded blends at a heating rate of 10°C/min.

	MELTING VALUES			CRYSTALLIZATION VALUES		
	ΔH_h (J/g)	$PEAK_h$ (oC)	$ONSET_h$ (oC)	ΔH_c (J/g)	$PEAK_c$ (oCJ/g)	$ONSET_c$ (oC)
MDPE-A	135.8	134.1	113.9	-116.7	74.0	86.6
HDPE-F/2	121.6	132.9	114.5	-111.5	76.9	87.7
HDPE-F/10	132.8	133.3	116.9	-116.2	79.6	88.8
HDPE-F/20	136.3	138.3	116.6	-122.1	76.5	89.1
HDPE-F	190.5	143.7	124.0	-171.5	88.1	98.9

i) Data from compression moulded sheet except HDPE-F (pellets).
ii) Subscript h refers to the heating cycle, c to the cooling cycle.

TABLE 6.3: Heating and crystallization data from HDPE-F compounded blends at a heating rate of 100oC/min.

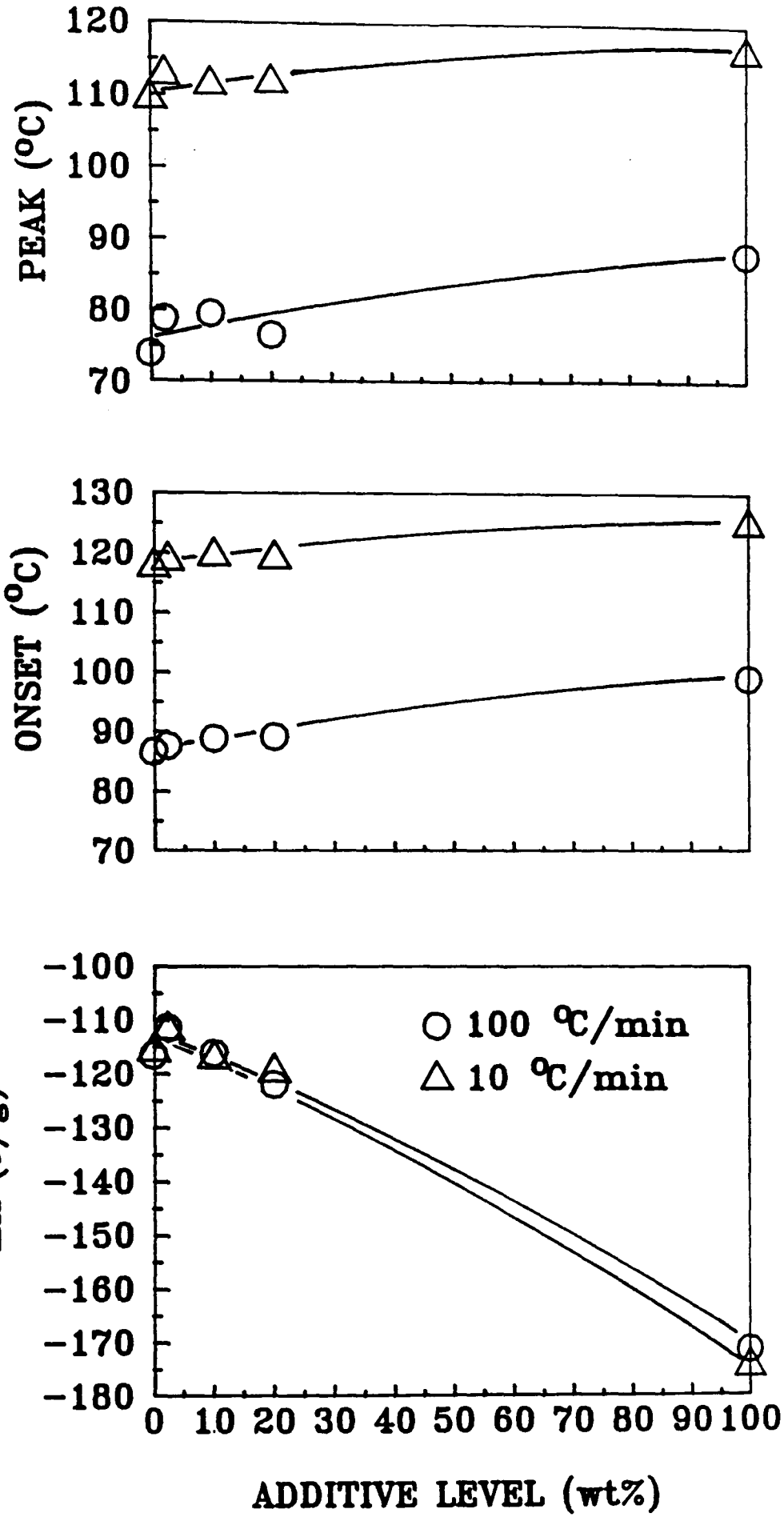

FIGURE 6.3: Crystallization behaviour of HDPE-F blends.

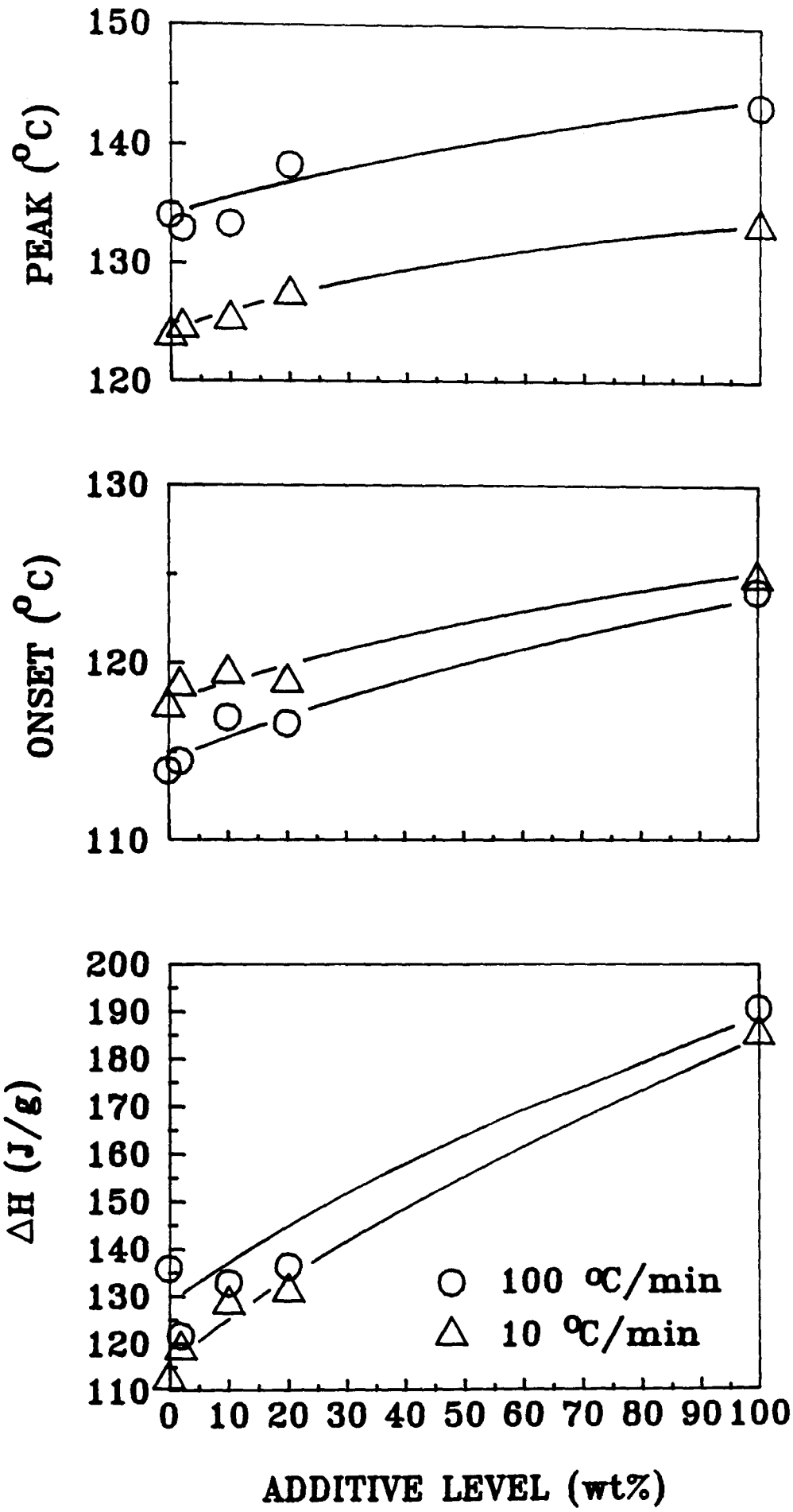

FIGURE 6.4: Heating behaviour of HDPE-F blends.

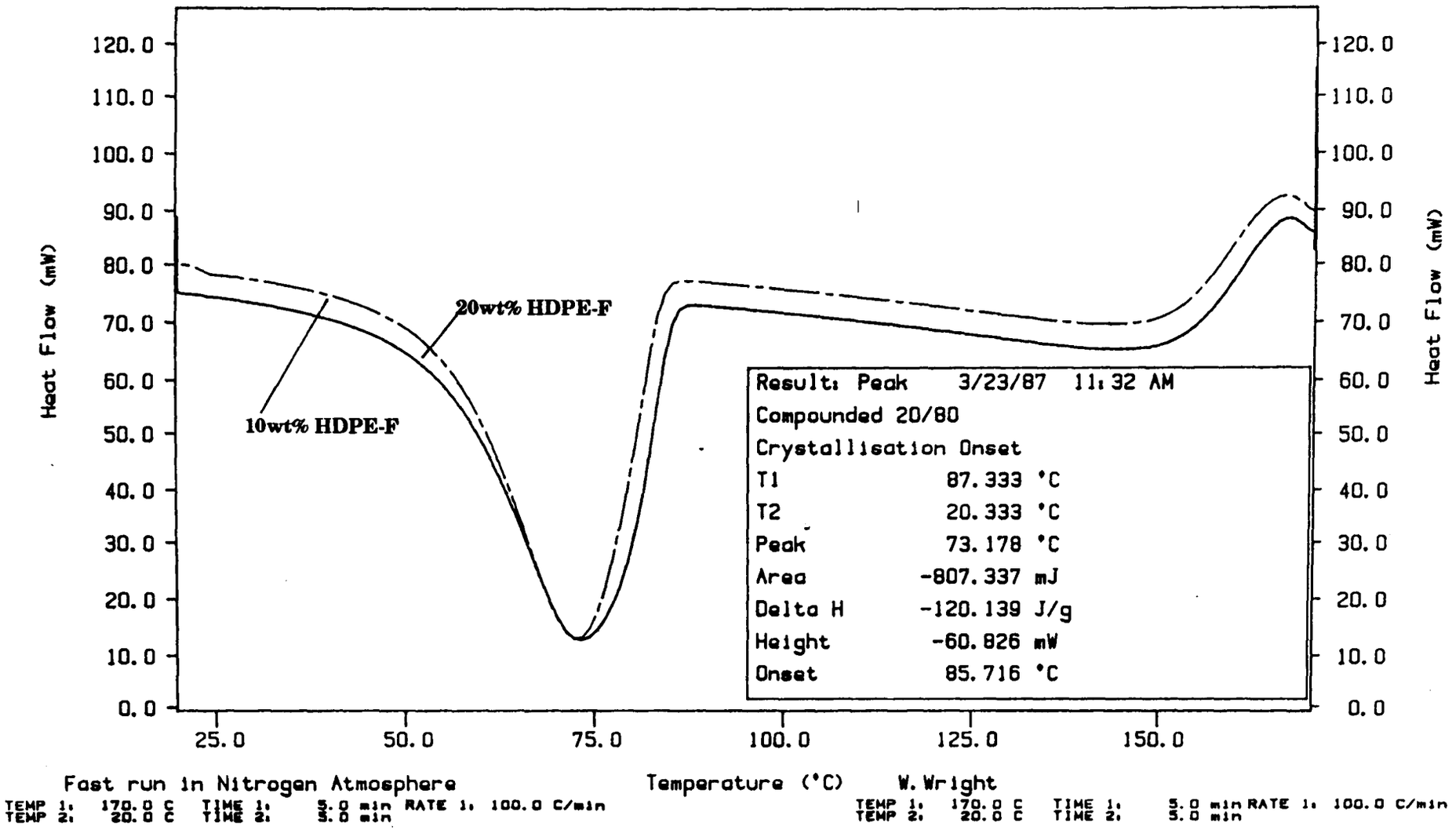

FIGURE 6.5: Typical DSC curve for 10 and 20wt% compounded HDPE-F blends at a crystallisation rate of 100°C/min.

	MELTING VALUES			CRYSTALLIZATION VALUES		
	ΔH_h (J/g)	$PEAK_h$ (oC)	$ONSET_h$ (oC)	ΔH_c (J/g)	$PEAK_c$ (oC)	$ONSET_c$ (oC)
MDPE-A/55	144.4	125.9	111.7	-128.0	119.0	114.3
HDPE-B/2	139.57	126.1	111.9	-124.8	119.4	114.3
HDPE-B/5	139.3	126.4	111.8	-116.4	118.7	114.6
HDPE-B/10	137.1	127.8	111.4	-128.2	119.0	114.6
HDPE-B/20	127.8	127.4	112.2	-112.9	120.4	115.0
HDPE-B	158.2	129.2	-172.8		113.9	121.7116.9

i) Data from compression moulded sheet except HDPE-B (pellets).
ii) Subscript h refers to the heating cycle, c to the cooling cycle.

TABLE 6.4: Heating and crystallization data from HDPE-B compounded blends at a heating rate of 10°C/min.

	MELTING VALUES			CRYSTALLIZATION VALUES		
	ΔH_h (J/g)	$PEAK_h$ (oC)	$ONSET_h$ (oC)	ΔH_c (J/g)	$PEAK_c$ (oC)	$ONSET_c$ (oC)
MDPE-A/55	144.4	125.9	119.0	-128.0	111.7	114.3
HDPE-M/2	129.7	126.0	118.9	-120.4	113.4	115.6
HDPE-M/5	132.6	126.5	118.5	-119.6	113.5	116.2
HDPE-M/10	137.5	127.1	119.3	-126.4	113.6	116.3
HDPE-M/20	136.4	127.8	117.6	-124.1	113.7	117.0
HDPE-M	157.9	130.8	120.5	-137.7	115.4	118.6

i) Data from compression moulded sheet except HDPE-M (pellets).
ii) Subscript h refers to the heating cycle, c to the cooling cycle.

TABLE 6.5: Heating and crystallization data from HDPE-M compounded blends at a heating rate of 10oC/min.

	MELTING VALUES			CRYSTALLIZATION VALUES		
	ΔH_h (J/g)	$PEAK_h$ (oC)	$ONSET_h$ (oC)	ΔH_c (J/g)	$PEAK_c$ (oC)	$ONSET_c$ (oC)
MDPE-A/55	144.4	125.9	119.0	-128.0	111.7	114.3
MDPE-P/2	220.3	125.6	118.4	-116.5	112.4	114.6
MDPE-P/5	210.2	125.8	118.3	-119.8	112.8	114.9
MDPE-P/10	215.3	126.1	117.9	-118.0	112.3	114.8
MDPE-P/20	201.4	126.4	117.1	-123.3	113.0	115.3
MDPE-P	147.4	127.5	116.4	-119.5	112.9	115.9

i) Data from compression moulded sheet except MDPE-P (pellets).
ii) Subscript h refers to the heating cycle, c to the cooling cycle.

TABLE 6.6: Heating and crystallization data from MDPE-P compounded blends at a heating rate of 10°C/min.

	MELTING VALUES			CRYSTALLIZATION VALUES		
	ΔH_h (J/g)	$PEAK_h$ (oC)	$ONSET_h$ (oC)	ΔH_c (J/g)	$PEAK_c$ (oC)	$ONSET_c$ (oC)
MDPE-A/55	144.4	125.9	119.0	-128.0	111.7	114.3
MDPE-D/2	133.6	126.3	119.6	-115.3	111.6	114.3
MDPE-D/5	129.8	126.1	119.7	-123.2	112.1	114.4
MDPE-D/10	140.2	126.7	119.1	-121.1	112.1	114.6
MDPE-D/20	139.0	126.5	119.5	-121.7	112.4	114.6
MDPE-D	145.6	126.5	120.2	-133.7	112.4	114.9

i) Data from compression moulded sheet except MDPE-D (pellets).
ii) Subscript h refers to the heating cycle, c to the cooling cycle.

TABLE 6.7: Heating and crystallization data from MDPE-D compounded blends at a heating rate of 10°C/min.

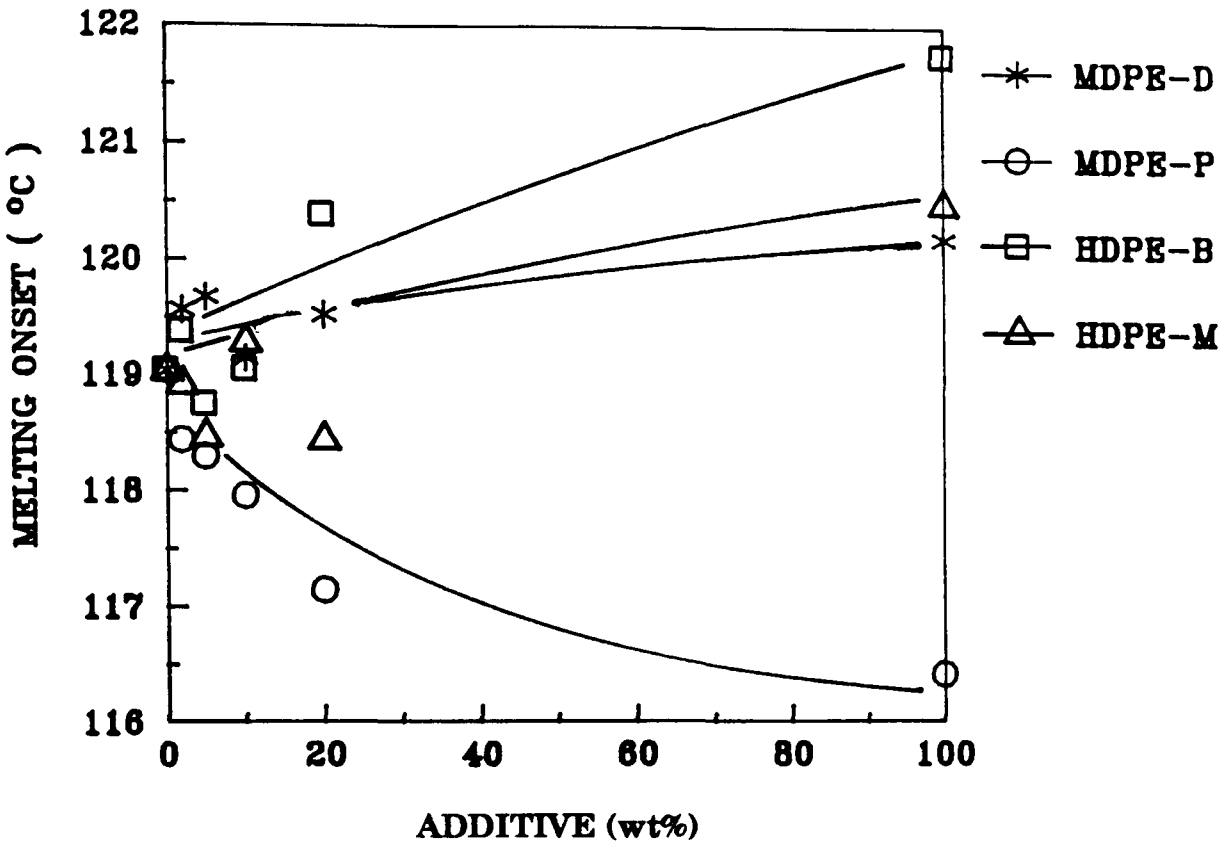

FIGURE 6.6: Melting temperature behaviour of 55mm pipe blends.

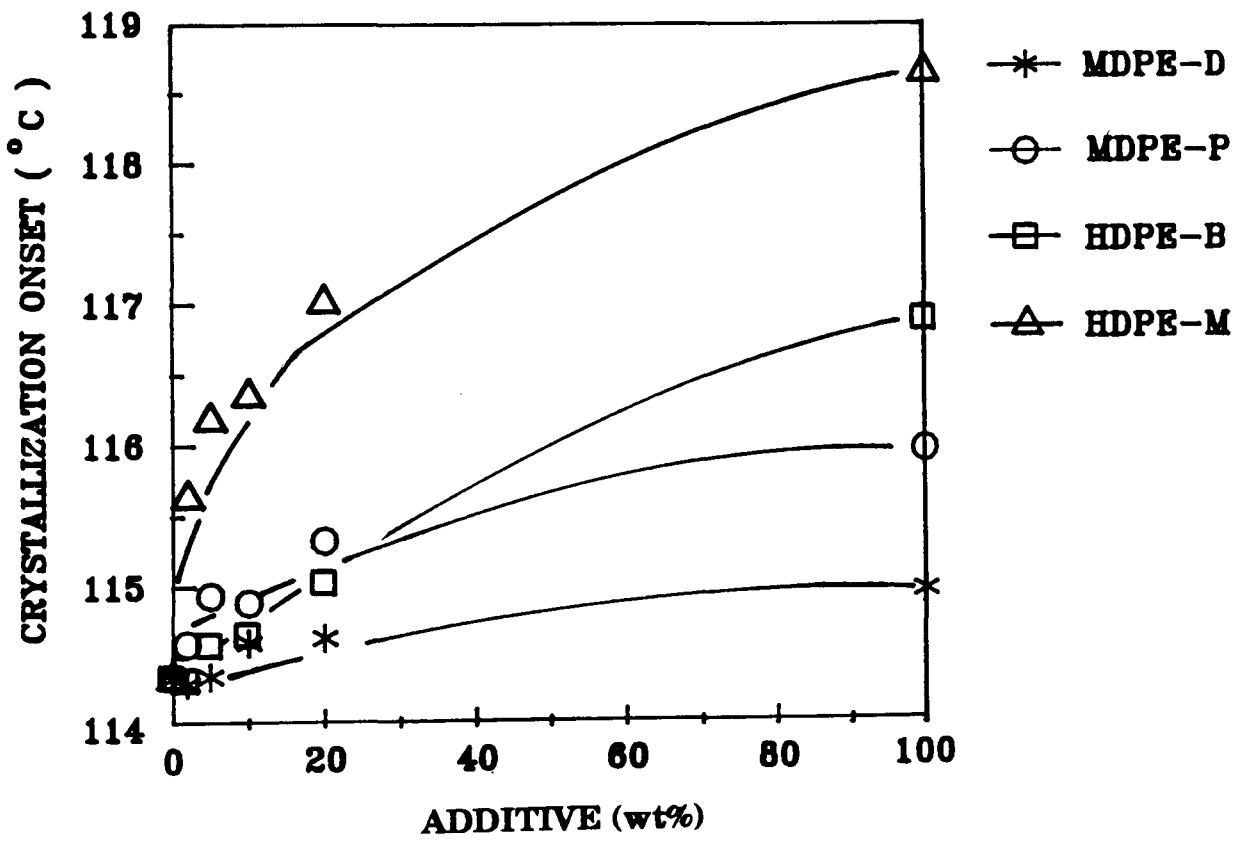

FIGURE 6.7: Crystallization temperature behaviour of 55mm pipe blends.

6.2.3 MICROSCOPY

Microscopy is a powerful and rapid tool for assisting in blend homogeneity evaluation, and was used both for determination of the microstructure of extruded pipe and for evaluation of the crystallization of blends. Figures 6.8 and 6.9 shows that by the addition of the HDPE-F material into the base resin at 20wt% the spherulitic structure of the MDPE-A resin (Figure 6.8) is completely altered to fine featureless spherulitic structures (Figure 6.9). For the compounded blend at this same addition level the spherulites appear smaller and more uniform showing the uniformity of the blend.

Microscopy work on samples from 55mm pipe showed similar structures to that produced for HDPE-F blends. These are illustrated at 20wt%, all the blends reducing the spherulitic structure of the MDPE-A resin to the fine/featureless morphology, (Figure 6.10 and 6.11).

Microscopy has identified poor mixing within the uncompounded blends, especially in 55mm pipe samples, where Figure 6.12a) illustrates this point. Here under non-polarized transmitted microscopy a clear streak of MDPE-D additive within a matrix of yellow pigmented polyethylene blend is seen. Changing the analyser light conditions through 90^{o} one can see the spherulitic organization of the matrix around the additive streak (Figures 6.12 b) and c)). What is evident from the micrograph is that on its own the MDPE-D material has a crystallization behaviour that produces a non-spherulitic structure but within a matrix that normally produces large spherulites the additive itself has large spherulites and causes the matrix to have small spherulites.

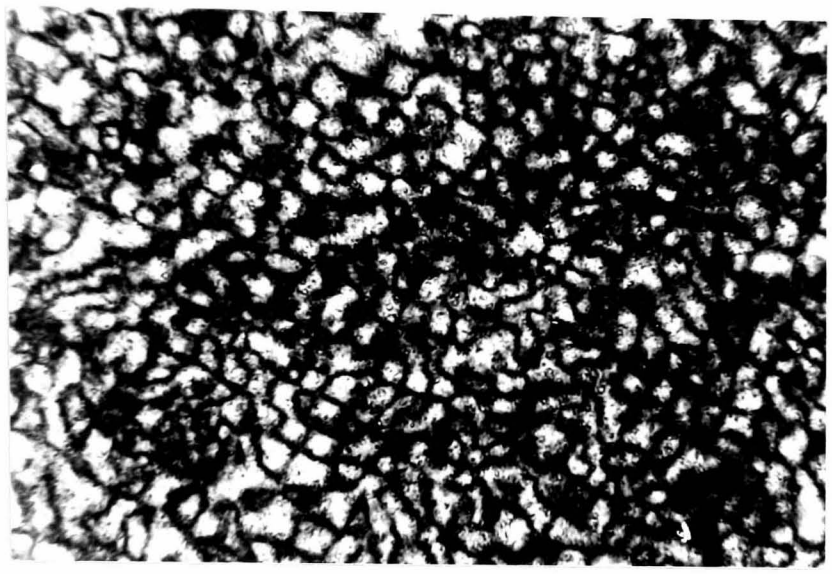

20μm

FIGURE 6.8: Microtome of 32mm MDPE-A pipe.

a)

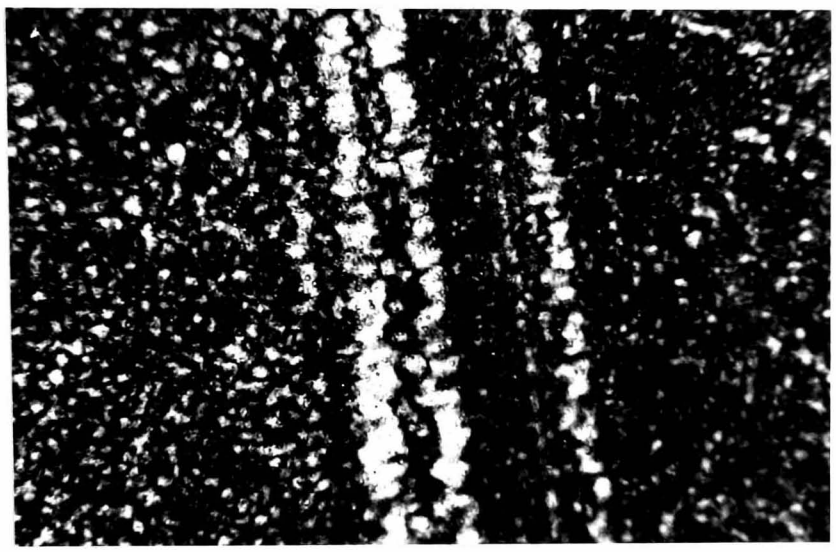

20μm

b)

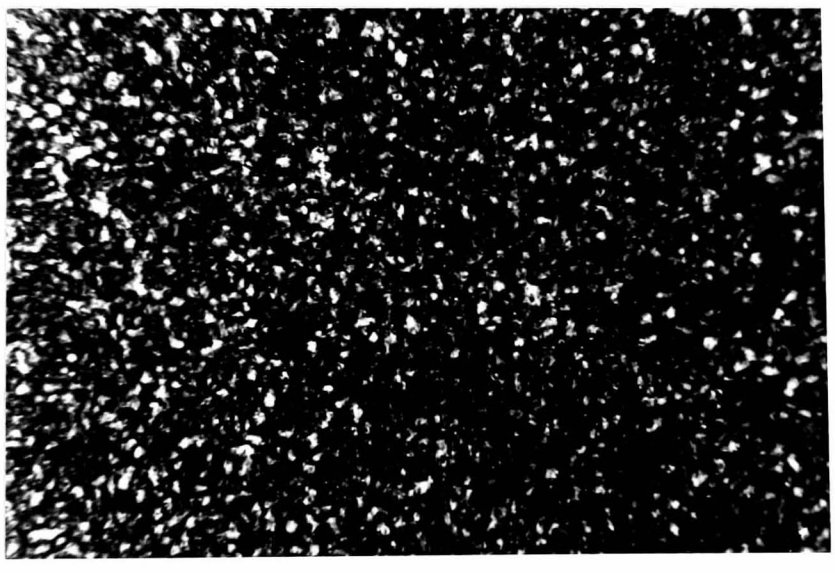

20μm

FIGURE 6.9: a) Microtome of 20 wt% HDPE-F in 32mm uncompounded pipe.
b) Microtome of 20 wt% HDPE-F in 32mm compounded pipe.

a)

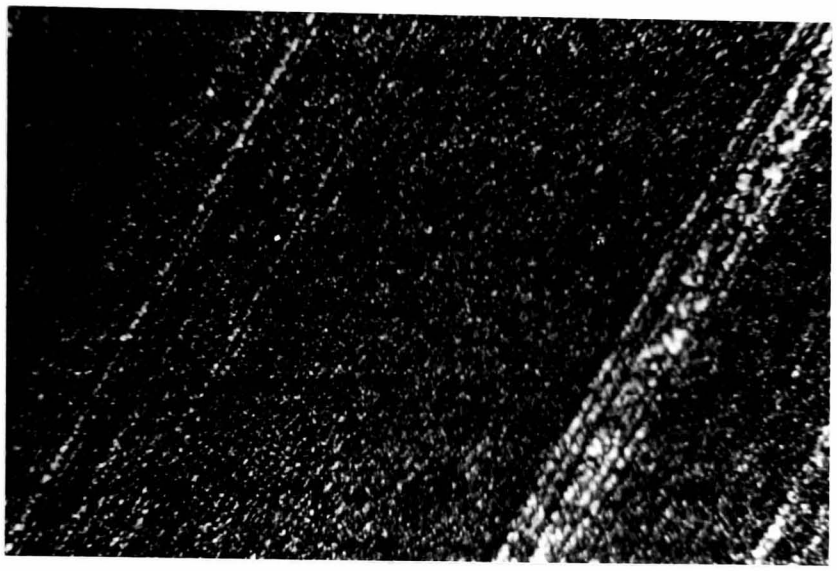

20μm

b)

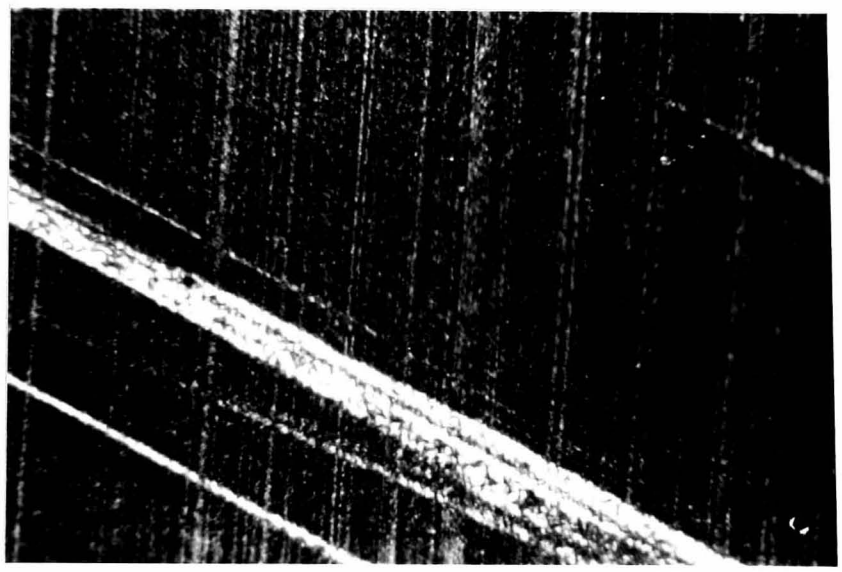

20μm

FIGURE 6.10: a) Microtome of HDPE-B/20 in 55mm pipe.
b) Microtome of HDPE-M/20 in 55mm pipe.

a)

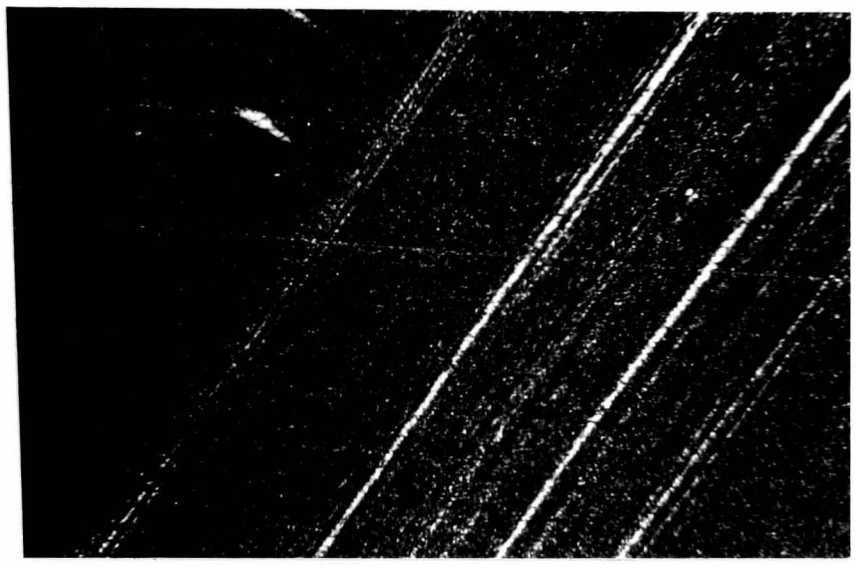

20μm

b)

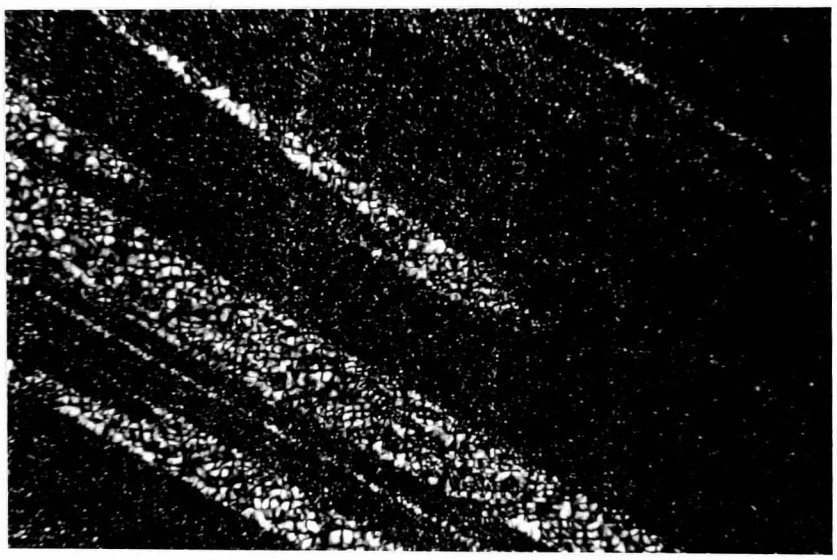

20μm

FIGURE 6.11: a) Microtome of MDPE-P/20 in 55mm pipe.
b) Microtome of MDPE-D/20 in 55mm pipe.

a)

50μm

b)

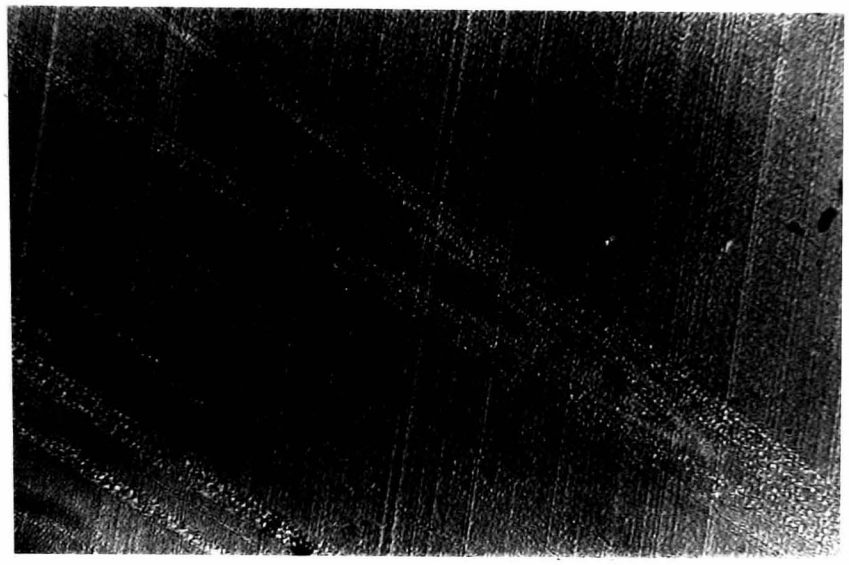

50μm

c)

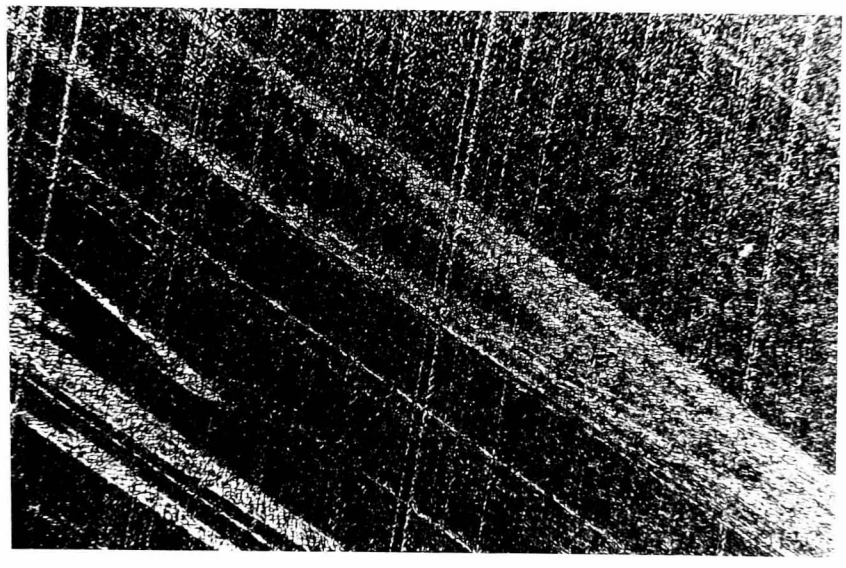

50μm

FIGURE 6.12: a) MDPE-D/20 sample under non-polarized light.
b) MDPE-D/20 in transistion stage.
c) MDPE-D/20 sample under polarized light.

6.3 DISCUSSION

6.3.1 DYNAMIC MECHANICAL THERMAL ANALYSIS

From compression moulded samples we have found that there are no reasons to believe that there are phase segregations within the HDPE-F blends. What is seen is the constant single peak variation of the γ and α regions corresponding to the two materials. However the slight presence of an increase in β transition at around $0^{o}C$ for 20wt% HDPE-F may infer either instrument error from poor clamping or molecular interactions within the blends [110]. Further work is needed to evaluate this area. In applying these results to the stress rupture performance of the blends it must be noted that the DMTA values were taken from compression moulded samples of blends that were compounded. Chapter 5 has shown how compounded pipe samples produced poorer stress rupture properties than uncompounded blends. This illustrates the point that uniform properties of the blends have no bearing on the stress rupture performance, and in fact appear to be more deleterious when compared to the hopper mixed blends (Figure 5.10).

6.3.2 DIFFERENTIAL SCANNING CALORIMETRY

This technique adequately supplemented work reported from DMTA..Single peaks were obtained for all blends at all additive additions even under fast heating / cooling regimes. Datta and Bailey [44] have found similar relationships with their LLDPE/HDPE blends, illustrating that their blends all showed cocrystallization. For their blends this relationship was reflected in good mechanical properties, although their testing was for short term mechanical properties alone.

The results from work on the HDPE-F blends were repeated with all the other blend systems. What is interesting is that there appears to be a direct relationship with the failure times exhibited for the blends with the onset of crystallization temperature, in that the most dramatic reductions in lifetimes were exhibited by the resins which moved the crystallization temperature of the blend to higher values (Figure 6.7). MDPE-D was the additive that caused minimal change in the 80°C performance of the MDPE-A resin; it was also the additive that had the least influence on the crystallization behaviour of the MDPE-A resin. Chapter 7 discusses this in more detail.

6.3.3 MICROSCOPY

It has been implied that larger spherulitic structures, have a reduced ESCR and stress rupture performance when compared to a material with finer spherulitic features. What we have found in this study is that by adding polyethylene grades to the MDPE-A resin (which had distinct spherulitic features), we destroyed that structure to produce a fine / featureless morphology. This fine / featureless morphology was evident in all the blends produced. Therefore we obtained poor stress rupture performances (HDPE and MDPE-P blends) , as well as good stress rupture performances (MDPE-D blends) with this type of morphology, illustrating the difficulties in allying spherulitic morphology to pipe performance.

However this change in microstructure is not uncommon. Bubeck and Baker [47] found that with ethylene / octene copolymers of similar molecular weight the increase in hexyl branch concentration increased the spherulitic size of the material, with the resultant decrease in density and increase in ESC . They proposed that the mechanism of crack propagation under ESC

conditions was due to the the decreased spherulitic size providing more internal spherulitic surface area for crack movement and hence a reduced ESC value. Maxfield and Mandelkern [54] also found that by mixing a non-spherulitic forming polyethylene with a spherulitic forming polyethylene, a decrease in the spherulitic structure of the blend was obtained . This observation was also evident for polyethylene pipe blends studied in this research project where the non-spherulitic structure of the phases decreased the large spherulitic structure of the MDPE-A material. However in the MDPE-D case the resultant morphology produced *good* 80°C performance. Using Bubeck and Bakers [47] work as a guideline they would imply a reduced 80°C performance.

In the precompounded HDPE-F blends the resultant morphology was found to be more uniform and finer than the uncompounded blends, implying that poor mixing was the main cause of non-uniform spherulitic structures in the uncompounded blends. Bhateja and Andrews [41] obtained similar results from blending UHMWPE with HDPE. They postulated that poor mixing could be at a microlevel (between crystallites). Bubeck and Baker [47] found that non-uniform spherulitic sizes in a material caused delamination between spherulitic layer boundaries. However in this present study it was the *non-uniform* structure (uncompounded blends) that produced better 80°C stress rupture performance than the *uniform* blends (compounded blends). Also DMTA and DSC results have shown that we have compatible blends in all cases and that phase segregation would be immediately identified by these techniques. Although the microstructure of HDPE-M and HDPE-B blends shows that there are localized regions of poor mixing of the components, this is principally due to the different viscosities of the additives, HDPE-M and HDPE-B at 190°C [4]. But as was mentioned before the decrease in stress rupture performance by twin-screw compounding

with the HDPE-F blends implies that poor mixing was not the cause of the marked fall off in performance, but some other mechanism was responsible.

The changes in microstructure of the base resin when blends are produced shows that the crystallization behaviour of the base resin is severely disrupted. The crystallization onset of the blends throws more light on this area. What is observed is that the introduction of a second polyethylene material raises the temperature of crystallization of the blend and in effect increases both the onset and the peak crystallization temperature. The magnitude of the increases in crystallization temperature can range from fractions of a degree (MDPE-D blends) to nearly 3°C (HDPE-M blends). However for all blends there is a single crystallization exotherm (Figure 6.5). This implies that the additive (if it has a higher crystallization temperature than the MDPE-A resin), will crystallize at a temperature between its normal crystallization temperature and that of the MDPE-A material within a blend.

This nucleation effect of the additive can be easily illustrated by using the simple experiment outlined in section 4.5.2 where two microtomed samples of pure HDPE-F and MDPE-A are made to overlap one another. By observing the cooling and crystallization of the sample from above the melting temperature it was found that the sample of HDPE-F crystallized first to produce a spherulitic morphology. As the temperature decreased the interface, that is where the two materials overlapped, formed spherulites and finally the MDPE-A material crystallized (Figure 6.13) . The nucleating effect is seen to be adequately proven for the HDPE-F material. What was even more remarkable was the fine spherulitic structure observed for the blend at the interface between the two polymers (Figure 6.13).

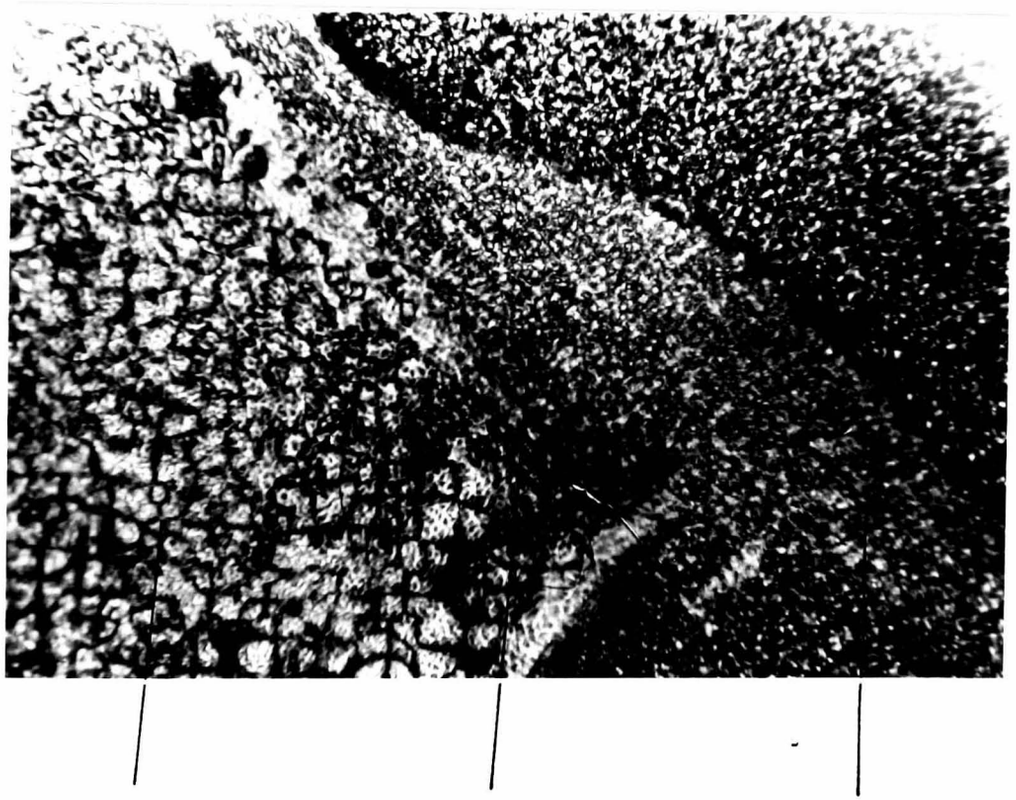

FIGURE 6.13: Transmitted optical micrograph showing nucleating influence of HDPE-F on MDPE-A.

What this chapter has shown is that the poor stress rupture performances of the majority of the polyethylene blends are not caused by phase segregation and poor mixing. DMTA, DSC and microscopy techniques have all demonstrated that cocrystallization takes place within the blends studied. Also, the changes in the large spherulitic microstructure of the MDPE-A material, to fine/featureless spherulites for all the blends investigated have strongly highlighted the weaknesses of attributing large spherulitic structures with poor stress rupture performance. It also nullifies the hypothesis that fine spherulitic structures ensure good stress rupture performances, and shows that the mechanisms controlling stress rupture performance lies deeper than *spherulite size*. Chapter 7 will attempt to expose these microstructural depths.

CHAPTER 7

FRACTOGRAPHY AND FAILURE MECHANISMS

7.1 INTRODUCTION

The previous chapters have shown the influence that blending has on the structure and performance of a known pipe grade resin. It is hoped that this chapter on fractography and failure mechanisms will illuminate some of the reasons influencing the pronounced deterioration of stress rupture properties when various polyethylene grades are blended.

7.2 FRACTOGRAPHY FEATURES OF UNNOTCHED PIPE

7.2.1 HDPE-F UNCOMPOUNDED BLENDS

The introduction of HDPE-F into the base resin grade MDPE-A significantly reduced the 80°C stress rupture performance of the blend, with increased additive levels progressively reducing performance. Figure 7.1a illustrates the brittle fracture surface of the unblended MDPE-A pipes under 80°C stress rupture conditions at 0.955 MPa internal pressure. The fracture surface is characteristic of slow crack growth pipe failure and is widely documented in several articles [4,6,67]. Here we see the microductility on the surface appearing to increase in fibril height as the crack progresses from

a)

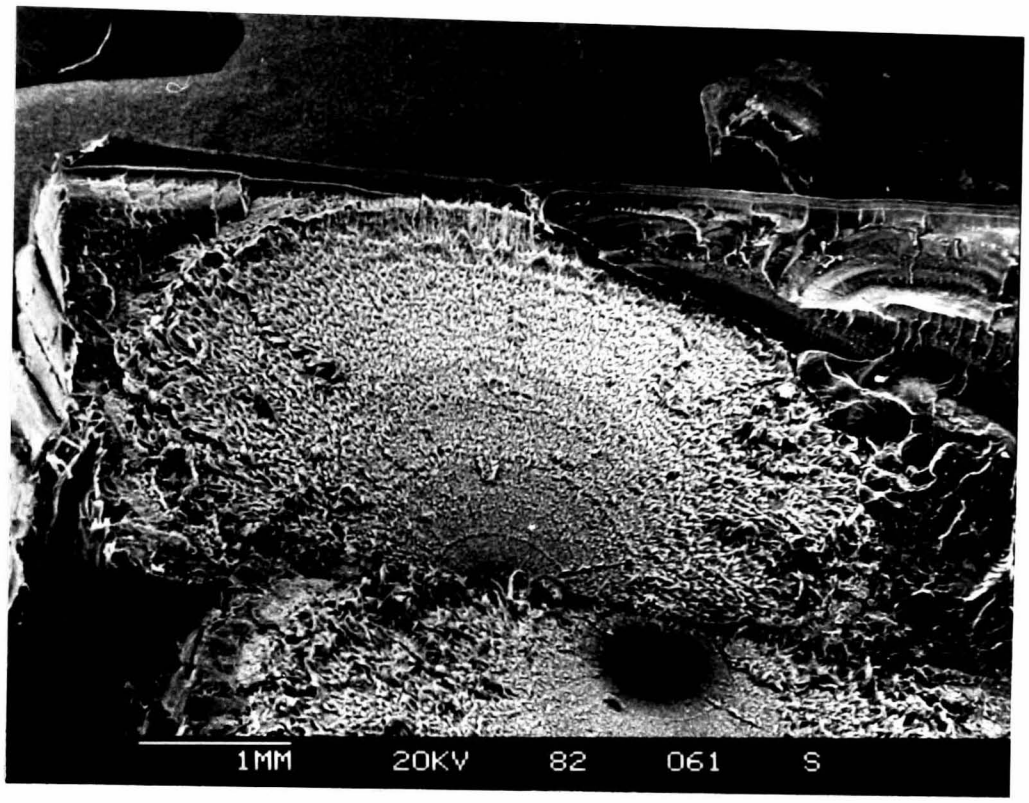

b)

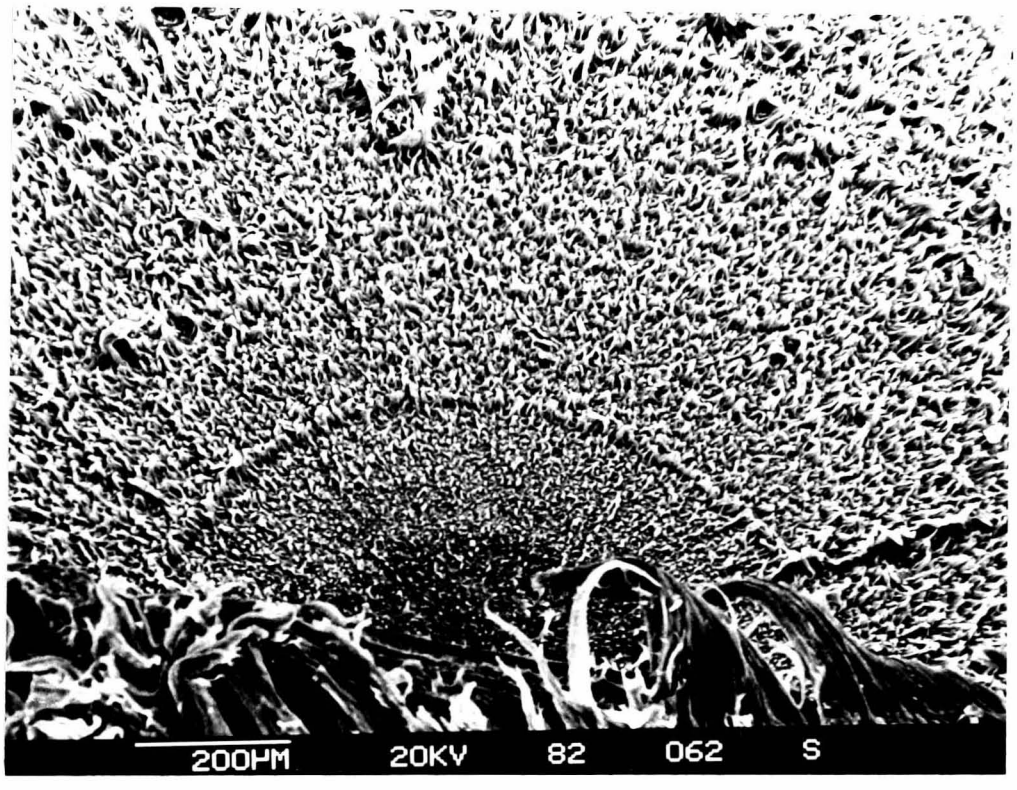

FIGURE 7.1: a) Fracture surface of 32mm MDPE-A pipe.
b) Fracture surface of 32mm MDPE-A pipe.
A void is shown initiating fracture.

the bore of the pipe to the outside. In this example the initiation region is at the bore. In another case a void is seen approximately 200μm from the bore of the pipe (Figure 7.1b). For both samples illustrated here, the initiation region at the bore is surrounded by an area of limited microductility.

Figure 7.2 a) and b) display the failed pipe fracture surfaces of 2 and 20wt% HDPE-F uncompounded blends. What can be seen is that overall the microductility is reduceed and the initiation site is shifted towards the centre of the pipe. If the fractured fibre heights on the fracture surface were measured the value expressed would be significantly less than that of the base MDPE-A material (Figure 7.1a). Here we see that the introduction of a material with similar molecular weight values has an influence on the long term fracture surfaces exhibited from its blends. Another observation from Figures 7.2a) and b) is the minimal fibrillar or low microductility region as compared with Figures 7.1a) and b). This region is defined in the diagram shown schematically in Figure 7.3a) and is graphically illustrated in Figure 7.3b) for HDPE-F uncompounded blends.

7.2.2 HDPE-F COMPOUNDED BLENDS

For HDPE-F compounded blends initiation from particles was evident in many of the formulations. The majority of the particles were of a non-metallic nature rather than metallic. Figure 7.4a) and b) show typical fracture surfaces for 2 and 10wt% HDPE-F compounded blends, Figures 7.5a) and b) are examples of 20wt% compounded blends. From these blends the fracture surfaces not only involved initiation from particles but the involvement of several fracture planes in the crack movement from the bore to the outside of the pipe. Again the presence of a large area of limited

microductility is clearly visible in the 20wt% compounded blend.

7.2.3 FRACTURE SURFACES OF 32mm HDPE-M AND HDPE-B BLENDS

Typical fracture surfaces of HDPE-B and HDPE-M at an additive level of 10wt% in MDPE-A are shown in Figures 7.6a) and b). Failure initiation sites are seen near the bore of the pipe. However although the fracture surfaces appear the same in terms of fibre height the movement of the crack throughout the pipe wall in the HDPE-M material is seen as crack arrest lines rather than the smooth crack progression of the HDPE-B material.

A Links elemental analyzer (attached to the Scanning Electron Microscope) was used to examine the initiation particles present within the fracture surfaces of pipe equations. A typical trace is shown for the initiation particle of Figure 7.4b) in Figure 7.7. In this case the particle was found to be calcium rich.

7.3 FRACTOGRAPHY FEATURES OF NOTCHED PIPE

7.3.1 FRACTURE FEATURES OF NOTCHED MDPE-A PIPE

The principle failure path for the crack in unnotched pipe is initiation at or close to the bore of the pipe and crack propagation towards the outside wall of the pipe. However the introduction of an external notch in the pipe produces a crack which grows from the outside to the inside wall of the pipe.

Chapter 5 has illustrated how the lifetime of 32mm notched pipe to 32mm [illegible] nd , that is the performance decreases.

a)

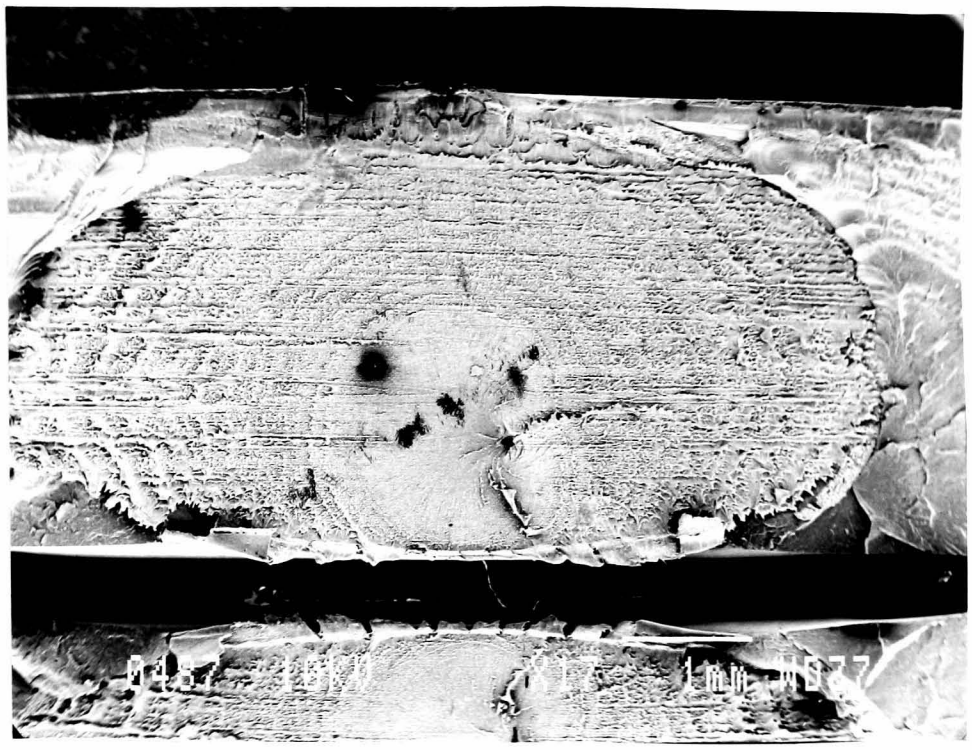

b)

FIGURE 7.2: a) Fracture surface of 32mm HDPE-F/2 pipe.
b) Fracture surface of 32mm HDPE-F/20 pipe.

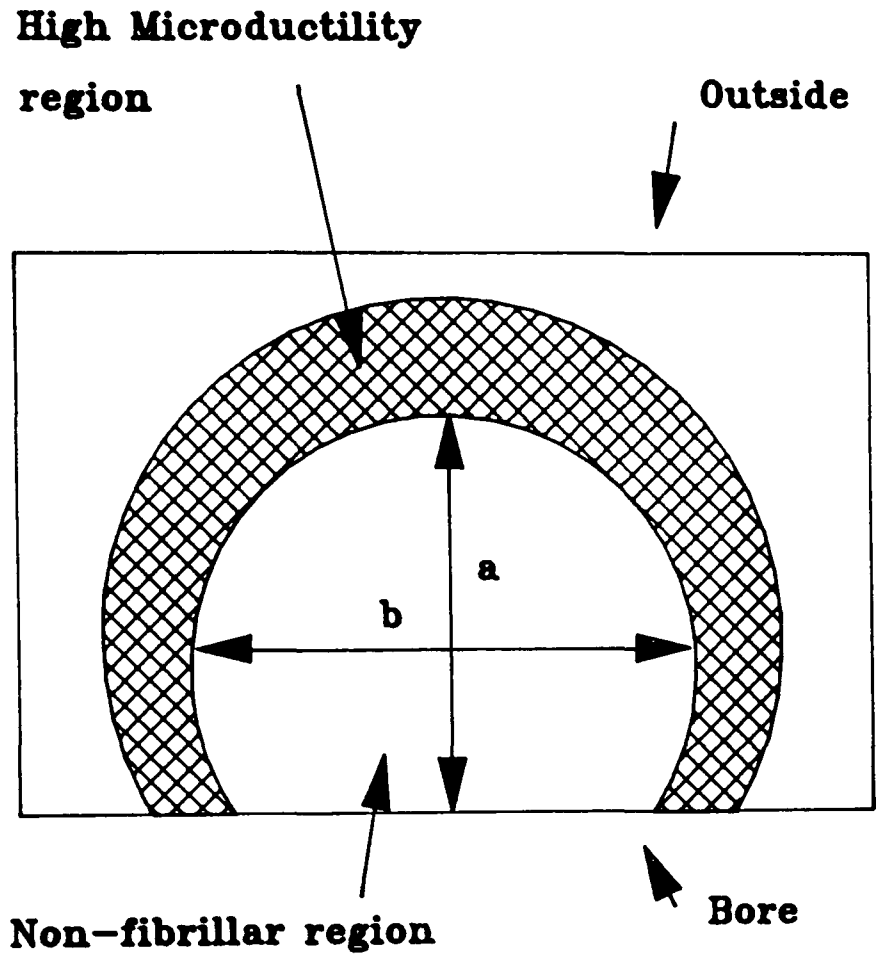

FIGURE 7.3a): Schematic representation of non-fibrillar region in pipe fracture surfaces.

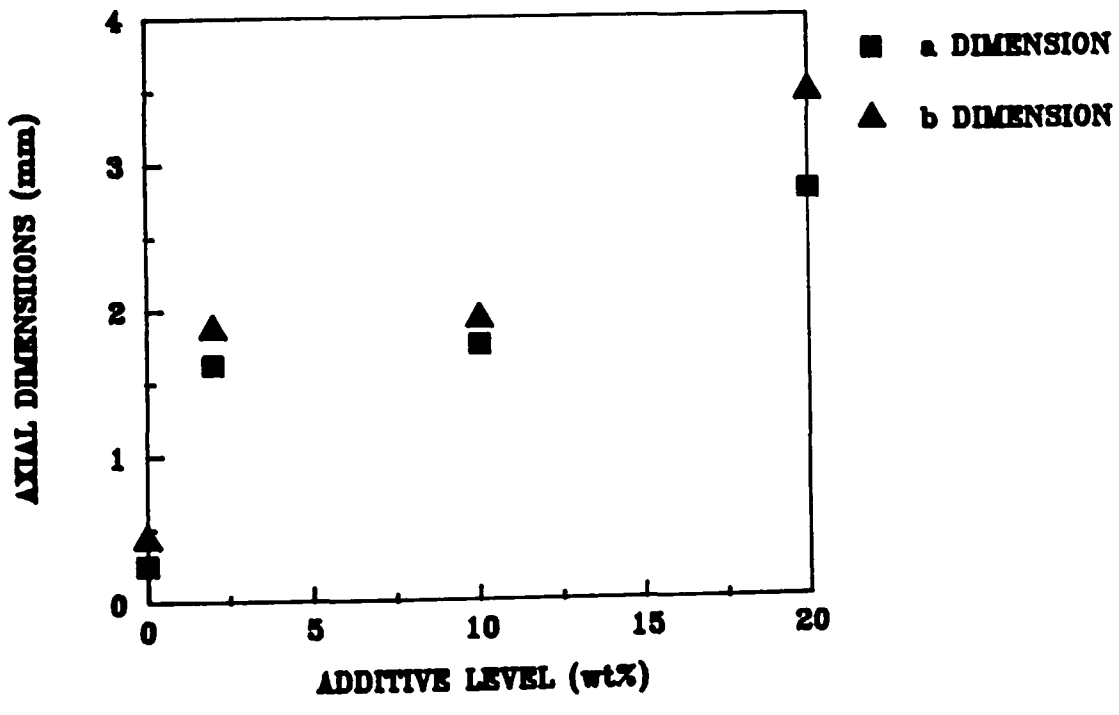

FIGURE 7.3b): Axial length variations with HDPE-F additions.

a)

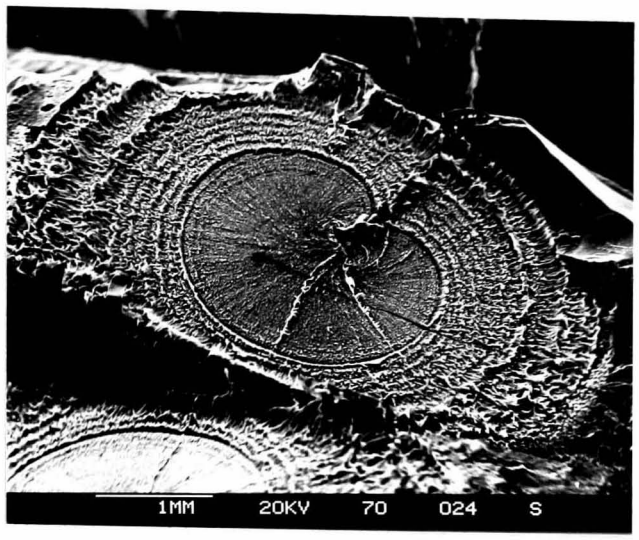

b)

FIGURE 7.4: a) Fracture surface of 32mm CHDPE-F/2 pipe.
b) Fracture surface of 32mm CHDPE-F/10 pipe.

a)

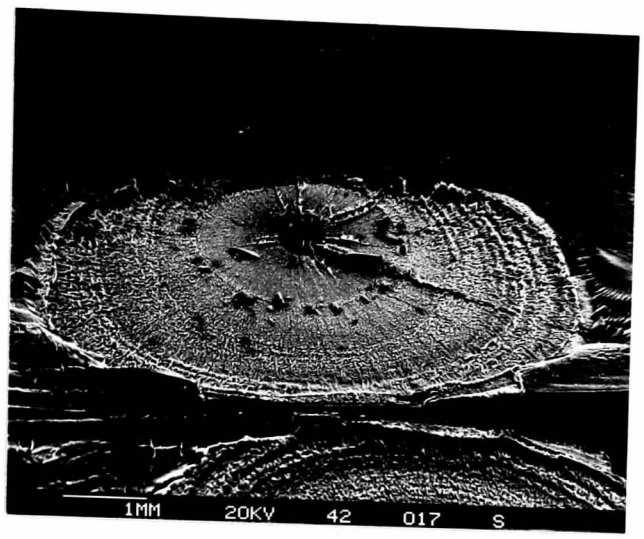

b)

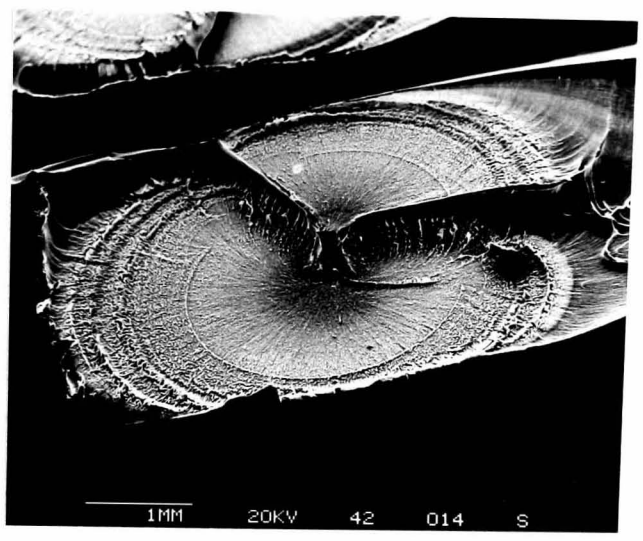

FIGURE 7.5: a) Fracture surface of 32mm CHDPE-F/20 pipe.
b) Fracture surface of 32mm CHDPE-F/20, pipe, showing fracture on two planes.

a)

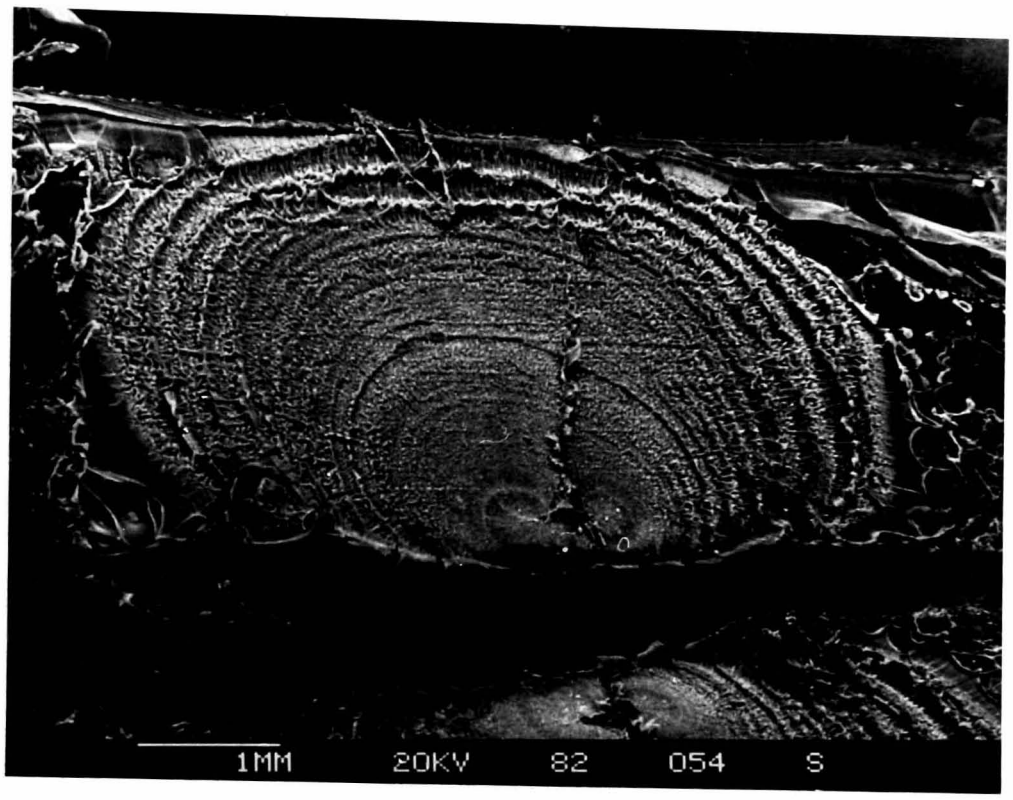

b)

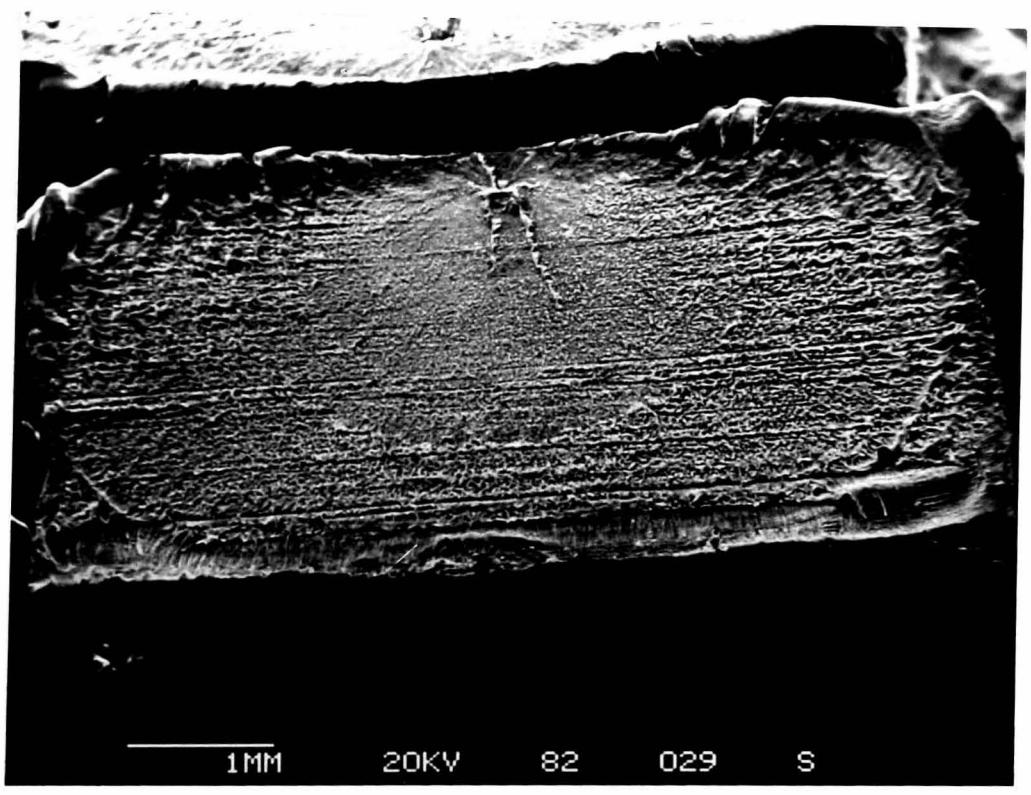

FIGURE 7.6: a) Fracture surface of 32mm HDPE-B/10 pipe.
b) Fracture surface of 32mm HDPE-M/10 pipe.

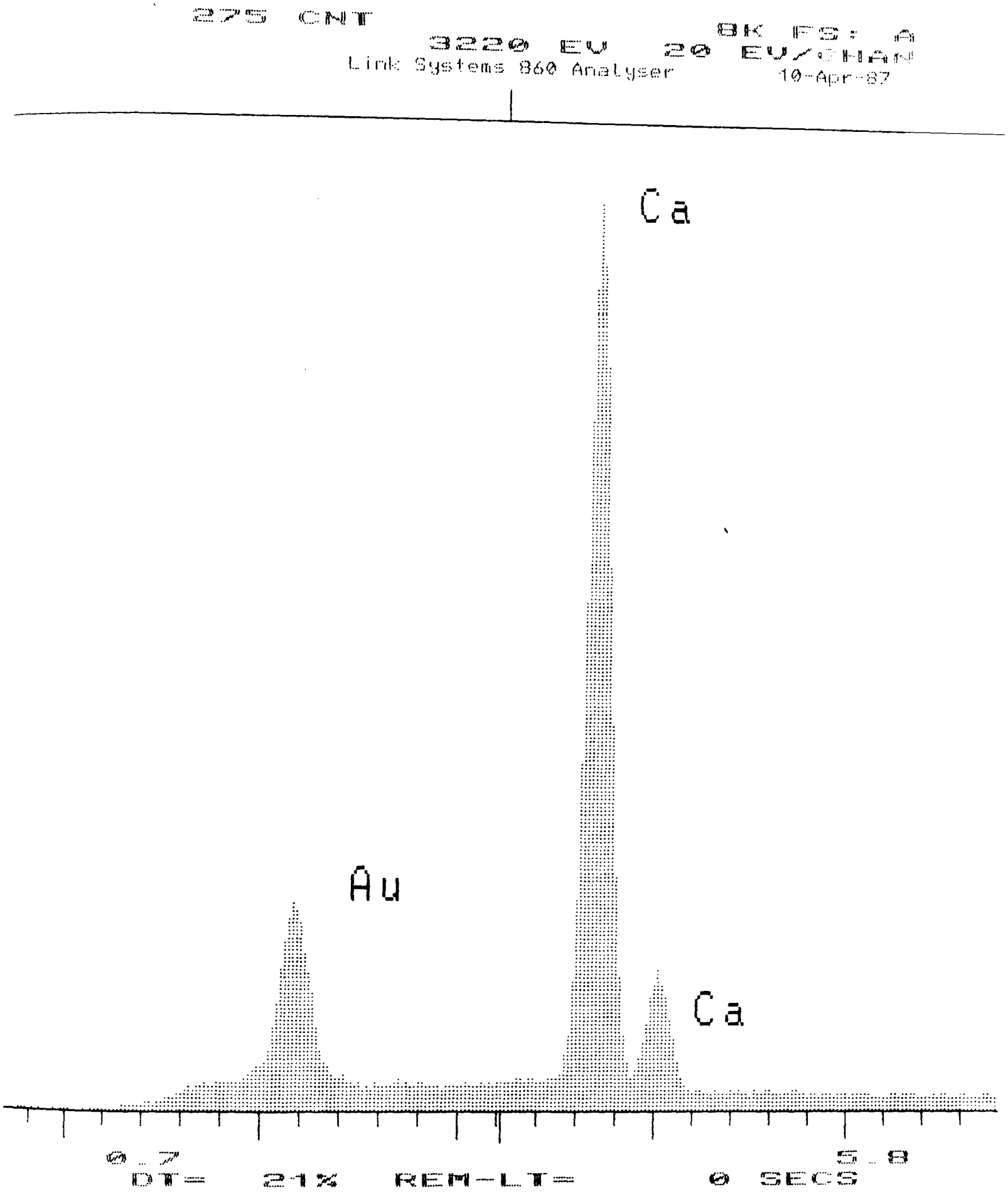

FIGURE 7.7: Typical S.E.M elemental trace of a particle near the fracture initiation site of a pipe sample

a)

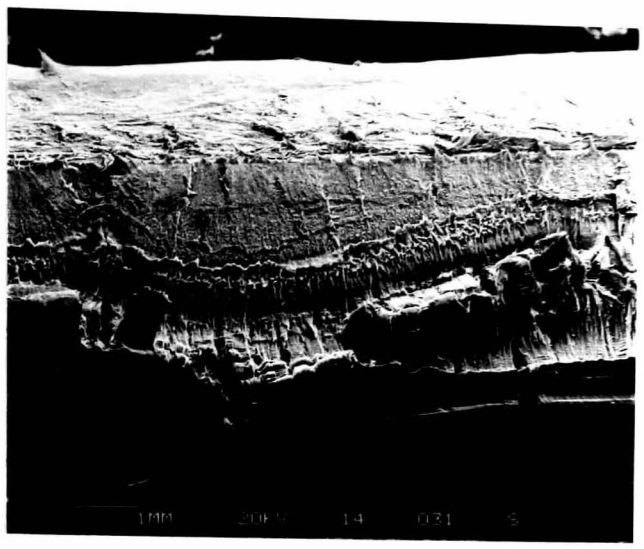

b)

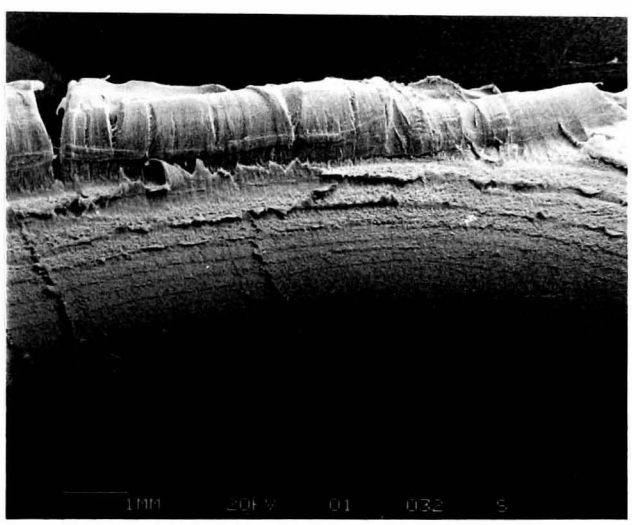

c)

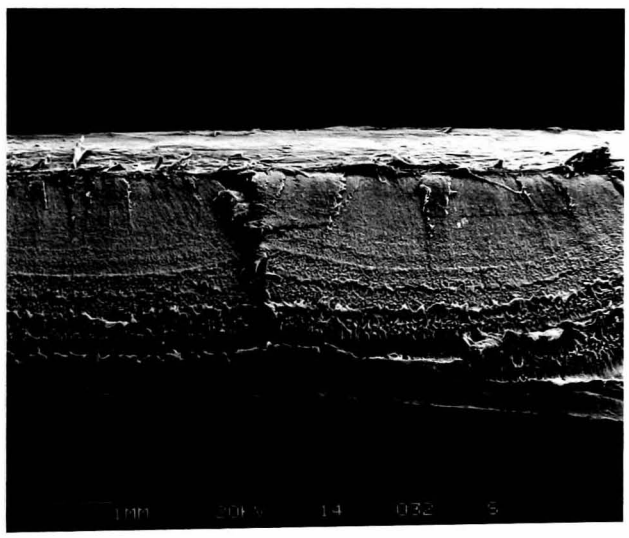

FIGURE 7.8: a) Notch fracture surface of 55mm MDPE-A pipe at 0.9MPa.
b) Notch fracture surface of 55mm MDPE-A pipe at 0.8MPa.
c) Notch fracture surface of 55mm MDPE-A pipe at

However the lifetime performance of notched pipe was found to be comparable with uncompounded blends at 20wt% additive addition level. The fracture surfaces of these notched pipe were found to be similar in appearance to fracture surfaces of unnotched pipe.

Figures 7.8a-c) show typical brittle fracture surfaces of notched 55mm SDR11 MDPE-A pipe at 0.9,0.8 and 0.7MPa internal pressure. One common feature between the micrographs is the movement of the crack from the notch to the outside portion of the pipe. However the similarity ends there, the fracture surface of the 0.9MPa sample clearly showing greater microductility than the 0.7MPa sample. The axial crack length, that is the horizontal movement of the crack along the notch, increased as the pressure increased.This axial length increase with internal pressure was found to be reflected in all the samples. A schematic definition of axial length is shown in Figure 7.9.

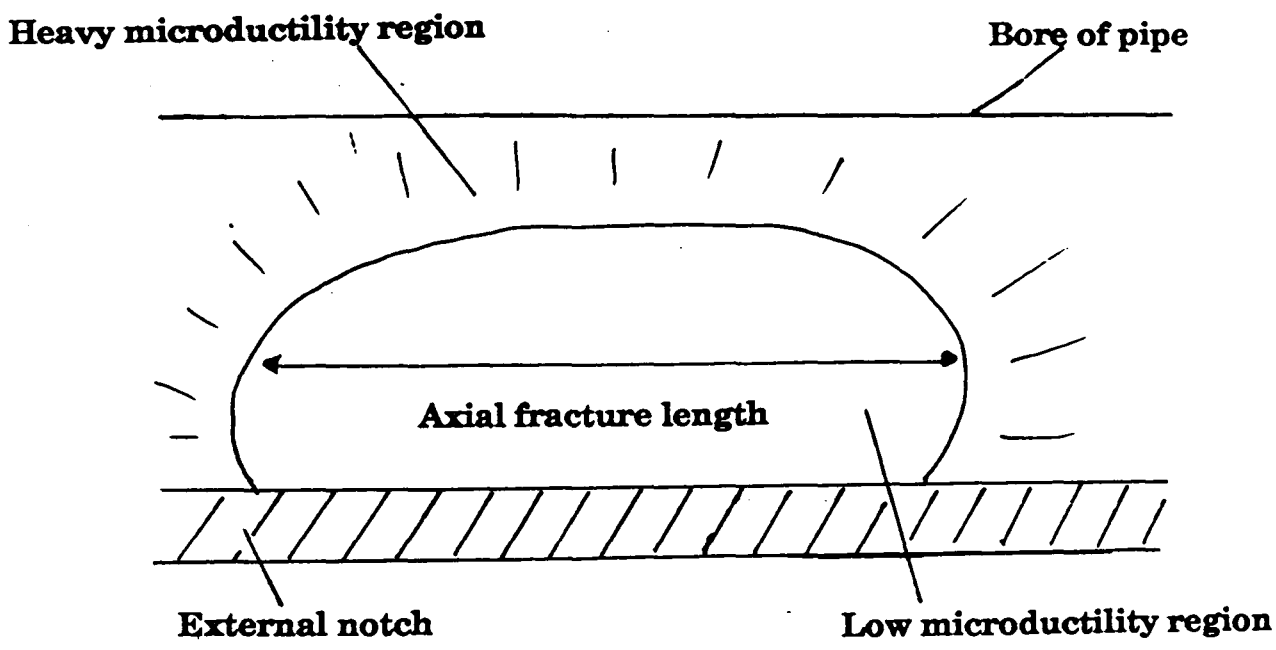

FIGURE 7.9: Schematic definition of axial fracture length.

7.3.2 AXIAL LENGTH VARIATIONS OF NOTCHED BLENDS

i) Notched HDPE-F Uncompounded Blends

Figure 7.10 shows the observed straight line relationship of average failure time as a function of average axial fracture length for notched HDPE-F uncompounded blends from values expressed in Table 7.1. Unfortunately data was not available for axial length variations of notched MDPE-A pipe. However we can postulate the possible axial fracture length from a knowledge of the 32mm notch failure times of the HDPE-F blends. From Figure 7.10 the equation of the line is of the form:

$$t_u = 2.8\text{x}10^{-4} \text{ x } 2.1^{a} \qquad [7.1]$$

where t_u = Uncompounded HDPE-F blend lifetime (hrs)

a_x = Axial fracture length (mm)

Assuming that at 0wt% the failure time of notched MDPE-A is 10,000 hrs then ax = 23.4mm; and for an assumed notch failure time of 40 hrs for a 50wt% HDPE-F blend, then a_x = 15.9mm. However it must be stated that this relationship is only for a limited range of blends at a single pressure and temperature value. The following sections show that the axial length values for 55mm notched fracture surface do not take the form of the equation just derived [7.1] and is therefore only applicable for this particular blend system.

ii) Fractography of HDPE-B Blends

Figure 7.11 illustrates results from Table 7.2 of the axial length variations

	HDPE-F LEVEL IN MDPE-A (wt%)		
	2	**10**	**20**
AVERAGE NOTCH FAILURE TIME (hrs)	5,644	1,785	98
AVERAGE AXIAL FRACTURE LENGTH (mm)	22.1	21.0	18.6

TABLE 7.1: Notch failure time / Axial length data for uncompounded HDPE-F blends.

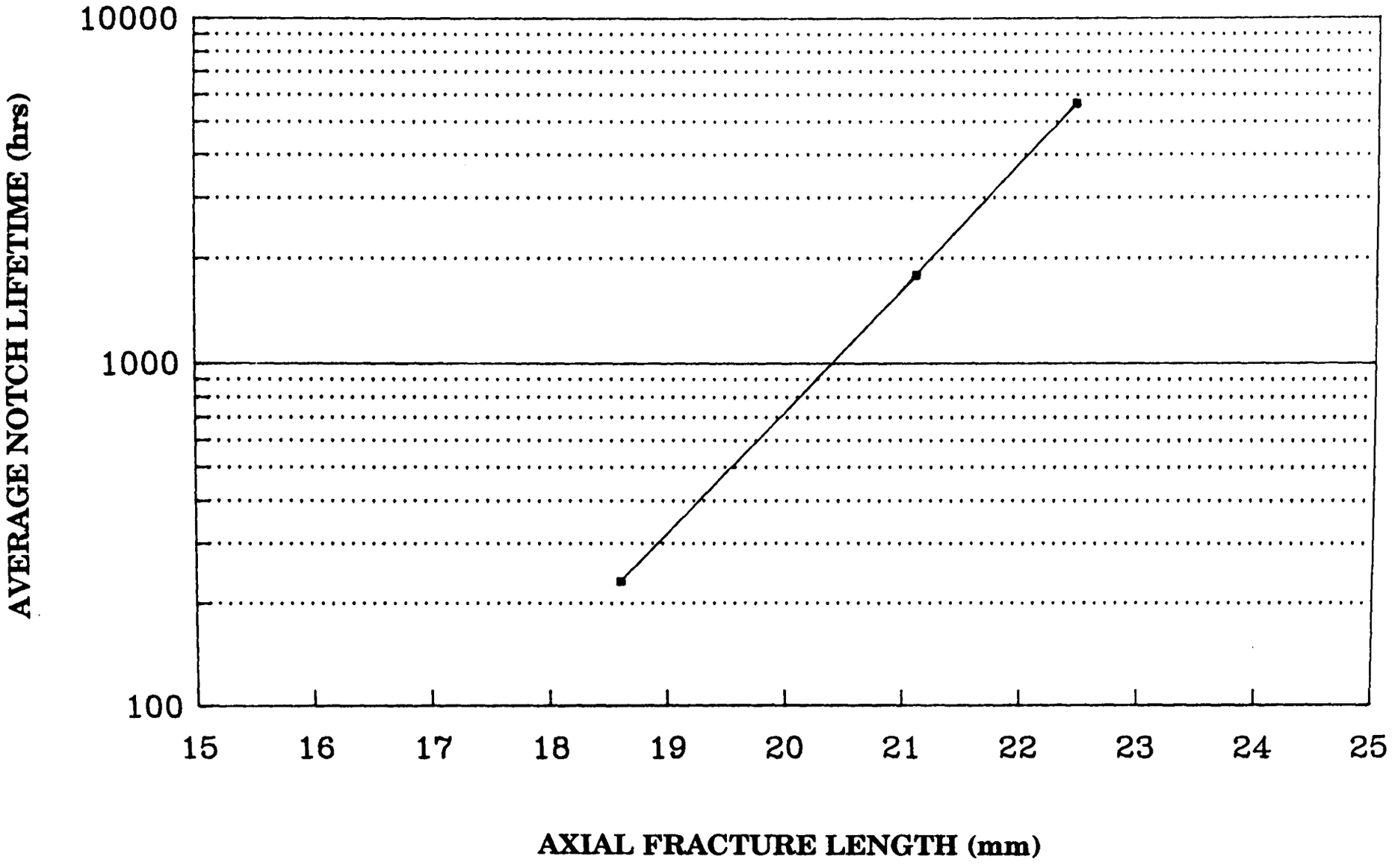

FIGURE 7.10: Average failure time / Axial fracture length graph for notched HDPE-F uncompounded blends.

	AXIAL FRACTURE LENGTH (mm)		
	0.7MPa PRESSURE	**0.8MPa PRESSURE**	**0.9MPa PRESSURE**
MDPE-A/55	42.05	45.70	58.30
HDPE-B/2	-	-	34.10
HDPE-B/5	36.90	32.98	67.50
HDPE-B/10	-	-	37.40
HDPE-B/20	17.20	22.50	46.00

TABLE 7.2: Axial fracture length data for HDPE-B pipe blends.

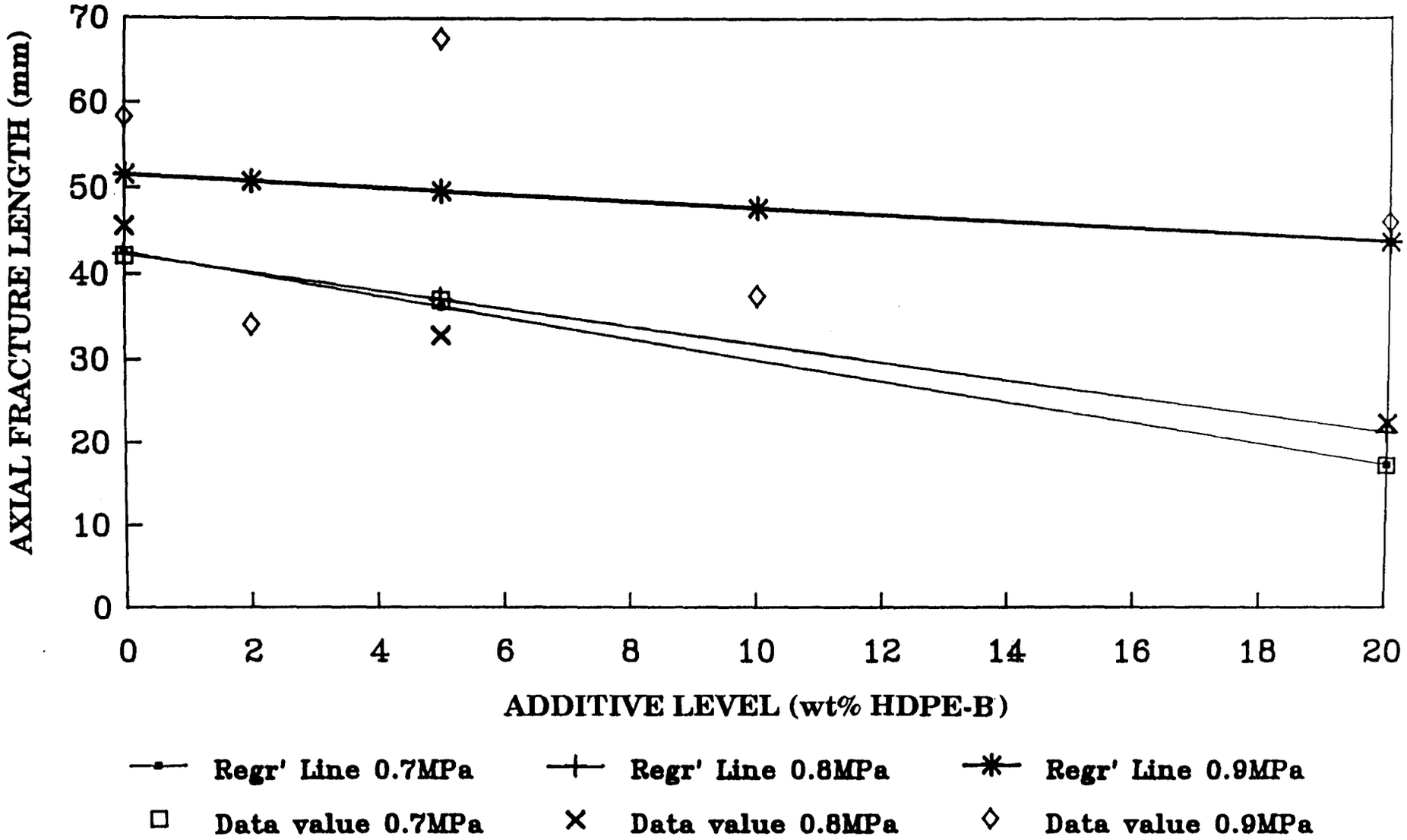

FIGURE 7.11: Axial fracture length graph for 55mm notched HDPE-B blends.

at each pressure level. The graph shows that the axial length decreases with increases in addition and stress levels. Visually the fracture surface appearance is different from the MDPE-A pipe with very little microductility on the fracture surface and showing very little crack arrest regions (Figure 7.12c).

iii) Fractography of HDPE-M Blends

The failure time against axial length curve is shown for HDPE-M blends in Figure 7.13 (values in Table 7.3) with gradual axial length increases with additive additions at the majority of testing pressures. The fracture surfaces exhibited an increase in initiation sites with higher testing pressures and high additive contents. Figures 7.14a) and b) illustrates the increase in initiation sites for a 20wt% blend at a test pressure of 0.9MPa compared with the 0.7MPa test pressure sample. Again for the great proportion of the crack growth a minimal fibrillar region is evident before the yielding of the final ligament before fracture.

iv) Fractography of MDPE-P Blends

The failure time against axial length curve was very unusual for the MDPE-P blends at all addition levels and pressures (Figure 7.15, from values expressed in Table 7.4). The influence of the blends was found initially to produce a decrease in performance down to approximately 5wt%, after which the performance increased up to at least 20wt%. Figure 7.15 reflects this change in performance with axial lengths reaching a maximum at 5wt% and decreasing to 20wt% at the two pressures shown (Table 7.4). The micrographs of a typical fracture surface for the blends are shown in Figures 7.16a) and b) at 5 and 20wt% and 0.7MPa pressure, illustrating this

a)

b)

c)

FIGURE 7.12: a) Notch fracture surface of 55mm HDPE-B/20 pipe at 0.9MPa.
b) Notch fracture surface of 55mm HDPE-B/20 pipe at 0.8MPa.
c) Notch fracture surface of 55mm HDPE-B/20 pipe at

	AXIAL FRACTURE LENGTH (mm)		
	0.7MPa PRESSURE	**0.8MPa PRESSURE**	**0.9MPa PRESSURE**
MDPE-A/55	42.05	45.70	58.30
HDPE-M/2	-	-	57.90
HDPE-M/5	41.30	37.10	63.20
HDPE-M/10	-	-	87.30
HDPE-M/20	38.60	55.90	97.50

TABLE 7.3: Axial fracture length data for HDPE-M pipe blends.

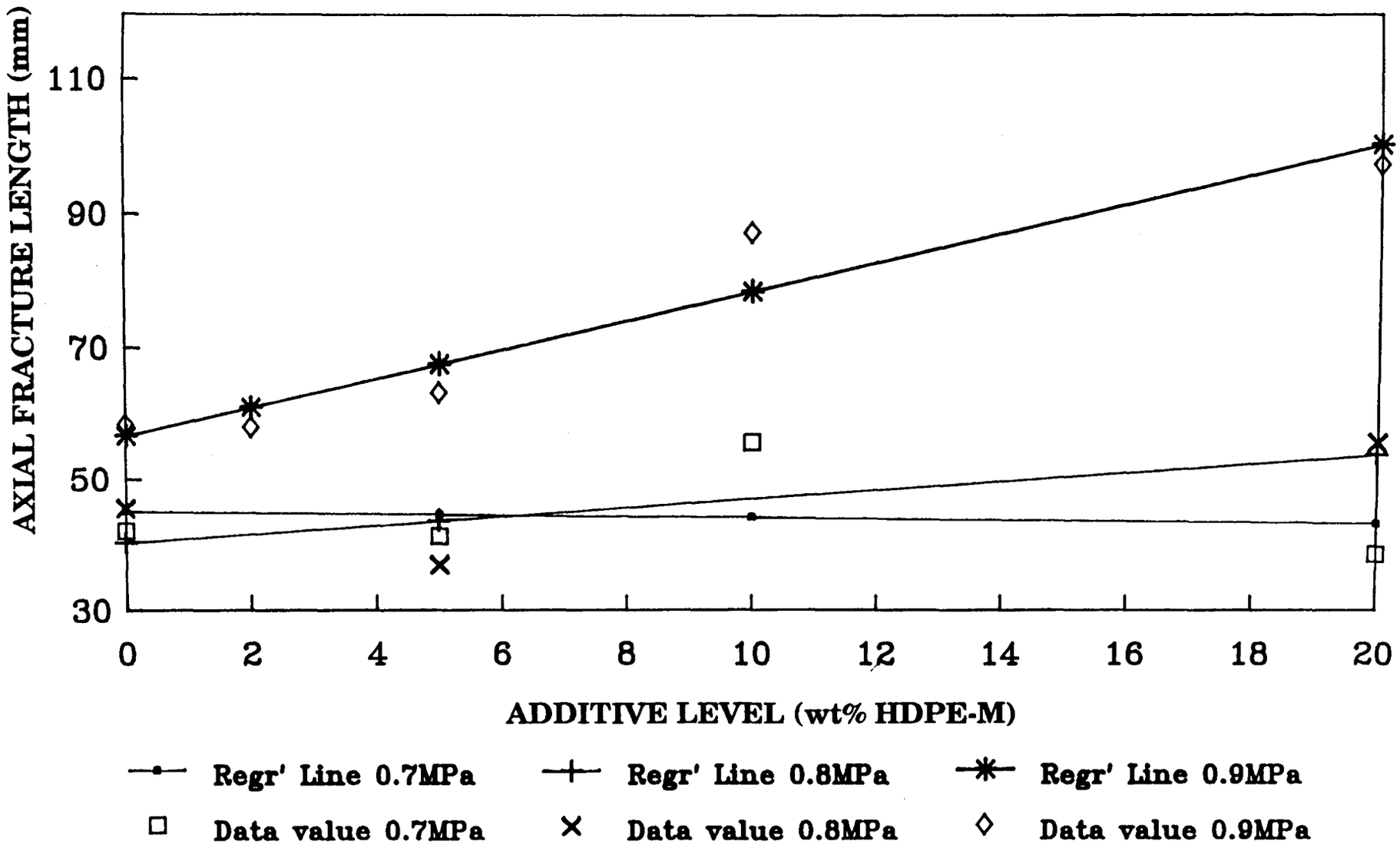

FIGURE 7.13: Axial fracture length graph for 55mm notched HDPE-M blends.

a)

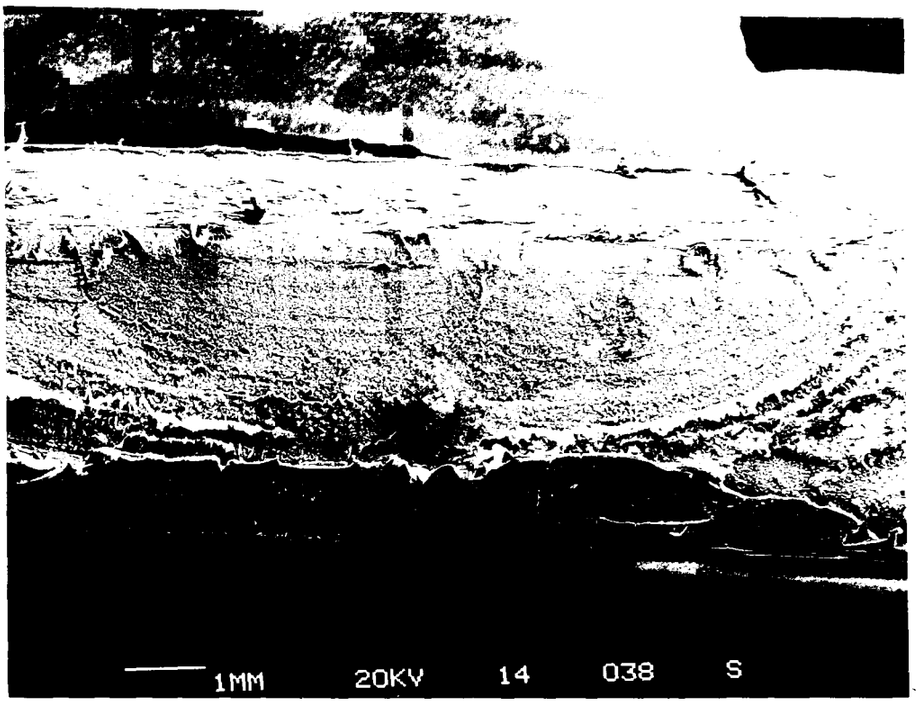

b)

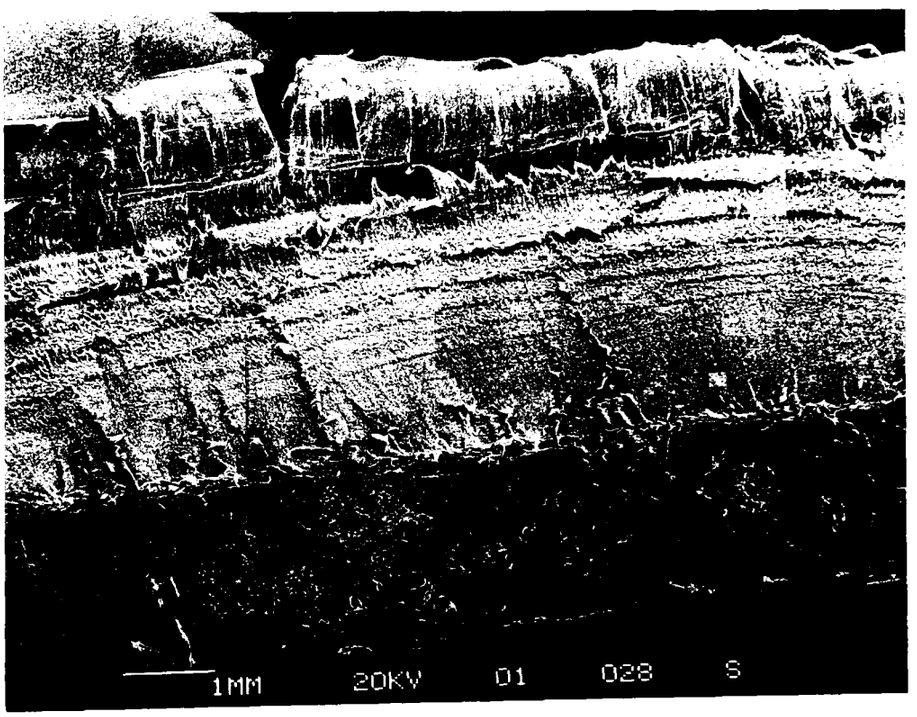

FIGURE 7.14: a) Notch fracture surface of 55mm HDPE-M/20 pipe at 0.9MPa.
b) Notch fracture surface of 55mm HDPE-M/20 pipe at

	AXIAL FRACTURE LENGTH (mm)		
	0.7MPa PRESSURE	**0.8MPa PRESSURE**	**0.9MPa PRESSURE**
MDPE-A/55	42.05	45.70	58.30
MDPE-P/2	-	-	76.10
MDPE-P/5	69.65	36.80	80.50
MDPE-P/10	-	-	62.00
MDPE-P/20	45.20	39.20	71.40

TABLE 7.4: Axial fracture length data for MDPE-P pipe blends.

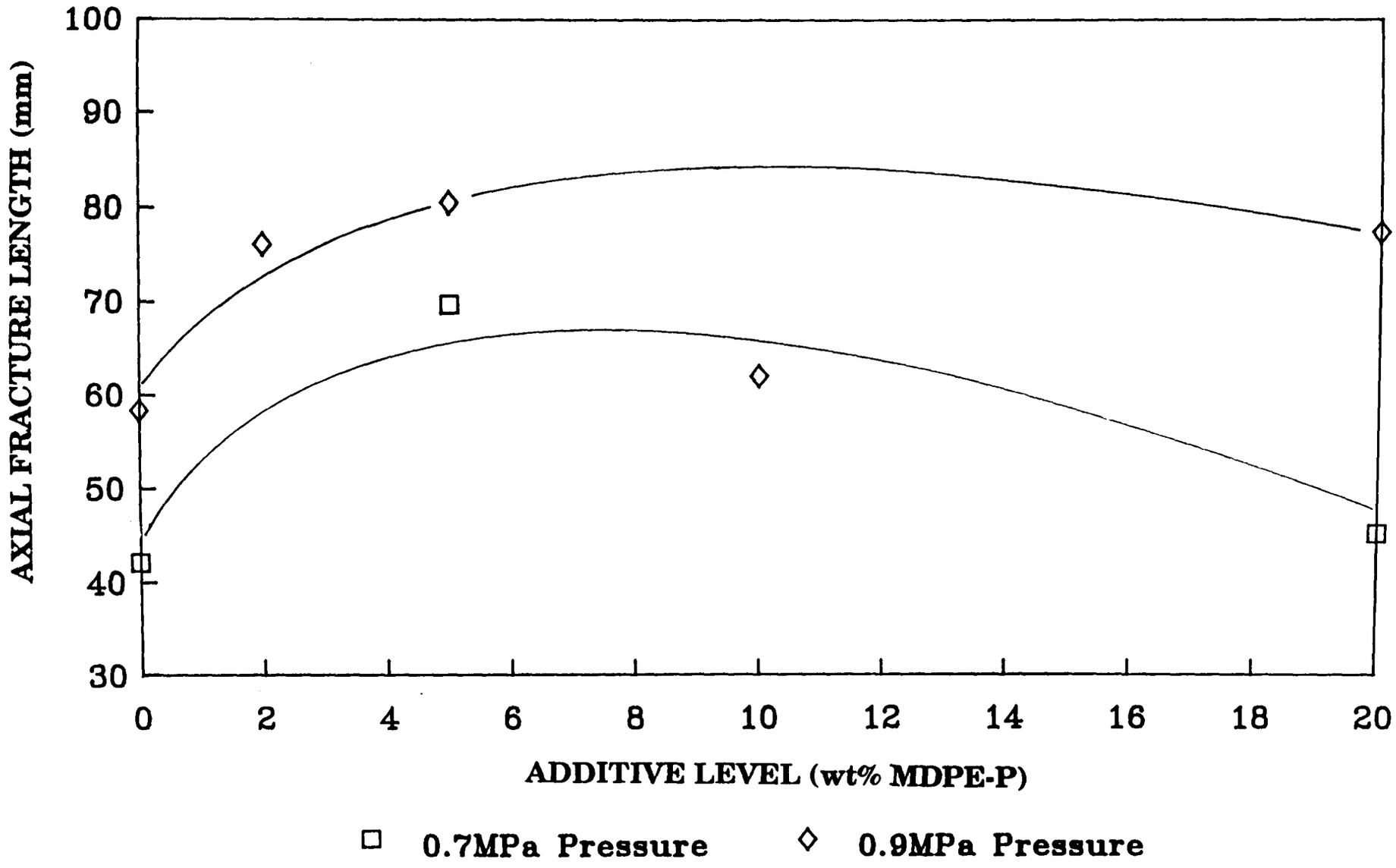

FIGURE 7.15: Axial fracture length graph for 55mm notched MDPE-P blends.

a)

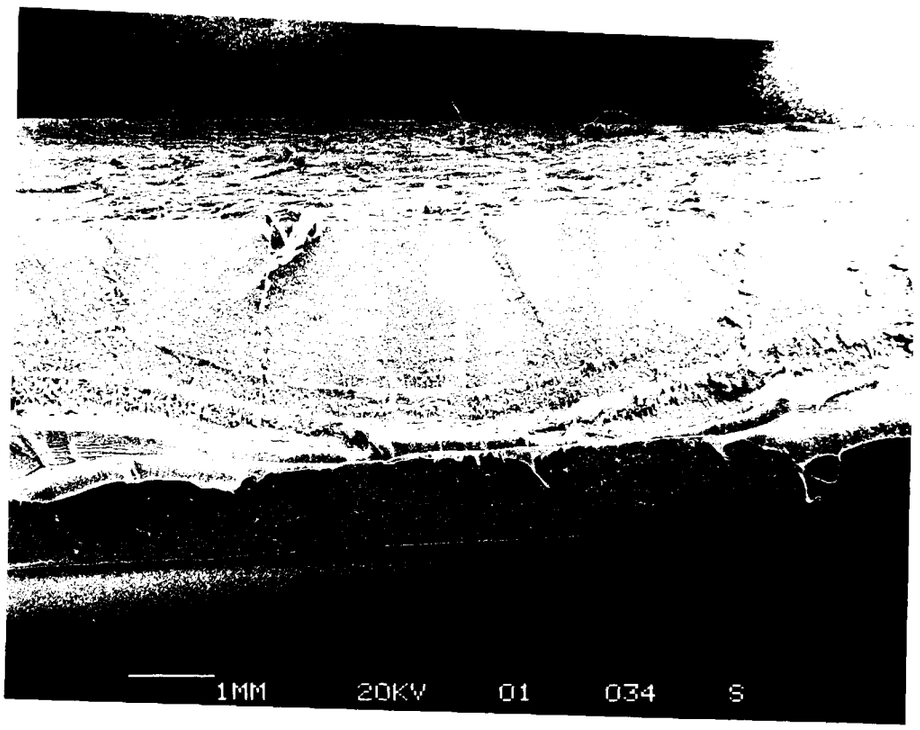

b)

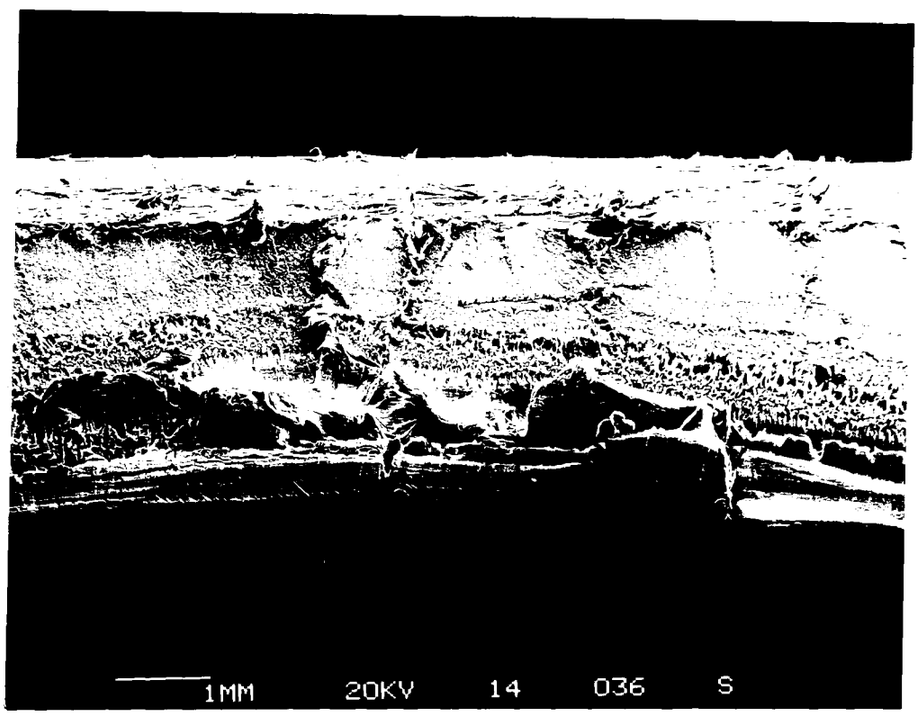

FIGURE 7.16: a) Notch fracture surface of 55mm MDPE-P/5 pipe at 0.9MPa.
b) Notch fracture surface of 55mm MDPE-P/20 pipe at

increase in initiation sites at the 5wt% addition level.

v) Fractography of MDPE-D Blends

The stress rupture results reported in Chapter 5 for these blends showed that they were the most compatible with the MDPE-A resin, maintaining stress rupture performance levels at all additive additions. Figure 7.17 shows a linear regression line of the values in Table 7.5. Only a gradual increase in axial length is obtained with increases in the MDPE-D content. The fracture surfaces of 20wt% at test pressures of 0.7 and 0.9MPa display the good microductility evident in MDPE-A samples. (Figure 7.18a) and b)). This blend shows that good stress rupture performance of a material can be characterized by this fibrous type of fracture surface.

7.4 DISCUSSION OF RESULTS

7.4.1 UNNOTCHED PIPES

It appears that for good stress rupture performance or lifetime a fracture surface having the features shown in Figure 7.1a) is desirable, that is one which is composed of a large amount of microductility from the bore region to the outside of the pipe. The fracture surface of the MDPE-A material is thought to be formed by craze formation followed by slow crack growth through the craze. The semi-circular *ridges* in the fracture surface are thought to correspond to a discontinuous crack advance mechanism. This is where the crack tip becomes stationary and the craze zone ahead of the crack tip yields, ruptures and crack advance takes place leaving behind the characteristic fibrous hump. The process is repeated when the crack is

	AXIAL FRACTURE LENGTH (mm)		
	0.7MPa PRESSURE	**0.8MPa PRESSURE**	**0.9MPa PRESSURE**
MDPE-A/55	42.05	45.70	58.30
MDPE-D/2	-	-	59.90
MDPE-D/5	50.65	-	58.70
MDPE-D/10	-	-	57.20
MDPE-D/20	46.50	44.90	72.70

TABLE 7.5: Axial fracture length data for MDPE-D pipe blends.

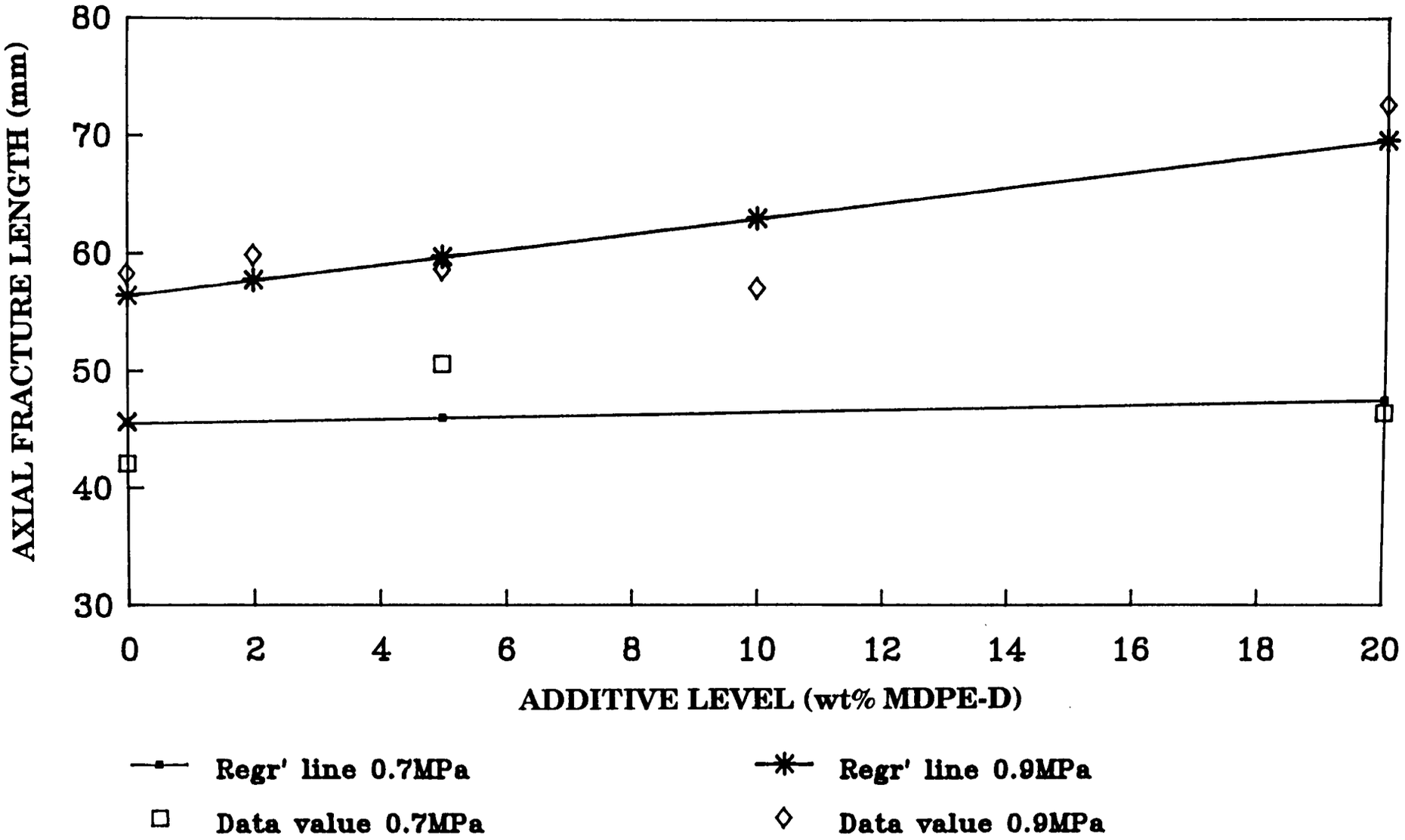

FIGURE 7.17: Axial fracture length graph for 55mm notched MDPE-D blends.

a)

b)

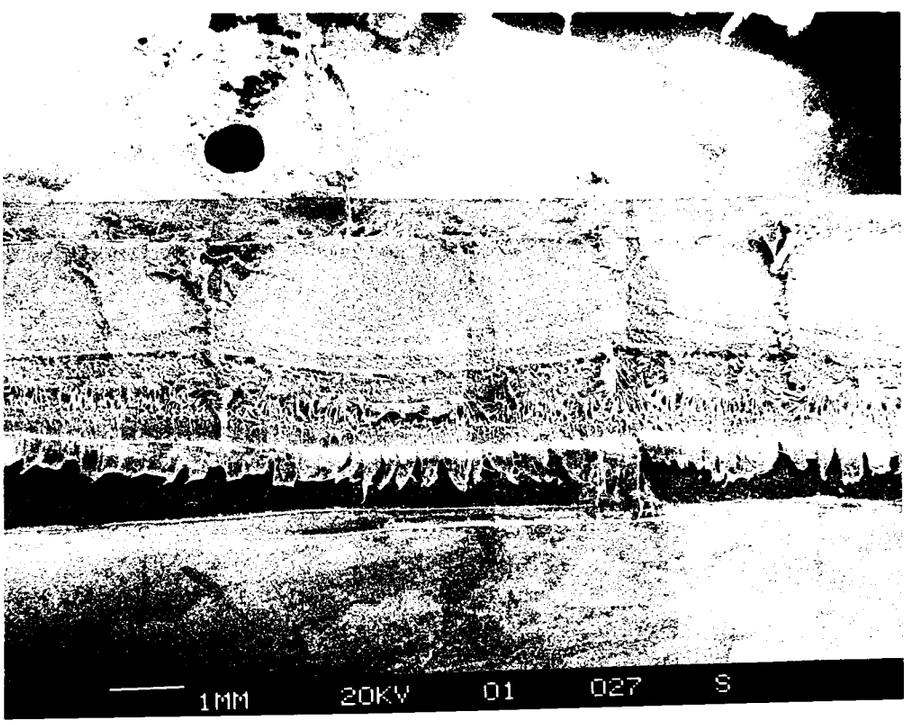

FIGURE 7.18: a) Notch fracture surface of 55mm MDPE-D/20 pipe at 0.9MPa.
b) Notch fracture surface of 55mm MDPE-D/20 pipe at

further arrested.

The presence of the minimal-fibrillar structure evidenced by the HDPE-F blends is not unknown. Lu et al [70] found that a minimal fibrillar region was evident in their linear polyethylene materials under slow crack growth tests. However with polyethylenes with hexene as the comonomer they obtained good microductility characteristics on the fracture surface. Ifwarson and Eriksson [91] found that PE pipes which had an oxidation layer on the bore of the pipe were the predominant initiation sites for failure. These regions were characterized as minimal-fibrillar from SEM studies.

However our samples were blended with a polymer of similar molecular weight and still experienced this reduced microductility feature on the fracture surfaces. Also the O.I.T results from the HDPE-F blends displayed the sample to be well stabilized in the bore region of both the compounded and uncompounded blends. What is evident from the results is that the fracture of the blends is being dictated on a micromolecular basis.

Lee and Epstein [93] studied the fracture surface features of various polyethylene pipe samples and found that the fibrous region changed in response to the crack growth rate. Therefore they found that by increasing the applied pressure (increasing K value), the fracture surface feature changed from fibrous to very fibrous. This area may be a feature in this work whereby the minimal-fibrillar region could be the result of increasing the crack growth rate from the blending of the second phase. Lu and Brown [70] found that by using polyethylene with a comonomer the slow crack growth rate was 10^2 to 10^3 times slower than a polyethylene homopolymer. They cite that the presence of the comonomer decreased the rate of disentanglement of molecules during stress rupture conditions and is

a mechanism which governs slow crack growth.

What is evident from the fracture surfaces of the HDPE-F blends is that during a large proportion of the cracks life the variation in the fibre heights are practically constant (8μm) over the minimal fibrillar region. Once the fibre height changes it is reasonable to assume that the stress intensity factor is changing and a separate mechanism of discontinuous growth is followed until failure [70].

7.4.2 APPLICATION OF K TO NOTCHED BLENDS

From notched pipe data it was attempted to apply K to the failure data. Figure 7.19 illustrates the regression lines for notched 2, 10 and 20wt% uncompounded HDPE-F blends. What is seen is a change in slope of the blend at high addition levels. These can be summarized by producing an equation to represent the data as:

$$\ln t_n = \ln A - b.\ \ln K_{int} \qquad [7.2]$$

where t_n = notched pipe failure time.

A = graph intercept, constant.

K_{int} = initial applied stress intensity factor ($MPam^{1/2}$)

b = exponent

The above equation can be rewritten as:

$$t_n = A\ K_{int}^{-b} \qquad [7.3]$$

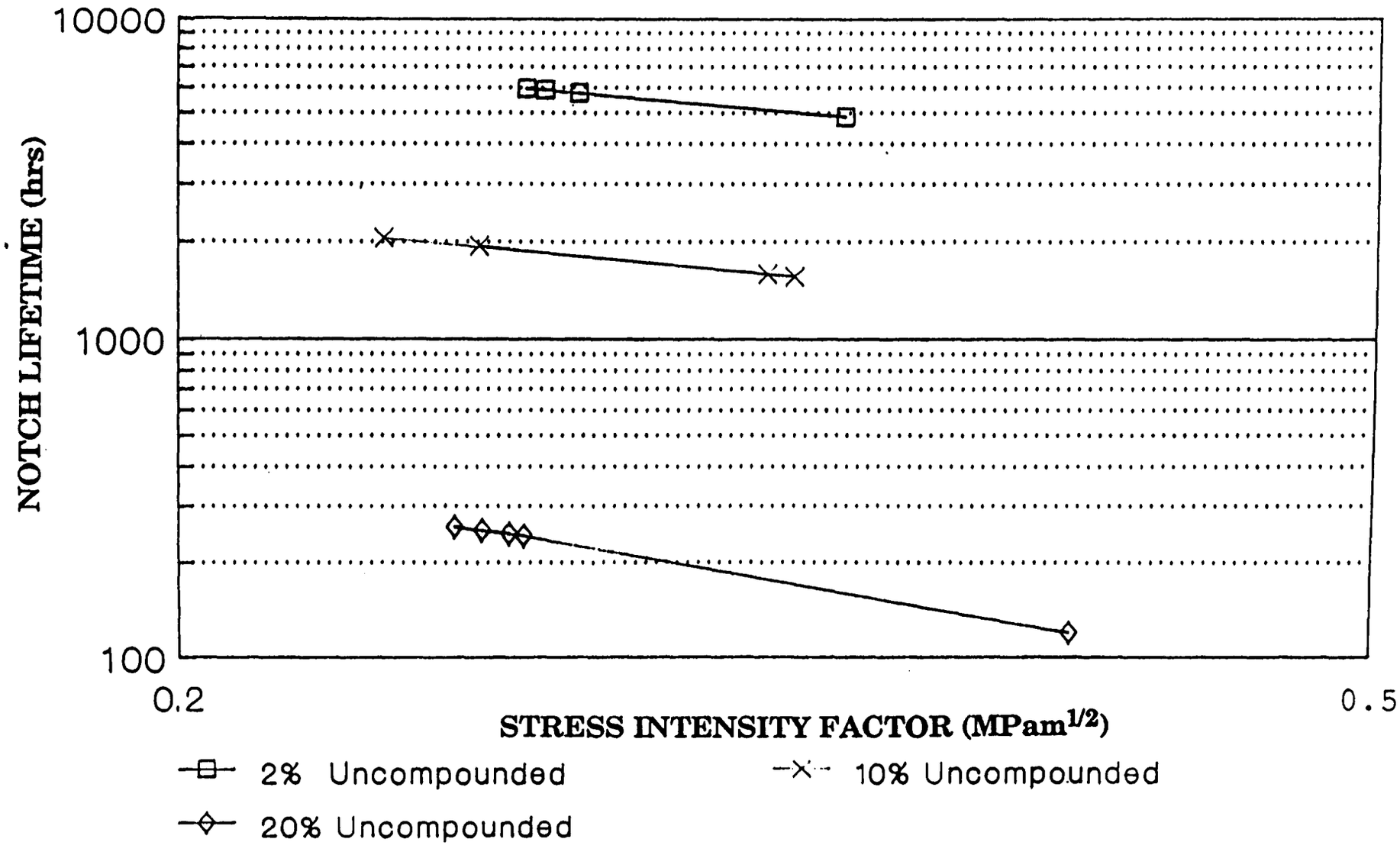

FIGURE 7.19: Lifetime / K_{int} regression line plots for 32mm notched uncompounded HDPE-F blends.

This equation has similarities with equation [3.10] in Chapter 3. For the blends, A and b in equation [7.2] becomes :

2wt% HDPE-F: $t_n = 1870\ K_{int}^{-0.82}$ [7.4]

10wt% HDPE-F: $t_n = 447\ K_{int}^{-1.02}$ [7.5]

20wt% HDPE-F: $t_n = 15\ K_{int}^{-1.99}$ [7.6]

For this particular set of blends A decreases while b increases. Greig and Lawrence [109] while testing pipes under fatigue found similar relationships for a group of polyethylene pipe materials and used the notched failure time / K curve as a means of ranking materials. However equations [7.2 and 7.3] only apply to these particular pipe blends at this particular nominal pipe hoop stress level (4.6MPa) and temperature (80°C). Unfortunately similar curves for the other blend systems did not show similar trend behaviour. Figure 7.20 shows a similar curve for HDPE-M blends at 0.9MPa and illustrates the need for greater data points to establish better correlation of the slopes. K_{int} values for all the blends are displayed in Appendices 16-20.

Although equation [7.3] is similar to the lifetime prediction of equation [3.10] in Chapter 3, it cannot be used to estimate the failure time of a component due to the change in K along the fracture surface. This equation only considers the initial applied K. In fact not even equation [3.10] could be applied, as the criterion for this equation is a slow stable crack growth throughout the specimen, which we have shown in this study to be varying over the fracture surface.

Although it was difficult to see the minimal fibrillar structure in most of the notched pipe fracture surfaces, one thing was apparent in that all the MDPE-D blends had fracture surfaces displaying crack arrest lines. The

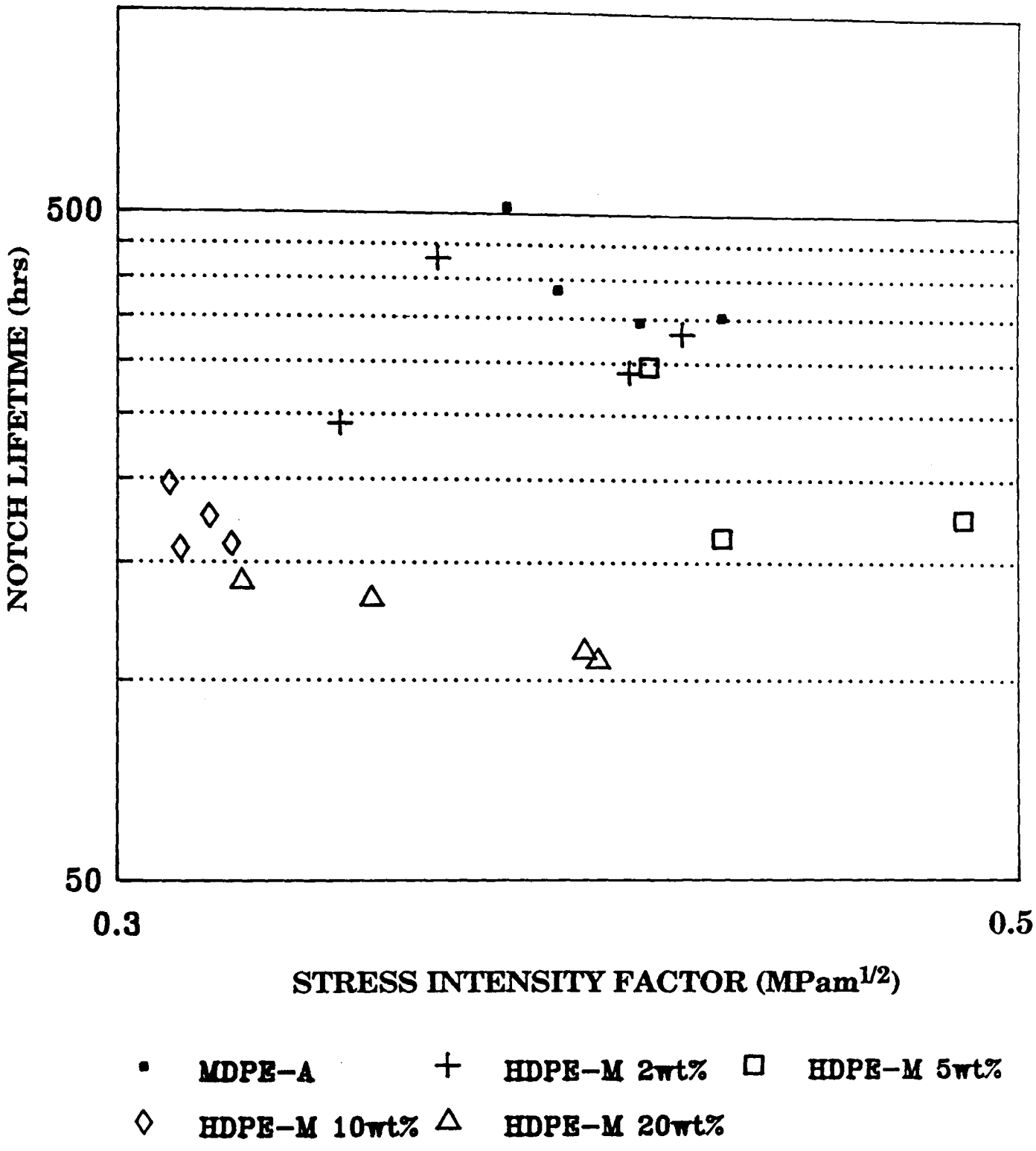

FIGURE 7.20: Lifetime / K_{int} data points for notched 55mm HDPE-M pipe blends.

20wt% MDPE-P blend also illustrated this feature, but the 5wt%MDPE-P blend had more initiation sites along the fracture length (axial length) than the 20wt% blend. This leads us into an area not yet discussed; crack initiation time. In the fracture mechanics analysis a known flaw size is assumed. Bragaw [92] has illustrated that the time spent initiating cracks is important and should be considered in any fracture mechanics approach. What we have here with the MDPE-P blend is that the change in material properties by blending disrupts the ability of the base resin to conform to its usual molecular structure, the resultant structure is one which could be susceptible to crack initiation. It is only when the second phase is at an addition level greater than 5wt%, that a blend is produced which has 80°C stress rupture properties similar to that of the base resin from the increased molecular weight of the additive.

7.4.3 USE OF NOTCHING IN THE BLENDING STUDY

Unfortunately it has been shown that by notching all the 0.8MPa samples last, the stress rupture lifetime data for the MDPE-D and MDPE-P blends nearly concurred with the 0.7MPa data. This was thought to be due to the cutter being significantly blunter than when used for the 0.7 and 0.9MPa samples. This would of course not only affect the lifetime results but the application of K_{int} for the crack tip where the blunting of the root radius would influence the stress around the crack tip [71]. What we have found is that notching of polyethylene pipe using the British Gas Standard (BGC/PS/PLC, Part 1, appendix O) procedure is only viable for ranking materials *within* a batch.

7.5 FAILURE MECHANISMS AND MODELING BLEND BEHAVIOUR UNDER STRESS RUPTURE CONDITIONS

7.5.1 FAILURE DUE TO MOLECULAR PARAMETER VARIATIONS

i) Branching

By blending polyethylenes several fracture characteristics have been found with the additives :

a) An increase in initiation sites with increase in additive additions HDPE-M, MDPE-P blends).

b) A minimal fibrillar region evident with low and high molecular weight additives (HDPE-M, F and B).

c) Fracture on several planes (HDPE-B and F).

What is apparent from these blends is that they all produced poor stress rupture performances even though one of the materials had a large Mw in comparison to the base resin. The main difference in properties between the HDPE and MDPE-P additives and the MDPE-A resin is of course branch length and branch distribution. All the HDPE and MDPE-P resins have hexene as their comonomer. Crack opening micrographs from Lu et al [70] show how the craze fibrils take part in the fracture process and do not as readily fracture as do samples of polyethylene without a comonomer. It is known that increasing the branch length of the comonomer increases the stress rupture lifetime in the brittle region up to a limiting value of branch length [115]. Ishikawa et al [51] have in addition shown that branch distribution, especially on the high molecular weight tail region is important in conferring good stress rupture characteristics to the material. What we

have definitely identified in this study is that blending of different types of branched polymer reduces the 80oC stress rupture performance *regardless* of molecular weight for addition levels up to 20wt%.

The influence of branching on the brittle failure process can be examined under kinetic considerations. At 80oC the amorphous region is above the glass transition temperature of the blend so it is expected that the rate determining process for fractures is the sliding of molecular chains through the crystalline regions of the fibrils in the crack forming process [94] . This would be expected to be more difficult for chains with hexyl branches (octene comonomer) than the butyl branches from the hexene comonomer additives. Lu et al [70] point out that the changes in fracture surface features of minimal fibrillar height are the result of comonomer variations. Fibrillar height is of course influenced also by molecular weight but we have seen that with a similar molecular weight additive, the fracture features changed significantly due to the branch type of the additive. However we cannot rule out branch distribution as a variable in the poor stress rupture performance of the blends. Ishikawa et al [51] showed that with similar molecular weight polyethylenes, the good stress rupture performance was obtained with a butene comonomer which had high branching levels on the high molecular weight tail in comparison with octene, 4 methyl pentene-l and hexene comonomers which had lower branching levels on the high molecular weight tail. From our results branching levels in the high molecular weight tail (M_Z) of Table 5.6, illustrate that the levels of branching were comparable for MDPE-A and MDPE-D resins. However the MDPE-P resin had very much lower branching levels than the other pipe resins. This implies that the high molecular weight tail is a much more linear molecule and according to Ishikawa et al [51] should have poorer stress cracking and creep properties than the MDPE-A and MDPE-D resins.

ii) Density

Density has been known to influence the brittle portion of the stress rupture curve. For similar molecular weight distributions, decreasing the density moves the brittle stress rupture curve to higher failure times [5,7]. By blending in either HDPE-F or HDPE-B, the density of the blend was shown to increase. This would increase the volume fraction of the crystalline region of the blend and decrease the amorphous content and hence may reduce the tie molecule concentration [106]. Density is strongly influenced by branching levels so that the high density of the HDPE-F is an indication of the linearity of the chain. As we have shown in the previous section the reduction of branching levels on the high molecular weight tail will reduce creep rupture times. It is probable with these HDPE blends that a reduction of tie molecules (due to the increased density and the linearity of the chain), led to blends of poor 80°C performance.

iii) Molecular weight and molecular weight distribution

The increased molecular weight (M_W and M_Z) of two of the additives (MDPE-P and HDPE-M) had no beneficial influence on the 80°C stress rupture performance of the MDPE-A resin and, in the case of the HDPE-M blends, reduced the performance at all addition levels. However molecular weight does have an influence and was proven for the low molecular weight HDPE-B additive where the blends 80°C performances were poor in comparison to the other HDPE blends. The similarities in lifetimes of the HDPE-F and HDPE-M blends in 32mm pipe testing showed that molecular weight is not the major influence and molecular weight distribution may play a significant part. The significant low molecular weight portion shown

in Figure 5.19 of the HDPE-M additive may offset any good stress rupture benefits from the high molecular weight tail. Bunniyat-Zade and Azimova [110] showed this clearly by removing the low molecular tail portion of a polyethylene hexene comonomer material and found increased stress cracking resistance.

This low molecular weight tail may be a feature in the MDPE-P blends where initially the 80oC performance was reduced and then increased to comparable MDPE-A levels at 20wt%. The introduction of the additive may possibly deplete tie molecule concentration due to the presence of the low molecular weight species and the increases in crystallization temperature, but may be offset at 10wt% by the increased levels of branching and high molecular weight tail within the blend.

iv) Crystallization and Melting Temperature

The crystallization temperature of the MDPE-A resin has been shown to be influenced by the addition of all the additives moving the blend to high crystallization temperature. This is reflected in the melting temperatures where, apart from the MDPE-P blends the melting temperatures are moved to higher values. Using the Hoffmann-Weeks equation [2.8] we can infer that the lamellae is getting thicker due to the melting point of the blend increasing (Figure 6.3) and decreasing for the MDPE-P blends. What appears to be happening is that the crystallization of the blends produces structures that have alien characteristics in resisting slow crack growth. This can easily be demonstrated by taking the example of HDPE-M blends. Due to its higher crystallization temperature the HDPE-M molecules will start to nucleate first being a longer and linear molecular species. As the temperature decreases the MDPE-A molecules grow on the existing nascent

HDPE-M crystals. Therefore there is a blend organization of MDPE-A/HDPE-M lamellar crystals growing at a *compromise* crystallization temperature. As we have found, the negligible disruption of the crystallization process from the MDPE- D blends may have greater significance than is presently known.

Although the mechanism of crystallization of polyethylene blends is complex several authors have found segregation under isothermal crystallization conditions [57,58,113] . They found non-segregation of the polyethylene blends under normal quenching conditions with the characteristic single peak from the DSC, showing increased cocrystallisation with increased undercoolings. This work could be of benefit to our studies in that although the blends have cocrystallised, under quenching conditions at a particular crystallization temperature the molecules may begin to seperate into their own species at elevated temperatures and produce lamellae which are energetically favorable to them. That is why Norton and Keller [113] and Rego Lopez et al [57,58] produced isothermally crystallized blends with distinct large and small lamellar regions corresponding mostly to the individual components.

7.5.2 FAILURE OF 32mm HDPE-F COMPOUNDED PIPE BLENDS

There has been many papers and articles outlining the advantages of precompounding materials in order to obtain maximum properties [42,44] . However we have obtained deleterious stress rupture results when precompounded blends are produced into pipe. Although there is no oxidational influences of the material (section 5.5.3) and no discernable changes in molecular weight of the blends (section 5.3.2), the changes could be attributed to the large initiation particles evident in some of the fracture surfaces (eg Figures 7.4&5) which could be degraded particles or polymeric

contamination from the screw of the compounder. It is widely known that impurities can largely influence the failure times of polyethylene pipes [67,73].

7.5.3 MODELLING THE BRITTLE FAILURE OF POLYETHYLENE PIPE BLENDS

Using the concepts described in the previous sections, an attempt is made to model the crystallization of the blends and hence describe the possible molecular confirmations that have reduced the overall stress rupture performance of the MDPE-A resin.

A simple two dimensional model can be used to explain these concepts. Figure 7.21a) shows an HDPE molecule forming into several lamellae crystals *above* the crystallization point of the MDPE-A phase which is in the melt around it. Chapter 6 has discussed this molecule being a nucleant for growth of other polyethylene molecules on its faces. It is also likely that this molecule will be a high molecular weight linear chain (or one with very few branches) due to the low molecular weight species and heavily branched chains crystallizing at lower temperatures [22]. As the temperature is decreased crystal growth proceeds until the conditions are energetically favorable to epitaxially nucleate a MDPE-A molecule *above* its normal crystallization temperature (Figure 7.21b). The MDPE-A molecule conforms to the crystal lattice dimensions of the lamallae and takes part in the crystallization process of other lamallae crystals. What is being built up is a lattice of molecules of each component because the next molecule may be an HDPE-M molecule which is of a low molecular weight and heavily branched. (Figure 7.21c)). It is a simple representation and does not consider defects such as screw dislocations, chain ends or entanglements of chains which are prevalent in the melt. However it shows the conditions

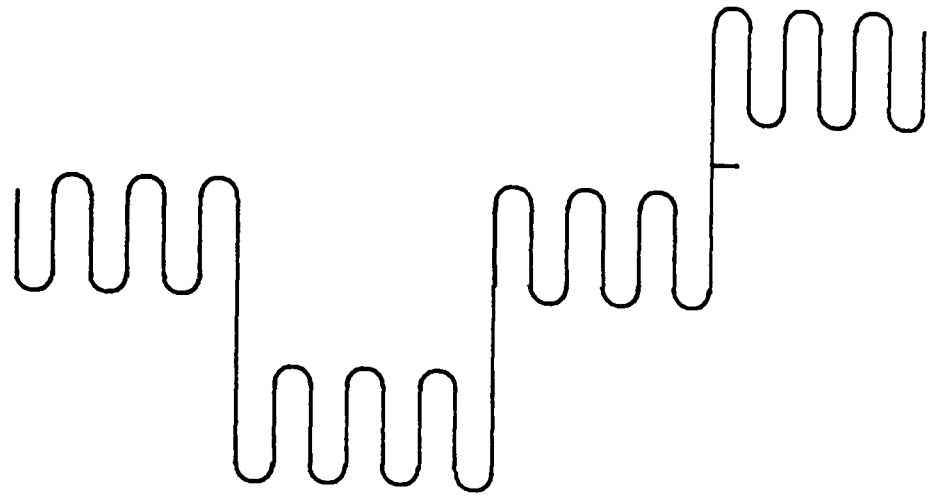

FIGURE 7.21a): A simplified model of the crystallization behaviour of a polyethylene molecule.

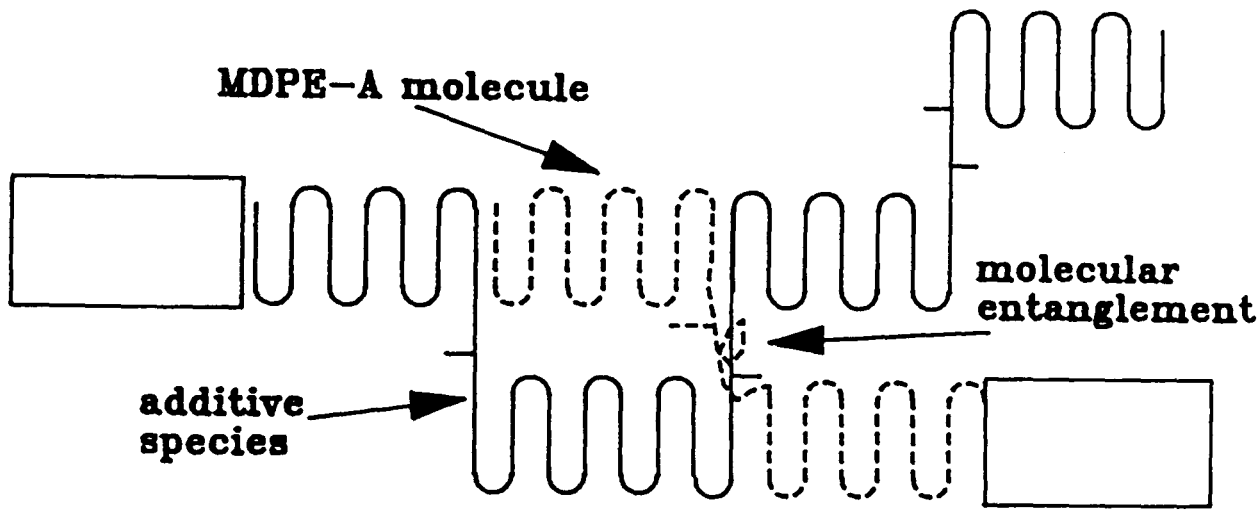

FIGURE 7.21b): Involvement of a MDPE-A polyethylene molecule in the crystallization of the additive, showing entanglement regions.

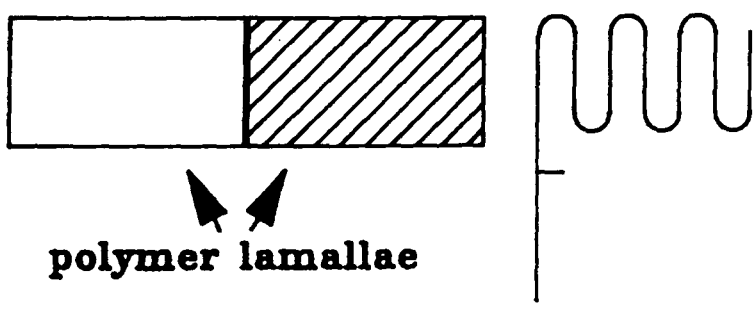

FIGURE 7.21c): The crystallization of a polyethylene molecule on the formed polymer lamellae.

favorable for slow crack growth in that the linear molecule can be more easily pulled out of the crystal lattice than a branched one, whereas the presence of a low molecular weight species reduces the tie molecule concentration by bridging fewer crystallites.

This model can be used to explain the failure mechanisms of the pipe blends. With the HDPE resins all the grades had hexene as the comonomer. Assuming the branch distribution along the polymer chains were similar to one another it can be postulated that only molecular weight and molecular weight distribution influences were of importance in ranking the additives in terms of their stress rupture performance as seen in Figure 5.12. With the HDPE-B resin the presence of the polyethylene molecule could reduce the amount of effective tie molecules due to the low molecular weight chains not bridging as many crystallites [108]. A similar mechanism can be applied to HDPE-F where although the molecular weight of the materials were comparable the reduced branching levels of the HDPE material led to more crystalline regions within the blend and a reduction in tie molecule concentration. The HDPE-M blends were unusual in that they had 80°C stress rupture lifetimes comparable to 10wt% HDPE-F blends. This could indicate the significant role of the low molecular weight species of this additive overcoming any effective stress rupture benefits from the high molecular weight tail. The linearity of the material in regards to branch levels as well as the type of branch would make molecular movement of the HDPE molecule easier than an MDPE-A molecule.

With the pipe grade polyethylene additives the situation is a little more complex due to the improvement in stress rupture performance of the MDPE-P blends after 10wt%. What is thought to occur with this blend is that at low addition levels the presence of a linear high molecular weight

tail increases density and increases the slow crack growth process. Also the low weight species of this additive may aid slow crack growth in the initial stages. However at 5wt% the additive is in sufficient quantities where molecular entanglements between high molecular weight species occurs (Figure 7.21b)). Further additions shows a decrease in density (Table 6.6) and probably an increase in entanglements of the high molecular weight species of the MDPE-P molecules. At these higher concentrations of MDPE-P the mechanism of slow crack growth will not only require chain pull-out but also the breaking of entangled chains, the bond energy of the carbon-carbon backbone being very much greater than chain pull-out. That is why UHMWPE has very good stress rupture properties due to entanglements of molecules rather than the level of branching on the chain [42].

It is not difficult to understand the good stress rupture behaviour of MDPE-D blends. This additive had molecular weight, branching levels, branch type and even similar crystallization temperature to the MDPE-A material. Therefore compatible blends were produced and stress rupture performances maintained.

The molecular pull-out of the chain under stress rupture conditions will be reflected in the fracture surface by the length of the molecule and branching concentration and molecular entanglement of the blend. The minimal fibrillar region of the fracture surface could be the result of the lack of the molecular resistance to deformation within the fibrils of the craze zone [70]. By using the models shown, it possible that the HDPE blends would be susceptible to this type of deformation. This may be true for the MDPE-P blends at low additions, where there is minimal molecular entanglement to offset the more linear high molecular weight chain being pulled out of the lamellae.

Even though tie molecule concentration and density/branching concentrations are important there is an optimum relationship for overall long and short term properties. If the fraction of molecules incorporated in the crystalline molecules is too low, then the material will display high ductility but also low stiffness. For the polyethylene pipe to resist exterior soil loadings underground, good stiffness properties need to be maintained. Therefore a balance must be established. In our studies this balance was offset when good short term (stiffness) properties of the blend were obtained but at the expense of the long term stress rupture performance. From this work on the blending of polyethylenes it is not the simple relationship of increasing molecular weight as was first postulated in Chapter 1. It has been found that the keys to good blending probably lies with materials with similar branch lengths (and distributions), molecular weight (or higher) and similar crystallization temperatures.

CHAPTER 8

CONCLUSIONS AND SUGGESTIONS FOR FURTHER WORK

8.1 INTRODUCTION

From the objectives outlined in Chapter 1 several areas have been explored and it has been found that the simple concept of increasing a polymers stress rupture performance by the addition of a high molecular weight material is much more complicated than was at first anticipated. The conclusions from the influence of blending HDPE-F, M and B and MDPE-P and D materials with the MDPE-A base resin are outlined in the following sections.

8.2 INFLUENCE OF BLENDING ON SHORT TERM PROPERTIES

The good short term behaviour of the HDPE-F blends was in stark contrast to the poor stress rupture properties of the pipes produced from these blends. This adequately shows the need for the final artifact to be tested under experimental conditions that will induce failures similar to those observed in the field. Stress rupture testing was found to be very sensitive not only to small changes in the base materials properties but in distinguishing between levels of additives within the base resin.

8.3 INFLUENCE OF TWIN SCREW COMPOUNDING ON THE STRESS RUPTURE PERFORMANCE OF HDPE-F BLENDS

Compounding of HDPE-F blends prior to extrusion was found not to offer any substantial improvements in the 80°C performance when compared to pipe produced with the MDPE-A and HDPE-F polymers mixed together before being fed into the hopper.

In fact the MDPE-A 80°C performance was reduced by 14% for 2wt% uncompounded blends in comparison to 90% for 2wt% compounded blends. Non-metallic defects were thought to be contributory to the compounded blends poor performance; even though at 20wt% HDPE-F the failure times under stress rupture conditions of compounded and uncompounded blends were similar showing that a material factor rather than a defect factor was influencing the overall reduction in 80°C performance. O.I.T tests showed that degradation of the pipe had not taken place and was not a factor in the reduction of 80°C performance.

8.4 COMPATIBILITY OF BLENDS

Miscibility studies revealed the compatibility of the blends used in the study. DMTA and DSC were techniques that showed the mechanical compatibility and cocrystallisation of the blend components through the single peaks produced in the experiments. Microscopy identified the nucleating influence of the additives on the crystallization behaviour of the blend and the change in spherulitic structure of the blends. The large spherulitic structure of the MDPE-A resin was destroyed by the additions of all the additives even at very small addition levels. This contradicted work by several authors **83,84,108** who emphasize reduced spherulitic structures as

an indication of good ESCR stress rupture properties. It was found that blends could be produced which had good and poor stress rupture performances with fine/featureless spherulitic morphologies. Spherulites have been demonstrated to be a poor guide in assessing a materials stress rupture properties.

8.5 INFLUENCE OF BLENDING ON THE STRESS RUPTURE PERFORMANCE OF THE MDPE-A RESIN

The HDPE additives all reduced the 80°C stress rupture performance of the MDPE-A resin with the HDPE-B producing the poorest properties of the three materials. The pipe grade resins behaved differently. At low additions the MDPE-P reduced the performance, but not as badly as the HDPE additives, however the performance started to increase after the 5wt% addition level and at levels of 20wt% the stress rupture performance was restored to the level of the base resin. The MDPE-D resins maintained 80°C performance at all addition and pressure levels.

8.6 FRAGOGRAPHY OF BLENDED PIPE

The features of the fracture surfaces of pipe made with HDPE blends displayed the reduced microductility features when compared to the MDPE-A fracture surfaces. For the 32mm unnotched HDPE-F blends a minimal fibrillar region was identified and found to increase with addition levels. The reduced performance of the MDPE-P was reflected in the fracture features of notched pipe where the axial length increased up to 5wt% and decreased to 20wt% addition levels.

8.7 FRACTURE MECHANICS BEHAVIOUR OF PIPE BLENDS

An attempt was made to correlate the failure times of notched pipe with the stress intensity factor at the notch tip. Although a relationship of the form below was obtained for 32mm uncompounded HDPE blends, no such correlation could be established with the 55mm pipe blends due to insufficient data points. For the 32mm notched pipes the relationship was given by:

$$t_n = A\, K_{int}^{-b}$$

where: t_n = Notch pipe failure time.

K_{int} = Initial applied stress intensity factor.

A,b = Constants.

For the 55mm pipes it was concluded that there was a need for further data points to reduce the scatter evident in the results.

The increase in failure time of the blends at 0.8MPa pressure in comparison to 0.7MPa have shown that the notch tip geometry from the cutter could be different than for notched pipe specimens tested at 0.7 and 0.9MPa. As a batch procedure notching has been shown to be valuable in ranking materials, but not in comparison with materials notched with a different cutter or a cutter which has been extensively used.

8.8 INFLUENCE OF MOLECULAR FACTORS UPON THE STRESS RUPTURE PERFORMANCE OF POLYETHYLENE BLENDS

From the data produced it was concluded that the following molecular

parameters influenced blend performance.

i) Branching levels, type and distribution.

ii) Density.

iii) Molecular weight and molecular weight distribution.

iv) Crystallization temperature.

The density of the blend was increased by using HDPE-B and HDPE-F materials. A simple model demonstrated that this would not only increase the crystalline portion of material within a blend but could probably decrease the tie molecule concentration. The decreased branching levels of the chain would help the movement and dis-entanglement of chains under stress to be pulled out. The type of branching was also identified to be a major asset for the polymer with the hexyl branches of the MDPE-A molecule offering greater chain pullout resistance than the butyl side chain of the HDPE additives.

The molecular weight distribution of the additives was found to be important, with the low molecular weight component being thought to influence the properties of the HDPE-M and MDPE-P blends. For the MDPE-P blends the reduction in entanglement density of the high molecular weight chains was thought to be major contributory factor to the reduced performance of blends up to 5wt%. At 20wt% there was enough entanglements of the high molecular chains to influence the resistance of molecular pullout of chains and therefore increased 80^{o}C performance levels in comparison to the MDPE-A material.

Crystallization temperatures of the blends all increased with higher additive levels. However MDPE-D blends reduced the disruption of the

crystallization behaviour of the blend the least. These blend materials were the ones that maintained stress rupture performance of the MDPE-A material at all addition levels.

From these studies on the blending of a number of polyethylene additives on a known pipe grade resin, it was thought that the keys to good blending lies with materials with similar branch lengths (and distributions), molecular weight distribution (or higher molecular weight tail) and similar crystallization temperature.

8.9 SUGGESTIONS FOR FURTHER WORK

As blends up to 20wt% have been studied, it would be interesting to evaluate the performance at 80°C at addition levels greater than 20wt%, especially for the MDPE-P additive where it appears that the stress rupture performance may continue to increase. It will also be interesting to see whether the full failure time / addition level curve for the HDPE-M blends exhibits the same behaviour as the MDPE-P blends and start to increase after 20wt%. This would support the theory of the entanglement of the high molecular weight chains in the MDPE-P blends after 5wt%.

Although poor performance resulted from blending, it does not imply from 80°C work that poor stress rupture performances would also be a feature at 20°C. Palermo [114] has found that even though a material has poor stress rupture properties at 80°C it could easily have good performance properties at 20°C due to the change in the time / temperature Arrhenius curve. At the time of writing 55mm pipe blends have been under creep rupture testing conditions at 60°C, 0.8 and 0.9 MPa pressure. At least one other temperature will be needed to correctly establish a possible estimation of

the lifetime of the blends at 200C using extrapolation techniques [114].

The consequences of blending may have far reaching implications. For example the welding of dissimilar materials may leave a weld interface which is a source of failure. The molecular interaction at the weld interface may have reduced tie molecule or entanglement concentrations. The use of socket fusion couplers or even electrofusion fittings, (which are thought to be able to weld dissimilar pipe systems [115]) may produce weld blends which are a source of failure. Further studies in the welding of dissimilar pipes under stress rupture conditions will evaluate whether for example the welding of a polyethylene with octene as its comonomer with a polyethylene with hexene as its comonomer will produce a weld interface which is a source of failure, as this work implies.

Lee and Epstein [93] and Lu et al [70] found changes in fracture surface features with different polyethylene samples. It may be advantageous to try and correlate the crack growth rate from slow crack growth experiments on notched or C-shaped notched specimens with the fracture surface features of pipe blends. Lee and Epstein [93] have been able to correlate the fibre height on the fracture surface with the applied stress intensity factor associated with the crack growth rate. Further work would elucidate if the minimal fibrillar region which is prevalent in the blend samples is a result of the change in crack growth rate of the MDPE-A resin or some other mechanism.

The keys to good blending have been thought to involve branching levels and distribution along the chain. Selected experiments could establish exactly the influence of branch distribution on the stress rupture performance. For example using MDPE-A as a reference and blending in

similar octene comonomer polyethylenes with :

a) All the hexyl branches in the low molecular weight portion of the MWD.

b) All the hexyl branches in the middle molecular weight portion of the MWD.

c) All the hexyl branches in the high molecular weight tail of the MWD.

These materials will definitely alter the crystallization behaviour of the MDPE-A resin. By using small angle X-ray scattering or neutron scattering methods, the lamellae dimensions can be evaluated after melt blending and after stress rupture testing to identify if any changes in lamellae dimensions can be correlated to stress rupture failure times.

REFERENCES

1 EUROPEAN PLASTICS NEWS. May (1988).

2 J WHITEHEAD. Plastics and Rubber Weekly. April 2nd (1988).

3 J A BOWMAN. Brunel University, England. Private Communication.

4 BRITISH GAS STANDARD., BGC PS/PLC, Part 1, Pipes, June (1986).

5 W MULLER and E GAUBE. Kunststoffe. **72** (1982) 297.

6 P ERIKSSON and M IFWARSON. Proc. 6th International Conference on Plastics Pipes, York, England. March (1985).

7 K RICHARD, G DIEDRICH and E GAUBE. Kunststoffe. **49** (1959) 516.

8 ASTM D2837-76. ASTM, Book of Standards. **34** (1977) 390.

9 E GLOOR. Modern Plastics. **36** (1958) 144.

10 S N ZHURKOV. Int. J. Fract. Mechs. **1** (1965) 311.

11 F R LARSON and J MILLER. Trans. Am. Soc. Mech. Eng. **74** (1952) 765.

12 S GLADSTONE, K J LAIDLER and H EYRING. The Theory of Rate Process, McGraw-Hill, New York (1941).

13 B D COLEMAN. J. Polym. Sci. **20** (1956) 447.

14 H GEBLER. Kunststoffe. **73** (1983) 73.

15 J SKARELIUS. Quality Assurance of Polymeric Materials and Products, ASTM STP 846, F T GREEN, R W MILLER and V L TURNER, Eds., American Society for Testing and Materials (1985) 118.

16 R L MILLER. Polymer Handbook , J Brandrup and E H Immergut, Editors, First Edition, Interscience, New York, (1967), 295.

17 J HASLAM, H A WILLIS and D C M SQUIRRELL. Identification and Analysis of Plastics, Second Edition, Iliffe Books, London, (1972).

18 J TECL. Int. Polym. Sci. Tech., **4** (1987) 14.

19 J SPEVACEK. Polymer., **19** (1978) 1150.

20 D L BEACH and Y V KISSIN . Encyclopedia of Polymer Science and Engineering., **6** (1986) 454, John Wiley and Sons, New York.

21 R J YOUNG. Introduction to Polymers, Chapman and Hall Ltd., London. (1981).

22 L MANDELKERN. Crystallization of Polymers, McGraw-Hill., New York. (1964).

23 A KELLER and A O'CONNOR. Disc. Faraday Soc. **25** (1958) 114.

24 A LOW, D VESELY, P ALLAN and M BEVIS. J. Mat. Sci. **13** (1978) 711.

25 D C BASSETT, A M HODGE and R H OLLEY. J. Polym. Sci., Phys. Ed. **17** (1979) 627.

26 P J FLORY. Am. Chem. Soc. **84** (1962) 2857.

27 D Y YOON and P J FLORY. Faraday Disc. Chem. Soc. **68** (1979) 288.

28 R SEGUELA and F RIETSCH. Polymer. **27** (1986) 703.

29 G CAPACCIO and I M WARD. J. Polym. Sci., Polym. Phys. Edn. **22** (1984) 132.

30 C FRANCE, P J HENDRA, W F MADDAMS and H A WILLIS. Polymer. **28** (1987) 710.

31 E MARTUSCELLI. J. Macromol. Sci.-Phys. **B11**(1) (1975) 1.

32 J MARTINEZ DE SALAZAR and F J BALTA CALLEJA. J. Crystal Growth. **48** (1979) 283.

33 J D HOFFMAN. Spe. Trans. **4** (1964) 315.

34 H D KEITH, F J PADDEN and R G VADIMSKY. J. Polym. Sci. **A-2,18** (1980) 2307.

35 A TSURATA, T KANAMOTO, K TANAKA and R S PORTER. J. Polym. Sci., Polym. Phys. Edn. **23** (1985) 429.

36 A LUSTIGER and R D CORNELIUSEN. J. Polym. Sci., Polym. Phys. Edn. **24** (1986) 1625.

37 L A UTRACKI. Polym. Eng. Sci. **22** (17) (1982) 1166.

38 L M ROBESON. Polym. Eng. Sci. **24** (8) (1984) 587

39 B B STAFFORD. J. Appl. Polym. Sci. **9** (1965) 729

40 A P PLOCHOCKI. Polymer Blends. D R PAUL and S NEWMAN, Editors, Academic Press., New York. **2** (1978) 319.

41 S K BHATEJA and E H ANDREWS. Polym. Eng. Sci. **23** (16) (1983) 888.

42 M M DUMOULIN, L A UTRACKI and J LARA. Polym. Eng. Sci. **24** (2) (1984) 117.

43 F P La MANTIA and D ACIERNO. Plast. Rubb. Process. Appl. **5** (2) (1985) 183.

44 N K DATTA and A W BIRLEY. Plast. Rubb. Process. Appl. **3** (3) (1983) 237.

45 A F MARGOLIES. S.P.E. J. **27** (1971) 44.

46 S COHEN. Mod. Plast. **4** (1974) 88.

47 R A BUBECK and H M BAKER. Polymer. **23** (1982) 1680.

48 P LUCCHESI. Union Carbide Corp., Canadian Patent. 1,106,521 (1981).

49 R SEGUELA and F RIETSCH. J. Mat. Sci. **23** (1988) 415.

50 L D CADY. Plast. Eng. Jan. (1987)

51 N ISHIKAWA, T SHIMIZU, Y SHIMAMURA, Y GOTO, K OMORI and N MISAKA. Proc 10th Plastics Fuel Gas Pipe Symnposium, New Orleans USA, Nov. (1987) 175.

52 F W BAILEY and W M WHITTE. Phillips Petroleum Comp., U.S. Patent. 4,547,551 (1985).

53 J L WAY, J R ATKINSON and J NUTTING. J. Mat. Sci. **9** (1974) 293.

54 J MAXFIELD and L MANDELKERN. Macromol. **10** (5) (1977) 1141.

55 L MANDELKERN and J MAXFIELD. J. Polym. Sci., Polym. Edn. **17** (1979) 1913.

56 N BROWN and I M WARD. J. Mat. Sci. **18** (1983) 1405.

57 J M REGO LOPEZ, M T CONDE BRANA, B TERSELIUS and U W GEDDE. Polymer. **29** (1988) 1045.

58 J M REGO LOPEZ and U W GEDDE. Polymer. **29** (1988) 1037.

59 F R LARSON and J MILLER. Trans. Am. Soc. Mech. Eng. **74** (1952) 765.

60 A D WHYMAN and E SZPAK. S.P.E. J. **29** (1973) 73

61 S J BARTON and B W CHERRY. Polym. Eng. Sci. **19** (1979) 590.

62 O D SHERBY. Acta Metallurgica. **10** (1962) 135.

63 G M BARTENEV and Y S ZUYEV. Strength and Failure of Viscolastic Materials. (1962) 26.

64 B W CHERRY and C M HOLMES. J. Phys., Part D, **2** (1969) 821.

65 P L McGINLEY. Ph.D Thesis, Monash Uni. (1973).

66 J KUBAT, M RIGDAHL and R SELDON. J. Appl. Polym. Sci. **20** (2) (1976) 799.

67 C G BRAGAW. Proc. 5th International Conference on Plastics Pipes, York, England. Sept. (1982).

68 R L AYRES. Proc. 10th Fuel Gas Pipe Symnposium, New Orleans USA, Nov.(1987) 206.

69 J M GREIG. Plast. Rubb. Process. Appl. **1** (1981) 43.

70 X LU, X WANG and N BROWN. J. Mat. Sci. **23** (1988) 643.

71 M K V CHAN and J G WILLIAMS. Polymer **24** (1983) 234.

72 D P ROOKE and D J CARTWRIGHT. Compendium of Stress Intensity Factors, HMSO, London. (1976).

73 A GRAY, J N MALLINSON and J B PRICE. Plast. Rubb. Process. Appl. **1** (1) (1981) 51.

74 M W BIRCH, M D TAYLOR and G P MARSHALL. Plast. Rubb. Process. Appl. **3** (3) (1983) 281.

75 M K V CHAN and J G WILLIAMS. Polym. Eng. Sci. **21** (1981) 1019.

76 H NIKLAS and K EIFFLAENDER. Kunststoffe. **49** (1959) 109.

77 E GAUBE. Kunststoffe. **49** (1959) 446.

78 M IFWARSON and P.ERICKSSON. Proc. 5th International Conference on Plastics Pipes, York, England. Sept. (1982).

79 M FLEIβNER. Kunststoffe. **77** (1) (1987) 45.

80 G P MARSHALL, M D TAYLOR and A J DICKINSON. Proc. 5th International Conference on Plastics Pipes, York, England. Sept. (1982).

81 M F EDWARDS, D I ELLIS, S BEORGHIADES and R SMITH. Proc. 5th International Conference on Plastics Pipes, York, England. Sept. (1982).

82 J F INGENHOUSZ. Proc. 5th International Conference on Plastics Pipes, York, England. Sept. (1982).

83 B TERSELIUS, U W GEDDE and J-F JANSSON. Polym. Eng. Sci. **22** (7) (1982) 422.

84 U W GEDDE, B TERSELIUS and J-F JANSSON. Polymer Testing. **2** (1981) 85.

85 M J HANNON. J. Appl. Polym. Sci. **13** (1974) 3761.

86 H R BROWN. Polymer. **19** (1978) 1186.

87 G DIEDRICH, B KEMPER and K GRAF. Kunststoffe **69** (1979) 470.

88 M WOLTERS. Plast. Rubb. Process. Appl. **3** (4) (1983) 323.

89 E H ANDREWS. Fracture in Polymers., Oliver and Boyd, London. (1959) 516.

90 I WOLOCK and S B NEWMAN. Fracture Processes in Polymeric Polymers. Ed. by B ROSEN., Interscience, New York. (1964) 235.

91 P ERIKSSON and M IFWARSON. Proc 6th International Conference on Plastics Pipes, York, England. March (1985).

92 C G BRAGAW. Plast. Rubb. Mat. Appl. (Nov. 1979) 145.

93 C S LEE and M M EPSTEIN. Polym. Eng. Sci. **22** (9) (1982) 549.

94 A LUSTIGER and R L MARKHAM. Polymer **24** (1983) 1647.

95 SHOWA DENKO KK. Japanese Patent, 57,057,737, (1982).

96 IDEMITSU PETROCHEM KK. Japanese Patent, 61,057,638, (1986).

97 SUMITOMO CHEMICAL KK. Japanese Patent, 57,115,438, (1982).

98 G J SANDILANDS and J A BOWMAN. Blending Report to British Gas. (1985).

99 J F CAREY. Introduction to Polymer Science and Technology: An SPE Textbook., H S KAUFMAN and J J FALCETTA, Ed., John Wiley and Sons Inc., New York. (1977) 425.

100 J A BRYDSON. Flow Properties of Polymer Melts. 2nd Edition, George Godwin. (1981).

101 D W VAN KREVELEN. Properties of Polymers. 2nd Edition, Elsevier Scientific Publishing Company, Amsterdam. (1976) 486.

102 L P B M JANSSEN and J M SMITH. Plast. Rubb. Process. 1 (1980) 115.

103 A J DICKINSON. PhD Thesis. Manchester Polytechnic. (1986)

104 E J HEARN. Mechanics of Materials, Pergamon Press. (1980) Chapts. 9 and 10.

105 W C A WRIGHT and J A BOWMAN. Proc. 7th Internatiional Conference on Plastics Pipes, Bath. Sept. (1988).

106 J A SAUER and K D PAE. Introduction to Polymer Science and Technology. H S KAUFMAN and J J FALCETTA, Ed., John Wiley and Sons Inc.

107 K A HODD. Thermal Analysis Short Course, Brunel University. (1987).

108 J M SCHULTZ. Polym. Eng. Sci. **24** (10) 1984 770.

109 J M GREIG and C C LAWRENCE. Proc. 7th International Conference on Plastics Pipes, Bath. Sept. (1988).

110 A BUNIYAT-ZADE and A B AZIMOVA. Sov. Plast. En. Transl. **6** (1970) 38.

111 P D FRAYER. P PO-LUK TONG and W W DREHER. Polym. Eng. Sci. **17** (1) (1977) 27.

112 N K DATTA. PhD Thesis, Loughborough University. (1982).

113 D R NORTON and A KELLER. J. Mat. Sci. **19** (1984) 447.

114 E F PALERMO. Proc. 8th Plastic Fuel Gas Symposium, New Orleans, USA. Nov. (1983).

115 R WILKINS and J HORNE. Electrofusion the next step in Polyethylene. British Gas Corporation, ERS Report to Gas Engineering and Management Meeting. Leicester, Oct. (1983).

APPENDICES

RHEOLOGICAL PROPERTIES OF POLYETHYLENE COMPOUNDS

Sample name(5 letters)	=	MDPE-A
Transducer Range (psi)	=	5000
Radius of Die(mm)	=	1
1st die length (mm)LONG	=	40
2nd die length (mm)SHORT	=	25

RESULTS

	Shear Str (KPa)	ln(SHST)	Shear Rat (/s)	ln(SHSR)	Viscosity Pas	ln(Visc)
	114900	11.65181	37.25403	3.617760	3084.229	8.034057
	142476	11.86692	55.88105	4.023225	2549.629	7.843703
170 C	163158	12.00247	74.50807	4.310907	2189.802	7.691566
	206820	12.23960	111.7621	4.716372	1850.537	7.523231
	367680	12.81496	372.5403	5.920345	986.9534	6.894622
	459600	13.03811	558.8105	6.325810	822.4612	6.712301
	87324	11.37738	37.61727	3.627463	2321.380	7.749917
	114900	11.65181	56.42590	4.032928	2036.298	7.618889
190 C	135582	11.81733	75.23454	4.320610	1802.124	7.496721
	167754	12.03025	112.8518	4.726075	1486.498	7.304178
	282654	12.55197	376.1727	5.930048	751.3942	6.621930
	337806	12.73022	564.2590	6.335513	598.6718	6.394713
	82728	11.32331	38.23791	3.643827	2163.507	7.679485
	101112	11.52398	57.35686	4.049292	1762.857	7.474691
210 C	117198	11.67162	76.47582	4.336974	1532.484	7.334645
	149370	11.91418	114.7137	4.742439	1302.110	7.171741
	250482	12.43114	382.3791	5.946412	655.0619	6.484729
	303336	12.62259	573.5686	6.351877	528.8573	6.270718
	59748	10.99789	36.34151	3.592960	1644.069	7.404930
	78132	11.26615	54.51227	3.998425	1433.291	7.267729
230 C	91920	11.42867	72.68303	4.286108	1264.669	7.142565
	117198	11.67162	109.0245	4.691573	1074.968	6.980046
	222906	12.31450	363.4151	5.895545	613.3645	6.418959
	261972	12.47599	545.1227	6.301011	480.5742	6.174981

Viscosity values at 100/s

170 C	=	1937.975
190 C	=	1574.341
210 C	=	1375.940
230 C	=	1112.849

APPENDIX 9.1: Shear rate, shear stress and viscosity data for MDPE-A . at various temperatures.

RHEOLOGICAL PROPERTIES OF POLYETHYLENE COMPOUNDS

Sample name(5 letters)	=	HDPE-F
Transducer Range (psi)	=	10000
Radius of Die(mm)	=	1
1st die length (mm)LONG	=	40
2nd die length (mm)SHORT	=	25

RESULTS

	Shear Str (KPa)	ln(SHST)	Shear Rat (/s)	ln(SHSR)	Viscosity Pas	ln(Visc)
	147072	11.89867	46.10799	3.830986	3189.728	8.067691
	165456	12.01646	69.16199	4.236451	2392.296	7.780009
170 C	183840	12.12182	92.21599	4.524133	1993.580	7.597687
	206820	12.23960	138.3239	4.929598	1495.185	7.310005
	317124	12.66704	461.0799	6.133571	687.7852	6.533476
	349296	12.76367	691.6199	6.539036	505.0403	6.224638
	124092	11.72877	43.18188	3.765421	2873.704	7.963357
	156264	11.95930	64.77283	4.170886	2412.492	7.788415
190 C	174648	12.07052	86.36377	4.458568	2022.236	7.611959
	202224	12.21713	129.5456	4.864033	1561.024	7.353097
	312528	12.65244	431.8188	6.068006	723.7478	6.584443
	333210	12.71652	647.7283	6.473471	514.4286	6.243056
	105708	11.56843	40.98011	3.713086	2579.495	7.855348
	119496	11.69103	61.47016	4.118551	1943.967	7.572486
210 C	147072	11.89867	81.96022	4.406234	1794.431	7.492443
	179244	12.09650	122.9403	4.811699	1457.975	7.284804
	294144	12.59182	409.8011	6.015671	717.7725	6.576152
	319422	12.67426	614.7016	6.421137	519.6374	6.253131
	98814	11.50099	40.36447	3.697950	2448.043	7.803044
	108006	11.58994	60.54671	4.103415	1783.845	7.486526
230 C	128688	11.76514	80.72895	4.391097	1594.074	7.374048
	156264	11.95930	121.0934	4.796562	1290.441	7.162739
	273462	12.51891	403.6447	6.000535	677.4817	6.518382
	310230	12.64506	605.4671	6.406000	512.3811	6.239068

Viscosity values at 100/s

170 C =	1882.189
190 C =	1841.552
210 C =	1620.626
230 C =	1425.794

APPENDIX 9.2: Shear rate, shear stress and viscosity data for HDPE-F at various temperatures.

RHEOLOGICAL PROPERTIES OF POLYETHYLENE COMPOUNDS

Sample name(5 letters)	=	HDPE-B
Transducer Range (psi)	=	5000
Radius of Die(mm)	=	1
1st die length (mm)LONG	=	40
2nd die length (mm)SHORT	=	25

RESULTS

	Shear Str (KPa)	ln(SHST)	Shear Rat (/s)	ln(SHSR)	Viscosity Pas	ln(Visc)
	28725	10.26552	34.83630	3.550660	824.5707	6.714862
	37917	10.54315	52.25446	3.956125	725.6222	6.587029
170 C	45960	10.73552	69.67261	4.243807	659.6565	6.491719
	56301	10.93846	104.5089	4.649272	538.7195	6.289195
	122943	11.71947	348.3630	5.853245	352.9162	5.866230
	150978.6	11.92489	522.5446	6.258710	288.9295	5.666182
	21831	9.991086	34.10116	3.529331	640.1834	6.461754
	28725	10.26552	51.15174	3.934796	561.5644	6.330726
190 C	34470	10.44784	68.20232	4.222478	505.4079	6.225365
	45960	10.73552	102.3034	4.627943	449.2515	6.107582
	104559	11.55750	341.0116	5.831916	306.6141	5.725590
	127539	11.75617	511.5174	6.237381	249.3345	5.518795
	18384	9.819236	34.20599	3.532400	537.4496	6.286835
	22980	10.04237	51.30898	3.937865	447.8747	6.104513
210 C	28725	10.26552	68.41198	4.225548	419.8825	6.039975
	36768	10.51238	102.6179	4.631013	358.2997	5.881370
	88473	11.39045	342.0599	5.834985	258.6476	5.555466
	105708	11.56843	513.0898	6.240451	206.0223	5.327984
	14937	9.611596	33.77104	3.519603	442.3019	6.091992
	19533	9.879860	50.65656	3.925068	385.5965	5.954791
230 C	24129	10.09116	67.54209	4.212750	357.2438	5.878418
	31023	10.34248	101.3131	4.618216	306.2090	5.724268
	73536	11.20553	337.7104	5.822188	217.7486	5.383341
	91920	11.42867	506.5656	6.227654	181.4572	5.201019

Viscosity values at 100/s

170 C	=	550.7183
190 C	=	452.2333
210 C	=	361.9401
230 C	=	307.7315

APPENDIX 9.3: Shear rate, shear stress and viscosity data for HDPE-B at various temperatures.

RHEOLOGICAL PROPERTIES OF POLYETHYLENE COMPOUNDS

Sample name(5 letters)	=	HDPE-M
Transducer Range (psi)	=	10000
Radius of Die(mm)	=	1
1st die length (mm)LONG	=	40
2nd die length (mm)SHORT	=	25

RESULTS

	Shear Str (KPa)	ln(SHST)	Shear Rat (/s)	ln(SHSR)	Viscosity Pas	ln(Visc)
	170052	12.04385	46.71009	3.843960	3640.583	8.199899
	188436	12.14651	70.06514	4.249425	2689.439	7.897088
170 C	202224	12.21713	93.42019	4.537107	2164.671	7.680023
	229800	12.34496	140.1302	4.942572	1639.902	7.402391
	330912	12.70960	467.1009	6.146545	708.4378	6.563062
	395256	12.88728	700.6514	6.552010	564.1264	6.335278
	156264	11.95930	48.30650	3.877566	3234.843	8.081735
	179244	12.09650	72.45976	4.283031	2473.704	7.813471
190 C	193032	12.17061	96.61301	4.570713	1997.991	7.599897
	216012	12.28308	144.9195	4.976178	1490.565	7.306910
	284952	12.56007	483.0650	6.180151	589.8832	6.379924
	344700	12.75042	724.5976	6.585616	475.7123	6.164813
	142476	11.86692	46.34236	3.836056	3074.422	8.030872
	163158	12.00247	69.51354	4.241521	2347.139	7.760952
210 C	174648	12.07052	92.68473	4.529203	1884.323	7.541324
	186138	12.13424	139.0270	4.934668	1338.861	7.199574
	275760	12.52728	463.4236	6.138641	595.0494	6.388644
	335508	12.72340	695.1354	6.544106	482.6512	6.179294
	119496	11.69103	43.91064	3.782156	2721.344	7.908881
	142476	11.86692	65.86596	4.187621	2163.120	7.679306
230 C	153966	11.94448	87.82129	4.475303	1753.173	7.469183
	176946	12.08359	131.7319	4.880769	1343.227	7.202830
	257376	12.45829	439.1064	6.084741	586.1357	6.373551
	310230	12.64506	658.6596	6.490206	471.0019	6.154862

Viscosity values at 100/s

170 C	=	2066.103
190 C	=	1948.859
210 C	=	1767.453
230 C	=	1609.812

APPENDIX 9.4: Shear rate, shear stress and viscosity data for HDPE-M at various temperatures.

RHEOLOGICAL PROPERTIES OF POLYETHYLENE COMPOUNDS

Sample name(5 letters)	=	MDPE-P
Transducer Range (psi)	=	10000
Radius of Die(mm)	=	1
1st die length (mm)LONG	=	40
2nd die length (mm)SHORT	=	25

RESULTS

	Shear Str (KPa)	ln(SHST)	Shear Rat (/s)	ln(SHSR)	Viscosity Pas	ln(Visc)
	160860	11.98828	48.82917	3.888328	3294.341	8.099961
	179244	12.09650	73.24376	4.293793	2447.225	7.802710
170 C	193032	12.17061	97.65835	4.581475	1976.605	7.589136
	220608	12.30414	146.4875	4.986940	1505.984	7.317202
	326316	12.69562	488.2917	6.190913	668.2807	6.504708
	349296	12.76367	732.4376	6.596378	476.8952	6.167296
	128688	11.76514	42.95930	3.760253	2995.579	8.004892
	151668	11.92944	64.43895	4.165718	2353.669	7.763730
190 C	160860	11.98828	85.91860	4.453400	1872.237	7.534889
	193032	12.17061	128.8779	4.858865	1497.789	7.311745
	294144	12.59182	429.5930	6.062838	684.7038	6.528986
	349296	12.76367	644.3895	6.468303	542.0572	6.295371
	114900	11.65181	43.22231	3.766356	2658.348	7.885460
	128688	11.76514	64.83347	4.171822	1984.900	7.593324
210 C	147072	11.89867	86.44463	4.459504	1701.343	7.439173
	170052	12.04385	129.6669	4.864969	1311.452	7.178890
	271164	12.51047	432.2231	6.068942	627.3703	6.441537
	307932	12.63763	648.3347	6.474407	474.9583	6.163227
	91920	11.42867	42.00910	3.737886	2188.097	7.690787
	110304	11.61099	63.01365	4.143351	1750.477	7.467644
230 C	128688	11.76514	84.01820	4.431033	1531.668	7.334112
	156264	11.95930	126.0273	4.836498	1239.921	7.122803
	234396	12.36476	420.0910	6.040471	557.9648	6.324295
	261972	12.47599	630.1365	6.445936	415.7384	6.030056

Viscosity values at 100/s

170 C	=	1945.442
190 C	=	1722.211
210 C	=	1549.464
230 C	=	1398.787

APPENDIX 9.5: Shear rate, shear stress and viscosity data for MDPE-P . at various temperatures.

RHEOLOGICAL PROPERTIES OF POLYETHYLENE COMPOUNDS

Sample name(5 letters)	=	MDPE-D
Transducer Range (psi)	=	10000
Radius of Die(mm)	=	1
1st die length (mm)LONG	=	40
2nd die length (mm)SHORT	=	25

RESULTS

	Shear Str (KPa)	ln(SHST)	Shear Rat (/s)	ln(SHSR)	Viscosity Pas	ln(Visc)
	133284	11.80023	40.91028	3.711381	3257.958	8.088855
	165456	12.01646	61.36542	4.116846	2696.241	7.899613
170 C	188436	12.14651	81.82057	4.404528	2303.039	7.741985
	229800	12.34496	122.7308	4.809993	1872.389	7.534970
	349296	12.76367	409.1028	6.013966	853.8097	6.749708
	404448	12.91027	613.6542	6.419431	659.0811	6.490846
	105708	11.56843	38.14348	3.641354	2771.325	7.927080
	137880	11.83413	57.21522	4.046820	2409.847	7.787318
190 C	156264	11.95930	76.28696	4.334502	2048.370	7.624800
	193032	12.17061	114.4304	4.739967	1686.893	7.430643
	330912	12.70960	381.4348	5.943940	867.5452	6.765667
	390660	12.87559	572.1522	6.349405	682.7902	6.526187
	91920	11.42867	37.67057	3.628879	2440.100	7.799794
	124092	11.72877	56.50586	4.034344	2196.090	7.694434
210 C	137880	11.83413	75.34115	4.322026	1830.075	7.512112
	174648	12.07052	113.0117	4.727491	1545.397	7.343036
	307932	12.63763	376.7057	5.931464	817.4337	6.706169
	353892	12.77674	565.0586	6.336929	626.2924	6.439817
	87324	11.37738	37.69361	3.629490	2316.678	7.747889
	101112	11.52398	56.54042	4.034955	1788.313	7.489028
230 C	119496	11.69103	75.38723	4.322637	1585.095	7.368400
	147072	11.89867	113.0808	4.728103	1300.591	7.170574
	280356	12.54381	376.9361	5.932075	743.7757	6.611739
	335508	12.72340	565.4042	6.337540	593.3948	6.385860

Viscosity values at 100/s

170 C =	2078.798
190 C =	1799.368
210 C =	1626.268
230 C =	1380.986

APPENDIX 9.6: Shear rate, shear stress and viscosity data for MDPE-D at various temperatures.

	ZONE TEMPERATURES (°C)					MELT PRESS. (psi)	SCREW SPEED (RPM)	AMPS (A)
	1	2	3	4	5			
SET CONDITIONS	150	170	175	180	190	-	150	-
CHDPE-F/2/32	150	170	175	180	190	380	150	11
CHDPE-F/10/32	150	170	175	180	190	440	150	11
CHDPE-F/20/32	150	170	175	180	190	410	150	10.5

Notes: 1. Haul off rate = 1.8m/min.
2. Water bath temperature = 35°C.
3. Feed rate = 40 revs at a screw speed of 150 RPM.

APPENDIX 9.7: Twin screw compounding conditions for 32mm HDPE-F blends.

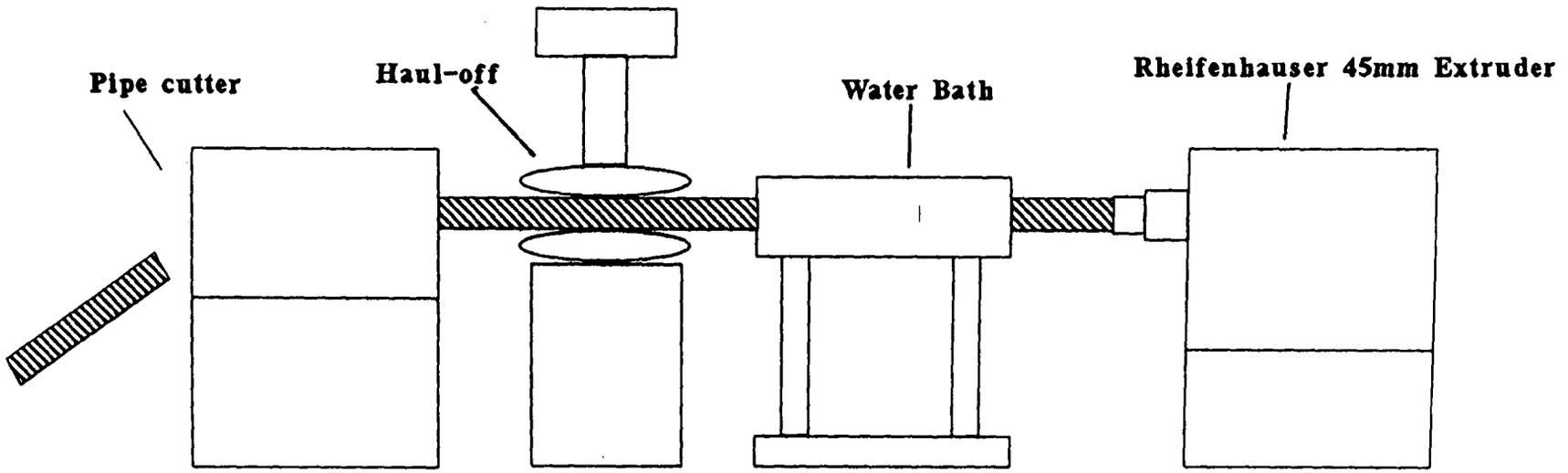

APPENDIX 9.8a): Extrusion layout for the production of 32mm pipe.

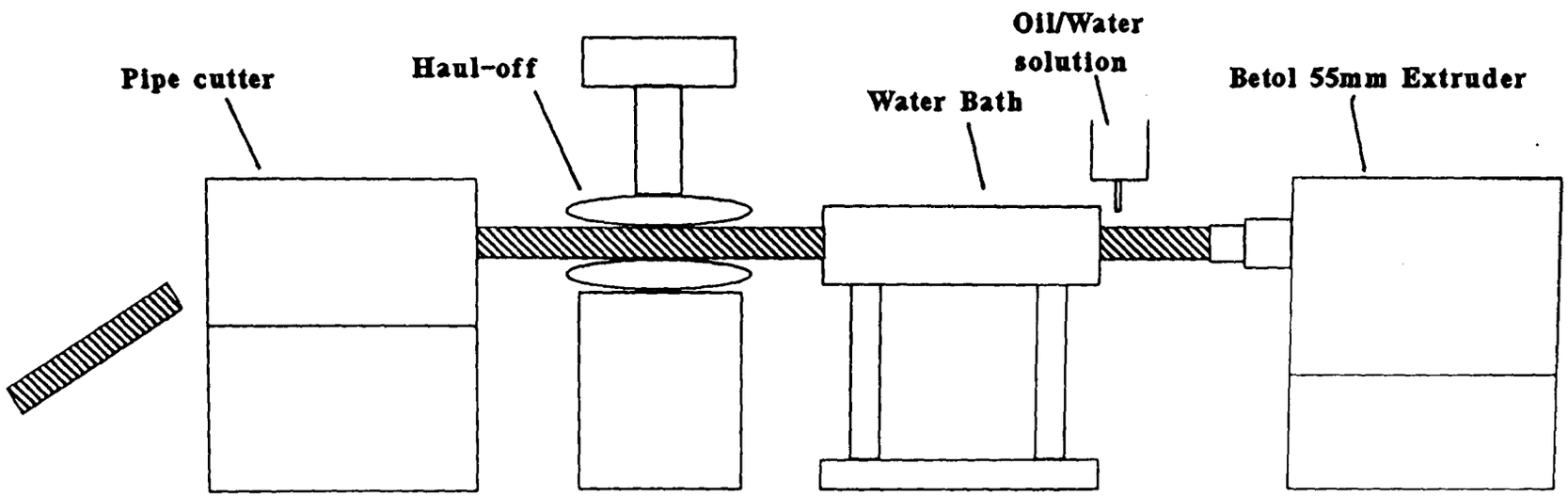

APPEENDIX 9.8b): Extrusion layout for the production of 55mm pipe.

	ZONE TEMPERATURES (oC)					DIE TEMP. (oC)		SCREW SPEED (RPM)	AMPS (A)
	1	2	3	4	5	6	7		
SET CONDITIONS	153	169	170	174	190	180	181	100	-
MDPE-A	153	169	170	174	190	180	180	150	11
HDPE-F/2	150	170	175	180	190	180	180	150	11
HDPE-F/10	150	170	175	180	190	180	180	150	11
HDPE-F/20	150	170	175	180	190	180	180	150	11

Notes: 1. Haul off rate = 3.6m/min.
2. Water bath temperature = 35oC

APPENDIX 9.9: Pipe extrusion conditions for 32mm HDPE-F blends

	ZONE TEMPERATURES (oC)					DIE TEMP. (oC)		SCREW (RPM)	AMPS SPEED (A)
	1	2	3	4	5	6	7		
SET CONDITIONS	153	169	170	174	190	180	181	80	-
MDPE-A	153	169	170	174	190	180	180	80	11
HDPE-M/10/32	150	160	166	175	195	180	180	75	10.5
HDPE-B/10/32	150	160	166	175	195	180	180	75	10.5

Notes: 1. Haul off rate = 3.6m/min.
2. Water bath temperature = 35oC

APPENDIX 9.10: Pipe extrusion conditions for 32mm HDPE-B and HDPE-M blends.

	Die Temp. (oC)		Zones Temp. (oC)				Melt Temp. (oC)	Screw (RPM)	Amps (A)	Haul -off (m/min)	Vac. (mmHg)	Melt Pressure (MPa)		
SET	200	200	190	180	170	160	-	-	-	-	-	-	-	-
MDPE-A	200	199	191	180	174	159	187	70.4	3.6	0.84	70	3.17	13.1	8.96
HDPE-B/2	200	200	192	180	173	160	187	70.4	3.6	0.78	70	3.03	15.8	8.2
HDPE-B/5	200	200	192	180	172	160	187	71.2	3.6	0.78	68	2.89	15.6	7.92
HDPE-B/10	200	200	190	180	172	160	187	71.2	3.6	0.78	68	2.79	15.2	8.62
HDPE-B/20	200	199	189	179	170	160	187	68.5	3.6	0.78	68	2.51	14.4	9.65
HDPE-M/2	195	200	190	180	176	160	188	72.4	3.5	0.63	68	3.24	16.5	6.06
HDPE-M/5	200	200	188	180	176	160	188	73.1	3.5	0.0.63	68	3.27	16.7	5.65
HDPE-M/10	200	200	188	180	178	160	188	73.1	3.5	0.63	68	3.72	17.8	4.96
HDPE-M/20	200	200	190	180	178	160	188	74.3	3.5	0.63	68	3.51	16.9	5.44

APPENDIX 9.11: Pipe extrusion conditions for 55mm HDPE-B and HDPE-M blends.

	Die Temp. (°C)		Zones Temp. (°C)				Melt Temp. (°C)	Screw (RPM)	Amps (A)	Haul-off (m/min)	Vac. (mmHg)	Melt Pressure (MPa)		
SET	200	200	190	180	170	160	-	-	-	-	-	-	-	-
MDPE-A	200	199	191	180	174	159	187	70.4	3.6	0.84	70	3.17	13.1	8.96
MDPE-P/2	200	199	192	181	174	160	188	70.4	3.6	0.76	68	3.14	14.5	7.79
MDPE-P/5	200	199	190	180	175	160	187	70.4	3.6	0.76	68	3.10	14.8	7.79
MDPE-P/10	200	199	190	181	176	160	187	71.8	3.6	0.75	68	3.24	15.0	6.54
MDPE-P/20	201	199	190	181	178	160	187	71.8	3.6	0.75	68	3.17	15.2	5.99
MDPE-D/2	200	199	193	180	175	160	187	73.4	3.6	0.77	70	3.24	-	10.1
MDPE-D/5	200	199	192	180	174	160	188	73.4	3.6	0.76	70	3.03	-	9.65
MDPE-D/10	200	200	192	180	174	160	188	70	3.6	0.76	72.5	3.10	-	9.58
MDPE-D/20	200	200	191	180	174	160	188	70	3.6	0.76	68	3.03	-	9.65

APPENDIX 9.12: Pipe extrusion conditions for MDPE-P and MDPE-D blends.

Sample	Failure Time (hrs)	Notch Depth (mm)	Wall Thickness (mm)	Hoop Stress (MPa)	Y	K (MPam$^{0.5}$)
MDPE-A	776.8	1.96	5.7	3.04	1.66	0.396
	1694.7	1.24	5.2	3.37	1.38	0.289
	1201.2	1.36	5.2	3.37	1.44	0.317
	1496.7	1.33	5.1	3.4	1.44	0.317
HDPE-B/5	663.1	1.11	5.3	3.30	1.31	0.255
	698.5	1.35	5.1	3.40	1.44	0.319
	211.9	1.42	5.2	3.37	1.47	0.330
	538.8	1.13	5.25	3.33	1.35	0.268
HDPE-B/20	61.7	1.25	5.7	3.04	1.35	0.257
	145.6	1.30	5.6	3.10	1.38	0.273
	171.1	1.24	5.6	3.1	1.37	0.265
HDPE-M/5	652.3	1.10	5.0	3.48	1.35	0.276
	803.2	1.26	5.0	3.48	1.42	0.310
	1113.5	1.19	5.1	3.44	1.38	0.290
	1246.1	1.22	5.3	3.30	1.37	0.279

APPENDIX 9.13: 32mm notched pipe data at 0.955MPa pressure and 80^{o}C.

Sample	Failure Time (hrs)	Notch Depth (mm)	Wall Thickness (mm)	Hoop Stress (MPa)	Y	K (MPam$^{0.5}$)
MDPE-A	776.8	1.96	5.7	3.04	1.66	0.396
	1694.7	1.24	5.2	3.37	1.38	0.289
	1201.2	1.36	5.2	3.37	1.44	0.317
	1496.7	1.33	5.1	3.4	1.44	0.317
HDPE-B/5	663.1	1.11	5.3	3.30	1.31	0.255
	698.5	1.35	5.1	3.40	1.44	0.319
	211.9	1.42	5.2	3.37	1.47	0.330
	538.8	1.13	5.25	3.33	1.35	0.268
HDPE-B/20	61.7	1.25	5.7	3.04	1.35	0.257
	145.6	1.30	5.6	3.10	1.38	0.273
	171.1	1.24	5.6	3.1	1.37	0.265
HDPE-M/5	652.3	1.10	5.0	3.48	1.35	0.276
	803.2	1.26	5.0	3.48	1.42	0.310
	1113.5	1.19	5.1	3.44	1.38	0.290
	1246.1	1.22	5.3	3.30	1.37	0.279
HDPE-M/20	979.2	1.31	5.0	3.48	1.44	0.321
	1174	1.46	5.2	3.33	1.48	0.334
	606.1	1.50	5.1	3.40	1.52	0.355
MDPE-P/5	709.8	1.17	4.8	3.68	1.41	0.314
	569.7	1.17	4.8	3.63	1.40	0.308
	486.2	1.42	5.1	3.48	1.49	0.346
	975.5	0.91	5.0	3.51	1.3	0.244
MDPE-P/20	1179.3	1.37	5.1	3.44	1.45	0.328
	947.9	1.16	4.9	3.55	1.38	0.296
	681.7	1.24	5.1	3.40	1.39	0.295
	976.7	1.14	4.9	3.55	1.37	0.291
MDPE-D/5	1629.1	0.97	5.3	3.30	1.30	0.236
	1461.3	1.12	5.2	3.37	1.35	0.269
	1297.1	1.12	5.4	3.23	1.33	0.254
	1006.8	1.03	5.3	3.26	1.30	0.241
MDPE-D/20	1852.4	1.21	5.5	3.26	1.37	0.275
	1423.5	1.09	5.4	3.23	1.33	0.252
	1438.8	1.17	5.4	3.23	1.35	0.264
	1231.5	1.19	5.2	3.33	1.37	0.279

APPENDIX 9.14: 55mm notched pipe data at 0.7MPa pressure and 80°C.

Sample	Failure Time (hrs)	Notch Depth (mm)	Wall Thickness (mm)	Hoop Stress (MPa)	Y	K (MPam$^{0.5}$)
MDPE-A	658.5	1.59	5.0	4.47	1.59	0.502
	1530.6	1.17	5.2	4.33	1.36	0.357
	1933	-	-	-	-	-
	2189	-	-	-	-	-
HDPE-B/5	506.1	1.35	5.1	4.42	1.45	0.417
	574.6	1.40	5.1	4.37	1.46	0.423
	164	1.46	5.2	4.33	1.48	0.434
	339.5	1.52	5.1	4.37	1.53	0.462
HDPE-B/20	97.4	1.50	5.6	3.99	1.46	0.399
	115.7	1.45	5.5	4.07	1.45	0.397
	132.1	1.45	5.5	4.07	1.45	0.397
	155.9	1.47	5.4	4.1	1.46	0.407
HDPE-M/5	664.4	1.24	4.9	4.57	1.42	0.404
	687.9	1.23	5.2	4.33	1.39	0.373
	1156.3	1.47	5.2	4.33	1.47	0.432
HDPE-M/20	170.3	1.31	5.0	4.47	1.44	0.412
	180.5	1.31	5.1	4.37	1.43	0.401
	299.9	1.45	5.0	4.52	1.52	0.463
	230.2	1.43	5.1	4.42	1.48	0.438
MDPE-P/5	1101.4	1.41	4.95	4.57	1.50	0.456
	1073.6	1.32	5.20	4.33	1.44	0.401
	623.6	1.54	5.00	4.52	1.56	0.490
	1674	-	-	-	-	-
MDPE-P/20	1544.1	1.22	5.2	4.33	1.39	0.372
	1375.7	1.24	4.8	4.67	1.43	0.416
	>1900	-	-	-	-	-
	>1900	-	-	-	-	-
MDPE-D/5	>2200	-	-	-	-	-
MDPE-D/20	1196.6	1.17	5.3	4.24	1.35	0.347
	1599.7	1.29	5.3	4.19	1.40	0.374
	1843	-	-	-	-	-
	1600	-	-	-	-	-

APPENDIX 9.15: 55mm notched pipe data at 0.8MPa pressure at 80°C.

Sample	Failure Time (hrs)	Notch Depth (mm)	Wall Thickness (mm)	Hoop Stress (MPa)	Y	K ($MPam^{0.5}$)
MDPE-A	385	1.19	5.0	4.52	1.39	0.384
	351.2	1.53	5.4	4.11	1.48	0.421
	344.6	1.25	5.0	4.52	1.42	0.402
	511.4	1.35	5.5	4.07	1.41	0.373
HDPE-B/2	340.5	1.24	5.3	4.24	1.38	0.365
	263.5	1.37	5.3	4.24	1.44	0.400
	257.2	1.39	5.1	4.42	1.46	0.426
HDPE-B/5	92.4	1.82	5.2	4.33	1.68	0.549
	162.7	1.37	5.0	4.47	1.46	0.428
	130.6	1.28	5.5	4.37	1.42	0.393
	153	1.29	5.1	4.42	1.43	0.402
HDPE-B/10	104.2	1.09	5.3	4.24	1.31	0.324
	175.6	1.35	5.3	4.25	1.40	0.387
	166.6	1.26	5.25	4.28	1.39	0.374
HDPE-B/20	34.4	1.52	5.3	4.24	1.5	0.439
	61.5	1.42	5.6	3.95	1.34	0.353
	59.1	1.47	5.5	4.07	1.43	0.395
	60.6	1.14	5.3	4.24	1.48	0.375
HDPE-M/2	427.2	1.13	5.0	4.47	1.35	0.359
	241.5	1.02	5.0	4.52	1.33	0.340
	289.1	1.27	5.0	4.47	1.42	0.400
	331.6	1.31	5.0	4.47	1.44	0.413
HDPE-M/5	163.4	1.39	5.1	4.37	1.46	0.421
	174.7	1.60	5.1	4.37	1.56	0.484
	296.6	1.44	5.4	4.15	1.45	0.405
	226.2	1.44	5.1	4.42	1.49	
HDPE-M/10	159.7	1.06	5.3	4.24	1.31	0.320
	175.8	1.10	5.4	4.11	1.31	0.316
	196.7	0.96	5.1	4.37	1.29	0.309
	157.3	1.09	5.5	4.07	1.31	0.311
HDPE-M/20	140.3	1.05	5.2	4.28	1.31	0.322
	107	0.95	5.3	4.19	1.72	0.394
	132.5	1.09	5.1	4.42	1.34	0.346
	110.5	1.25	5.1	4.42	1.41	0.390
MDPE-P/2	293	1.35	5.0	4.52	1.46	0.429
	312.7	1.11	4.9	4.62	1.36	0.370
	421.1	1.31	4.9	4.62	1.45	0.429
	208.8	-	-	-	-	-
MDPE-P/5	255.3	1.17	4.9	4.57	1.38	0.382
	216.3	1.07	5.4	4.15	1.31	0.315
	312.7	1.12	5.1	4.42	1.35	0.354

contd.

Sample	Failure Time (hrs)	Notch Depth (mm)	Wall Thickness (mm)	Hoop Stress (MPa)	Y	K ($MPam^{0.5}$)
MDPE-P/10	626.1	1.38	5.5	4.07	1.42	0.380
	595	1.40	5.3	4.24	1.45	0.407
MDPE-P/20	318.4	1.09	5.3	4.24	1.32	0.327
	385.4	1.25	5.3	4.24	1.38	0.366
	304.2	0.95	5.1	4.42	1.29	0.311
MDPE-D/2	449.8	1.39	4.9	4.57	1.48	0.446
	667	1.37	5.3	4.19	1.44	0.396
	480.9	-	-	-	-	-
	693.4	-	-	-	-	-
MDPE-D/5	342	1.43	5.1	4.42	1.48	0.438
	352.9	1.44	5.3	4.19	1.5	0.423
	305.7	1.56	5.2	4.33	1.54	0.466
	384.1	1.67	5.4	4.11	1.55	0.461
MDPE-D/10	562.3	1.30	5.3	4.24	1.41	0.381
	440	1.49	5.1	4.42	1.51	0.456
	603.5	1.26	5.3	4.19	1.38	0.364
	449.8	1.16	5.5	4.07	1.33	0.326
MDPE-D/20	337.8	1.27	5.4	4.15	1.38	0.362
	342.4	1.18	5.4	4.11	1.34	0.335
	338	1.16	5.5	4.07	1.33	0.326
	410.5	1.15	5.3	4.24	1.34	0.341

APPENDIX 9.16: 55mm notched pipe data at 0.9MPa pressure and 80°C.